Modulating stress responses to boost resilience in the nematode *C. elegans*

Dissertation

zur Erlangung des Doktorgrades der Mathematisch-Naturwissenschaftlichen Fakultät der Universität zu Köln

vorgelegt von

Jan Eike Dinort

aus Siegen

Cambridge, 26 May 2026

The work described in this dissertation was conducted between December 2021 and May 2026 under the supervision of Dr. Martin Denzel. Until April 2022, the work was conducted at the Max Planck Institute for Biology of Ageing, Joseph-Stelzmann-Straße 9b, D-50931, Cologne, Germany. The majority of the work was conducted with Altos Labs at the Cambridge Institute of Science, Portway Building, Granta Park, Great Abington, Cambridge, CB21 6GP, United Kingdom.

Die in dieser Dissertation beschriebenen Arbeiten wurden zwischen Dezember 2021 und Mai 2026 unter der Leitung von Dr. Martin Denzel durchgeführt. Bis zum April 2022 wurde die Arbeit am Max-Planck-Institut für Biologie des Alterns, Joseph-Stelzmann-Straße 9b, D-50931, Köln, Deutschland, durchgeführt. Der Großteil der Arbeit wurde bei Altos Labs in Cambridge Institute of Science, Portway Building, Granta Park, Great Abington, Cambridge, CB21 6GP, Großbritannien durchgeführt.

CONTENTS

ABSTRACT

Increased susceptibility to cellular stress is a key characteristic of aging and disease. Determining the molecular mechanisms underlying this decline of organismal resilience is critical for understanding the transition from healthy aging to disease-associated collapse. Here we present a fundamental investigation into the determinants of physiological frailty in a *C. elegans* model for Duchenne Muscular Dystrophy (DMD). Centered on the hypothesis that a chronic homeostatic burden reduces the responsiveness to acute perturbation, we assess physiological and molecular responses to stress to outline mechanisms driving frailty. While defects in locomotion and mitochondrial calcium metabolism are well described in the DMD model, the causal drivers in this phenotype remain elusive.

In this project, we identify a hypersensitivity of the dystrophin mutant *dys-1(eg33)* to heat and mitochondrial stress, which can be alleviated by boosting UPR^{mito} stress response capacity. We apply RNAseq to describe high-resolution kinetics of the heat stress response, identifying previously overlooked signatures including suppressed proteolysis, a transient burst in histone expression, and a systematic reduction in mitochondria encoded transcripts. This uncovered a reduced response of the UPR^{mito} in the *dys-1(eg33)* mutant, supporting reports of mitochondrial dysfunction caused by increased calcium influx into mitochondria.

We demonstrate that augmenting UPR^{mito} capacity effectively alleviates stress hypersensitivity in DMD animals, offering a potent metabolic axis for therapeutic intervention that could complement current gene-therapy and anti-inflammatory strategies. Our findings indicate that resilience is governed by a complex interplay of response mechanisms active in resolving chronic and acute challenges throughout life. Ineffective management of resource allocation, and exceeding homeostatic thresholds shifts the system from hormetic adaptation toward programmed lethality. These results provide a multi-faceted framework for understanding the systemic impact of disease and accumulation of environmental burdens in age on cellular homeostasis and suggest that targeting organismal resilience may offer a robust path to improving healthspan in aging and chronic illness.

ZUSAMMENFASSUNG

Eine erhöhte Anfälligkeit für zellulären Stress ist ein prominentes Merkmal des Alterns und bei Krankheit. Die Bestimmung der molekularen Mechanismen, die diesem Rückgang der organismischen Resilienz zugrunde liegen ist entscheidend für das Verständnis des Übergangs von gesundem Altern zu einem krankheitsassoziierten Kollaps. Hier präsentieren wir eine grundlegende Untersuchung der Determinanten physiologischer Fragilität in einem *C. elegans*-Modell für Duchenne-Muskeldystrophie (DMD). Ausgehend von der Hypothese, dass eine chronische homöostatische Belastung die Reaktionsfähigkeit auf akute Störungen verringert, bewerten wir physiologische und molekulare Stressantworten, um die Mechanismen zu skizzieren, die diese Fragilität vorantreiben. Während Defekte in der Fortbewegung und im mitochondrialen Kalziumstoffwechsel im DMD-Modell gut beschrieben sind, bleiben die kausalen Ursachen dieses Phänotyps bisher ungeklärt.

In diesem Projekt identifizieren wir eine Hypersensitivität der Dystrophin Mutante *dys-1(eg33)* gegenüber Hitze und mitochondrialem Stress, die durch eine Steigerung der UPR^{mito}-Stressantwortkapazität gemildert werden kann. Wir setzen RNA-Seq ein, um die hochauflösende Kinetik der Hitzestressantwort zu beschreiben, wobei wir bisher übersehene Signaturen identifizieren, darunter eine unterdrückte Proteolyse, einen vorübergehenden Anstieg der Histonexpression und eine systematische Reduktion mitochondrial kodierter Transkripte. Diese Arbeit deckt eine verminderte Antwort der UPR^{mito} in der *dys-1(eg33)*-Mutante auf, was Berichte über mitochondriale Dysfunktion stützt, die durch einen erhöhten Kalziumeinstrom in die Mitochondrien verursacht wird.

Wir demonstrieren, dass die Stärkung der UPR^{mito}-Kapazität die Stresshypersensitivität in DMD-Tieren effektiv lindert und somit eine vielversprechende metabolische Achse für therapeutische Interventionen bietet, die aktuelle Gentherapien und antiinflammatorische Strategien ergänzen könnte. Unsere Ergebnisse deuten darauf hin, dass Resilienz durch ein komplexes Zusammenspiel von Reaktionsmechanismen gesteuert wird, die aktiv chronische und akute Herausforderungen im Laufe des Lebens bewältigen. Ein ineffektives Ressourcenmanagement und das Überschreiten homöostatischer Schwellenwerte verschieben das System von einer hormetischen Anpassung hin zu programmierter Letalität. Diese Ergebnisse bieten einen facettenreichen Rahmen für das Verständnis der systemischen Auswirkungen von Krankheiten und der Akkumulation von Umweltbelastungen im Alter auf die zelluläre Homöostase. Sie legen nahe, dass die gezielte Beeinflussung der organismischen Resilienz einen robusten Weg zur Verbesserung der Gesundheitsspanne im Alter und chronischen Krankheiten bieten könnte.

LIST OF FIGURES

LIST OF TABLES

ABBREVIATIONS

aa amino acid

AA antimycin A

ATP adenosine triphosphate

ATF activating transcription factor

cDNA complementary DNA

CDS coding sequence

C. elegans Caenorhabditis elegans

CHOP C/EBP homology protein

CReP constitutive repressor of eIF2alpha phosphorylation

CRISPR clustered regulary interspaced short palindromic repeats

DMD Duchenne Muscular Dystrophy

DMSO dimethyl sulfoxide

DNA deoxyribonucleic acid

DR dietary restriction

FLInt fluorescent landmark interference

FUDR 5-Fluoro2'-deoxyuridine

GFP green fluorescent protein

GO gene onthology

HDR homology directed repair

HSR Heat Shock Response

HSF Heat Shock Factor

IGF insulin-like growth factor

IIS insulin/IGF-like signalling

IPTG isopropyl beta-D-1-thiogalactopyranoside

IRE1 inositol-requiring protein 1

ISR Integrated Stress Response

L4 *C. elegans* larval stage 4

mRNA messenger RNA

NAD nicotinamide adenine dinucleotide

NADH nicotinamide adenine dinucleotide hydride

NGM nematode growth media

nt nucleotide

OA over-activation

OE over-expression

ORF open reading frame

PAM protospacer-adjacent motif

PC Principal Component

PCA Principal component analysis

PERK PKR-like endoplasmic reticulum kinase

PKR protein kinase R

RNA ribonucleic acid

RNAi RNA interference

RNAseq RNA sequencing

RT-qPCR reverse transcriptase - quantitative polymerase chain reaction

SD standard deviation

SEM standard error of the mean

SNP single nucleotide polymorphism

syn synuclein

TC ternary complex

TF Transcription Factor

TM Tunicamycin

uORF upstream open reading frame

UPR unfolded protein response

UPR-ER Endoplasmic Reticulum Unfolded Protein Response

UPR-mt Mitochondrial Unfolded Protein Response

UTR untranslated region

WT wild type

1 INTRODUCTION

1.1 More than longevity: Why we study aging

The scientific challenge to understand aging has evolved significantly from a pursuit of the "fountain of youth" into a rigorous scientific necessity driven by a global demographic shift (DementiaForecasting 2022). As modern medicine has successfully reduced mortality caused by infections or trauma and increased global life expectancy, we are experiencing a staggering rise in age-related pathologies (Guo et al. 2022). While we are living longer, our "healthspan", the period of life spent in good functional health, has not kept pace with our lifespan (Garmany, Yamada, and Terzic 2021). This disparity has resulted in an unprecedented rise in the prevalence of age-related conditions, most notably sarcopenia, Parkinson's disease (PD), and various neurodegenerative dementias. Among these conditions, Alzheimer's Disease (AD) arguably exerts the strongest impact on modern society. It causes a progressive and irreversible collapse of cognitive architecture, currently affecting over 55 million people worldwide and projected to nearly triple by 2050 (DementiaForecasting 2022; Scheltens et al. 2021). However, the progressive decline of muscle mass and strength in sarcopenia can also occur without genetic predisposition, and represents a critical risk factor for age-related frailty (Cruz-Jentoft and Sayer 2019). Consequently, there is an urgent clinical, but also social and economic incentive to move beyond treating individual symptoms toward understanding the fundamental biological drivers of these age-related conditions (Kennedy et al. 2014).

The consequences of the demographic shift by far exceed the medical implications of a longer lifespan, as its effects are universal, and extend to significant social and economical challenges. With rising life expectancy and an increase in age-related disease the overall cost to treat them and maintain health throughout life increases with it (Jaba, Balan, and Robu 2014; Atella et al. 2019). The investments in the healthcare systems hereby improve life expectancy itself (Ranabhat et al. 2018; Gürler and Özsoy 2018), which creates a "paradox of success" where high investment into the healthcare system increases lifespan, which in turn demands higher investments as people live longer. This simplified example shows how deeply these topics are connected, and how wide-reaching the effects of improvements in modern medicine are. Considering the differences in healthcare and social systems between countries, there is also a political aspect, as not all countries provide free healthcare and access to treatments. This also generates a social hurdle guarding access to health, especially in age. With this comes the fear that healthy aging will be reserved to those who can afford it, making healthy aging a luxury.

The past decades have transformed the understanding of aging from a process of linear decline into a genetically regulated and dynamic state. This paradigm shift was ignited by landmark publications using the nematode *Caenorhabditis elegans* (*C. elegans*). Using this model researchers demonstrated that a single mutation more than doubled the organism's lifespan (Kenyon et al. 1993; Klass 1983). This discovery proved that aging is not merely a stochastic accumulation of damage, but a process governed by conserved signaling pathways such as the Insulin/IGF-1 signaling (IIS) pathway that integrates nutrient sensing with cellular maintenance. Organising the complex mechanisms driving aging, the field converged on the "Hallmarks of Aging", a framework popularized by López-Otín et al. 2013, which identifies key drivers such as genomic instability,

telomere attrition, and mitochondrial dysfunction. Collapse of protein homeostasis, or proteostasis, is another important driver of aging. Loss of proteostasis is a systemic failure of the cellular machinery responsible for maintaining the health, folding, and degradation of proteins. In this context aging is characterized by a failure of the cellular quality control machinery to fold or degrade damaged proteins, resulting in accumulation in aggregates and imbalance of homeostasis (Labbadia and Morimoto 2014). These hallmarks do not exist in isolation, but are in constant interplay where a failure in one, such as collapse of protein homeostasis, triggers a systemic decline in cellular resilience.

Today, aging research addresses aspects of the hallmarks to reverse diseases and also uses systemic treatments, moving beyond a descriptive understanding toward targeted therapeutic interventions. By isolating pathways causing mitochondrial dysfunction, proteostasis collapse, or cellular senescence, researchers are developing strategies designed to restore youthful function to compromised processes and tissues (Amorim et al. 2022; Ocampo et al. 2016). This resulted in the establishment of pharmacological interventions using drugs that can serve as "Geroprotectors", which target the biological pathways that regulate metabolism and cellular repair in accordance with the hallmarks. Most prominently, Rapamycin and Metformin cause a range of health benefits in aging (Harrison et al. 2009; Li, Kim, and Blenis 2014; Barzilai et al. 2016). While Rapamycin is used in a narrow range due to its immune-modulating effects, Metformin is commonly prescribed in metabolic disorders (Group 1998; Lv and Guo 2020). Many of the drugs explored in treatment of age-related disorders, just like Metformin which is used for over 60 years, are older than modern aging research itself, highlighting the trend of re-purposing drugs rather than inventing novel molecules.

Aging is a complex, multi-faceted process and is much more than the increasing number of years and becoming more physically vulnerable in old age. It is an inter-disciplinary topic and does not just affect the health of an individual, but has wide-reaching impact on the social, economical, and political landscape (Gianfredi et al. 2025). With increasing age and a demographic shift (Collaborators et al. 2020), we also experience an increase in overall cost of living throughout life and maintaining health, which drives the need for better care. The full consequences this entails remain to be uncovered, but we start to experience the impact on our everyday lives and modern politics with debates addressing problems in state pension plans and effects on the retirement age, which as a consequence of an older population and a reduced workforce would eventually require people to work longer. While not every scientist can directly shape the socio-economic effects of the research, we should take responsibility to ensure treatments are affordable and accessible to everyone. This should be a fundamental driver of not just aging research but science, to provide knowledge and access to its benefits for all of society.

1.1.1 Healthspan: Improving health in aging and disease

Chronological age is measured in years and does not represent the state of physical health. We have therefore adopted new metrics to measure health and performance to determine biological timers, moving away from an individual number toward assessing fitness, vitality and molecular biomarkers in the determination of "functional age" (Baker and Sprott 1988). Combining assessment of physical performance with molecular parameters, functional age captures a more complete representation of overall health. Physical tests to assess grip-strength, balance and cardiorespiratory fitness are hereby complemented by determination of metabolic markers to assess overall health (Mandsager et al. 2018; Leong et al. 2015; Mutz, Iniesta, and Lewis 2024). An important advancement in this field was the discovery of aging clocks, measuring modifications of the DNA which correlate with age, and can serve as a predictor of biological age (Horvath 2013). This has since been

advanced to include clinical biomarkers like glucose and albumin levels to better inform health outcomes and mortality risk (Levine et al. 2018; Lu et al. 2019).

While genetics provide the fundamental blueprint for aging biology, health and its decline throughout life is heavily modulated by additional factors such as nutrition and exercise. The amount of nutrient intake is as important as the frequency, and intermittent fasting has been a popular method to optimise nutritional health benefits (Francesco et al. 2018). By active lifestyle choices we are moving from the treatment at the onset of symptoms to the proactive modulation of the aging process. These effects are difficult to quantify, but a balanced diet is reported to affect a range of factors contributing to functional benefits in age (Fontana and Partridge 2015). Based on these discoveries, the integration of precise nutrition with physiological monitoring is fundamentally reshaping the boundaries of elite sports. By aligning dietary intake with metabolic demands, athletes can optimise their nutrition plans to maximise performance (Hawley and Leckey 2015; Impey et al. 2018). Additionally, high-protein diets have been demonstrated to facilitate greater overall weight and fat loss while essential lean mass is preserved, representing a critical factor for maintaining power-to-weight ratios (Phillips 2006). Refining these nutritional strategies and synchronizing them with the continuous assessment of performance parameters such as maximal oxygen uptake and lactate threshold (San-Millán and Brooks 2018), professional athletes are transforming their respective sports. As an example of this, human performance has recently been taken to the next level with the first recorded sub 2 hour marathon in an official race by Sabastian Sawe and Yomif Kejelcha at the 2026 TCS London Marathon. It remains to be shown what is possible by precise nutrition and advancements in sports science, as the limits of professional performance keep shifting. We are witnessing a continuous expansion of what is possible by precise nutrition and advancements in sports science, and it remains to be shown where the limits lie, as yesterday's records are becoming today's baseline. Witnessing this shift in the limits of performance, we need to ask what this means for health and aging itself. While nutrition and exercise is a key determinant of health, it needs to be balanced to optimise its benefits, and excessive exercise is not synonymous with increased healthspan.

Overall, systematic comparison of age-related metrics on cell, tissue, and organ level has become a reliable tool in aging research to detect patterns of disease, and determine the state of an individual's health. With the rise of artificial intelligence (AI) and the use of machine learning, analysis of health metrics is expecting a revolution in prediction and diagnosis of age-related diseases (Wilczok 2025; Li et al. 2026). There are currently a variety of methods that are being explored in the pursuit of increased healthspan, ranging from nutrient supplementation, re-purposing of drugs, specific diets and exercise regimes, to alterations of the microbiome (Wilmanski et al. 2021; Harrison et al. 2009). While long-term effects of either of these methods remain to be shown, the most reliable path to a healthy life appears to be a well balanced diet, measured exercise, and sufficient amount of sleep. Additionally, a key driver appears to be the amount of stress that is endured throughout life, may it be physical or psychological (Cohen et al. 2012).

1.1.2 Reduced resilience as a driver of aging

In the context of aging, resilience is defined as the fundamental homeostatic plasticity required to orchestrate a precise, "on-demand" protective response to acute challenges, allowing an organism to recover from systemic disturbances and return to its pre-stress state (Ukraintseva, Yashin, and Arbeev 2016). While the exact definition of resilience in this context is still debated, the consensus is that resilience is defined as the ability to return to an original state following deviation from this steady state (Whitson et al. 2016; Ukraintseva, Yashin, and Arbeev 2016). As a major contributing factor determining organismal resilience, protein homeostasis,

or proteostasis, is the complex interplay of molecular pathways that ensures proteins are correctly folded, trafficked, and degraded (Hoppe and Cohen 2020; Höhfeld et al. 2021). In line with the aging hallmarks, the aging process is fundamentally characterized by a progressive decline in the organism's ability to maintain proteostasis in the face of internal and external challenges (Labbadia and Morimoto 2014; López-Otín et al. 2013). At the heart of this decline is a sophisticated cellular signaling network designed to sense proteotoxic, metabolic, or oxidative imbalances and orchestrate a corrective physiological shift, commonly described as the proteostasis network (PN) (Labbadia and Morimoto 2014; Jayaraj, Hipp, and Hartl 2020). Key processes supporting efficiency of the PN are chaperone-mediated folding, the ubiquitin-proteasome system (UPS), and the autophagy-lysosome pathway. They function in parallel to lift proteostatic burdens, and are shown to have reduced efficiency in aging (Hipp, Kasturi, and Hartl 2019). This decline creates a permissive environment for the transition from resolvable protein damage to overt disease.

In this study we understand resilience to entail three stages in overcoming homeostatic challenges. In the initial stage the organism reacts to the deviation from the homeostatic state and drives a machinery of pathways affecting protein interaction, organelle dynamics, and the rapid expression of response genes to resolve immediate damage. The capacity of these response mechanisms rely heavily on the maintenance of the folding, trafficking, and clearance of proteins, and robust mitochondrial function to ensure that cellular faults can be resolved effectively. Following this first line of response, the organism experiences a phase of adaptation to adjust to the new environmental conditions, and endure the stress as long as possible. Once stress subsides, the system will attempt to restore pre-stress conditions, returning to homeostasis in the stage of stress recovery.

The decline of resilience is described as a key manifestation of aging (Ukraintseva et al. 2021; Fulop et al. 2010), and enables the progression of age-related diseases (Labbadia and Morimoto 2014). As an organism ages, its ability to effectively respond to acute stress, such as proteotoxic or mitochondrial insults, becomes compromised, and a loss of the balance between sustained damage and repair results in a progressive decline of resilience in aging (Haigis and Yankner 2010; Ukraintseva et al. 2021). By viewing health through the lens of resilience, we recognize that vulnerability to neurodegenerative pathologies is not merely a product of genetic defects but a consequence of the organism losing its ability to resolve underlying cellular stress through a decline in resilience. This progressive decline in resilience acts as a primary driver of aging according to the loss of proteostasis (López-Otín et al. 2023), turning once-manageable environmental or metabolic challenges into triggers for chronic frailty and systemic decline. Targeting the loss of integrity of the proteome and mitochondrial network as hallmark of aging, some interventions now focus on a "help-it-help-itself" approach, aiming to boost stress response signaling to restore youthful resilience (Sidrauski et al. 2015; Zhu et al. 2026). In this approach, increased lifespan is a secondary benefit of enhancing this internal capacity, as modern research is shifting from simple longevity toward maximizing an organism's workload capacity and homeostatic plasticity. Ultimately, addressing this loss of resilience allows the fine-tuning of physiological responses, effectively closing the gap between rising life expectancy and the onset of frailty.

Quantifying the decline of homeostatic capacity in age and disease

The decline of homeostatic capacity marks a transition into a state of "frailty", also characterised as a "non-specific state of vulnerability, which reflects multi-system physiological change" (Fulop et al. 2010). This state is not an abrupt failure but a gradual erosion caused by a chronic stress stimulus which builds

up a burden on the homeostatic system, and ultimately exhausts molecular chaperones and quality control pathways (Morimoto 2008). This exhaustion is typically the result of a chronically accumulated burden, which can be driven by genetic defects, persistent low-grade inflammation, or extreme environmental conditions (Hipp, Park, and Hartl 2014). The consequence is a profound reduction in the plasticity of stress responses, and a hypersensitivity to perturbation. In this state of homeostatic frailty, the system's capacity to buffer changes is severely diminished. The threshold of failure, referred to as resilience threshold, represents the level of stress the organism can absorb without suffering permanent damage (Fig. 1). It is significantly reduced in age and disease, and resulting from this reduction in buffer capacity the rapid, "on-demand" expression of protective elements, such as stress-responsive chaperones, becomes blunted and leads to homeostatic frailty.

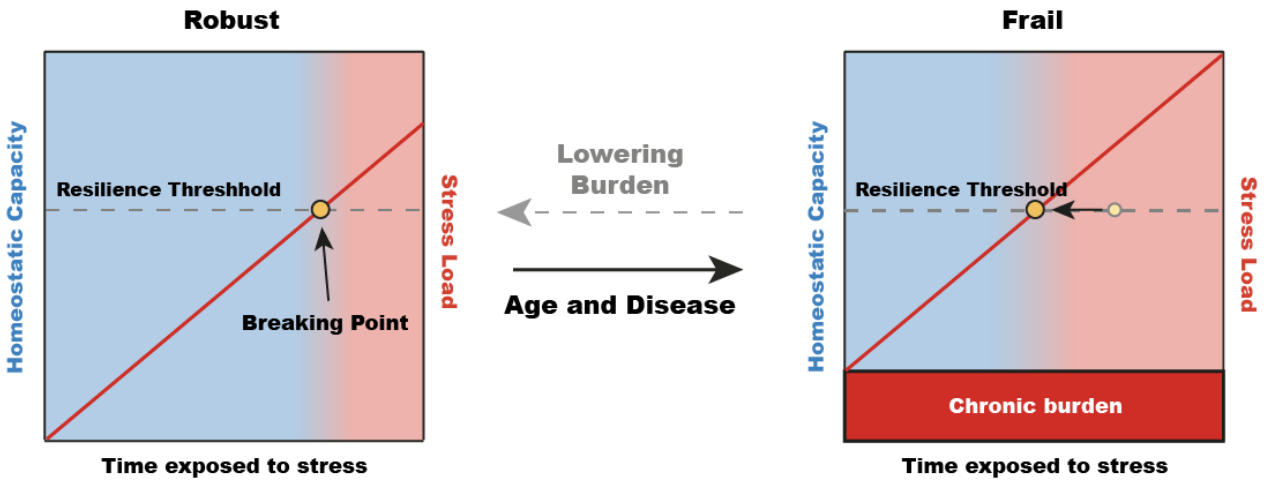

Figure 1: ***Homeostatic Capacity in Age and Disease.*** *During constant exposure to stress, the stress accumulates over time building an increasing burden on the system. If the stress load reaches a level exceeding the resilience threshold, the system takes damage from which it will not be able to recover, representing the breaking point. The capacity to buffer stress is determined by the availability of resources which is reduced in aging and disease by a chronic burden or reduced energy availability, reaching this point after a shorter time of exposure.*

We hypothesise that as an organism experiences a chronic homeostatic burden, the threshold for the additional, acute stress it can endure is reduced, because respective stress response mechanisms are occupied. Exposure to additional perturbation will therefore reach this threshold earlier, as the buffering capacity is no longer sufficient to absorb and resolve the acute stress. When the cumulative stress surpasses the breaking point, the organism can no longer resolve damage induced by the stress, resulting in permanent dysfunction and irreversible damage. This accelerates the trajectory of age-related disease and mortality. In this frail state, the breaking point is shifted so that a shorter exposure time or a lower concentration of a stress which a young, resilient organism would easily overcome, is now sufficient to induce systemic collapse, ultimately reducing overall health and longevity. The cumulative impact of age-related molecular damage, inherited genetic predispositions, and acute or chronic environmental perturbation constitutes a relentless burden on the organism. This continuous pressure is what drives the system from a state of resilience towards frailty (Kirkwood 2005; Kennedy et al. 2014).

1.1.3 Age-related diseases with reduced proteostatic capacity

A collapse in PN capacity leads to the accumulation of misfolded proteins and aggregates, which serve as the primary drivers for several age-related pathologies, including AD, and PD (Hipp, Park, and Hartl 2014; Santra, Dill, and Graff 2019). In neurodegenerative contexts like AD, the pathology is fundamentally a "protein-folding disease" where the deficit lies in the failure to clear amyloid-beta ($A\beta$) plaques and hyperphosphorylated tau. Age-related impairment of the autophagy pathway prevents the clearance of these toxic oligomers, chronically exhausting the Unfolded Protein Response (UPR) and leading to persistent translational repression that manifests as cognitive decline and memory loss (Hipp, Kasturi, and Hartl 2019). Similarly, in PD, the accumulation of α-synuclein into Lewy bodies is compounded by failures in mitophagy, the selective autophagy of mitochondria. When the PINK1/Parkin pathway declines with age, damaged mitochondria are not removed, resulting in oxidative stress and proteostatic collapse within dopaminergic neurons, leading to the characteristic muscle rigidity and tremors (Narendra and Youle 2011).

Beyond the brain, this proteostatic failure is a critical driver of metabolic dysfunction. Type 2 Diabetes (T2D) is increasingly viewed as a proteostatic disease of the pancreatic β-cells (Arunagiri et al. 2019; Back and Kaufman 2012). As insulin demand rises, the accumulation of Islet Amyloid Polypeptide (IAPP) triggers chronic ER stress (Laybutt et al. 2007). In these states, stress response mechanisms shift from an adaptive repair mechanism to a pro-apoptotic signal, resulting in a permanent loss of β-cell mass (Back and Kaufman 2012). A critical insight from recent research is the convergent nature of these pathologies, as the same chaperones that are overloaded in AD are also sequestered in Diabetes (Klaips, Jayaraj, and Hartl 2018). This suggests that proteotoxicity is a systemic driver of aging, where tissue-specific symptoms are simply manifestations of which cell type is most vulnerable to the specific protein burden. Consequently, developing therapies that restore proteostasis globally, rather than targeting individual aggregates, represents a promising strategy to bolster an organism's capacity to resolve chronic cellular stress.

1.1.4 Duchenne Muscular Dystrophy

While many age-related diseases only become apparent at later stages of life, there are progressive diseases that affect patients from the very onset. Duchenne Muscular Dystrophy (DMD) represents a unique intersection between early-onset genetic pathology and the accelerated manifestation of mechanisms typically associated with systemic aging. It is a progressive X-linked neuromuscular disorder characterized by severe muscle-wasting, caused by mutations in the structural muscle protein dystrophin (Falzarano et al. 2015). As it is inherited through the X-chromosome, it appears more severe in males, being present in approximately 1 out of 3.600 to 6.000 live male births (Deconinck and Dan 2007; Falzarano et al. 2015). DMD can be viewed as an accelerated muscle frailty disease, or "myopathy", that shows aspects of the progressive loss of muscle mass and function seen in sarcopenia, the age-related decline of skeletal muscle (Merlini, Bonaldo, and Marzetti 2015). While sarcopenia is the natural, age-related loss of muscle mass, and DMD is a genetic disease caused by the lack of dystrophin, both conditions suffer from nearly identical cellular, metabolic, and structural breakdown pathways in the muscles (Merlini, Bonaldo, and Marzetti 2015; Yuan and Larsson 2023). However, where sarcopenia is driven by a gradual attrition of regenerative capacity over decades, DMD presents a rapid collapse of muscle integrity due to the absence of the scaffolding domain of the structural protein dystrophin. Resulting from these structural defects, muscle fibers are constantly damaged and repaired and experience a mechanical stress (Höhfeld et al. 2021), eventually overwhelming the cellular machinery responsible for protein folding and quality control (Duan et al. 2021).

There is currently no cure for DMD, while commonly prescribed drugs such as the corticosteroid prednisone have been shown to slow the disease progression (Matthews et al. 2016). Additionally, antioxidants and metabolic modulators like Idebenone have been investigated for their potential to improve respiratory and muscular function by targeting deficits in DMD (Buyse et al. 2013; McDonald et al. 2016). The most promising trends in the development of a treatment are found in gene therapy, with drugs in clinical trials aiming to restore the production of functional protein by gene therapy like exon-skipping (Verhaart and Aartsma-Rus 2019; Duan et al. 2021). In January 2026, Sarepta reported that patients treated with the AAV vector-based gene therapy Elevidys showed a 70% reduction in functional decline over three years compared to external controls. However, while this drug has been approved for use in patients, long-term studies will have to show how efficient this treatment is, as concerns have been raised about the presence of adverse effects (Crudele 2025). Additionally, introduction of a microdystrophin has shown promise in SGT-003 gene therapy in early DMD trials (Flanigan et al. 2025). Importantly, this comes from an early stage trial, and long-term effects need to be considered among observations of high efficacy and improvement of biomarkers of muscle integrity. Thus, while gene therapy remains a promising avenue in treating DMD, it is far from clear that it will be a stand-alone treatment. Therefore research and development explores alternative means to treat DMD.

As a model for myopathy and the resulting frailty phenotype, there has been extensive research in mice using the mdx mouse model, which is representative of mammalian mutations in the dystrophin gene found in humans (Bulfield et al. 1984). Studies in mdx mice and human DMD biopsies have demonstrated a significant effect on mitochondria, describing them as dysfunctional and fragmented in DMD (Kelly-Worden and Thomas 2014). This mitochondrial pathology correlates with increased mitochondrial calcium levels, establishing mitochondrial frailty as a driver of DMD progression (Dubinin et al. 2020).

1.1.5 Restoring cell health by rejuvenation and reprogramming

For the past decades, researchers have attempted to uncover what determines the "age" of a cell, and how a youthful cellular state can be defined. A fundamental milestone in modern aging research was set by the discovery of cellular reprogramming using four transcription factors, also known as the "Yamanaka factors" (Takahashi and Yamanaka 2006). Here, induction of Oct4, Sox2, Klf4, and c-Myc was sufficient to transform differentiated somatic cells into pluripotent stem-cells (Takahashi et al. 2007). This discovery transformed the understanding of cell differentiation being a one-way process, and serves as a pioneer paper to establish related approaches as a strategy for restoring resilience in aging and disease.

While full reprogramming de-differentiates cells back into a pluripotent, stem-cell-like state, a more targeted approach known as partial reprogramming allows cells to regain a respectively youthful functional identity without losing their specialized roles. Leveraging this method, partial cellular reprogramming to "rejuvenate" compromised tissues has been applied to restore cellular and tissue function Chondronasiou et al. 2022. In this application, using a timely restricted, pulsed expression of the four factors is used not to reverse the cell to a pluripotent state, but to revert its cellular properties to a more stem-cell-like state, constituting a "rejuvenated" cell. This approach is shown to affect the epigenetic landscape, to correct the DNA methylation patterns that change throughout life. By resetting these epigenetic markers, researchers have restored a epigenetically more youthful state (Lu et al. 2020).

This restoration of functional identity provides a path to reinforce the system's homeostatic buffer, epigenetically rejuvenating the cell, and potentially restoring function of a cell or tissue. However, the use of this method has also been heavily discussed, as a consistent expression of the four factors can lead to cells showing cancer-like behavior. To turn this into a targeted medicine, these negative and unwanted effects need to be understood to precisely orchestrate the use of the Yamanaka factors. Therefore, current research is aiming to understand the underlying mechanism of cellular rejuvenation using reprogramming, to refine the process and advance our understanding of the mechanisms driving benefits in the "black box" which is OSKM reprogramming.

1.2 The nematode *C. elegans* in aging research

The use of the nematode *C. elegans* as a model organism has evolved from its origin in developmental biology to becoming a cornerstone of aging and stress research. Since Sydney Brenner's seminal work in the 1960s established its use in developmental biology (Brenner 1974), the worm has offered unmatched transparency, both physically and genetically, for investigating how complex life processes decline over time. Because *C. elegans* has a highly tractable genome and a short lifespan of approximately 3 weeks, *C. elegans* enabled high-throughput genetic screenings to identify variants that confer stress resistance phenotypes or are overall drivers of increased health (Jorgensen and Mango 2002). One of the most powerful tools in the *C. elegans* toolkit is the use of fluorescent transcriptional reporters (Hutter 2006). These transgenic constructs are coupled to the promoters of well-established stress marker genes, acting as a direct readout into the cell's internal response, to monitor the organism's response to treatments and environmental changes.

Following the discovery of the IIS pathway as a primary regulator of lifespan (Kenyon et al. 1993), mutations in genes like the insulin/IGF-1 (insulin-like growth factor 1) receptor *daf-2* were shown to not only double the worm's lifespan but also drastically improve its resilience to environmental insults (Lithgow et al. 1995; Kenyon et al. 1993). Beyond aging and resilience research, *C. elegans* has emerged as a premier model for systems neuroscience and metabolic profiling due to its fully mapped connectome and highly conserved genetic architecture (Roussos et al. 2023; Salzer and Witting 2021). Researchers utilize the nematode's 302 precisely defined neurons to investigate the molecular basis of complex behaviors, such as associative learning and memory, which serve as foundational analogs for human neurobiology (Roussos et al. 2023). By over-expressing human disease-associated genes in these specific neurons, the worm provides a high-throughput platform for modeling neurodegenerative conditions in real-time. Furthermore, advanced mass spectrometry has enabled the detailed mapping of the *C. elegans* metabolome, identifying critical biomarkers that link metabolic health to lifespan (Salzer and Witting 2021). This combination of structural simplicity, mapped neuronal circuit, and metabolic complexity allows for rapid, whole-organism drug discovery and the validation of disease interventions.

1.2.1 Investigating resilience in *C. elegans*

Since the discovery of programmed modulation of lifespan the investigation of biological resilience in *C. elegans* has transitioned from observing simple survival to mapping the sophisticated molecular "switches" that dictate an organism's homeostatic plasticity. It has been studied to explain fundamental mechanism comprising the PN (Hoppe and Cohen 2020), and has shown the systematic coordination of not just cellular mechanisms but cross-tissue interaction (Charmpilas, Li, and Hoppe 2025). A landmark discovery in this field revealed that proteostatic capacity is not lost randomly but is part of a programmed developmental shift (Labbadia and Morimoto 2015). The capacity to respond to heat stress mediated by the Heat Shock Response (HSR) undergoes a sharp repression upon the onset of reproductive maturity, significantly limiting thermal stress recovery in post-reproductive life (Labbadia and Morimoto 2015). Furthermore, this decline can be alleviated and resilience artificially preserved through modulation of germline signaling. Altering expression levels of genes such as *glp-1* and the histone demethylase *jmjd-3.1* facilitates epigenetic remodeling by shifts in histone acetylation, and support the maintenance of heat tolerance and proteome stability long after the typical developmental decline (Arantes-Oliveira et al. 2002; Labbadia and Morimoto 2015). Ultimately this has also been shown to be linked to the insulin/IGF-1 pathway, highlighting the interaction of these resilience pathways, and implementing the use of *daf-2* mutants as the "gold-standard" for improved resilience (Hsin

and Kenyon 1999; Arantes-Oliveira et al. 2002).

Beyond traditional heat shock factors and IGF-signaling, recent research has highlighted the Integrated Stress Response (ISR) as a critical determinant of resilience, balancing the immediate need for protein synthesis inhibition with the long-term requirement for cellular repair (Derisbourg et al. 2021). Modulation of stress response pathways has potential therapeutic implications beyond simple survival, as the induction of thermal stress responses has been demonstrated to alleviate tau toxicity, suggesting that the mechanisms governing heat resilience can be leveraged to combat neurodegenerative protein aggregation (Stanley et al. 2024). A critical area of investigation involves the intrinsic trade-offs and distinctions between lifespan and acute stress resistance, as organisms frequently prioritize survival mechanisms over long-term longevity under perturbation (Dues et al. 2019).

As one of the most robust methods to enhance resilience, studies have focused on the impact of Dietary Restriction (DR) (Houthoofd et al. 2003). As discussed, the impact of nutrition governed by caloric intake, feeding frequency, and food quality is wide-reaching and affects energy metabolism, overall health, and performance. While DR is often associated with simple caloric reduction, it is increasingly viewed as a tool for optimizing resource management and energy availability in *C. elegans* (Hansen et al. 2008; Mair et al. 2009). Under DR, the organism avoids the metabolic challenges caused by excessive nutrient intake, which otherwise prohibits improvements in workload capacity by exceeding the system's maximum processing limit at any given time. By maintaining the organism at this metabolic optimum, DR enables a sustained state of high-alert proteostasis and mitochondrial efficiency, effectively extending the period during which the animal can autonomously resolve acute homeostatic insults. Strikingly, DR has been shown to improve resilience in proteotoxicity (Steinkraus et al. 2008), making it a robust method to improve resilience in *C. elegans*.

1.2.2 Methods to assess physiology and resilience in *C. elegans*

Adding to the advantages of using *C. elegans* in research related to aging and health is the simple assessment of fitness and survival using physiological assays. In *C. elegans*, fitness and physiological performance are determined by the dynamic interplay between genetic programming, energy metabolism, functional integrity of the tissues like the muscle, and the impact of environmental factors that affect homeostasis. While measuring lifespan remains a foundational metric, it is increasingly recognized that longevity does not always correlate with healthspan, as increased lifespan is not equivalent with the extension of fitness and active life (Bansal et al. 2015). Therefore, the assessment of an organism's performance requires a multidimensional approach that moves beyond simple mortality curves to evaluate the "functional integrity" of the animal across its short but invariant life cycle.

To capture the nuances of physiological decline, researchers employ several metrics that quantify the "quality" of life. Investigating pharyngeal pumping, animals are assessed for the contraction rate of the pharynx, which declines as worms age. It therefore serves as a proxy for muscular and neural integrity, which is often used to assess metabolic fitness and the onset of frailty (Cho et al. 2025). As one of the most used readouts, locomotion can be assessed in various contexts to assess fitness, where measuring body bend rates, crawling speed, or distance travelled in a set time allows researchers to quantify the age-related degradation of body-wall muscle or acute effects of stress treatments (Brenner 1974; Liu et al. 2013). Adding to the analysis of basic functions of fitness, another readout for health has been identified in the assessment of reproductive fitness, or fecundity. The total brood size and the timing of egg-laying are critical indicators of

resource allocation. Genetic manipulations that extend life often result in a "trade-off" where reproductive output is reduced or delayed (Hughes et al. 2007).

Over the past decade, automated systems to assess motility, strength, and even response to compounds has been a major frontier in *C. elegans* research (Zavagno et al. 2024; Chaudhuri, Parihar, and Pires-daSilva 2011; Rahman et al. 2020). Utilizing automated tracking to measure motility in liquid or crawling speed allows researchers to quantify the age-related degradation of body-wall muscle activity, or assess behaviour in regards to movement patterns and location in respect to their food (Zavagno et al. 2024). Using these systems, researchers have assessed locomotion in AD models, and established a screening platform suited for commercial assessment of behaviour upon treatment with compounds (Vivek-Ananth et al. 2025). In the future, this field will be heavily impacted by the advancements of automated behaviour analysis by AI (Xu et al. 2026), which will make analysis of movement and behaviour even more accessible, and comparable across experimental settings.

In the context of resilience, *C. elegans* has been used in various contexts, assessing the behaviour upon treatment with compounds or exposure to chemical, mechanical, or environmental cues (Romussi et al. 2024; Yasuda et al. 2021; Bargmann, Hartwieg, and Horvitz 1993). Often, assays measure the ability to recover from any of these systemic disturbances, which is fundamentally determined by their homeostatic capacity to respond to the respective challenge. Beyond mere survival, these assays evaluate the induction kinetics of protective pathways under stress, utilising tools for the analysis of underlying molecular changes. Complementary to assays that measure the tolerance to a stress in assessment of endurance of organismal stress are recovery assays. These are usually performed at a moderate stress and include a period of recovery under non-stress conditions to measure the return to pre-stress homeostasis, covering a key aspect of resilience in stress recovery. A popular assay in this category is measuring thermorecovery, where populations of animals are exposed to heat stress for a short period, and recovery of this stress is scored 24 hours later (Labbadia and Morimoto 2015). By assessing entire populations of isogenic animals, researchers can obtain a highly quantifiable readout of systemic resilience comparing recovery rates between populations. Expanding this considering the convergence of stress responses as a determinant of resilience, experimental setups can be customised to address specific aspects of resilience and interaction of stress response pathways. As an example for complex assessment of resilience, combination of two stresses such as pre-treatment with the pro-oxidant paraquat followed by heat shock, can unmask hidden mitochondrial vulnerabilities that a single stress might fail to trigger (Dilberger et al. 2019). Complementing physical aspects, the use of fluorescent reporter strains which express GFP under stress-specific promoters provide a real-time, non-invasive window into the animal's molecular response, facilitating sophisticated epistasis analysis (Link et al. 1999; Calfon et al. 2002). In this context, changes in fluorescent signal intensity allow researchers to determine whether specific genetic mutations or interventions have successfully bolstered or critically compromised the organism's primary stress-signaling architecture.

1.2.3 *C. elegans* transgenesis and modulation of gene expression

To analyse the underlying molecular processes determining resilience and stress survival, a range of tools to manipulate gene expression or monitor stress response pathways have been developed in *C. elegans*. The genetic tractability of *C. elegans* hereby offers a diverse toolkit that ranges from transient gene silencing to precise, permanent genomic editing. These methods allow researchers to interrogate gene function with unparalleled speed and scale, enabling the assessment of the systemic knockdown of entire pathways to the

insertion of fluorescent tags at specific loci (Hobert and Loria 2016; Miller et al. 1999).

The era of extensive genetic manipulation of *C. elegans* took off with the establishment of gonadal microinjection, a technique standardized by Mello et al. 1991 that allows the injection of DNA directly into the distal gonad arms of adult nematodes. The injected DNA would then form heritable, multi-copy extrachromosomal arrays, which are inherited upon random integration into the genome facilitated by causing DNA damage. While these arrays provide high expression levels, their inherent variability and susceptibility to germline silencing led to the development of Mos1-mediated Single Copy Insertion (MosSCI) (Frøkjær-Jensen et al. 2008), providing a method to precisely insert single-copy transgenes into genomic locations for more predictable results. This push for precision was revolutionised by the discovery of CRISPR-Cas9, which was pioneered in the nematode by Dickinson et al. 2013 and Friedland et al. 2013, and enabled seamless endogenous tagging and surgical genome editing. Since then, the field has expanded to include high-throughput CRISPR guide feeding via bacteria to achieve activation of gene expression facilitated by CRISPR activation (CRISPRa), which utilises the targeting mechanism of CRISPR-Cas9, in combination with a transcriptional activator domain (Fischer et al. 2022; Luo et al. 2022). This complements conventional tools for modulation of gene expression, based on the discovery of RNA interference (RNAi) by (Fire et al. 1998) which introduced a transformative method for gene silencing. This eventually scaled into whole-genome feeding libraries developed by that allow for the systematic knockdown of nearly every gene encoded in the nematode genome (Kamath et al. 2000; Kamath et al. 2003), which remains to be the "gold-standard" in knockdown studies.
As a recent advancement in *C. elegans* transgenesis, fluorescent landmark interference (FLInt) has been developed to increase efficiency and improve identification of successfully edited animals (Malaiwong, Porta-de-la-Riva, and Krieg 2023). This method uses CRISPR/Cas9 to facilitate the integration of designed inserts into "safe harbour" landing sites on a set of almost 300 loci over all 6 chromosomes of *C. elegans*. These loci encode a fluorescent marker, which loses its signal upon successful restriction by Cas9, and enables a fast selection process of potentially edited animals. While this method is still being optimised (Malaiwong et al. 2026), it provides a valid alternative to mosSCI, and promises fast turnaround of genetic editing in the future.

Overall, there are a variety of methods to tune gene expression in *C. elegans*. These tools add real power to the use of the nematode in epistasis analysis and genetic screening (Kamath et al. 2000; Jorgensen and Mango 2002). As an example, by combining a permanent fluorescent reporter with a systemic knockdown mediated by RNAi, researchers can rapidly map signaling hierarchies. This scalability makes *C. elegans* the premier model for identifying "resilience genes" that can be targeted to support cellular health during aging or disease.

1.2.4 Duchenne Muscular Dystrophy in *C. elegans*

C. elegans has emerged as a powerful platform for modeling physiological frailty and neuromuscular decay. In this capacity, it has emerged as a great tool for studying muscle frailty as a model for DMD, assessing physiology and relevant molecular processes in mutants of *dys-1*, the ortholog of the human dystrophin gene (Hewitt et al. 2018; Higashitani et al. 2023). This mutant has been shown to be a great model recapitulating key aspects of the disease, with the worm's simplified muscular structure providing a clear platform to monitor DMD phenotypes and enabling the rapid identification of genetic modifiers and potential drug candidates (Ellwood, Piasecki, and Szewczyk 2021).

The effects of the *dys-1* mutation manifest in clear phenotypes representing physical frailty, as described in mammalian DMD models (Gaud et al. 2004). *C. elegans dys-1* consists of similar domains found in the human

protein, with a C-terminal actin-binding domain followed by spectrin repeats, which can also bind actin, and a more complex N-terminal region with various domains interacting with proteins in the sarcolemma (Ellwood, Piasecki, and Szewczyk 2021). This N-terminal domains serve important scaffolding functions, and support sarcolemma stability and interactions. There are two mutant strains that are commonly used in *C. elegans*, *dys-1(eg33)* and *dys-1(cx18)*, which are both nonsense mutations leading to a premature stop, consequently expressing a truncated version of the dystrophin protein (Ellwood, Piasecki, and Szewczyk 2021). They have been compared on physiological and molecular level, including transcriptomic analysis of mutants to identify distinct signatures in pre- and post-symptomatic stages, providing a molecular map of how muscle-specific decay initiates (Hrach et al. 2020). Central to the pathology in *C. elegans* is a chronic shift in cellular calcium levels, the disruption of mitochondrial calcium regulation, and increased mitochondrial fragmentation (Sudevan et al. 2019). Elevated cytosolic Ca^{2+} levels and increased calcium uptake into mitochondria are defining features of DMD progression in *C. elegans* (Zhan et al. 2014; Higashitani et al. 2023). This calcium overload is intrinsically linked to mitochondrial dysfunction via the UPR^{mito}, mediated by regulators such as CLPP-1, serving as a critical cellular checkpoint in maintaining organelle proteostasis during these pathological shifts (Haynes et al. 2007). While these features are well-studied in the context of both aging and DMD, the direct impact of these perturbations on acute stress resistance and the ability of the organism to recover from environmental shifts remains poorly understood.

Research utilizing *C. elegans* DMD models has successfully identified a variety of pharmacological and genetic interventions that mitigate muscle-wasting phenotypes. Firstly, conventional treatments using Prednisone and Melatonin have been shown to partially restore muscle function, highlighting the role of antioxidant pathways in stabilizing the sarcolemma, and supporting prevention of muscle function decline (Gaud et al. 2004; Hewitt et al. 2018). Metabolic supplementation with sulfur amino acid and hydrogen sulfide have demonstrated efficacy in rescuing DMD-related muscle phenotypes (Ellwood et al. 2022; Ellwood et al. 2021). Similarly, Mitochonic Acid 5 (MA-5) has been identified as a promising candidate for rescuing mitochondrial health in *dys-1(eg33)* mutant backgrounds (Wu et al. 2022). Addressing the wider context of progressive muscle decline in age, discoveries in *C. elegans* DMD can also inform age-related sarcopenia, as key phenotypes are shared across genetic and age-related muscle frailty (Merlini, Bonaldo, and Marzetti 2015).

1.3 Mechanisms of homeostasis

1.3.1 Stress responses in aging and disease

The decline of efficient function of mechanisms constituting the PN is a main driver of the loss of proteostasis in age and disease (Labbadia and Morimoto 2014; Jayaraj, Hipp, and Hartl 2020). The PN is comprised of a set of defined molecular pathways activated in response to stress, with main response mechanisms related to resilience being the heat shock response (HSR), the unfolded protein response (UPR) at the endoplasmic reticulum (ER) and mitochondria, and the integrated stress response (ISR) (Walter and Ron 2011; López-Otín et al. 2023). In a youthful state, these stress responses are robust and highly plastic, efficiently resolving challenges to cellular homeostasis, before they manifest as systemic pathology in progressive aging. In *C. elegans*, the decline of proteostasis capacity has been described as an early event driving the aging process (Ben-Zvi, Miller, and Morimoto 2009), highlighting the importance of efficient stress response mechanisms in aging.

When cells can no longer resolve the accumulation of misfolded proteins or damaged mitochondria the result is a permissive environment for disease progression. Consequently, dysregulation or reduced efficiency of stress responses results in increased vulnerability to neurodegenerative disorders like PD and AD, and sarcopenia (Stanley et al. 2024; Brown and Naidoo 2012; Ghemrawi and Khair 2020). It is understood not merely as a result, but as a contributing factor to age-related diseases. By identifying the causal drivers of this decline in stress response capacity, we seek to shift the medical paradigm from treating symptoms to restoring the organism's innate homeostatic plasticity. Accordingly, targeting the protein homeostasis network and improving stress response capacity has been proposed as a potential target for improvement of disease outcomes and improving health (Balch et al. 2008). While there is evidence of a strong connection between the various mechanisms in response to stress stimuli, there are distinct mechanisms to resolve stress in the cytosol, the ER, and mitochondria, which is why these three response pathways have frequently been assessed individually.

1.3.2 The HSF-1 dependent heat shock response

As the primary transcriptional defense mechanism against cytosolic proteotoxic stress, the transcription factor (TF) HSF-1 (Heat Shock Factor 1) drives the cellular response to thermal stress. Under physiological conditions, HSF-1 is maintained in an inactive, monomeric state through associations with molecular chaperones (Labbadia and Morimoto 2014). Upon sensing an accumulation of misfolded or denatured proteins, as induced by heat or oxidative stress, HSF-1 assembles in trimers and translocates to the nucleus. There, it binds to Heat Shock Elements (HSE) on the DNA, enabling transcription and massive up-regulation of heat shock proteins (HSPs) that function as chaperones to refold or degrade damaged proteins, thereby preserving the integrity of the proteome (Jayaraj, Hipp, and Hartl 2020).

The HSR is a highly conserved stress pathway and was shown to be a determinant of longevity in *C. elegans* (Morley and Morimoto 2004). By comparing the molecular HSR in activated and impaired HSF-1 mutants, the transcriptional response to heat stress has been outlined in detail comparing steady-state stress conditions in the nematode (Brunquell et al. 2016; Kyriakou, Taouktsi, and Syntichaki 2022). Adding to the assessment of direct HSF-1 dependent effects, these expression changes have been assessed in extreme temperature

conditions to reveal the HSR as a highly dynamic process (Jovic et al. 2017). Despite this complex analysis, the consequences of heat induced damage are numerous, and it remains challenging to identify causal drivers of heat-induced lethality. However, as one of these mechanisms, heat induced calcium leakage has been described to cause damage in mitochondria in bodywall muscle, directly contributing to physiological failure (Momma et al. 2017).

In addition to the canonical HSR, HSF-1 activity affects a wide range of mechanisms, as HSEs are also found in a range of other genes and even non-coding RNA (Schreiner et al. 2019). Furthermore, HSF-1 has also been shown to have an important function in development, highlighting the versatility and universal involvement of key drivers of homeostasis (Li et al. 2016). Based on its wide reaching effects, modulation of the HSR has previously been proposed as a therapeutic strategy in toxicity related to protein aggregation (Stanley et al. 2024). This has also been explored in *C. elegans*, where transient pulses of non-lethal heat stress primes the organism to show an increased resilience in heat stress, defined in the biological concept of hormesis (Kumsta et al. 2017; Xu et al. 2023).

1.3.3 The Unfolded Protein Response

The endoplasmic reticulum Unfolded Protein Response

The Unfolded Protein Response of the Endoplasmic Reticulum (UPR^{ER}) is a fundamental homeostatic mechanism that maintains proteostasis by coordinating the cellular response to misfolded proteins in the ER (Walter and Ron 2011). It is governed by three transmembrane sensors in the ER membrane, IRE-1, ATF-6, and PERK, which collectively monitor the ER lumen and initiate a signaling cascade to expand folding capacity and reduce protein load upon detection of unfolded proteins (Fig. 2)(Ron and Walter 2007). Another major component are ER chaperones like BiP, in *C. elegans* the orthologs HSP-3 and HSP-4. They are not just among the key effectors up-regulated as a consequence of UPR^{ER} signaling, but are also involved in facilitating UPR^{ER} activation. While the exact mode of action remains contested, BiP/HSP-4 reacts to misfolded proteins in the ER and by dissociation from the transmembrane sensors enables efficient UPR^{ER} induction (Pincus et al. 2010).

A driving branch of this response involves the ribonuclease activity of IRE-1, which catalyzes the unconventional splicing of *xbp-1* mRNA to produce a potent transcription factor that up-regulates an extensive network of molecular chaperones (Calfon et al. 2002; Lee, Iwakoshi, and Glimcher 2003). Furthermore, IRE-1 serves a dual function and is also active in Regulated IRE1-Dependent Decay (RIDD), where it degrades mRNAs to avoid their translocation into the ER before they can add to the burden of the protein-folding machinery (Maurel et al. 2014). Contrasting the mode of action of IRE-1, the transmembrane protein ATF-6 undergoes a unique transformation from sensing ER stress to function as a nuclear transcription factor (Lei et al. 2024). Under non-stress conditions, ATF-6 is sequestered in the ER membrane. When misfolded proteins accumulate, BiP/HSP-4 dissociates from ATF6 to assist in protein folding, and ATF-6 is cleaved by specific proteases for its N-terminal domain to be released into the cytosol and ultimately function as a transcription factor in the nucleus (Lei et al. 2024). The third branch of the UPR^{ER} is orchestrated by the ER kinase PERK. It also facilitates expression of ER chaperones in response to protein misfolding, however, it achieves this through activation of the Integrated Stress Response (ISR) (Ron and Walter 2007).

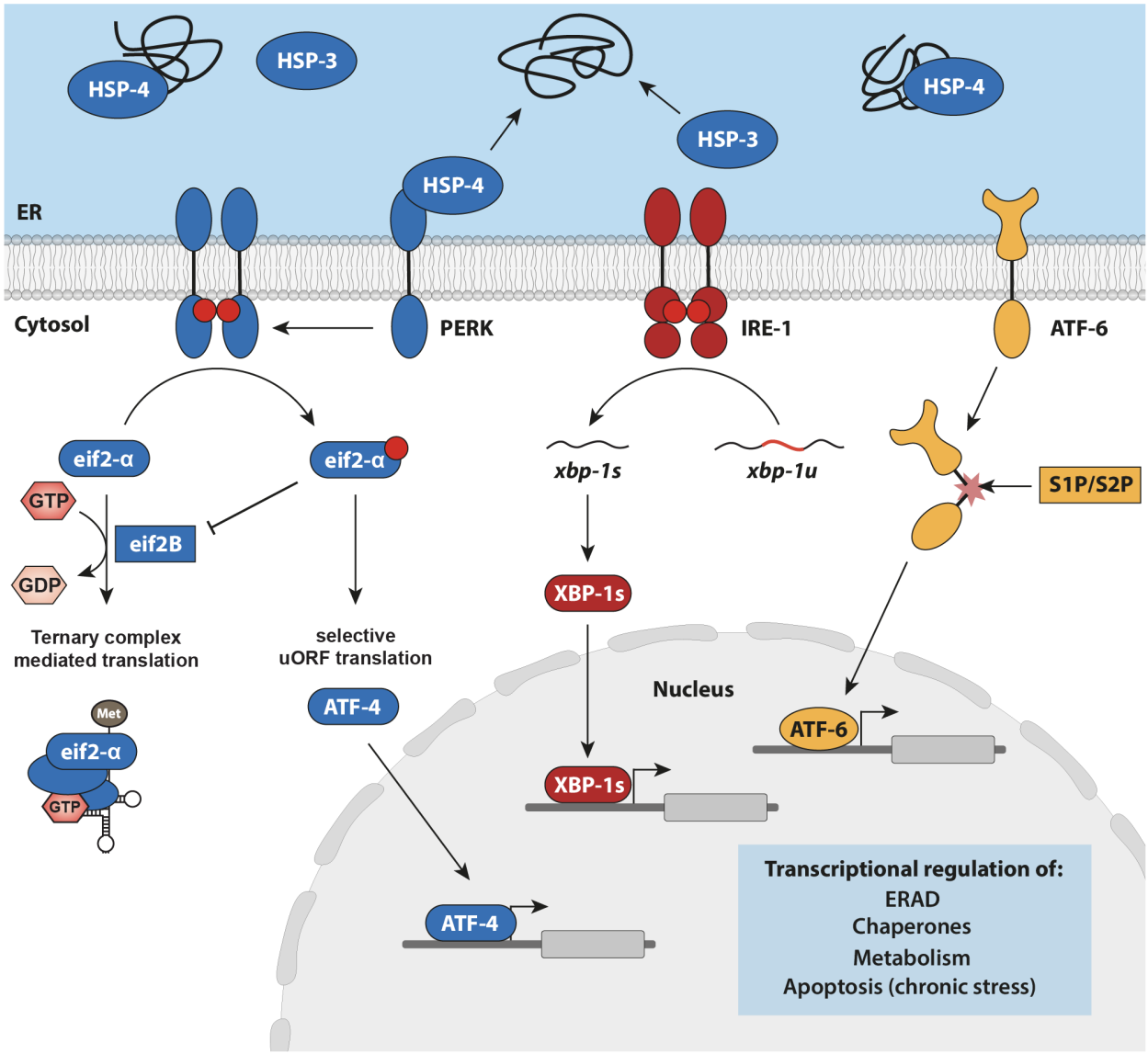

Figure 2: ***The unfolded protein response at the ER.*** *During misfolding of proteins in the ER, the unfolded protein response is induced by release and activation of three distinct UPR kinases, PERK, IRE-1, and ATF-6. PERK dimerises and autophosphorylates, to induce the ISR by phosphorylation of eIF2α. Consequently, global translation mediated by the ternary complex is reduced favouring preferred translation of response genes like ATF-4. The IRE-1 branch induces selective splicing of xbp-1 mRNA, which subsequently acts as a transcription factor in the nucleus. ATF-6 is cleaved by S1P and S2P proteases, and also translocates to the nucleus. All three distinct mechanisms induce the transcription of stress response genes acitve in ER-associated degradation (ERAD), Metabolism, protein folding, or signaling.*

Beyond its role as a response system to acute perturbation, the UPR^{ER} has been defined as a master regulator of long-term homeostatic regulation, determining the resilience of an organism to chronic proteotoxic challenges (Walter and Ron 2011). Loss of UPR capacity erodes cellular resilience and creates a permissive environment for the accumulation of toxic protein aggregates. This loss is shown to be age-related (Taylor and Dillin 2013), and ER stress resolution is a central driver in the pathogenesis of neurodegenerative disorders, including Alzheimer's and Parkinson's diseases, where the failure to resolve underlying protein faults leads to irreversible cellular dysfunction and death.

The Integrated Stress Response

Activated by the PERK branch of the UPR^{ER}, the ISR is a sophisticated signaling network that allows eukaryotic cells to adapt to environmental and internal perturbations by dynamically tuning the rate of protein synthesis (Costa-Mattioli and Walter 2020). While it is intrinsically linked to the ER through PERK, the ISR acts as a central hub that integrates signals from various cellular stresses to determine the metabolic and proteostatic fate of the cell. Initiation of the ISR occurs by phosphorylation of the alpha subunit of the eukaryotic translation initiation factor 2 *eIF2*α, which is performed by four distinct kinases reacting to ER stress (PERK), amino acid starvation (GCN2), heme deficiency and oxidative stress (HRI), or viral infection (PKR) (Wek, Jiang, and Anthony 2006; Pakos-Zebrucka et al. 2016). Phosphorylated *eIF2*α (*eIF2*α-phospho) acts as a potent inhibitor of its own Guanine Nucleotide Exchange Factor (GEF), eIF2B, which facilitates the assembly of the ternary complex (TC) required for initiation of mRNA translation. Reduction of TC results in a global reduction of mRNA translation initiation, which prohibits misfolding of proteins in acute stress conditions and enables the selective translation of mRNAs that carry upstream open reading frames (uORFs) (Derisbourg, Hartman, and Denzel 2021). In mammals, the crucial downstream effector is the transcription factor ATF4, which orchestrates a gene expression program aimed at restoring homeostasis or, if the stress is chronic, inducing apoptosis through CHOP (Pakos-Zebrucka et al. 2016; Costa-Mattioli and Walter 2020). In *C. elegans eIF2*α is phosphorylated by either GCN-2 or the PERK ortholog PEK-1. Here, mutations leading to reduced activation of the ISR are shown to enhance lifespan and survival in various stress contexts (Derisbourg et al. 2021).

The mitochondrial Unfolded Protein Response

Complementary to the UPR^{ER}, the Unfolded Protein Response of mitochondria (UPR^{mito}) is a conserved retrograde signaling pathway that ensures mitochondrial proteostasis by communicating organelle distress to the nuclear genome (Charmpilas, Li, and Hoppe 2025). Mitochondria are particularly vulnerable to proteostatic collapse due to their dual-genome origin, the stoichiometric mismatch between nuclear-encoded and mitochondrial-encoded proteins can lead to an accumulation of misfolded or orphaned subunits within the matrix (Haynes and Ron 2010; Nargund et al. 2015). This imbalance, often triggered by metabolic stress, ROS production, or mtDNA mutations, disrupts the delicate environment required for oxidative phosphorylation (OXPHOS), the metabolic pathway cells use to produce energy in form of adenosine triphosphate (ATP). To prevent irreversible damage, the UPR^{ER} acts as a surveillance mechanism that monitors mitochondrial import efficiency, linking the organelle's functional health directly to the cell's transcriptional output (Shpilka and Haynes 2018).

In *C. elegans* this response is orchestrated by the bZIP transcription factor ATFS-1, which possesses both a mitochondrial targeting sequence (MTS) and a nuclear localization signal (NLS). Under homeostatic conditions, ATFS-1 is efficiently imported into healthy mitochondria and degraded by the LON protease (LONP-1). However, when mitochondrial import is compromised upon mitochondrial dysfunction, ATFS-1 import is compromised and it instead translocates to the nucleus (Nargund et al. 2012). This "import-efficiency switch" is supported by the peptide transporter HAF-1 and the ubiquitin-like protein UBL-5, which facilitate the activation of the response in coordination with the complementary DVE-1 transcription factor (Haynes et al. 2010).

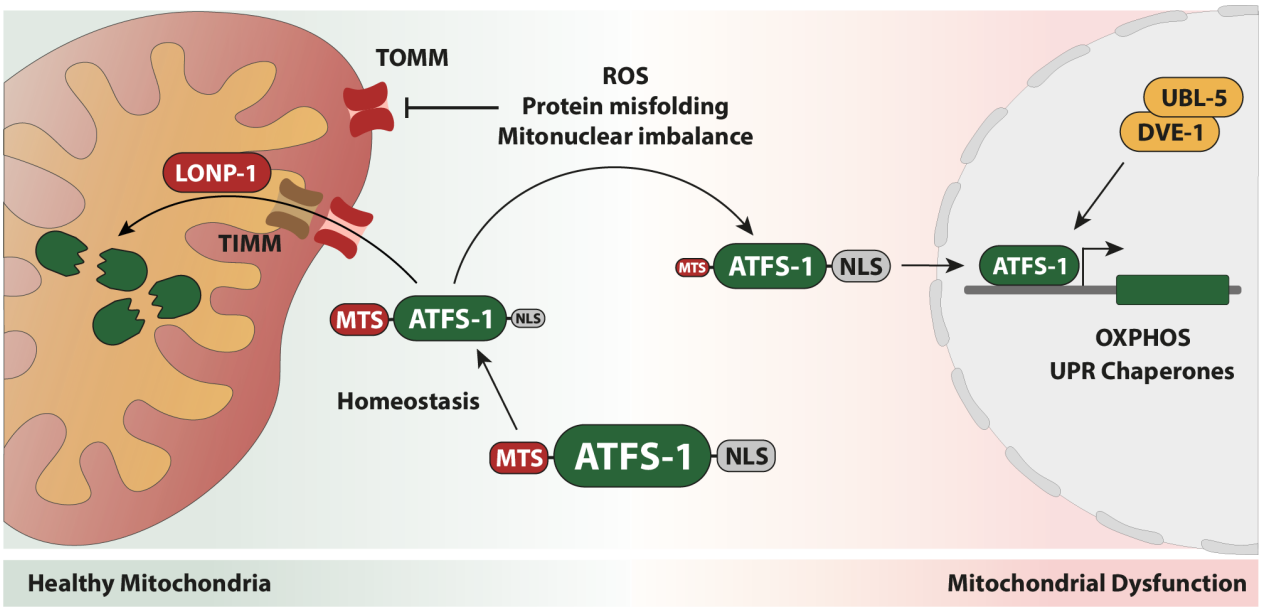

Figure 3: ***The UPR^{mito} in C. elegans.*** *Schematic overview of the ATFS-1 dependent UPR^{mito} in C. elegans. In non-stress conditions, ATFS-1 is translocated to mitochondria facilitated by a mitochondrial targeting signal (MTS), where it is cleaved by the protease LONP-1. Upon stress, translocation via TOMM is prohibited and ATFS-1 is translocated to the nucleus to induce expression of response genes together with the transcription factor DVE-1, and UBL-5.*

Once active in the nucleus, ATFS-1 induces a robust transcriptional program designed to recover mitochondrial function and promote organismal resilience. Downstream effects include the up-regulation of mitochondrial chaperones, such as HSP-6 and HSP-60, and proteases like CLPP-1, which work to refold or clear damaged proteins (Yoneda et al. 2004). Beyond proteostasis, the UPR^{mito} reconfigures cellular metabolism by shifting toward glycolysis and increasing the expression of ROS-detoxifying enzymes and innate immunity genes. In addition to this, ATFS-1 has also been shown to directly regulate expression of OXPHOS components (Nargund et al. 2015), highlighting the broad role in mitochondrial homeostasis and energy metabolism.
Overall, UPR^{mito} activation influences mitochondrial dynamics, typically favoring mitochondrial fission to segregate damaged portions of the network for degradation via autophagy, or shifting the balance toward fusion to maximize ATP production under mild stress (Shpilka and Haynes 2018). Chronic failure of this signaling and the resulting accumulation of misfolded proteins are implicated in the transition from hormetic adaptation to programmed cell death, contributing to the progression of various mitochondrial myopathies (Labbadia et al. 2017).

1.3.4 Mitochondria: Not just the powerhouse of the cell

Energy metabolism in mitochondria

As essential providers of ATP, the functional capacity of mitochondria determines the energetic "ceiling" of a cell and organism, ultimately governing its ability to maintain homeostatic processes, power mechanical work, and survive acute physiological stress. Should this energy production fall short of cellular demands, there will be irreversible consequences for the cell, and subsequently the entire organism (Tsang and Lemire 2003). Chronic burdens or faults in mitochondrial maintenance, such as impaired energy production or

imbalanced dynamics, are consequential effects of aging, and contribute to a depletion of cellular homeostasis capacity, preconditioning the organism for increased frailty during sudden spikes in energy demand (Palikaras, Lionaki, and Tavernarakis 2015).

Mitochondrial health is governed by a delicate balance of fission and fusion, mitochondrial proteostasis, and efficient OXPHOS. Disturbances to these dynamics are hallmarks of various diseases, characterized by "leaky" OXPHOS leading to excessive Reactive Oxygen Species (ROS) production, and calcium imbalances (Pan et al. 2013). The Mitochondrial Calcium Uniporter (MCU-1) plays a crucial role in regulating these levels, and its dysfunction can lead to (Ca^{2+}) overload. Mitochondrial (Ca^{2+}) uptake is tightly regulated and follows precise mechanism which in turn determine the state of this highly selective calcium channel (Petrungaro et al. 2015). In *C. elegans*, calcium imbalance and extracellular matrix (ECM) degradation have been identified as primary drivers of muscle damage and myopathy phenotypes (Sudevan et al. 2019; Baines et al. 2017). Furthermore, persistent mitochondrial dysfunction is a known causal factor in systemic muscle atrophy (Hyatt et al. 2019).

Therapeutic Strategies targeting mitochondrial health has become a key frontier in both clinical and athletic science. Strategies include boosting mitophagy, the selective degradation of damaged mitochondria to maintain a healthy pool of organelles (Campbell and Zuryn 2024). Furthermore, inducing mitohormesis, a concept that mild, non-lethal mitochondrial stress like low-level ROS or transient energy deficits can trigger adaptive responses that bolster overall cellular defense and longevity, appears promising in improving mitochondrial health (Ristow and Schmeisser 2014; Cheng, Liu, and Finkel 2023). In this framework, the transient bursts of mitochondrial ROS act not as toxic byproducts, but as essential signaling molecules that prime antioxidant defenses. Additionally, food supplements like Coenzyme Q10 (CoQ10), PQQ, and NAD+ precursors like Nicotinamide Riboside have been used to support OXPHOS efficiency and mitochondrial biogenesis (Ishii et al. 2004; Yang et al. 2021; Mouchiroud et al. 2013). Next to application in disease, these methods are also being assessed in the context of sports and athletics, as boosting mitochondrial energy levels is vital for peak performance and recovery. Enhancing mitochondrial density and efficiency through targeted training and nutrition allows athletes to sustain higher workloads and delay the onset of metabolic exhaustion. As the field advances, standardized methods for assessing the (UPR^{mito}) and mitochondrial health, ranging from fluorescent reporters to metabolic flux assays, are essential for identifying new therapeutic targets and understanding the nuances of organelle-driven resilience (Haeussler and Conradt 2022).

Mitochondrial dynamics in stress

Mitochondria also serve as an important sensory hub of the cell, integrating environmental cues to orchestrate systemic adaptive responses. Mitochondrial morphology and functionality are dictated by a fine balance between fission and fusion, which coordinate mitochondrial dynamics and determine the efficiency of respiration and biogenesis in a changing cellular environment (Liu et al. 2019; Tondera et al. 2009). When encountering physiological perturbations, the mitochondrial network undergoes rapid structural remodeling. Under conditions of mild metabolic stress or nutrient deprivation, mitochondria often engage in Stress-Induced Mitochondrial Hyperfusion (SIMH) (Tondera et al. 2009). This elongation of the network allows for the sharing of membrane components and matrix enzymes, maximizing the OXPHOS efficiency in challenging conditions and buffering the impact of localized damage. Conversely, severe or chronic stress triggers DRP1-mediated fission, fragmenting the network to isolate dysfunctional organelles. This fragmentation is a crucial prerequisite

for mitophagy, a quality control mechanism that prevents the accumulation of damaged mitochondria and the subsequent release of pro-apoptotic factors (Palikaras, Lionaki, and Tavernarakis 2015).

Beyond structural transitions, stress significantly alters mitochondrial biogenesis and energetic efficiency to meet the cell's shifting requirements. The transcriptional coactivator PGC-1α acts as a master regulator in this context, driving the synthesis of new mitochondria to compensate for increased energy demands (Halling and Pilegaard 2020). However, acute stressors such as extreme temperature or oxidative shifts can lead to the "uncoupling" of the electron transport chain. Although this metabolic uncoupling decreases the efficiency of ATP synthesis relative to oxygen consumption, it functions as a vital defensive strategy to attenuate the formation of superoxide and other Reactive Oxygen Species (ROS). By lowering the mitochondrial membrane potential, this mechanism prevents oxidative "bursts" that would otherwise cause irreversible damage to mitochondrial DNA and structural lipids (Brand 2000).

Calcium metabolism as determinant of mitochondrial health

Calcium serves as a critical secondary messenger that bridges cellular signaling with mitochondrial bioenergetics (Alvarez et al. 2020). Under homeostatic conditions, mitochondria act as vital buffers that sequester transient increases in cytosolic Ca^{2+} through the mitochondrial calcium uniporter (MCU) complex. This uptake is not merely a storage mechanism, but under non-stress conditions regulates controlled increase in mitochondrial Ca^{2+} levels required by dehydrogenases within the tricarboxylic acid (TCA) cycle. This supports efficient management of ATP production and adjusts it to the current metabolic demands of the cell (Cárdenas et al. 2010). Therefore, mitochondrial health is fundamentally connected to the organelle's ability to sense and buffer calcium oscillations, a process that ensures energetic flexibility during physiological transitions.

The maintenance of this sensitive balance is frequently disrupted by structural defects or chronic cellular stress, leading to a state of calcium overload. In models of muscular dystrophy and neurodegeneration, the loss of sarcolemmal integrity or "leaky" sarcoplasmic reticulum (SR) channels results in a persistent influx of Ca^{2+} into the mitochondrial matrix (Sudevan et al. 2019). This chronic imbalance forces the mitochondria to prioritize sequestration over respiration, leading to a dissipation of the membrane potential and a rapid increase in ROS production (Higashitani et al. 2023). The consequences of systematic dysregulation of calcium levels are particularly evident in *C. elegans* models of DMD, where the truncation of dystrophin increases calcium influx at the sarcolemma, ultimately mediating calcium-mediated problems in mitochondria (Zabłocka, Górecki, and Zabłocki 2021; Hughes et al. 2018). The chronic sequestration of excess cytosolic Ca^{2+} by the mitochondria leads to a progressive alteration of the mitochondrial membrane potential and the deleterious activation of calcium-dependent proteases (Joyce et al. 2012). These proteases facilitate the proteolytic degradation of the sarcomere and other structural proteins from within the muscle fiber. This breakdown in mitochondrial calcium homeostasis serves as a molecular hallmark of the transition from adaptive homeostatic maintenance to cellular frailty.

1.4 Aims of this study

The central aim of this study is to identify modulators of disease through the comparison of dynamic gene expression changes during the response to stress. We intend to study gene expression differences between wild type and stress sensitive disease models to uncover changes in stress response expression patterns. The driving hypothesis is that distinct stress response pathways converge to determine the physiological resilience of an organism. This is governed by the capacity of the responsiveness of the combined stress response mechanisms and availability of metabolic resources to react to acute perturbation. Consequently, any chronic burden, whether pathological or age-related, would act as a constant drain that diminishes response capacity to acute stress by adaptive mechanisms. Beyond testing this hypothesis, my objective is to pinpoint the underlying molecular changes that cause a system to be frail and subsequently develop targeted interventions to restore organismal resilience. We argue that comparison of steady-state transcriptomes is not sufficient to uncover the full extent of relevant expression differences, as highly dynamic changes during the response to stress require precise wiring. Understanding how stress responses interact during stress to determine resilience and outlining the role of these mechanisms in frailty might illuminate new ways to improve the ability to overcome homeostatic challenges. Utilising models that are hypersensitive to certain stressors will help identify pivotal points in this wiring of stress responses, and help guide novel treatments that boost overall stress resilience.

In this framework, we define frailty as a state of exhausted homeostatic "buffering" capacity, characterized by a significantly lowered stress-tolerance threshold which ultimately determines reduced resilience (Fig. 1). Informing this concept, we learn from specific genetic modulators of resilience, such as the inhibition of the IIS pathway via *daf-2* mutation, which can increase overall resilience. This suggests that this capacity can be tuned in both directions, highlighting the potential of increasing buffer capacity as a means to improve resilience. However, while *daf-2* mutants exhibit remarkable lifespan extension and health benefits, we hypothesize that such resilience is accompanied by trade-off effects necessitated by the convergence of stress-response pathways on a limited resource pool. This is supported by the documented reductions in fecundity and locomotion phenotypes in long-lived IIS mutants, suggesting that the expansion of the stress-tolerance threshold in one domain incurs a mandatory physiological cost in others (Bansal et al. 2015).

Scientific Questions

Question 1: Are *C. elegans* disease models hypersensitive to stress? We aim to investigate disease models for increased sensitivity to stress. We intend to quantify physiological frailty, and ultimately uncover the driving mechanisms required to endure, resolve, and ultimately recover from stress.

Question 2: Can we identify molecular differences in hypersensitive *C. elegans* stress responses? We aim to outline molecular changes in stress responses in stress hypersensitivity and intend to uncover differences in stress response mechanisms by outlining gene expression changes in dynamic stress induction.

Question 3: Can we devise novel ways to improve *C. elegans* resilience? We will employ genetic and pharmacological treatments to find ways of boosting stress recovery. We will use diverse treatments and interventions to help guide strategies with the aim to improve the organisms ability to buffer stress.

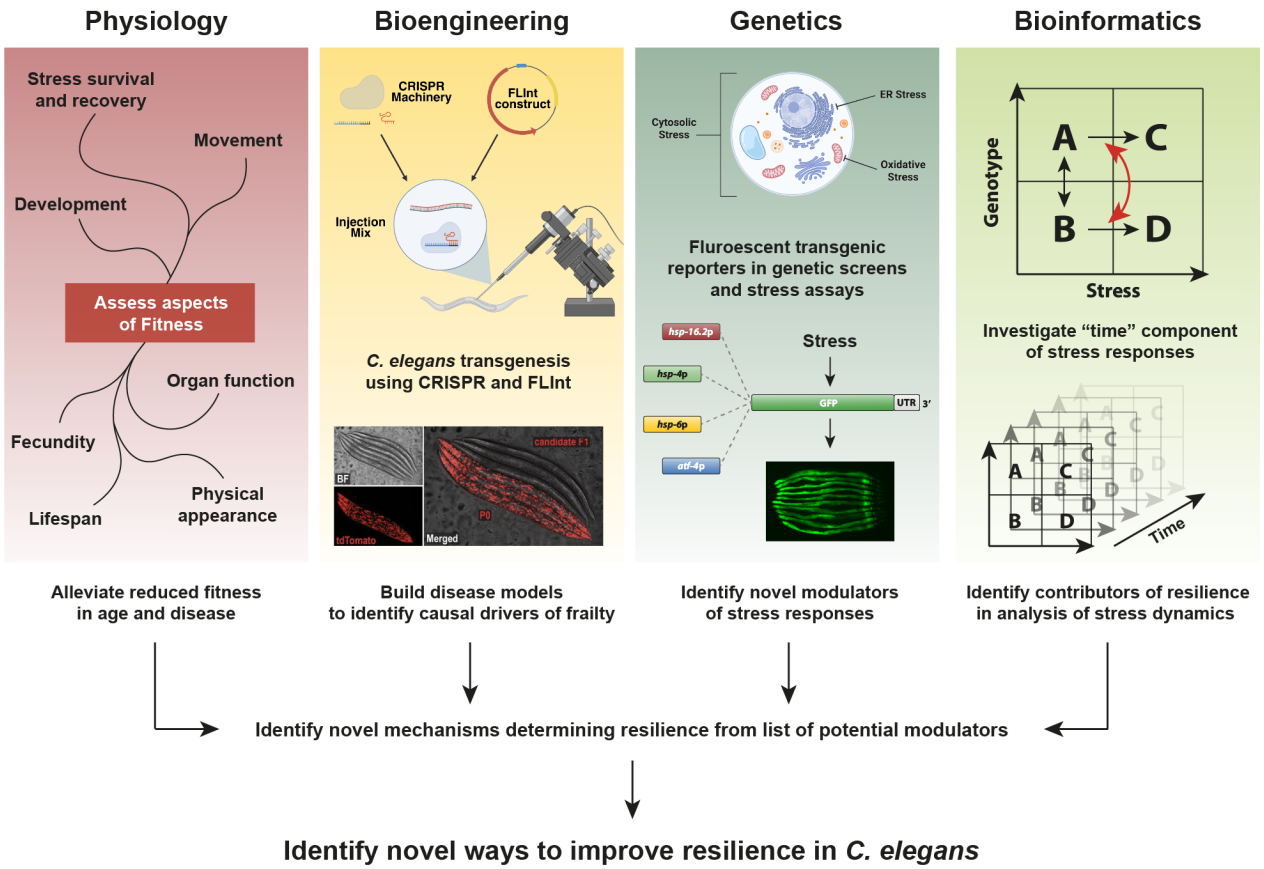

Figure 4: ***Project Approach.*** *By application of various methods in physiology, bioengineering, genetics, and bioinformatics we will compile a list of candidates which will be explored for their potential to increase resilience in C. elegans. We will assess aspects of physiology in genetic and pharmacological modulation of gene expression, comparing parameters of frailty across disease models to identify causal changes in expression determining frailty. Worm images in the bioengineering section are used from Malaiwong et al., G3, 2023.*

To address these questions, I combine state-of-the-art methods in genetics, bioengineering, and bioinformatics to identify and guide novel methods to improve *C. elegans* resilience. Physiological frailty will be characterised by assays defining parameters of fitness assessing motility, development and survival during stress, and will ultimately serve as a readout for successful interventions (Fig. 4). Leveraging recent advancements in precise genome engineering, I will employ Fluorescent Landmark Interference (FLInt) to generate transgenic *C. elegans* strains specifically engineered to recapitulate reduced homeostatic resilience. A comprehensive physiological comparison of these nascent models, alongside established disease models, will serve to validate our metabolic resource availability hypothesis. Once we identify a disease model, comparative analysis will delineate the transcriptomic and physiological signatures of frailty, ultimately facilitating the identification of key molecular determinants and causal drivers underlying homeostatic frailty.

The genetic approach encompasses previous work related to the ISR, screening for novel modulators using a fluorescent reporter of the main effector, *atf-4*. To achieve a more holistic understanding of organismal resilience, we have expanded this toolkit into utilising a broader set of fluorescent reporters under the promoters of well characterised stress response genes, each responding to a different type of stress. By this, we not only cover individual stress pathways for detailed analysis of resilience mechanisms, but can also

investigate interaction of these pathways. By systematically cross-referencing various stressors against this reporter set, we aim to identify critical regulatory hubs and pivot points in stress-response connectivity.

To identify causal molecular mechanisms of physiological stress hypersensitivity, I will employ multi-dimensional RNA sequencing (RNA-seq) designed to resolve causal mechanisms of frailty by analysing time resolved stress response dynamics. Unlike traditional steady-state transcriptomics, this approach utilizes a stress-augmented comparative analysis, pairing disease models with wild type cohorts under both basal and perturbed conditions. This methodology is specifically designed to uncover latent transcriptional differences, molecular shifts that remain masked under homeostatic conditions but drive frailty under exogenous pressure. This integrative strategy will generate a curated candidate library of resilience modulators. We will modulate gene expression of these candidates and analyse the effects on established physiological assays, to identify novel ways to modulate resilience and increase stress response capacity in *C. elegans*.

2 RESULTS

2.1 Stress resilience is reduced in *C. elegans* DMD

2.1.1 Investigating disease model frailty and resilience in physiological assays

We hypothesise that disease models with chronically affected proteostasis carry a homeostatic burden, which would reduce acute responsiveness to additional stress. To test this hypothesis, we aimed to characterise available *C. elegans* models recapitulating aspects of disease in physiological assays and pharmacological perturbation. Outlining a robust framework for assessment of physiological and homeostatic costs of a chronic burden, we evaluated several *C. elegans* disease models characterized by distinct metabolic and physical burdens. We prioritized strains with phenotypes likely to confer hypersensitivity to secondary environmental perturbations, aiming to highlight the respective frailty associated with these conditions.

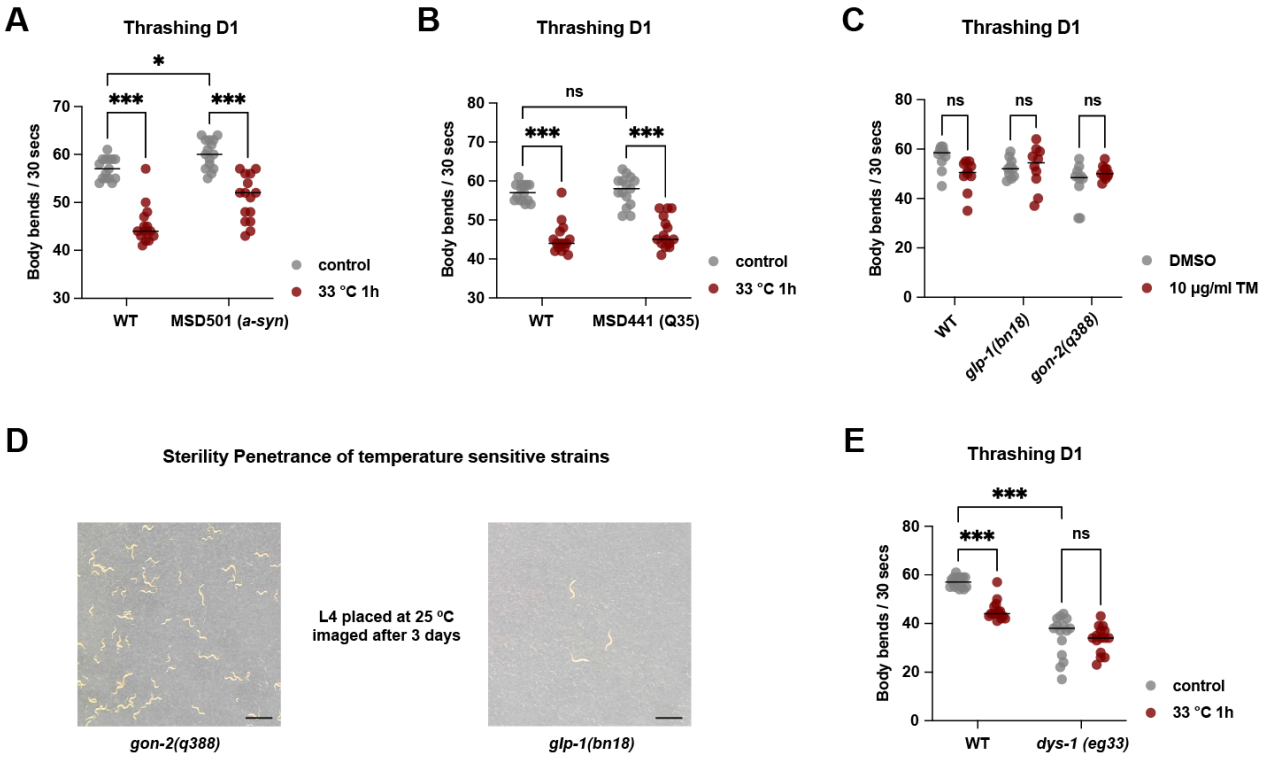

Figure 5: ***Day 1 Locomotion of diverse C. elegans mutants in mild stress.*** *(A)-(B) Locomotion assay on day 1 animals of α-synuclein or polyglutamine accumulation models in mild heat stress compared to the wild type. Significance tested by two-way ANOVA Sidak's post hoc test; *p<0.05, ***p<0.005. (C) Locomotion assay on day 1 WT animals compared to glp-1(bn18) and gon-2(q388) mutants in response to mild ER stress. Significance tested by two-way ANOVA Sidak's post hoc test; *p<0.05 versus WT control). (D) Sterility penetrance test comparing glp-1(bn18) and gon-2(q388) sterility after one generation. (E) Locomotion assay using day 1 animals of the dys-1(eg33) mutant in mild heat stress compared to the wild type. Significance tested by two-way ANOVA Sidak's post hoc test; ***p<0.005.*

To quantify this vulnerability, we initially relied on locomotion as a parameter for fitness and health using day 1 adult animals, which had been described as a readout for physiology measuring lateral body bends in liquid in 30 second intervals. This behavioral metric provides a standardized assessment of neuromuscular integrity and energetic capacity, serving as a baseline for determining how diverse chronic and acute burdens compromise organismal fitness and resilience.

We tested two models that have been used in the assessment of disturbance of proteostasis. They are characterised by accumulation of α-synuclein or polyglutamine expansions (Q35), leading to the formation of aggregates (Morley et al. 2002; Lakso et al. 2003). Based on this proteostatic burden, we assessed their ability to respond to additional stress by its impact on locomotion. While the chosen stress significantly reduced thrashing rates, neither of the models showed a significant reduction in baseline locomotion or in the response to a short heat treatment at day 1 of adulthood (Fig. 5C-D). These models accumulate damage throughout life, and strong effects on fitness were only expected at later stages of life, commonly assessed at day 5 or 8 of adulthood (Morley et al. 2002). By adding stress in the form of heat, we assessed if this could already reveal differences in the response of the model in comparison to the wild type, which in this experimental setup it did not. From this, we learned that the right model for this study needed to fulfil certain criteria to be suited for further experiments and analysis of stress response dynamics. We therefore set the requirements to be a measurable phenotype on Day 1 of adulthood, which ideally would give us a certain room to leverage for treatments to improve a phenotype. Additionally, we needed it to be scalable for RNA-seq experiments, which required the model to not be significantly delayed in development of the worms or a broader distribution of when worms reach adulthood. While the α-synuclein and Q35 models could add value in the analysis at older age, the absence of a phenotype under these conditions made it difficult to assess them for stress response dynamics or scale for larger RNA-seq experiments.

Further investigation into models fulfilling the criteria lead us to use the temperature-sensitive (ts) mutant *gon-2(q388)*, which has established itself as a benchmark for use in RNA-seq (Roux et al. 2022). Upon temperature shift to 25 °C it becomes sterile, while otherwise retaining a wild-type-like phenotype. In comparison to this, we employed another ts mutant with a mutation in notch family receptor GLP-1 (Arantes-Oliveira et al. 2002). This mutant, *glp-1(bn18)*, is also characterised by temperature induced sterility, but has increased lifespan contrary to *gon-2(q388)* (Ewald et al. 2015). As both strains are temperature sensitive sterility mutants which lose their germ line at the non-permissive temperature, downstream analysis was expected to be less noisy and make the data more conclusive. In this setup, we reasoned that a direct comparison of these two mutants could reveal the mechanisms determining the increased resilience and stress response properties in the *glp-1(bn18)*.
Because the sterility phenotype is induced by a temperature shift, we used this opportunity to explore the effects of ER stress using Tunicamycin (TM) on locomotion. However, assessment of locomotion of day 1 of adulthood did not show any differences in thrashing rates between the genotypes or treatment (Fig. 5C). Additionally, the penetrance of the sterility phenotype appeared to strongly vary between the two strains as temperature shift of L4 stage larvae did not prohibit reproduction in the *gon-2(q388)*, while the *glp-1(bn18)* were fully sterile ((Fig. 5D)). Based on the lack of a phenotype and the incomplete penetrance, we decided to move on from this model comparison, as they were not suited in this scientific context.

To identify a model which would fulfil our criteria, we assessed the literature for disease models with clear physiological deficiencies on day 1 of adulthood. Using locomotion deficiency on day 1 adults as a proxy, we identified a model for Duchenne Muscular Dystrophy (DMD) as a suited candidate representing

physiological frailty and muscle weakness from day 1 of adulthood. This appeared of particular interest, as the model also show aspects of a homeostatic burden, with increased calcium uptake and reduced longevity described as secondary effects as a consequence of the *dys-1(eg33)* mutation (Sudevan et al. 2019). We confirmed the muscle phenotype portrayed by reduced motility assessing body bends, and detected a reduction by about 30% (Fig. 5E).

2.1.2 Generating disease models using Fluorescent Landmark INTerference

In parallel to the comparison of published *C. elegans* models for resilience and homeostatic frailty, we explored the option of engineering a transgenic model that suited our criteria. We searched for mutations leading to a physical frailty in a mechanism we know to be affected by acute stress. This lead us to the process of mRNA translation, as it is heavily affected by acute interference in response to stress (Yamasaki and Anderson 2008). It has further been described that mutations in ribosomal subunits can lead to error-prone translation with wide reaching effects, causing phenotypes related to frailty from shortened lifespan to physical weakness in mice (Shcherbakov et al. 2022). Based on this, we aimed to generate an analogous model in *C. elegans* with defects in translation, to subsequently assess fitness and stress response properties.

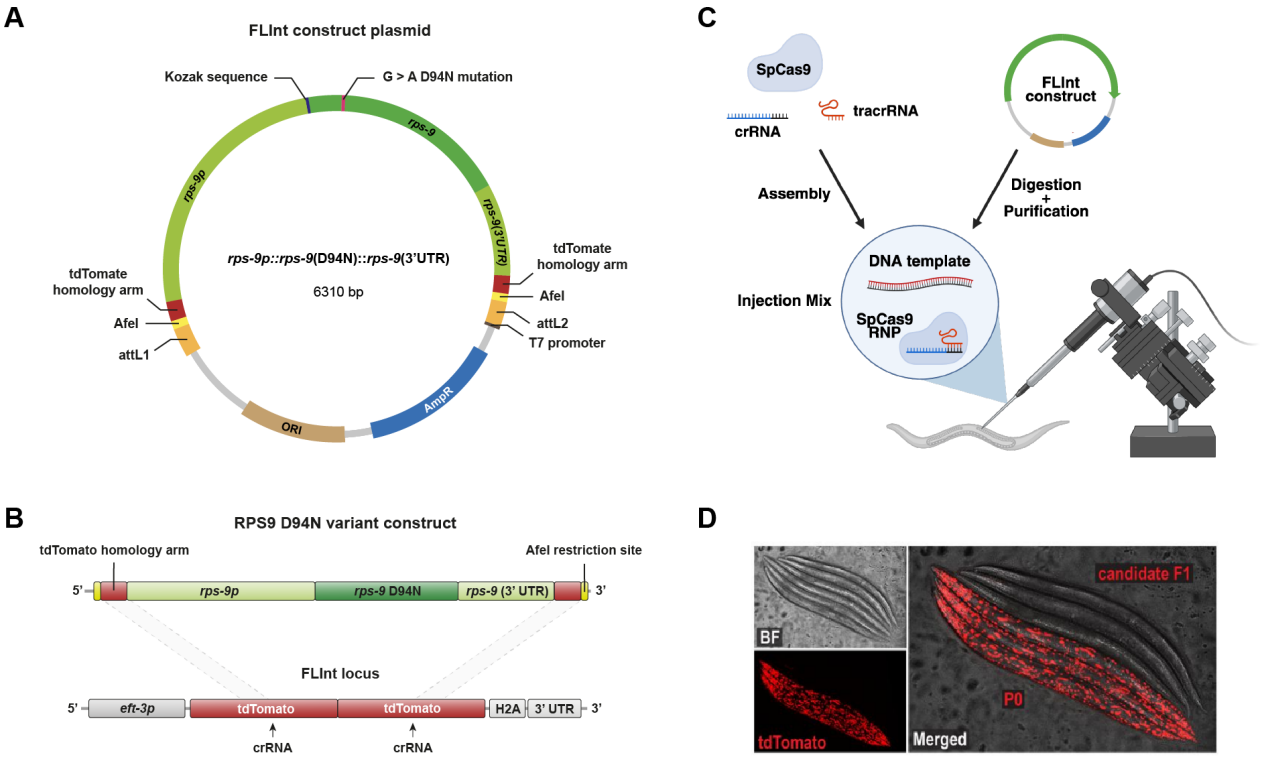

Figure 6: ***FLInt construct injection and integration.*** *(A) Schematic plasmid card of the FLInt construct, carrying the altered rps-9 gene with the D94N mutation, flanked by tdTomato homology arms and AfeI restriction sites for linearisation. Plasmid carrying (B) Integration of the RPS9 D94N construct into the FLInt locus. Marked are the homology arms and CRISPR-Cas9 targeting sites to illustrate the integration point. (C) Schematic overview of injection process: the CRISPR-Cas9 components are assembled in a CRISPR mix and combined with the linearised and purified template DNA in the injection mix. This is injected into the distal gonad arms of gravid adult C. elegans using microinjection. (D) Pictured are P0 worms expressing the tdTomato construct in the FLInt background, compared to successfully edited worms from the F1 generation. (Image from Malaiwong et al., G3, 2023).*

Advancing *C. elegans* transgenesis for the integration of large constructs via CRISPR-Cas9.

To generate this new model, we had to consider the severity of this mutation, as it has been described to be lethal when homozygous. Thus, we compared methods to build a model that carries the described mutation causing error-prone translation, without prohibiting a certain level of baseline mRNA translation leading to functional, "healthy" proteins. We theorised that providing a transgene expressing a mutated RPS-9 ribosomal subunit, while keeping the endogenous gene intact, should cause a certain level of errors in mRNA translation as we expected the machinery to establish a balance of ribosomes with endogenous and transgenic RPS-9. The transgene was designed using the endogenous gene and untranslated regions with a single nucleotide exchange causing a transition of an aspartic acid to an asparagine at residue 94 (Fig. 6A), analogous to the published error-prone translation mutation in mice (Shcherbakov et al. 2022).

While the ability to genetically manipulate *C. elegans* presents a significant strength, the integration of large constructs into its genome remains technically challenging and labor-intensive. Comparing methods of modern *C. elegans* transgenesis to build this model, we identified a novel approach termed Fluorescent Landmark INTerference (FLInt) as a suited method to integrate this transgene into the *C. elegans* genome (Malaiwong, Porta-de-la-Riva, and Krieg 2023). This method builds on a set of strains that carry a transgene expressing the fluorophore tdTomato under a ubiquitous promoter in save harbours on different locations of the genome. Targeting these regions with CRISPR-Cas9 and specific sgRNAs, constructs designed to carry corresponding homology regions can be targeted for integration at the FLInt locus (Fig. 6B), facilitated by homology-directed repair (HDR).
Ensuring high integration efficiency, we linearised the template, for which we included flanking AfeI restriction sites in the plasmid design. Following purification of the template DNA, it was combined with the assembled CRISPR-Cas9 components in the injection mix, and injected into the distal gonad arms of adult *C. elegans* of a strain carrying the FLInt locus (Fig. 6C). As additional means to increase the efficiency and facilitate integration, SpCas9 was co-injected as protein into both gonads, and worms were shifted to 25 °C for improved SpCas9 activity.

The F1 generation was assessed for tdTomato fluorescence. Identification of successful CRISPR-Cas9 editing in FLInt is further facilitated by an absence of tdTomato signal (Fig. 6D). From 45 injected worms, 16 produced F1 animals which were tdTomato negative, indicating SpCas9 and successful cutting. 143 singled F1 were genotyped to confirm integration of the construct using primers that spanned out from the insert to the FLInt locus sequence outside the integration site. In pooled genotyping we identified at least 7 candidates that carried the construct, which we confirmed with Sanger-sequencing.

Error-prone translation in *C. elegans* via RPS9 D94N

To characterise the physiological properties of the generated *rps-9*(D94N) model, we assessed how it performs in thrashing and lifespan assays, and in response to acute stress (Fig. 7). The *rps-9*(D94N) worms did not show alterations in locomotion or lifespan when compared to the wild type. Body bends did not seem to be affected by addition of the transgene, and just like the wild type, thrashing rates were not affected by treatment with tunicamycin (TM), which was chosen as an ER stress targeting mRNA translation via connection to the ISR. The lifespan assay was performed at 25 °C to make a potential phenotype more prominent in a taxing environment, and to use the *glp-1(bn18)* mutant as a positive control. While the positive control showed

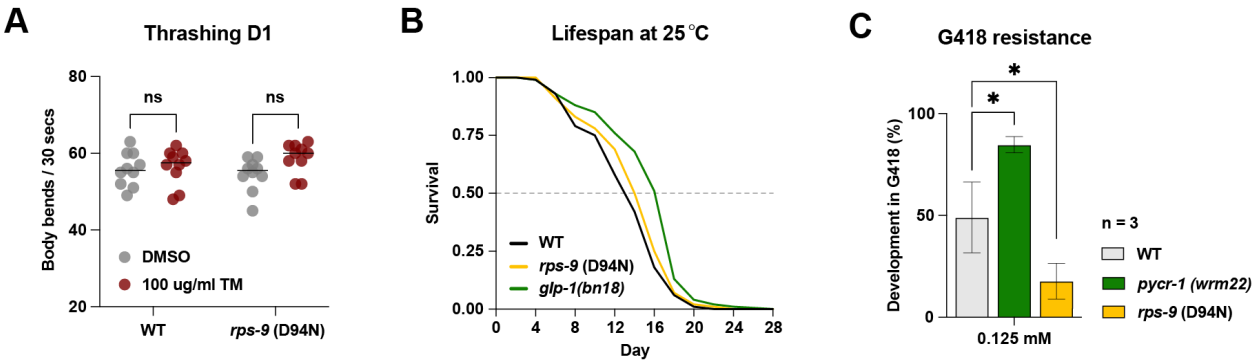

Figure 7: ***Physiological assessment of rps-9(D94N)*** *(A) Locomotion assay on D1 adults comparing wild type and rps-9(D94N) in ER stress. Significance determined by two-way ANOVA Sidak's post hoc test; *p<0.05. (B) Lifespan analysis at 25 °C comparing wild type and rps-9(D94N) survival. glp-1(bn18) serves as positive control. (C) Assessment of development in G418 of rps-9(D94N) compared to the wild type. The mutant pycr-1(wrm22) serves as positive control as it has been shown to be more resistant to this stress. Error bars represents means ±SD, one-way ANOVA Dunnett's post hoc test; *p<0.05.*

a significantly higher lifespan, the *rps-9*(D94N) transgenic animals did not show significant variation. To assess if there is any phenotype caused by the induced mutation, we addressed the direct mode of action of the RPS-9 protein and targeted mRNA translation elongation using the elongation blocker geneticin (G418). Assessment of development rates in treatment with G418 revealed an increased sensitivity to this compound in the *rps-9*(D94N) strain. A respective positive control was used with the mutant *pycr-1(wrm22)*, which has been described to be more robust in G418 stress (Denzel lab, unpublished). Overall, characterisation of the error-prone translation model *rps-9*(D94N), built using FLInt, showed a mild hypersensitivity to G418 stress, however, it did not show a reduction in lifespan at 25 °C, and did not have any alterations in locomotion. This pathology is likely founded in the way we engineered this strain. Because we expected the phenotype to be severe if we would edit the endogenous locus, we introduced the transgene separately, ultimately leading to a "pseudo-heterozygous" state, where the genome encode the same amount of copies for the endogenous gene as for the transgene. However, it has been impossible to determine the ratio of ribosomes carrying the endogenous to mutated subunit, making this experiment difficult to control.

Taken together, we were able to build and identify published disease models that are representing a homeostatic burden and show a phenotype representing frailty. Based on the presence of a clear locomotion phenotype on day 1 of adulthood in the *dys-1(eg33)* mutant, we decided to proceed with this strain as a model for frailty. This made it an ideal model to test our hypothesis further, as these effects would indicate a chronic burden that the organism would be spending resources on to retain basic activity and survival.

2.1.3 *C. elegans* model for DMD is hypersensitive to heat and mitochondrial stress

Progressive loss of muscle function in *C. elegans* DMD

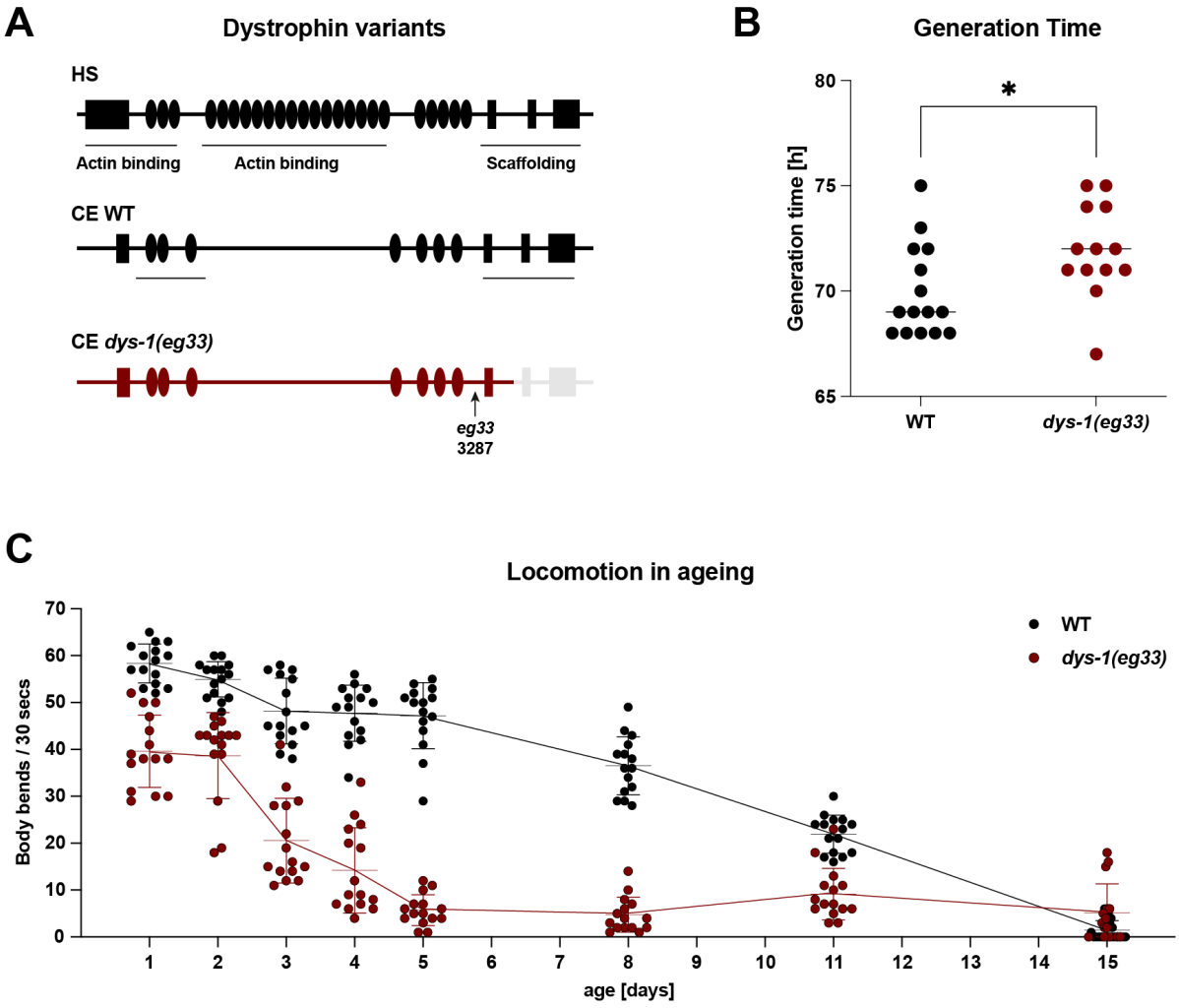

Figure 8: ***Progressive muscle loss in C. elegans DMD.*** *(A) Schematic representation of dystrophin comparing human and C. elegans variants. (B) Generation time assay comparing onset of egg-lay between wild type and dys-1(eg33) mutant. Significance was determined by unpaired t test; *p=0.0246. (C) Locomotion assay throughout 15 days of life comparing body bends/30 seconds of wild type and dys-1(eg33) mutant at different ages. Scored are body bends/30 seconds of 15 individuals per time point.*

In a systematic comparison of disease models, we ultimately identified a *C. elegans* model for Duchenne Muscular Dystrophy (DMD) to be well suited and fulfilling our required criteria. The strain *dys-1(eg33)* is defined by a single mutation in the structural muscle protein dystrophin at position 3287, resulting in a premature stop and subsequent expression of a truncated version of the protein, lacking an important scaffolding domain anchoring it in the cell membrane (Fig. 8A). To fully understand the pathology of the model, we assessed physiological metrics throughout life to determine necessary parameters for transcriptomic experiments, and characterise the effect of age on *dys-1(eg33)* mutant fitness. Assessment of generation time revealed a mild delay in development of the DMD model (Fig. 8B), for which we corrected in further assays

by an offset of 3 hours when synchronising the strains for experiments. To assess long-term health and fitness decline in the *dys-1(eg33)* mutant, we monitored locomotion throughout life in comparison to the wild type (Fig. 8C). In the wild type, we observed a steady gradual decline in motility in aging, with motility reduced by more than 50% after 11 days, and worms barely moved after 15 days of adulthood. The *dys-1(eg33)* mutant, characterised by an already lower baseline motility on day 1, described a steeper slope in locomotion decline, with the average motility rates being more than 50% reduced when compared to baseline on day 4 of adulthood. The DMD model therefore not just showed a generally reduced fitness on baseline, but displayed a more rapid decline in motility in age, with animals barely moving from day 5 of adulthood onward.
Taken together, the *dys-1(eg33)* mutant is a robust model for physical frailty, with a strong phenotype in the reduction in motility compared to the wild type. We could show that it also portrays a faster progression in the decline of the ability to move in aging, characterising it as a model for progressive loss of muscle function.

dys-1(eg33) mutant hypersensitivity to heat stress

According to our hypothesis, a chronic burden leading to reduced resilience characterises disease models with insults to proteostasis. We would therefore expect a model like the *dys-1(eg33)* mutant, which presents a clear frailty phenotype described to be linked to metabolic imbalance at mitochondria (Kelly-Worden and Thomas 2014), to be more sensitive to perturbation. To test this concept, we exposed mutant and wild type animals to various cellular stresses, and analysed survival or fitness following perturbation. We analysed the stress response properties in treatments that broadly target the cytosol, mitochondria, the ER, or mRNA translation. To investigate stress resilience in heat stress, we employed a thermorecovery assay, which measures the ratio of worms in a population that are moving normally following a 24 hour recovery after heat stress, compared to dead or non-motile animals. This was chosen as it covers not just the endurance of a stress, but also the ability to recover from it and adapt to changed environmental conditions. Initially, we performed a stress time course before recovery, to identify stress conditions that reveal a variation in recovery rates. The wild type showed a gradual decline in recovery rates from 4 hours of exposure to 33 °C, with about 25 % of animals recovering from heat stress at 33 °C for 10 hours ((Fig. 9A)). In contrast, *dys-1(eg33)* mutant animals started to show an impact after 3 hours of stress, describing a more severe drop in recovery rates than the wild type, leading to a recovery of less than 25 % of animals after just 6 hours of treatment.

Thermorecovery was consistently lower in the mutant from exposure to 3 hours of heat stress onward. Furthermore, the reduction of recovery in the DMD model described a steeper decline as portrayed by the gradual reduction observed in the wild type. As it showed the biggest separation of wild type and *dys-1(eg33)* mutant, we decided to proceed with a stress at 33 °C for 6 hours before recovery. In these conditions, wild type animals recovered at about 80 %, while the mutant showed recovery rates at about 20 % (Fig. 9B). Thermorecovery in the *dys-1(eg33)* mutant was significantly lower throughout experiments when compared to the wild type control, with recovery rates reduced by up to 60%. Taken together, we detected a strong heat stress hypersensitivity in the *dys-1(eg33)* mutant, with clear correlation of the duration of the stress before recovery. A steeper drop in thermorecovery in dependence of time in the *dys-1(eg33)* mutant stress recovery was equivalent to observations in locomotion. We identified a stress of 6 hours at 33 °C as a suitable window for assessment of this metric producing a robust phenotype with good separation, which we used for further comparison.

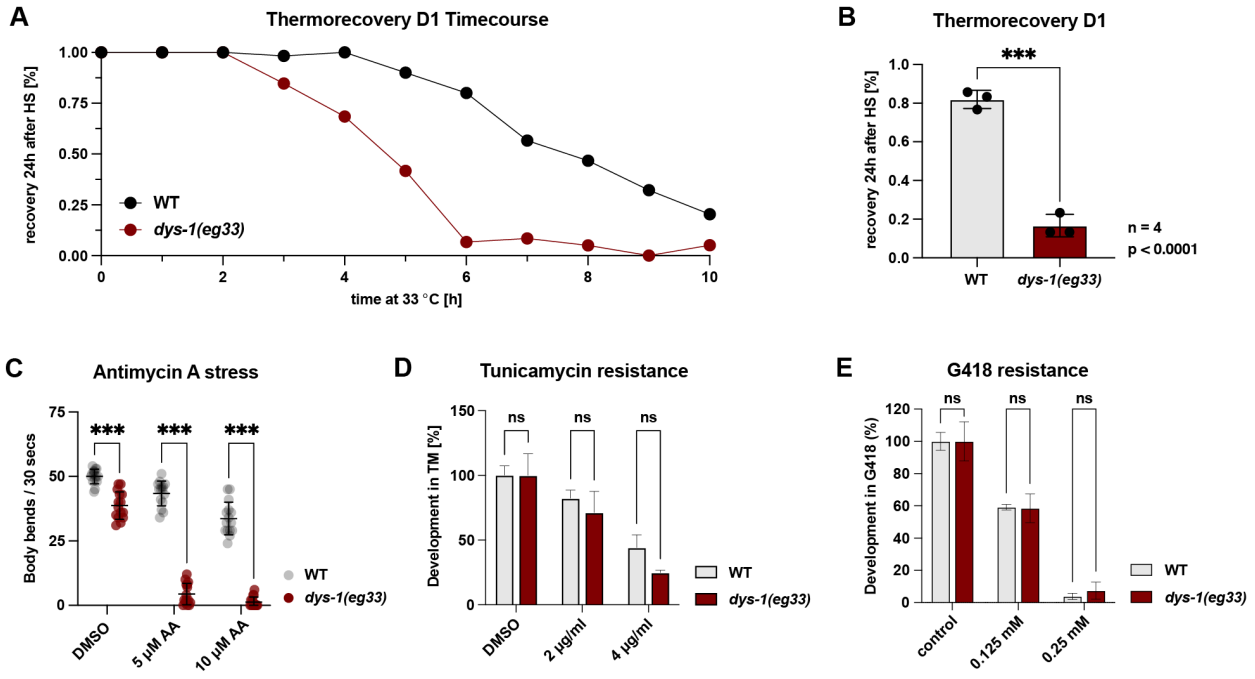

Figure 9: ***dys-1(eg33) mutant is sensitive to stress.*** *(A) Thermorecovery time course of day 1 adults. Animals were treated for up to 10 hours before the recovery period. (B) Thermorecovery assay of day 1 adults comparing wild type and dys-1(eg33) mutant recovery following heat shock at 33 °C for 6 hours. Error bars represents means ±SD, Welch's t-test; ***p<0.0001. (C) Locomotion assay of day 1 adults comparing wild type and dys-1(eg33) mutant motility following 24 hour treatment at different concentrations of Antimycin A. Significance tested by two-way ANOVA Turkey's multiple comparison test; ***p<0.0005. (D) Development stress assay comparing development rates of wild type and dys-1(eg33) animals from egg to adulthood on various concentrations of Tunicamycin. (E) Development stress assay comparing the same conditions on G418.*

dys-1(eg33) mutant hypersensitivity to mitochondrial stress

To assess if stress hypersensitivity expands to other contexts, we exposed the animals to mitochondrial stress by blocking complex III of the electron transport chain (ETC) by treatment with Antimycin A (AA). This compound is commonly used to measure the response by assessment of paralysed animals in a population (Sudevan et al. 2019). We theorised that if high concentrations paralyse the worms, moderate concentrations might affect motility in a range we could measure in assessment of body bends. To test this and uncover potential alterations in the response of the *dys-1(eg33)* mutant, we exposed day 1 animals to 5 and 10 μM AA for 24 hours, and assessed them for locomotion (Fig. 9C). As established, we found baseline locomotion reduced in the DMD model. Treatment with 10 μM AA significantly reduced body bends in the wild type, but only by less than 50 %. In stark contrast, the DMD model showed a strong reaction to the treatment, with animals barely moving after being exposed to the lower stress condition at 5μM AA for 24 hours.

Manifestation of stress hypersensitivity in *dys-1(eg33)* mutants

Additionally, we attempted to assess the effect of ER stress and mRNA translation stress on adult animals, however, we could not determine the ideal parameters for a phenotype in adult animals. Treatment with the ER stressor Tunicamycin (TM) on adult animals did not cause any changes in survival or motility following treatment for 24 hours with concentrations up to 100 μg/ml. As adult animals appeared to be rather robust

in this stress, we exposed wild type and *dys-1(eg33)* mutant animals to (TM) or G418 during development (Fig. 9D-E). We measured the development rates comparing development past the L4 larval stage, and could detect a dose-dependent reduction in development rates upon treatment with both compounds. Interestingly, we could not detect a significant difference in development rates of wild type and *dys-1(eg33)* mutant in treatment with either TM or G418 in development.
In conclusion, we identified a significant hypersensitivity to heat and mitochondrial stress in the *dys-1(eg33)* mutant. In accordance with our hypothesis, the DMD model showed reduced recovery rates following exposure to heat stress, which was defined by an onset of a reduction of recovery at a lower stress dose, a more severe reduction in recovery rates over time, and significantly lower recovery in comparison to the wild type throughout. Furthermore, the *dys-1(eg33)* mutant also showed increased sensitivity to mitochondrial stress, as treatment on plates containing AA revealed strong effects on locomotion. In both cases we identified a stress-dependent, gradual decline in the wild type during increased stress intensity. In contrast, the DMD mutant was more sensitive to both stresses, being affected at lower stress doses, and showing a stronger reduction in recovery rates at every condition. This matched the concept of a homeostatic frailty, and would recapitulate a lower threshold towards stress based on decreased stress response capacity.

2.1.4 Reduced IGF-signalling improves hypersensitivity in DMD

Published compound treatments for DMD in *C. elegans* fail to rescue hypersensitivity to stress

Next to a purely exploratory approach, we assessed the literature for a variety of treatments to improve either resilience or the muscle frailty phenotype of *dys-1(eg33)* mutants. Having identified a novel phenotype describing stress hypersensitivity in the *C. elegans dys-1(eg33)* mutant, we wondered if these effects could be alleviated by classical treatments for DMD used in both nematodes and mammals. These conventional treatments are mostly intended not to treat the cause of the disease, but alleviate symptoms by preventing or slowing the functional decline of the muscle. Treatment with the hormone Melatonin, alongside the synthetic corticosteroid Prednisone, has been described to slow decline of muscle function in *C. elegans* (Hewitt et al. 2018). We were also interested in the effects of the synthetic Coenzyme Q_{10} (CoQ_{10}) analog Idebenone, which functions as an electron carrier supporting the function of the ETC, and had been shown to alleviate symptoms in DMD (McDonald et al. 2016).

Another method is the targeted inhibition of calcium uptake into mitochondria by the mitochondrial calcium uniporter (*mcu-1*) blocker Ru360, which has been described to improve locomotion in DMD (Higashitani et al. 2023). Furthermore, we employed an inhibitor of lysosomal proteolysis, Chloroquine, which inhibits autophagy flux (Chapin et al. 2015). While autophagy is usually considered to be beneficial for survival, Chloroquine treatment has been shown to alleviate DMD phenotypes in mdx mice (Hirata et al. 2024). We therefore tested if treatment with Chloroquine can support recovery in acute stress of *dys-1(eg33)* mutants. Targeting broader cellular resilience, we explored treatments targeting relevant mechanisms in the context of stress. We hypothesised that boosting the expression of response genes could prime responsiveness to stress and support survival. In this context, Arimoclomol and Teprenone have been described to induce the expression of stress responsive chaperones (Penke et al. 2018).

To test the effect of these compounds on thermorecovery and locomotion, we raised animals on respective compound plates from birth, and assessed performance of day 1 adults. Treatment of wild type or DMD mutant worms with various concentrations of Idebenone, 1 mM Melatonin, and 5 μM Ru360 did not result in

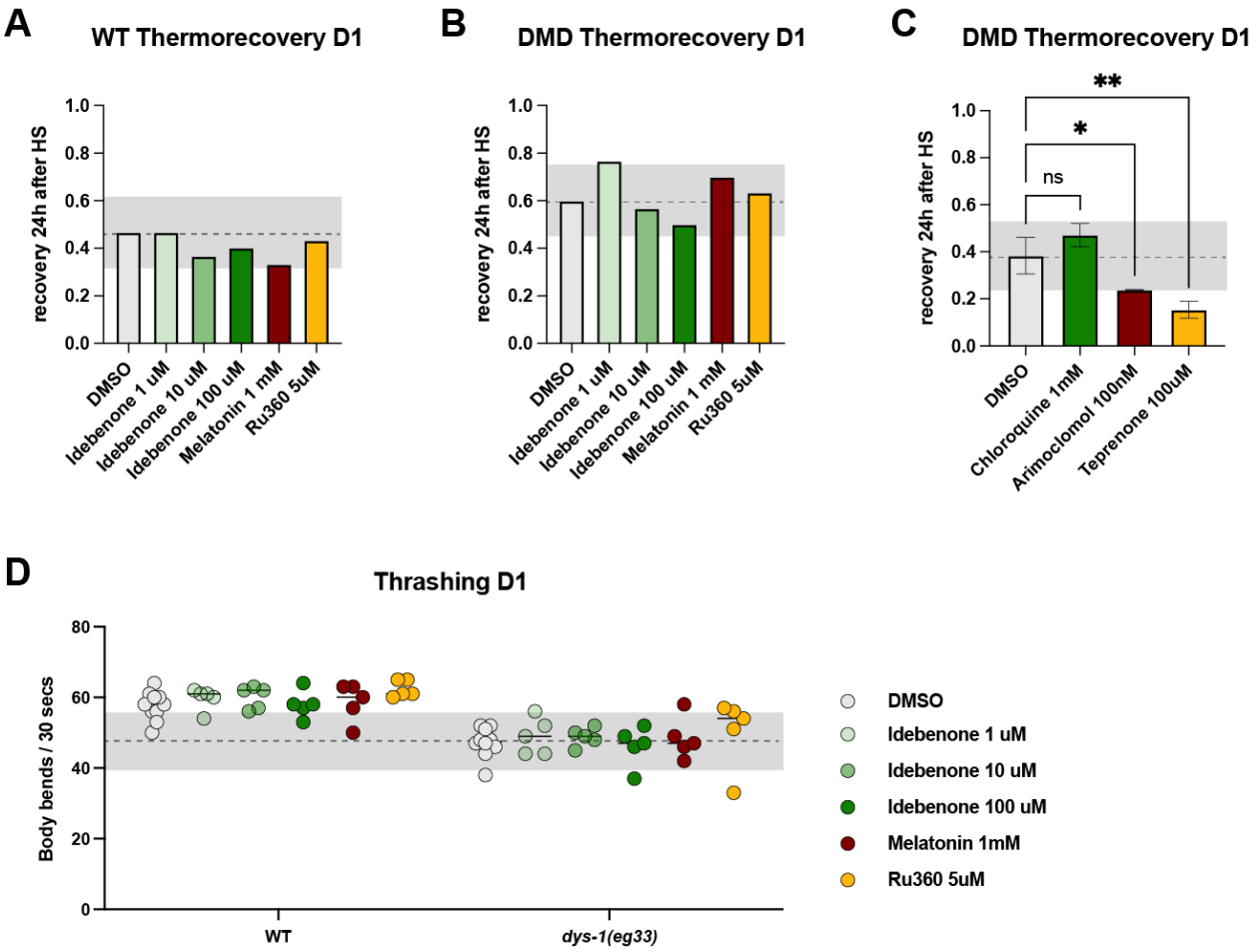

Figure 10: ***DMD frailty rescue with compounds.*** *(A) Thermorecovery assay using day 1 adults of the wild type raised on plates prepared with Idebenone, Melatonin, or Ru360. Animals were treated for 6 hours at 34 °C. (B) Thermorecovery assay using day 1 adults of the dys-1(eg33) mutant raised on plates prepared with Idebenone, Melatonin, or Ru360. Animals were treated for 6 hours at 33 °C. (C) Thermorecovery assay using day 1 adults of the dys-1(eg33) mutant raised on plates prepared with Chloroquine, Arimoclomol, or Teprenone. Animals were treated for 6 hours at 33 °C. (D) Locomotion assay on day 1 adults comparing the effects of treatment with Idebenone, Melatonin, or Ru360 on wild type worms or dys-1(eg33) mutants.*

significant changes of thermorecovery rates in our experimental conditions (Fig. 10A-B). Treatment with 1 mM Chloroquine did not significantly impact thernmorecovery of the dys-1(eg33) mutant, while treatment with Arimoclomol and Teprenone even reduced thermorecovery in trial experiments (Fig. 10C). Assessing effects on locomotion in trial experiments assessing body bends in 5 individuals, we did not detect any significant changes resulting from treatment with Idebenone, Melatonin, or Ru360 for either wild type or *dys-1(eg33) mutant*. This stands in contrast to published results, where treatment with Melatonin and Ru360 did result in a significant improvement of locomotion in dys-1(eg33) when compared to untreated controls (Hewitt et al. 2018; Higashitani et al. 2023). We identified a variety of potential causes for this lack of rescue, as compound treatments of *C. elegans* can prove difficult without a reliable way to confirm target engagement. Common limitations are related to solubility and drug uptake, as animals are placed on plates containing the compound, and subsequent uptake depends on permeability of the nematode cuticle, or is facilitated by ingestion of bacteria exposed to the compound. The overall efficacy of a compound is therefore unreliable, and we could not prove any of the treatments were effective.

In conclusion, we failed to show any significant effect of compound treatment on either locomotion or thermorecovery. Contrary to expectations, we could not reproduce published effects of treatment with Melatonin and Ru360, and explorative experiments using Idebenone, Chloroquine, Arimoclomol, and Teprenone did not show any effect in any of our assays. Although we used a range of concentrations for certain drugs to increase the chance of effective treatment, we failed to prove any of the compounds engaged their respective target, as we were lacking the relevant controls. We therefore cannot conclude if any of the drugs are affecting thermorecovery or locomotion in *dys-1(eg33)*.

Inhibition of calcium uptake into mitochondria fails to reproduce published data

As pharmacological interference did not result in measurable effects, we utilised genetic mutations implied to alleviate DMD phenotypes, which we expected to lead to more reliable results. The inhibition of calcium uptake has been shown to improve locomotion not just by pharmacological inhibition with Ru360, but also by genetic knockout of *mcu-1* (Higashitani et al. 2023). Here, we crossed the *mcu-1* knockout mutation *mcu-1(ju1154)* in the *dys-1(eg33)* mutant background, and investigated the double mutant for fitness and resilience in locomotion and thermorecovery assays.

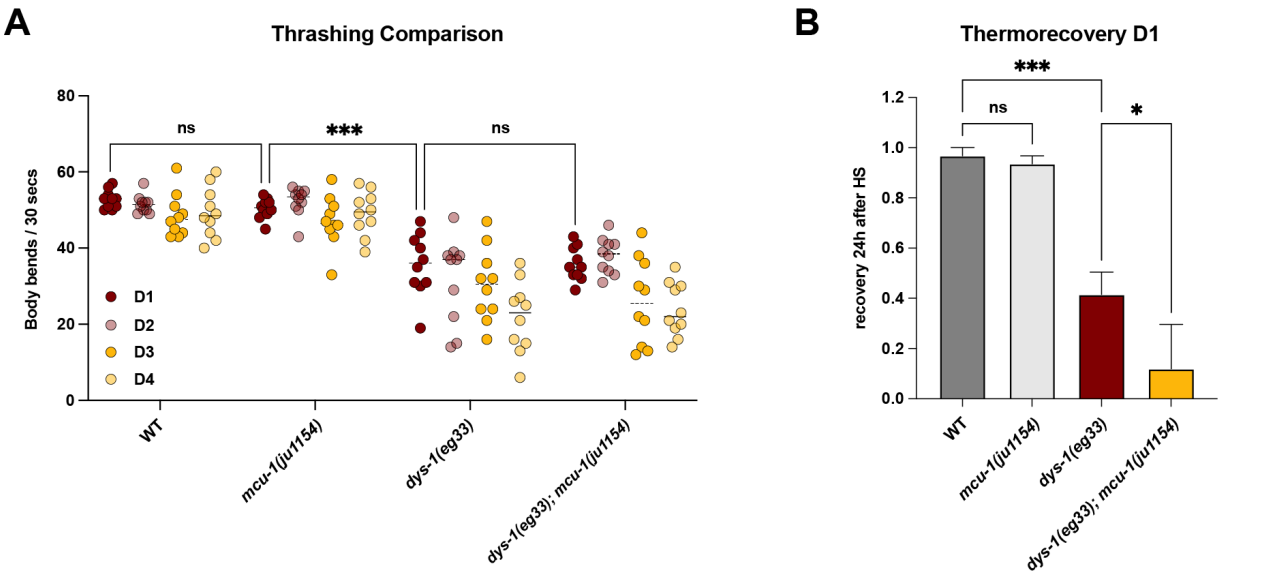

Figure 11: ***DMD frailty rescue by knockout of mcu-1.*** *(A) Locomotion assay of worms throughout the first four days of adulthood comparing wild type, mcu-1(ju1154) knockout mutant, dys-1(eg33) mutant, and dys-1(eg33); mcu-1(ju1154) double mutants. (D) Thermorecovery assay using day 1 adults of the same strains comparing recovery rates from heat stress for 6 hours at 33 °C.*

We assessed motility of the animals on four consecutive days starting from day 1 of adulthood, looking for improved locomotion in the double mutant (Fig. 11A). Surprisingly, we did not detect an improvement of locomotion, as the *mcu-1(ju1154)/dys-1(eg33)* double mutant portrayed the *dys-1(eg33)* phenotype showing reduced day 1 locomotion and a stronger decline throughout the experiment in comparison to the wild type. The *mcu-1(ju1154)* mutant alone did not show any variation in comparison to the wild type. Investigating the

effects of the *mcu-1(ju1154)* mutation on thermorecovery, it did not affect stress recovery in the individual mutant. However, we detected a significantly lower recovery in the *mcu-1(ju1154)/dys-1(eg33)* double mutant when compared to the individual *dys-1(eg33)* mutant, showing a further increase in DMD-mediated hypersensitivity.

Overall, the *mcu-1(ju1154)* mutation did not affect locomotion in our experiments, contrary to published observations (Higashitani et al. 2023). Strikingly, we found the *dys-1(eg33)*;*mcu-1(ju1154)* double mutant to be more sensitive to heat stress than the individual *dys-1(eg33)* mutant, while the *mcu-1(ju1154)* mutant by itself did not show any signs of increased sensitivity in heat stress than the wild type control.

Reduced IGF-signalling rescues stress hypersensitivity, but not motility

Because more targeted approaches aiming to alleviate DMD related phenotypes failed, we wondered if conventional methods to boost resilience in *C. elegans* could improve stress recovery in the *dys-1(eg33)* mutant. To test this, we employed a well characterised model for increased health with the *daf-2(e1370)* mutant as the "gold-standard" for improving health and longevity in *C. elegans* (Murphy et al. 2003). The mutation in *daf-2(e1370)* causes increased resilience across several environmental stressors, primarily mediated by the transcription factor DAF-16/FOXO (Dues et al. 2019; McColl et al. 2010). In this context, we aimed to uncover if the global health benefits observed in the *daf-2(e1370)* mutant could rescue the homeostatic frailty presented in the *dys-1(eg33)* mutant.

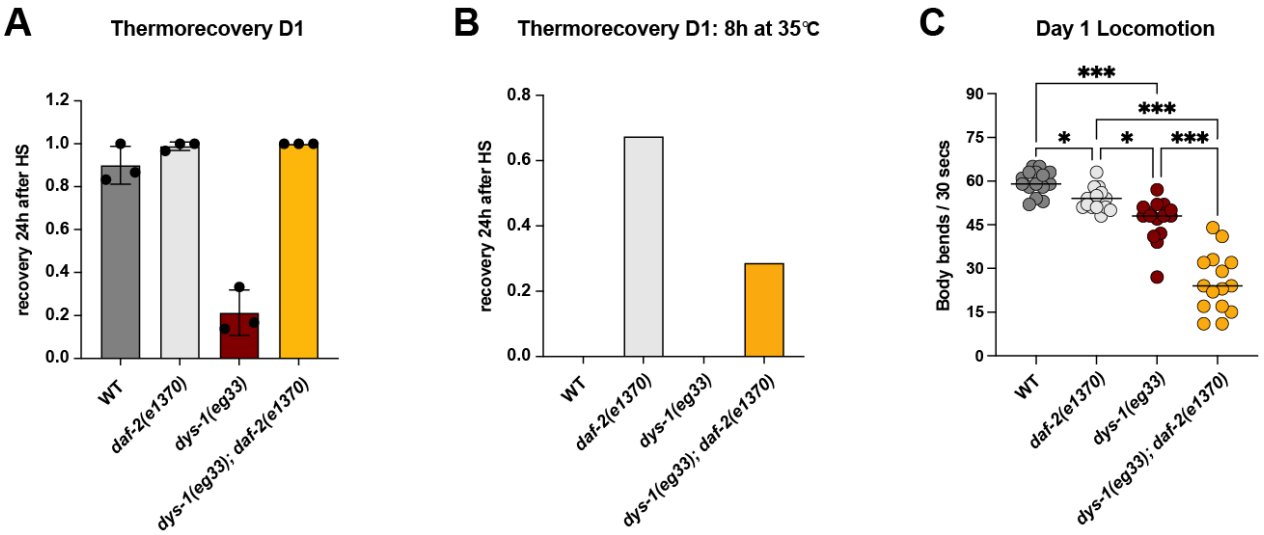

Figure 12: ***DMD rescue by reduced IGF-signalling.*** *(A) Thermorecovery assay using day 1 adults of daf-2(e1370), dys-1(eg33) and dys-1(eg33); daf-2(e1370) mutant strains compared to wild type. Animals were stressed for 6 hours at 33 °C. (B) Thermorecovery assay using day 1 adults of the same strains following treatment at 35 °C. (C) Locomotion assay using day 1 adult worms of daf-2(e1370), dys-1(eg33) and dys-1(eg33); daf-2(e1370) mutant strains compared to wild type.*

First, we assessed thermorecovery of individual mutants and the *daf-2(e1370)*;*dys-1(eg33)* double mutant following heat stress at 33 °C for 6 hours (Fig. 12A). The individual *daf-2(e1370)* mutant was not affected under usual experimental conditions in the thermorecovery assay, while the wild type and *dys-1(eg33)* mutant

followed established patterns, recovering at just over 80 % and about 20 % respectively. The double mutant of *dys-1(eg33)* and *daf-2(e1370)* recovered at 100%, improving thermorecovery to higher levels than the wild type and seemingly completely masking *dys-1(eg33)* frailty. To identify if we can still separate the individual *daf-2(e1370)* mutant from the double mutant in stress, we performed a thermorecovery at significantly higher temperatures, exposing the animals to 35 °C for 8 hours (Fig. 12B). Strikingly, the *daf-2(e1370)* mutant still recovered at over 60 %, while the double mutant with *dys-1(eg33)* showed recovery of about 30 % of the population. The wild type and *dys-1(eg33)* did not show survival of any individuals.
Based on this strong beneficial effect on thermorecovery, we wondered if the *daf-2(e1370)* could also alleviate the locomotion phenotype in the DMD model. Thus, we assessed motility of day 1 adult animals of the individual and double mutants compared to the wild type (Fig. 12C). The *daf-2(e1370)* mutant alone did show a slightly reduced body bend rate from the wild type, while presenting significantly higher motility than the *dys-1(eg33)* mutant. Surprisingly, the double mutant of *daf-2(e1370)* and *dys-1(eg33)* revealed strong motility deficits when combining the two mutations, describing a reduction of over 50 % in comparison to the individual *dys-1(eg33)* mutant. This synergistic effect was in contrast to the thermorecovery phenotype, where combination of both mutations lead to an overall more robust recovery from stress than the DMD model alone.

Taken together, we showed that modulation of the IIS pathway mediated by the *daf-2(e1370)* mutant significantly increases thermorecovery in the *dys-1(eg33)* mutant. The double mutant exceeded recovery levels of the wild type, but was still more sensitive than the individual *daf-2(e1370)* mutant when exposed to extreme stress, showing that the underlying detrimental effects in the DMD model are still present and not completely buffered. Assessment of locomotion, however, revealed reduced motility in the *daf-2(e1370);dys-1(eg33)* double mutant when compared to the individual *dys-1(eg33)* mutant strain. This could be explained in our hypothesis or a finite availability of resources and would indicate a trade-off, as the increase of thermorecovery facilitated by *daf-2(e1370)* would come at the cost of locomotion.

Reduced resilience and stress hypersensitivity in *dys-1(eg33)* mutant

In summary, we assessed various models for reduced proteostasis for their ability to respond to, endure, and recover from stress. We tested stress behaviour in ER, mitochondrial, mRNA translation, and heat stress to establish suited metrics to quantify stress resistance. While we did not find the right parameters for the use of TM and G418 in adult worms, we identified heat stress and AA stress to affect recovery and motility.

Ultimately, we showed that the *dys-1(eg33)* mutant is hypersensitivity to heat and mitochondrial stress in these assays. Recovery rates after heat stress were lower in mutant populations at a range of conditions, and motility was affected significantly stronger following exposure to AA stress. Having identified this physiological frailty, we aimed to uncover if this was caused by differences in the induction of canonical stress responses, which we addressed by outlining these mechanisms using transgenic reporters monitoring the HSR and the UPR^{mito}, respectively.

2.2 Outlining stress response induction and their overlap in *C. elegans*

Having described the effects of stress treatments on physiology in assays like thermorecovery and mitochondrial stress assay, we wanted to understand how the stress pathways are activated in response to stress on a molecular level. We aimed to monitor and compare the induction of respective stress responses, to uncover any potential differences in the response of the *dys-1(eg33)* mutant which could explain stress hypersensitivity. Visualising the induction of stress *in vivo*, we employed a set of transgenic reporter strains used to monitor stress response induction as increasing fluorescence under the promoter of respective response genes (Bar-Ziv et al. 2020). By this, we intended to bridge observations from physiological assays to the driving molecular response and investigate if differences in stress survival in DMD are caused by variation in the canonical stress response pathways.
We hypothesized that variation in stress responses could be caused by differences at the level of initial stress sensing, changes in intensity, or changes of timing of the expression changes covering the aspect of stress dynamics. To obtain a conclusive picture of stress response capacity, we probed the system from different angles, testing the response to three different stresses. Additionally, we wanted to investigate the interaction of stress response pathways by measuring induction of reporters during off-pathway stress. This should help understand how local stress responses are affected in global stress, and if the *dys-1(eg33)* strain shows any alteration in a potential connection.
Ultimately, the stress induction assays in the reporters were also aimed to facilitate the experimental design of RNA-seq, to set suitable parameters for comparison of wild type and DMD transcriptomes in a time course. Supported by initial reporter results, we aim to fully elucidate the molecular changes forming the molecular response to stress, and driving frailty in the DMD model.

2.2.1 Assessing stress response induction using fluorescent reporters

Determining the ideal stress dosage using fluorescent reporters: Heat stress

Transgenic reporter strains facilitate high-throughput genetic screening, epistasis analysis, and real-time monitoring of stress induction in *C. elegans*. In this study, we sought to characterize the induction dynamics of fluorescent reporters in response to specific challenges, establishing dose-dependent stress dynamics for the induction of heat, ER, and mitochondrial stress. With this, we wanted to outline stress dynamics and elucidate whether the hypersensitive *dys-1(eg33)* mutant exhibits a compromised capacity to mount a robust stress response, as this might contribute to its reduced stress response capacity. The experimental outline incorporated three distinct stressors, targeting a specific cellular environment (Fig. 13A). These included tunicamycin (TM), which induces ER stress by inhibiting N-linked glycosylation, Antimycin A (AA), respiratory chain complex III inhibitor targeting mitochondrial function, and thermal stress, inducing a global cytosolic stress response. These treatments are established to differentially up-regulate the transcriptional reporters *hsp-4*p::GFP, *hsp-6*p::GFP, and *hsp-16.2*p::GFP, respectively. By systematically titrating these stressors, we aimed to identify optimal concentrations that generate a robust, measurable signal while avoiding the saturating of the response. Determination of this ideal dose ensures that subtle variations in stress response changes are not masked during extreme, non-physiological stress exposure. Capacity of the *dys-1* mutant can be statistically discerned from the wild-type N2 background. Consequently, these established parameters are intended to facilitate the understanding of how dystrophin deficiency modulates cellular homeostasis under environmental pressure.

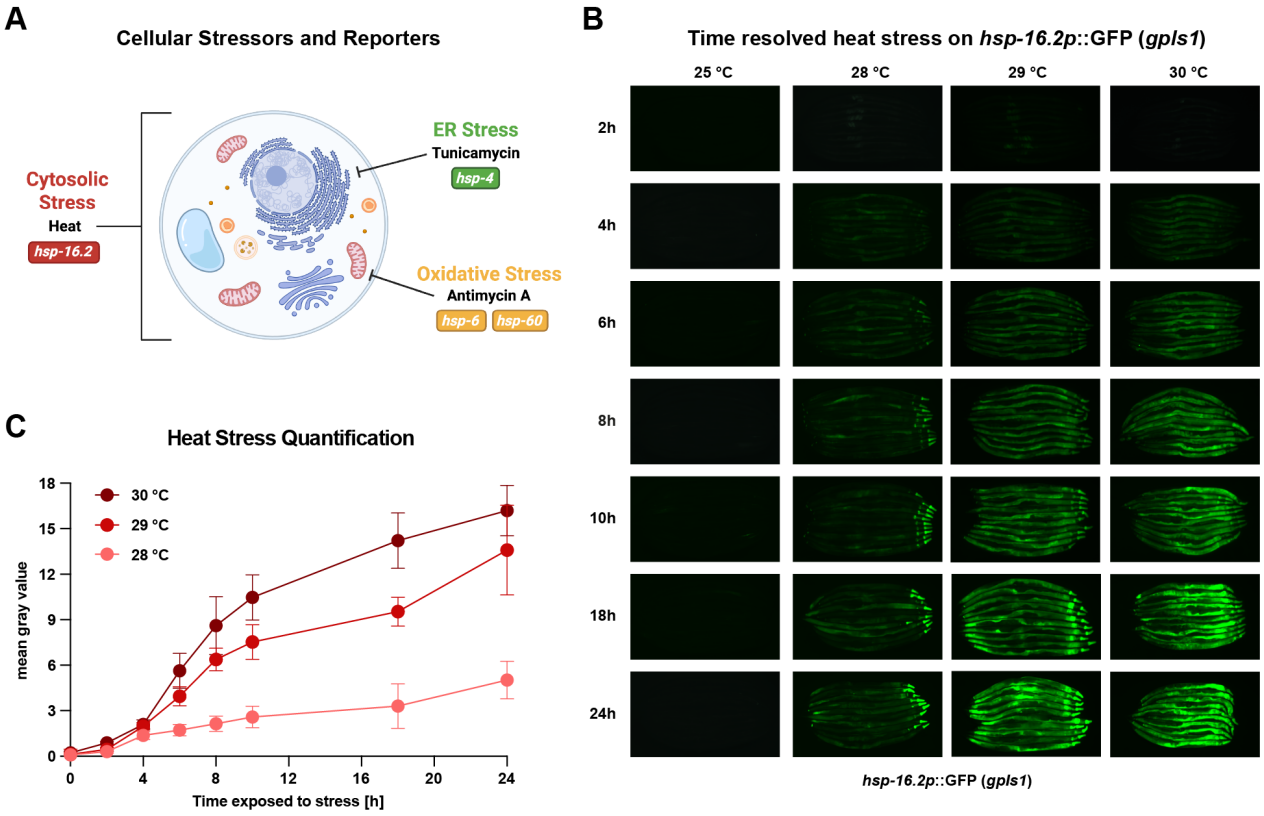

Figure 13: ***Heat stress dose finding using fluorescent hsp-16.2 reporter.*** *(A) Stress treatment overview showing respective treatments and responsive chaperones. (B) Heat stress time course at increasing temperatures comparing signal induction of day 1 adults of the fluorescent hsp-16.2p::GFP reporter. (C) Quantification of GFP signal of hsp-16.2p::GFP reporter time course measured as mean gray value of individual animals. Compared are the induction levels at 28 °C, 29 °C, and 30 °C over a duration of 24 hours.*

To outline the heat induced expression of the *hsp-16.2*p::GFP*(zcIs13)* reporter strain monitoring the cellular response to heat, we performed a time course experiment exposing day 1 animals to different temperatures over 24 hours (Fig. 13B). Worms were imaged using a fluorescent microscope to visualise GFP expression. At 25 °C, we could not detect any reporter induction in *hsp-16.2*p::GFP animals. Starting at 28 °C, we detected a steady time-dependent induction of GFP expression, increasing with higher temperature. Of note, animals treated at 28 °C presented a variation in expression pattern, as the signal appeared to be stronger in the pharynx, while remaining mild in the rest of the body. At higher temperatures, the signal was strongly increasing especially in the intestine. Quantification of the GFP, measured as mean gray value, described a dose dependent increase of reporter signal throughout the experiment (Fig. 13C). While showing a strong induction, treatment at 30 °C did not reach a plateau after 24 hours of treatment, which would indicate saturation of the response. Comparison of the signal described a great separation of the response at different temperatures, which in this context can be understood as the dose of this specific stress.

Taken together, we identified a treatment at 30 °C as a good dose for induction of the *hsp-16.2*p::GFP*(zcIs13)* reporter over 24 hours without saturating the response. Further experiments assessing intensity levels and molecular response to heat were performed at these conditions.

Determining the ideal stress dosage using fluorescent reporters: ER stress

Applying an analogous approach, we monitored the induction of the *hsp-4*p::GFP(*zcIs4*) reporter in a TM dose-response over 24 hours, to establish the ideal parameters for assessment of UPR^{ER} induction. Day 1 adult animals were transferred to TM plates, and imaged after exposure at different concentrations over 24 hours (Fig. 14A). This systematic titration from 1 to 100 μg/ml revealed a significant dose-dependent elevation in reporter fluorescence, confirming the dynamic range of the UPR^{ER} pathway (Fig. 14B). Notably, treatment at μg/ml dosage appeared to reach a plateau, suggesting a saturation of the transcriptional machinery and reinforcing the selection of a more moderate concentration for further experiments to ensure a linear rate of induction avoiding saturation. Despite the robust reporter activity, utilizing TM as a metric for physiological resilience in adult populations presented significant experimental challenges due to the absence of a measurable physiological phenotype in mature animals. Although larval development assays demonstrated a clear, dose-dependent sensitivity to TM between 1 and 4 μg/ml (Fig. 14C), we could not detect any impact on survival or locomotion in adult wild type animals at the highest used concentration of 100 μg/ml.

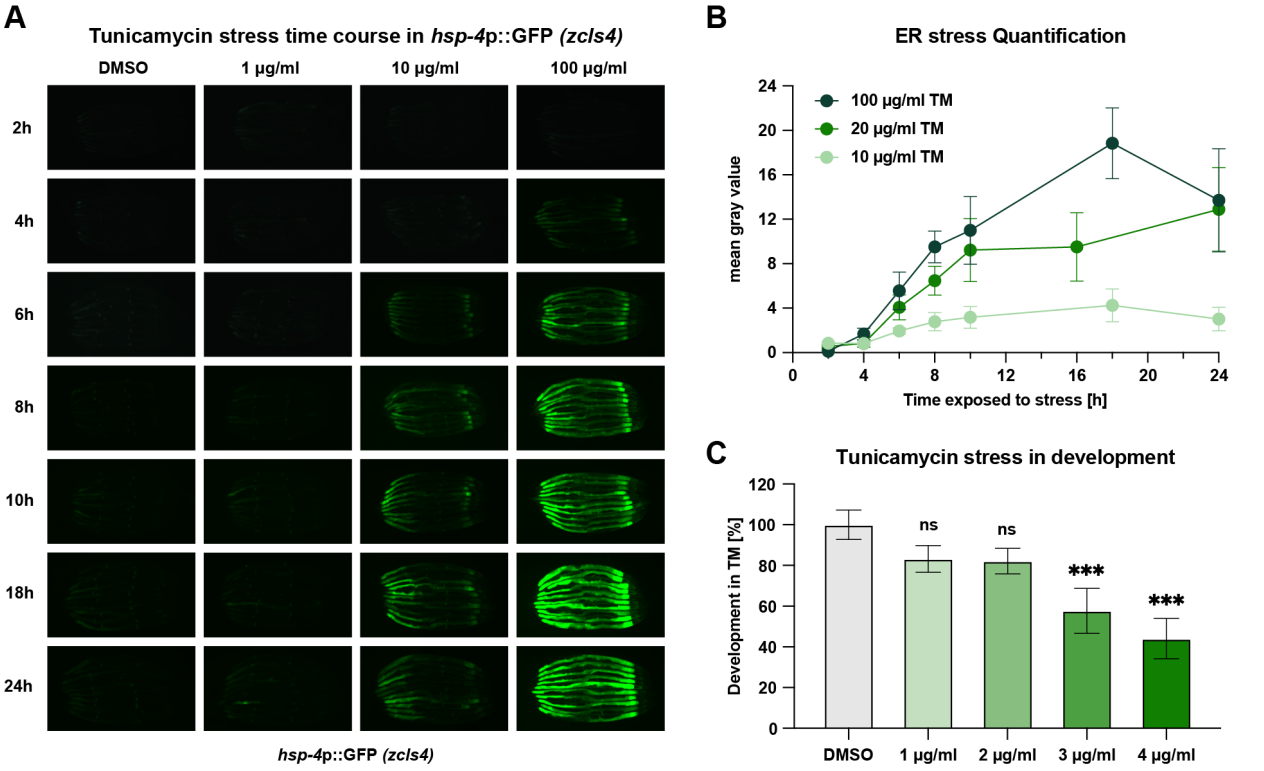

Figure 14: ***ER stress dose finding using fluorescent hsp-4 reporter.*** *(A) Tunicamycin stress time course induction of hsp-4p::GFP(zcIs4) reporter comparing GFP induction by various concentrations of Tunicamycin from 1 to 100 μg/ml over a duration of 24 hours. (B) Quantification of GFP signal of hsp-16.2p::GFP reporter time course measured as mean gray value of individual animals. Compared are the induction levels at 10, 20, and 100 μg/ml over a duration of 24 hours. (C) Development stress assay comparing development rates of wild type animals from egg to adulthood on various concentrations of Tunicamycin.*

While the *hsp-4*p::GFP(*zcIs4*) reporter presented a sensitive readout for UPR^{ER} stress induction, its utility as a proxy for survival-based stress resistance in adulthood is limited by this lack of phenotype. Consequently, based on this disconnect between molecular reporter activation and organismal resilience, we did not pursue this stress to outline differences in molecular response in RNA-seq.

Determining the ideal stress dosage using fluorescent reporters: Mitochondrial stress

Next, to assess the induction of the UPR^{mito}, we evaluated the induction profiles of fluorescent reporters induced by mitochondrial stress. Initial assessments in liquid culture demonstrated that while paraquat (PQ) treatment caused a mild up-regulation of *hsp-6*p::GFP(*zcIs13*), it failed to trigger significant expression of the *hsp-60*p::GFP(*zcIs9*) reporter (Fig. 15A-B). In contrast, exposure to AA in liquid did not yield a quantifiable fluorescent signal in either strain. It did, however, result in a clear reduction in body size and viability, which we annotated to acute organismal toxicity likely due to the severity of mitochondrial inhibition surpassing the animal's capacity for transcriptional adaptation in this experimental setup.

To overcome this acute toxicity, we adapted the treatment and attenuated concentration to 2 μM AA directly incorporated into the NGM media plates. In this context, we detected a time-dependent induction of *hsp-6*p::GFP(*zcIs13*) when placing day 1 adult animals on the plates (Fig. 15C). Notably, we established that a 24-hour exposure to moderate concentrations of 5 μM and 10 μM AA resulted in a statistically significant, dose-dependent decline in locomotion (Fig. 15D). This observation described a direct link between UPR^{mito} induction and a phenotypic deficit that can be utilized as a metric for physiological resilience in addition to the molecular readout.

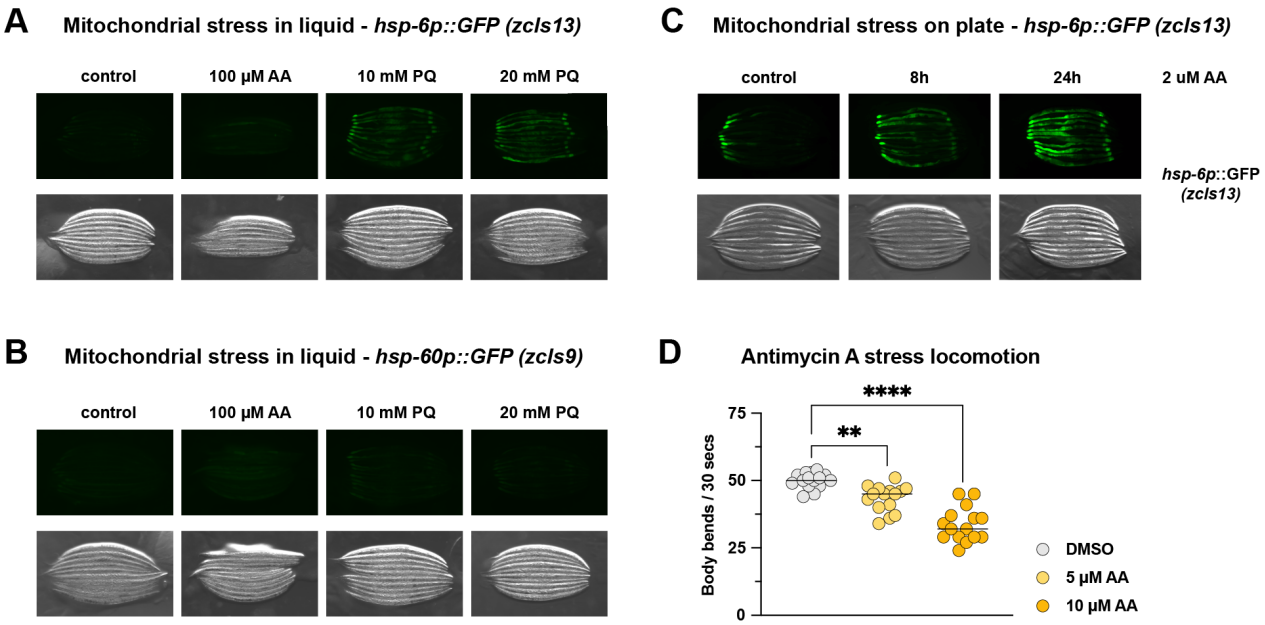

Figure 15: ***Antimycin A stress dose finding using fluorescent hsp-6 reporter.*** *(A) Antimycin A stress assay in liquid using day 1 animals of hsp-6p::GFP(zcIs13) reporter strain comparing induction of GFP in treatment with 100 μM Antimycin A, or 10 and 20 mM Paraquat. (B) Antimycin A stress assay in liquid using day 1 animals of hsp-60p::GFP(zcIs9). (C) Antimycin A stress assay on NGM plate containing 2 μM Antimycin A comparing induction of GFP of day 1 animals of hsp-6p::GFP(zcIs13). (D) Locomotion assay comparing body bend rates of wild type day 1 animals on various concentrations of Antimycin A.*

In conclusion, we showed that treatment for 24 hours at concentrations of 2-10 μM AA resulted in a stable induction of the UPR^{mito}, and a significant reduction in locomotion. By bridging the gap between mitochondrial proteostatic stress and functional decline, these findings validate the use of low-dose AA as a robust method for assessing homeostatic capacity.

2.2.2 Uncovering ISR independence of suspected *atf-4* reporter

We also aimed to include monitoring of the integrated stress response (ISR) activity in stress, as previous work of the lab focused on the benefits on lifespan and stress survival by inhibition of the ISR, highlighting the involvement of this pathway in organismal resilience (Derisbourg et al. 2021). The ISR sits at the intersection of different stress pathways sensing disturbance of homeostasis to the ER, facilitated by the PERK branch of the UPR^{ER}, and responding to metabolic disturbances signaling starvation. As the ISR converges various stress signals into a single hub, orchestrating a global shift in translation, we reasoned ISR activity would have a huge impact on resilience. To assess this, we used a published ISR reporter described to be an ISR-dependent fluorescent reporter under the promoter of the main effector, *atf-4* (Statzer et al. 2022).

To assess ISR induction and enable equivalent dose-finding experiments as described for the other reporters, we treated day 1 animals of the reporter with 50 μg/ml TM, aiming to induce the reporter via the UPR^{ER} kinase PEK-1 (Fig. 16A). As a reference, we used a reporter in the background of the ISR inhibition mutant *eif-2α (syb1385)*, which abolishes the key event required for ISR activity in the phosphorylation of *eif-2α*, and prohibiting downstream ISR signaling. Surprisingly, we detected strong levels of GFP induction in the *eif-2α (syb1385)* mutant. To understand what caused the signal, we performed this experiment in RNAi-mediated knockdown of key genes active in the response to TM stress. We uncovered that the induction was fully dependent on *xbp-1*, a main driver of the UPR^{ER} downstream of the IRE-1/XBP-1 branch, which is independent from usual ISR signaling. As this did not align with expectations of an *atf-4*p::GFP reporter, we wondered if the problem was caused by the reporter, or if there was a problem with the ISR inhibition mutant. To assess the state of the ISR in these strains, we performed a pulse-chase experiment assessing phosphorylation of *eif-2α*, incorporation of puromycin, and induction of GFP in acute stress by TM or Heat stress (Fig. 16B). We compared the protein levels of phosphorylated *eif-2α*, Puromycin, and GFP of day 1 adults of wild type, the *eif-2α (syb1385)* mutant, and an activator mutant for the reporter, E32. First, we confirmed that the *eif-2α (syb1385)* mutant did present the expected phenotype, only showing a faint band detected by the anti-phospho-*eif-2α (syb1385)* antibody, deemed to be background signal from un-phosphorylated *eif-2α*. Overall translation detected by puromycin incorporation appeared only mildly reduced in TM stress, while heat clearly reduced translation levels. Assessing GFP induction, we detected induction of GFP signal by TM in all strains, while heat did not induce the signal. The E32 activator mutant showed extreme levels of GFP throughout (Fig. 16C).

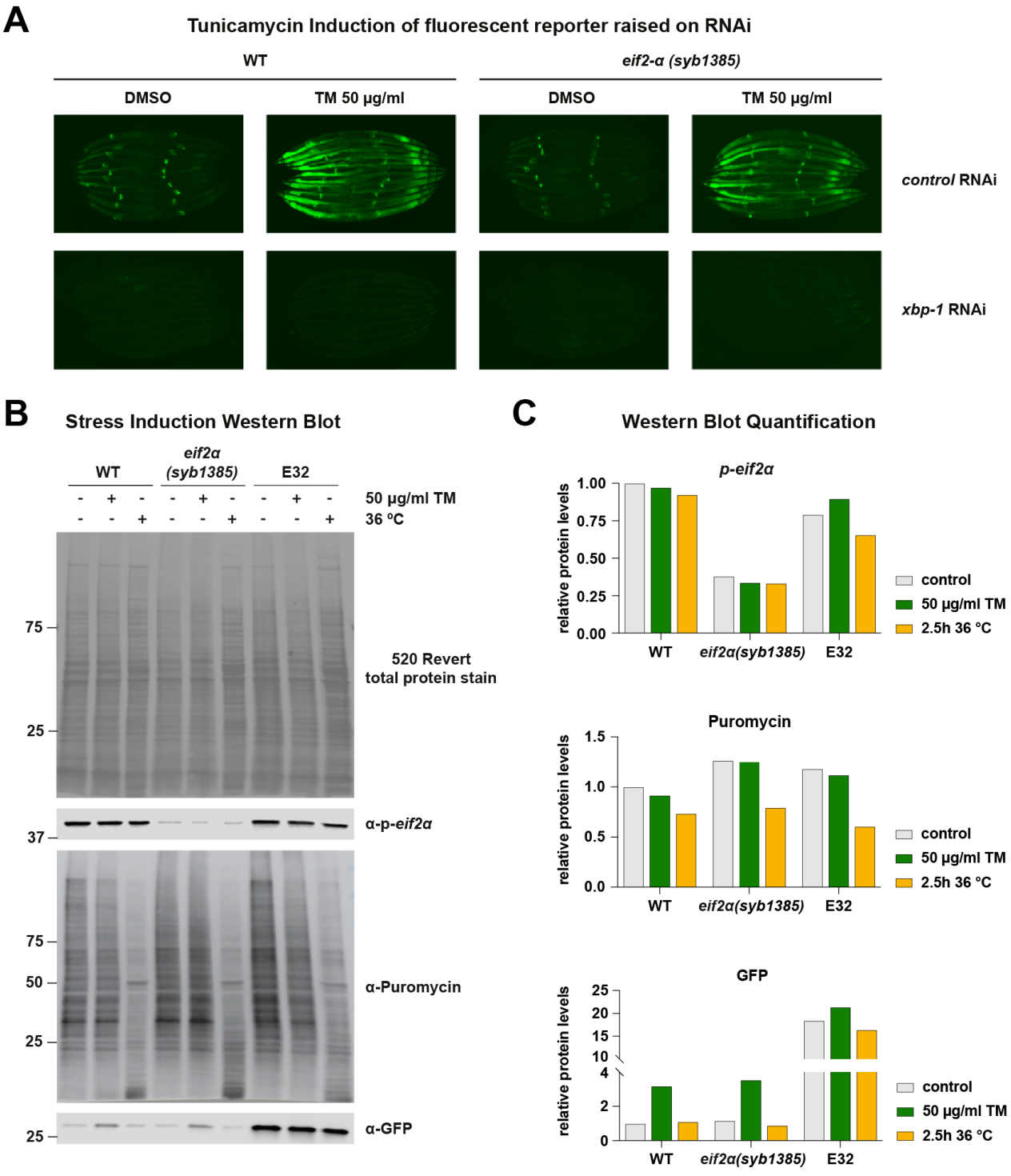

Figure 16: ***ISR mutant in heat stress and stress reporter induction.*** *(A) Tunicamycin stress assay using day 1 adults comparing wild type and ISR inhibition mutant eif-2α(syb1385) comparing GFP induction of a published atf-4p::GFP reporter in control and xbp-1 RNAi. (B) Western Blot of day 1 adult animals of wild type, eif-2α(syb1385) mutant, and E32, an activator mutant for the published atf-4p::GFP reporter. Compared are the incorporation of Puromycin into nascent proteins, and protein levels of phosphorylated eif-2α and GFP following stress treatment in liquid for 2.5h with 50 µg/ml Tunicamycin or heat treatment at 36 °C. (C) Quantification of protein levels detected in Western Blot comparing p-eif-2α, Puromycin, and GFP levels between wild type, eif-2α(syb1385), and E32 in TM and heat stress.*

Overall, we confirmed the *eif-2α (syb1385)* mutant to be an ISR inhibitor. While we did not detect any phosphorylation of *eif-2α*, it induced the GFP signal, therefore confirming the suspicion of the reporter to be ISR independent. The reduction of translation rates in heat stress was also observed in *eif-2α (syb1385)* mutant, and hence appeared to be ISR independent. This hints at an alternative mechanism involved in the reduction of translation in heat stress other than the ISR. Based on these results, we decided to sequence the reporter to understand the mechanism of its induction, as it seemed to be irregular and not aligned with the understanding of the translation of *atf-4*. Surprisingly, sequencing of the reporter revealed that indeed the promoter region was not that of the ISR effector *atf-4*, but the promoter of the well understood UPR chaperone *hsp-4*. This not just highlights the need for crucial controls, but also explains some of the obtained results, considering the reporter induction being the result of UPR^{ER} activity resulting in up-regulation of *hsp-4* via the IRE-1/XBP-1 branch of the UPR. Consequently, we abandoned any further work with this reporter.

2.2.3 *C. elegans* DMD model shows mild deficits in ER stress induction

Having determined ideal conditions for comparison of stress response pathway induction, we crossed the transgenic reporters in the *dys-1(eg33)* mutant background to assess if the changes in stress recovery are caused by changes in the ability to mount an effective stress response and to compare stress induction dynamics to the wild type. First, we compared the induction of the *hsp-16.2*p::GFP(*gpIs1*) reporter in response to heat, to identify if a variation in the canonical HSR accounted for a reduction in thermorecovery.

Heat stress reporter increases *dys-1(eg33)* hypersensitivity

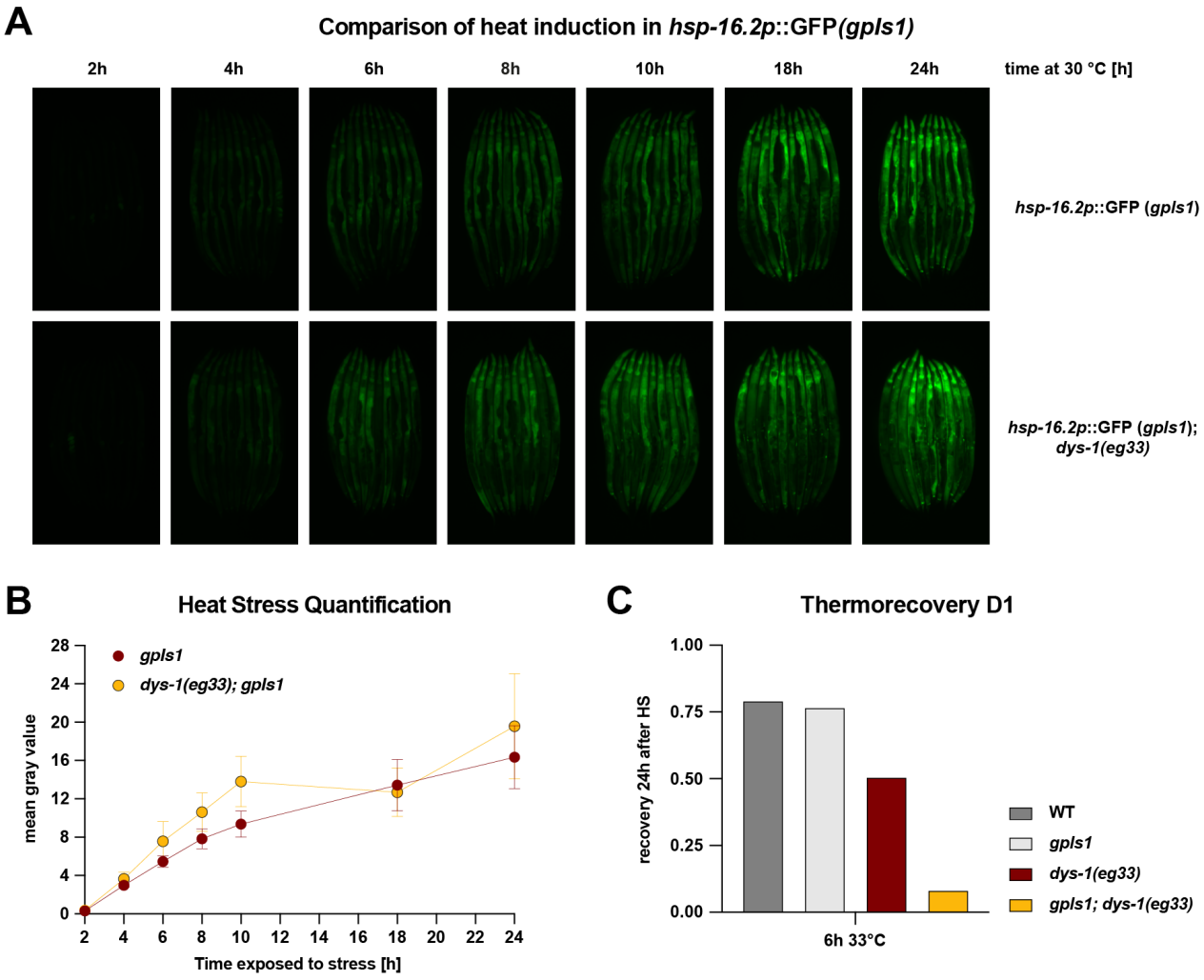

Figure 17: ***DMD mutant in heat stress reporter induction.*** *(A) Heat stress assay on day 1 adults of wild type and dys-1(eg33) mutant strains over 24 hours comparing induction of GFP in hsp-16.2p::GFP(gpIs1) reporter. (B) Quantification of GFP signal of hsp-16.2p::GFP reporter during time course induction measured as mean gray value of individual animals. Compared are the induction levels of the reporter crossed into the wild type or dys-1(eg33) mutant background. (C) Thermorecovery assay using day 1 adult animals of wild type, hsp-16.2p::GFP(gpIs1) reporter, dys-1(eg33) mutant, and a strain carrying hsp-16.2p::GFP(gpIs1) and dys-1(eg33) mutation. Compared is the recovery following heat stress at 33 °C for 6 hours.*

We exposed day 1 animals of the respective genotypes to heat stress at 30 °C over 24 hours, and quantified the signal as mean gray value (Fig. 17A-B). We could not detect a significant change in reporter signal, as the reporter in the *dys-1(eg33)* mutant background induced the signal following the same temporal dynamics and intensity as the wild type. Assessing the images at later time points it appeared that the induction in the DMD mutant was slightly "leaky", as we could see negative space in wild type induction around the area of the intestine, while *dys-1(eg33)* mutant worms showed a more uniform signal throughout the body.
To confirm that the *hsp-16.2*p::GFP(*gpIs1*) reporter by itself did not affect heat stress behaviour of the worms, we assessed the strains for thermorecovery at day 1 of adulthood (Fig. 17C). Surprisingly, we detected strongly reduced recovery rates in the dys-1(eg33) mutant when carrying the transgenic reporter. In contrast, the reporter in the wild type background did not show an increased vulnerability to heat stress, indicating that the GFP expression itself was not the cause of the drop in the *dys-1(eg33)* mutant reporter.

Overall, we showed that the *dys-1(eg33)* mutant induced the *hsp-16.2*p::GFP(*gpIs1*) reporter to the same extend as the wild type. This confirms that differences in stress recovery were not caused by changes in the canonical HSR or a delayed response to heat stress. Variation of expression pattern could indicate a less precise regulation of the induction, as the wild type expression appeared to be more defined. Additionally we found that the heat responsive reporter in the DMD background increased the sensitivity to heat stress compared to the *dys-1(eg33)* mutation alone. Aligning with the concept of finite energy availability, we theorise that this could be caused by a reduced availability of energy to respond to acute stress, as the translation machinery is occupied by the extreme expression of GFP in the reporter.

Only ER stress induction significantly varies from WT response

To analyse how the induction of the remaining transgenic reporters compares, we performed on-pathway stress induction on *hsp-16.2*p::GFP(*gpIs1)*, *hsp-6*p::GFP(*zcIs13*), and *hsp-4*p::GFP(*zcIs4*). Based on our observations in the detailed comparison of the HSR reporter, we reasoned that assessment of induction after 24 hours would be sufficient to confirm if there is a variation of stress induction in the *dys-1(eg33)* mutant, as either a delayed onset of induction or a reduced amplitude would result in a lower GFP signal.

To compare these induction levels, we transferred day 1 adults on plates containing the stress, alternatively in case of heat transferred the entire plate, and imaged for GFP after 24 hours of treatment (Fig. 18). We confirmed the results in regards to heat stress, and showed that treatment with 5 μM also recapitulated the signal induction observed in the wild type, as we could not detect a significant difference in induction of the *hsp-6*p::GFP(*zcIs13* reporter upon treatment for 24 hours (Fig. 17C-D). We then assessed the signal intensity of the *hsp-4*p::GFP (*zcIs4*) reporter in treatment with 20 μg/ml TM over 24 hours to investigate the response of the DMD model to UPR^{ER} stress. Here, we uncovered a significantly weaker GFP induction in the DMD model upon treatment with TM (Fig. 17E-F). While all individual animals were able to induce the reporter, the intensity was visibly lower.

In conclusion, we did not find any evidence that the detected stress hypersensitivity of the *dys-1(eg33)* mutant in heat and mitochondrial stress was linked to an alteration in the canonical stress responses activated in response to the respective stress. While we did detect a significantly lower induction of GFP in the *hsp-4*p::GFP (*zcIs4*) reporter during TM induced ER stress, we could not connect this to an increased sensitivity in any physiological readout, and therefore we could not leverage this reduction to a reduced stress resilience.

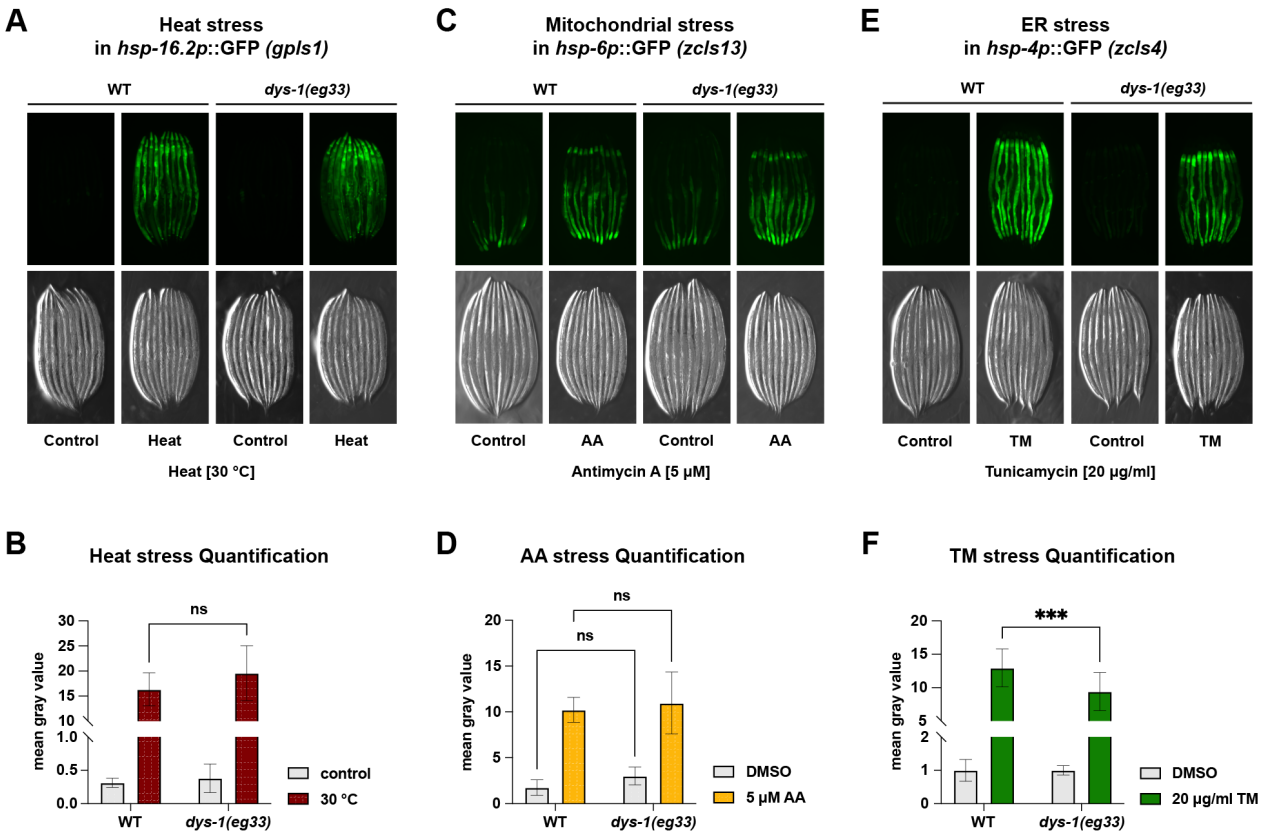

Figure 18: ***Fluorescent stress reporter induction in dys-1(eg33) mutant.*** *Stress induction of GFP signal in fluorescent reporter strains using day 1 adult animals of wild type and dys-1(eg33) mutant, crossed into the respective reporter strains. (A) GFP induction of hsp-16.2p::GFP(gpIs1) reporter following heat stress at 30°C for 24 hours. (C) GFP induction of hsp-6p::GFP(zcIs13) reporter following stress treatment on 5 µM Antimycin A for 24 hours. (E) GFP induction of hsp-4p::GFP(zcIs4) reporter following stress treatment on 20 µg/ml Tunicamycin for 24 hours. (B)(D)(F) Quantification of GFP signal of the respective reporter measured as mean gray value of individual animals. Compared are the induction levels in wild type and dys-1(eg33) normalised to the respective background signal.*

2.2.4 Elucidating stress response connectivity

While we used the transgenic reporters to investigate the stress-dependent induction of individual pathways, we argue that resilience comprises the complex interplay of a multitude of molecular responses. Based on this, we would expect cross-talk between local response pathways as a result of perturbation determining a combined stress response capacity. Previous research has described the induction of the *hsp-4*p::GFP*(zcIs4)* reporter in heat stress (Yoneda et al. 2004), however, they did not cover a time component in this context. To further investigate such a cross-talk, we extended the use of the fluorescent reporters from on-pathway stress to comparative treatment with all three to determine if they are also affected in stresses targeted at different mechanisms. Considering dose-finding experiments, we decided that imaging after 8 and 24 hours at the determined concentrations should be sufficient to probe for induction of GFP signal in the reporter strains.

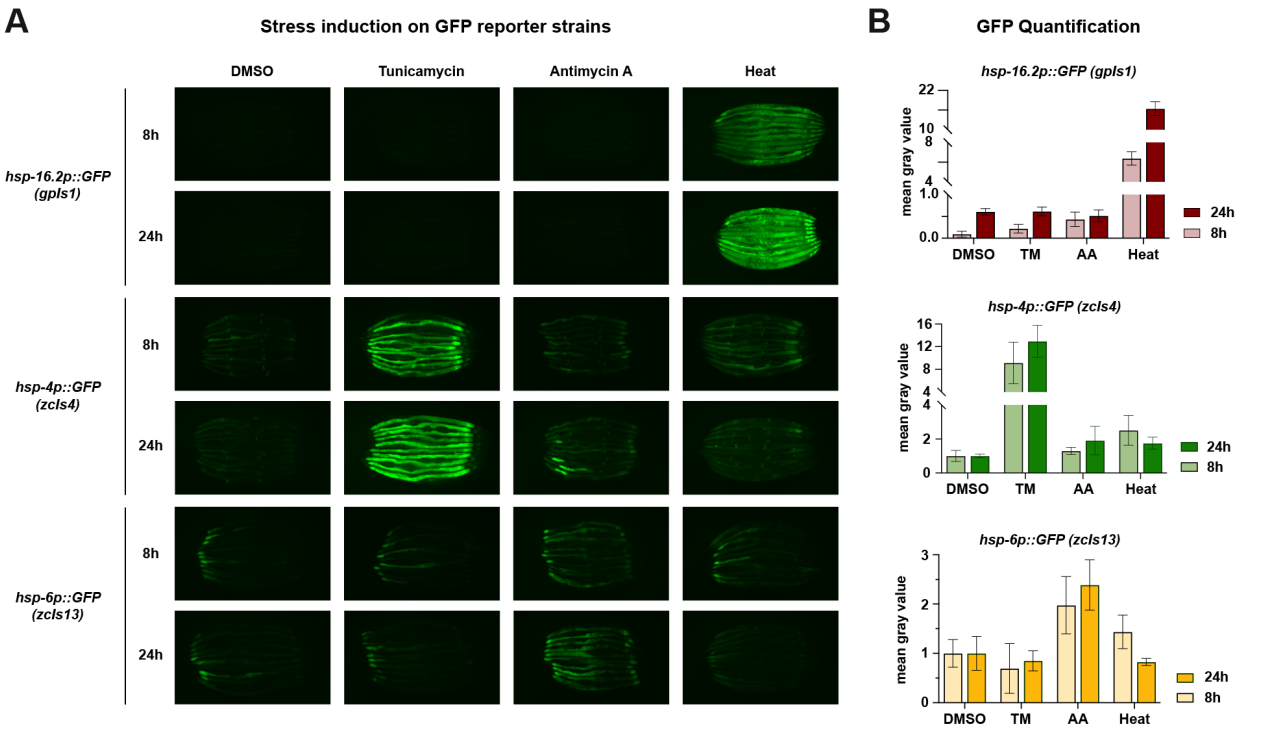

Figure 19: ***Cross-stress treatments on fluorescent reporters.*** *(A) Stress induction assay on day 1 animals of fluorescent reporter strains hsp-16.2p::GFP(gpIs1), hsp-4p::GFP(zcIs4), and hsp-6p::GFP(zcIs13) comparing GFP induction during treatment with 20 μg/ml Tunicamycin, 5 μM Antimycin A, or 30 °C. Induction was assessed by imaging after 8 and 24 hours. (B) Quantification of GFP signal of the respective reporter measured as mean gray value of individual animals. Compared are the induction levels during the stress treatment after 8 and 24 h normalised to the respective background signal.*

To address this, we imaged day 1 animals of the transgenic reporters after 8 and 24 hours of treatment with TM, AA, and thermal stress to obtain a comprehensive overview of reporter induction in response to these stresses (Fig. 19A). We found the *hsp-16.2*p::GFP (*gpIs1)* reporter showed increasing strong induction from 8 to 24 hours of heat stress, and was not induced by TM or AA. As expected, we detected a gradual increase in *hsp-4*p::GFP(*zcIs4*) signal in treatment with TM. However, we also saw a mild increase of signal in thermal stress of this reporter, which was mostly detectable after 8 hours, but not 24 hours of treatment. Additionally, AA also showed some fragmented induction in the *hsp-4*p::GFP(*zcIs4*) reporter at the 24 hour time point,

which appeared to be restricted to the distal intestine. Assessment of the *hsp-6*p::GFP(*zcIs13*) reporter showed a consistent background signal, but was significant induced upon treatment with AA (Fig. 19B). Quantification revealed a mild increase in *hsp-6*p::GFP(*zcIs13*) expression upon heat stress after 8 hours, and a mild reduction after 24 hours, as the background signal appeared to be reduced.

Overall, the on-pathway stresses did show the strongest induction in their respective reporters. The effects of thermal stress, however, appeared to be very broad and impacted all reporters. As this stress exposes the full organism to environmental changes, the entirety of a cell is subject to extensive heat stress, causing misfolding not only in the cytosol but globally. It was therefore not surprising to see this effect, however, it shows that there is an overlap of stress response mechanisms, as described in previous research (Yoneda et al. 2004). This indicates that the UPR^{ER} partially buffers the damage induced by thermal stress. We therefore state that the damage induced by heat stress is not in its totality resolved by the canonical HSR alone, and that homeostatic capacity in this scenario comprises additional mechanisms. Furthermore, the observed reduction of the background reporter signal of the *hsp-6*p::GFP(*zcIs13*) reporter in this context is intriguing, as this would not imply the active involvement of the UPR^{mito} in heat stress. Regarding the observation of fragmented induction of the *hsp-4*p::GFP(*zcIs4*) in AA stress, we assessed the literature for potential explanations. While not describing this effect in a transgenic reporter, increased transcript levels of *hsp-4* have been found in over-activation mutants for the UPR^{mito}(Soo et al. 2021a). However, the distinct pattern describing fragmented induction in the distal intestine remains to be explained.
Taken together, we found evidence showing a certain level of overlap of stress responses using transgenic reporters. Future research could focus on the nature of this overlap to discern if there is a direct interaction, or if this is mediated by secondary effects in the event of elevated energy demands in the cell during stress conditions.

Implications from the analysis of stress dynamics using transgenic reporter strains

In summary, studying the induction of stress response pathways using transgenic fluorescent reporters has proven valuable and expanded our understanding of stress response mechanisms underlying resilience. We outlined the dynamic induction of the canonical HSR in thermal stress and the UPR^{ER} by TM stress, and explored the induction of the UPR^{mito} during AA stress. This informed the comparison of stress induction of the *dys-1(eg33)* mutant, which revealed a reduced induction of the *hsp-4*p::GFP(*zcIs4*) reporter in TM stress, while reporters for heat and mitochondrial stress did not show significant variation. Hypersensitivity of the DMD model in heat and mitochondrial stress could therefore not be ascribed to malfunction of the canonical response mechanisms or reduce molecular responsiveness. Therefore, we utilised the established parameters to design a time course RNA-seq, to investigate not just individual stress response genes in transgenic reporters, but the global transcript changes unfolding during exposure to thermal stress over 24 hours.

Assessment of the ISR suggested that there is a distinct mechanism in the reduction of mRNA translation rates in heat stress, as the ISR inhibition mutant *eif-2*α *(syb1385)* still showed strong reduction in nascent protein levels following thermal stress. In regards to stress response cross-talk, we showed that thermal stress also affects the UPR^{ER}, and to a limited extent the UPR^{mito}. Furthermore, we detected fragmented expression of *hsp-4* in mitochondrial stress, describing a locally restricted connection of mitochondrial stress and the UPR^{ER}.

2.3 Transcriptome analysis in heat stress reveals baseline and dynamic changes in *C. elegans* DMD

As analysis of canonical response pathways with transgenic reporters failed to uncover causal changes for hypersensitivity in *dys-1(eg33)* mutants, we decided to analyse the global response to heat stress using RNA-seq in a time course of heat stress over 24 hours. By this, we aimed to capture the broader stress response and not only individual reporter genes. Having established key parameters of the stress treatment, we used the transgenic reporter induction as a proxy for global stress induction in TM and thermal stress. Based on the lack of a phenotype in day 1 adults during TM stress, and considering the significant changes in thermorecovery in the DMD model, we decided to use heat stress as the treatment in RNA-seq.
We assessed the literature for comparable experiments that could inform our experimental design. Investigation of transcriptomic changes has previously been addressed in the ts mutant *gon-2(q388)* (Roux et al. 2022), which fails to develop gonads at the non-permissive temperature of 25 °C (Sun and Lambie 1997). This is intended to avoid contamination by the germline, which accounts for a significant portion of the total mRNA and protein in the adult hermaphrodite (Reinke et al. 2000). Since we intended to use heat as the stress in our experiment, we abandoned the idea of using the *gon-2(q388)* mutant, as it would require application of heat prior to the stress treatment, which would alter the molecular response. Additionally, this method itself is not without fault, as other studies in addition to our observations in earlier experiments have documented an incomplete penetrance of the sterility phenotype (Roux et al. 2022).
We therefore opted for the use of chemical inhibition of propagation using the thymidylate synthase inhibitor 5-fluoro-2-deoxyuridine (FUdR). An important consideration was the effect of FUdR treatment on homeostasis, as it has also been described to affect HSR capacity and proteostasis (Shalgi et al. 2013). Considering the available options, we decided to proceed with the use of FUdR to induce sterility, using minimal concentrations, as we reasoned that the effects would be normalised with all worms raised at the same conditions.
Adding an insight into heat response dynamics, we found a data set describing temporal dynamics of *C. elegans* over a period of 12 hours of treatment at 35 °C (Jovic et al. 2017). This might help to outline HSR markers and trends, however, the choice of a severe stress presents a limitation of this study. We argue that dynamic changes in this data set are masked by saturation of the HSR and contaminated by signatures of dead worms as a consequence of lethal stress at later time points. By using a more moderate stress, we intended to cause a more consistent induction of the HSR without overwhelming the system. This was intended to ensure a good separation of time-dependent processes and produce a high-resolution data set that supports identification of subtle changes in the comparison of wild type and *dys-1(eg33)* mutant animals. Ultimately, we wanted to identify gene changes that could explain a stress hypersensitivity in the DMD model, and test these variations for a causal impact on thermorecovery in physiological recovery assays.

RNA-seq time course: experimental setup and quality control

To ensure our data set enables a detailed analysis covering mild expression changes and time-dependent separation, we carefully set the experimental parameters supported by transgenic reporter experiments. We decided to perform this experiment using heat stress at 30 °C, as this was sufficient to strongly induce the HSR without saturating it over 24 hours. Additionally, we decided to include untreated negative controls for every time point, as we reasoned that the animals age a full day throughout the experiment, which represents a significant proportion of their overall lifespan. Normalisation of the heat stressed samples to their respective negative control would thereby reduce variation and noise in the data.

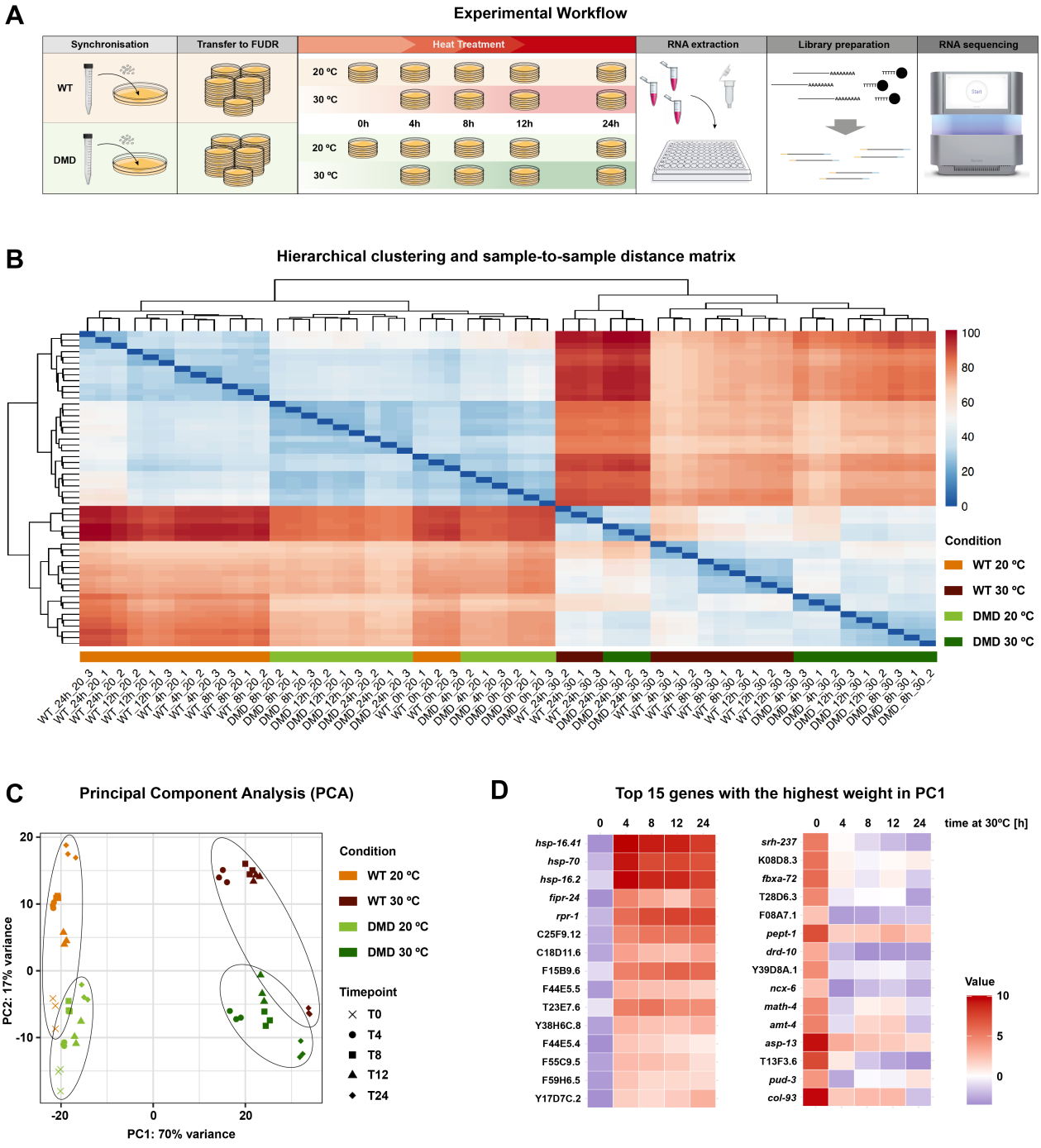

Figure 20: ***Experimental workflow and quality control.*** *(A) RNAseq experimental overview: wild type and dys-1(eg33) mutant animals were synchronised and raised on NGM plates until L4 larval stage. They were washed over to NGM plates containing FUDR to prohibit hatching of larvae during the experiment. Day 1 adult worms were heat stressed for 24 hours, with samples collected after 0, 4, 8, 12, and 24 hours. Worms were collected in TRIreagent for RNA extraction, library prep and sequencing was performed from randomised 96-well plates. (B) Hierarchical clustering and distance matrix showing similarity across each sample and condition. (C) Principal component analysis (PCA) for combined replicates of each condition. Analysed were all expressed transcripts; merged isoforms >10RPM. (D) Top 15 genes with the heaviest weight in PC1, up- and down-regulated.*

Adult populations of wild type and *dys-1(eg33)* mutant worms were synchronised and seeded on 10 cm NGM plates (Fig. 20A). *dys-1(eg33)* worms were synchronised 3 hours ahead of the wild type to normalise for a mild delay in development, and ensure all worms reach adulthood at the same time. After 62 hours at the L4 larval stage, the animals were transferred to plates containing FUdR to ensure sterility throughout the experiment. After 24 hours on FUdR plates, treatment was started by placing plates randomised in a large incubator at 30 °C. In parallel, control plates were kept at 20 °C, to normalise for aging-related changes. To achieve sufficient coverage of the response, we decided to collect samples in triplicates after 4h, 8h, 12h, and 24h of treatment at 30 °C. Following treatment, samples were collected in ice-cold buffer and stored at −80 °C until RNA was extracted in three replicate groups. RNA was extracted, purified, and handed over to the Altos Genomics Hub in a randomised 96-well plate for library preparation and RNA sequencing. The library preparation was performed using polyadenylated (Poly(A)) RNA Capture, selecting for protein-coding mRNAs. The samples were sequenced at 30 million reads per sample (RPS) depth on a Illumina NextSeq platform.

Following mapping of the reads to the *C. elegans* genome and technical quality control, we assessed overall sample variation and analysis of data quality by comparison of sample similarity. Hierarchical clustering in a sample-to-sample distance matrix showed that all replicates clustered together, with a clear separation between samples that were raised at 20 °C and 30 °C (Fig. 20B). While most of the samples of the same genotype clustered together, there were two outliers of this trend with the untreated wild type samples at time point 0 (T0), and the treated DMD samples at T24, clustering more with the respective treated or untreated wild type samples.
Principal component analysis (PCA) showed clustering of the four main conditions separated by temperature and genotype, with PC1 accounting for 70% of sample variance, and PC2 describing 17% variance (Fig. 20C). To understand the gene expression changes that drive this separation, we assessed the genes that had the strongest impact of separation by PC1. For this, we mapped the top 15 up- and down-regulated genes with the heaviest weight in PC1 in a heat-map, comparing their expression in the wild type throughout the experiment to visualise their overall expression trend in heat stress (Fig. 20D).

Overall, visualisation of the data in PCA portrayed robust data, as all samples clustered with their respective replicates. Separation of samples in PC1 was clearly driven by the factor stress, as samples were separated by treatment at 20 °C and 30 °C, respectively. PC2 appeared to have some aspect of genotype, but the wild type samples of untreated T0 and treated T24 showed more similarity with the DMD samples, showing that there were more aspects driving the variance described by PC2. Additionally, there appeared to be a directional time component separating samples in PCA, with the untreated samples clustering together in PC1, and showing time-dependent progression along the y-axis in PC2. The treated samples described a time-dependent progression along the x-axis in PC1, with the samples at T8 and T12 clustering closely together for both genotypes. As we identified stress treatment to be a major factor described by PC1, we understood this as a promising trend, as it indicated a change in gene expression pattern throughout this time course, which could be caused by dynamic changes. This was supported by initial assessment of the genes with the heaviest weight in PC1, as especially the up-regulated genes showed a high representation of key drivers of the heat shock response with *hsp-16.41*, *hsp-70*, and *hsp-16.2*.

2.3.1 Discovery of novel trends by analysis of heat shock response dynamics

Differential expression analysis was conducted using the limma-voom pipeline, as it offers a sophisticated linear modeling framework that is particularly well-suited for large-scale data sets with complex experimental designs (Law et al. 2014). While DESeq2 is highly sensitive for studies with small sample sizes due to its shrinkage estimation of dispersion, limma demonstrates superior computational efficiency and robust error rate control when handling high-volume studies. As this analysis included 54 transcriptomes across four distinct conditions, limma was prioritized for its ability to maintain high statistical power while effectively mitigating the influence of outliers by precision-weighting transformation. Consequently, this model provided the most stable and conservative platform for identifying authentic stress-induced transcriptional changes within our multi-condition comparison.

Changes of the canonical heat shock response

We reasoned that to discern changes in the response of the *dys-1(eg33)* worms, we would first have to understand the response mechanisms to heat stress in the wild type, and how they develop throughout the time course. To assess the initial response and confirm trends of the canonical HSR, we analysed the wild type transcript changes after 4 hours of treatment, comparing wild type T4 at 20 °C and 30 °C. Visualising significant changes in a volcano blot revealed 784 genes to be significantly weaker, and 411 genes to be significantly stronger expressed in heat stress at T4. The genes with the highest positive and negative fold-change were portrayed in a heat-map, covering their expression changes throughput the experiment (Fig. 21A-B). These revealed that most of the genes showing higher expression had their strongest expression levels at this time pint, while the genes showing reduced expression were consistently reduced throughout the heat treatment. Assessment of gene onthology (GO) revealed involvement of processes related to response mechanisms to protein unfolding, a major event in heat-mediated stress, and defense mechanisms of the innate immune response to bacteria among the top hits in up-regulated expression (Fig. 21C). GO terms of Biological Processes down-regulated in heat stress were dominated by representation of genes associated with proteolysis (Fig. 21D). We further found representation of genes related to fatty-acid metabolisms and amino acid transport.

As expected, we found the main drivers of the HSF-1-dependent heat shock response to be up-regulated after 4 hours of heat stress. The strongest effects were found in the expression of the heat responsive chaperones *hsp-16.2*, *hsp-16.11*, *hsp-16.41*, and *hsp-70*. Additionally, we found certain genes to be strongly up-regulated in heat that have not been described as drivers of the response with *rpr-1*, *fipr-24*, and *oac-14*. Comparison of the expression pattern throughout the experiment showed that the expression of these genes also followed the same trend as the HSF-1-dependent response, with a clear peak of expression at T4, before slightly dropping expression levels at later stages. Based on significant changes after 4 hours of heat stress, we found the GO terms of up-regulated genes to be related to known heat response mechanisms like the up-regulation of chaperones in response to unfolded proteins, as well as the general defense mechanisms to perturbation. Assessment of the genes down-regulated in heat stress did not show clear heat stress signatures as in the up-regulated genes. However, we did identify genes with significantly reduced expression connected to structural components and extracellular matrix (ECM), with certain collagens being amongst the genes with the strongest reduction in transcript levels. Additionally, we found proteolysis to be the biggest gene group to show reduced transcripts in heat stress, with the aspartyl protease *asp-13* showing the strongest drop in expression levels at T4.

Taken together, analysis of temperature dependent changes at T4 confirmed the induction of the canonical HSR, and served as a robust positive control for the treatment. GO term analysis did partially show the up-regulation heat-induced chaperones of the HSR, but also showed involvement of the response mechanism of the innate immune response. Comparison of GO terms associated with down-regulated genes revealed a strong trend of reduced proteolysis in heat stress.

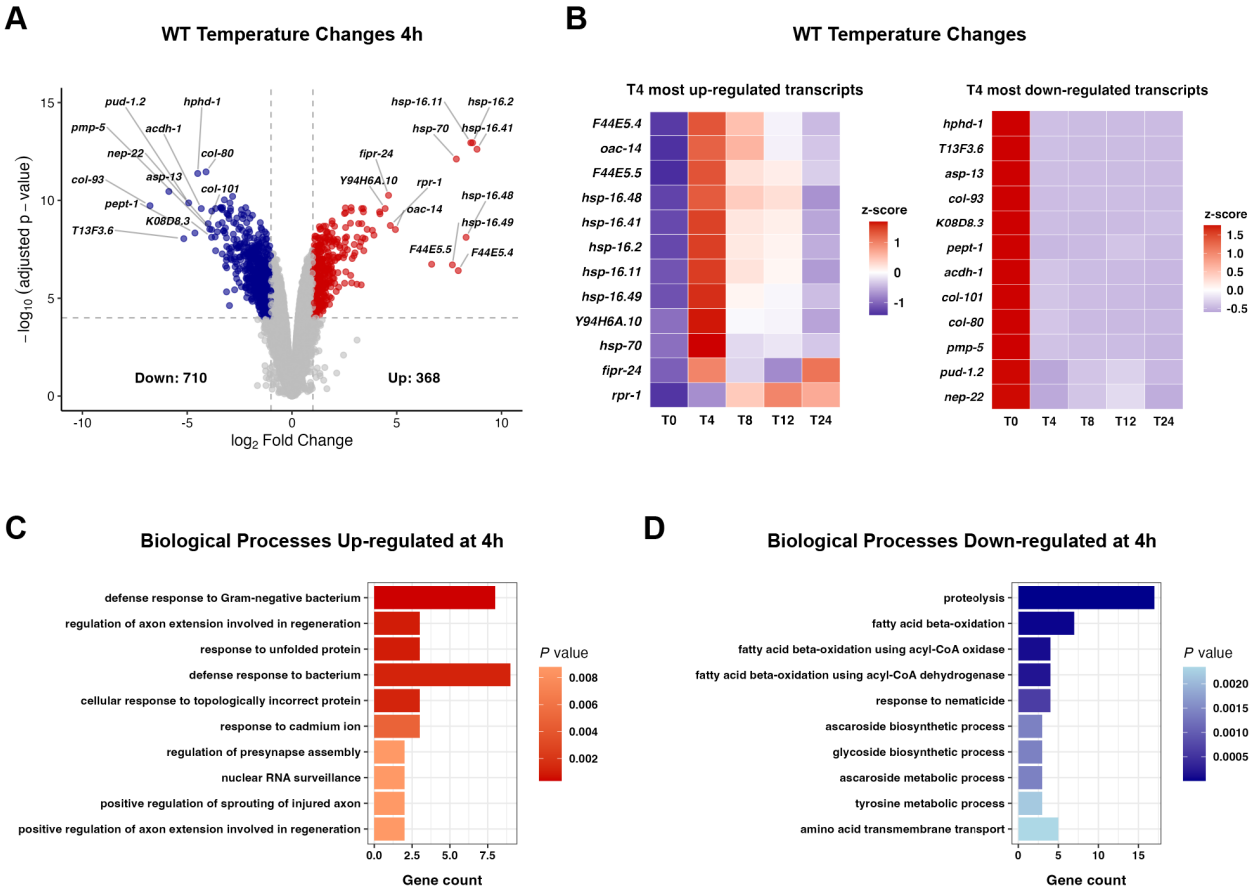

Figure 21: ***The canonical heat shock response after 4 hours at 30 °C.*** *(A) Volcano plot comparing merged transcript isoforms >10RPM of wild type day 1 animals raised at 20 °C or 30 °C after 4 hours of treatment. (B) Heatmap of the 10 genes with the highest positive and negative FC in expression between 20 °C and 30 °C comparing their expression at different time points. (C) Biological Processes GO terms of genes significantly higher expressed at 30 °C after 4 hours of heat stress (RED). Biological Processes GO terms of genes significantly lower expressed at 30 °C after 4 hours of heat stress (BLUE).*

Time-resolved dynamics of the canonical HSR

Following the validation of canonical HSR signatures at the initial time point, we sought to characterize the temporal progression of the transcript level changes throughout the experiment. First, we analyzed the expression of the most highly altered genes from the T4 time point (Fig. 21B), before systematically mapping global transcript level changes across all time points. To differentiate between consistent and transient stress signatures, we overlapped transcript changes of significantly changed genes of different time points against each other, to identify if changes occurred at precise time points or were present throughout. This comparative

approach enabled us to delineate how the thermal stress affected the genetic landscape over time, identifying consistent responses versus dynamic changes.

We selected main drivers of the HSF-1-dependent HSR, which we identified to be among the strongest increases of transcript levels at T4, and assessed their expression levels throughout the experiment (Fig. 22A). All selected genes described a similar trend, showing an explosive increase in transcript levels at T4, and declining after this initial peak. This reduction after T4 was in most cases gradual, and described a sharp drop in *hsp-70* from T4 to T8, before maintaining expression at this level. After 24 hours, the detected transcript levels had reduced strongly from T4, however, remained to be significantly higher compared to the untreated control. Based on this difference in the response of individual genes, we wondered what the overall response after 24 hours looked like, and how it compared to the changes at T4. Visualising significant gene expression changes at T24 by volcano blot, we found HSR genes to remain among the strongest up-regulated genes (Fig. 22B). Overall, we detected 2265 genes to show significantly lower, and 719 genes to present significantly higher transcript levels in heat stress after 24 hours.
We then compared the genes with significantly changed transcript levels at T4 and T24, to assess the overlap of differential gene expression of the early and late response to heat stress (Fig. 22C-D). Of the genes showing higher expression in heat stress, 25.4 % were exclusively detected at T4, 17.2% were shared between the time points, and 57.4 % were only found at T24. Assessment of the genes which showed a reduction in transcript levels, we found 4.9 % only at T4, 28.1 % were found in both groups, while 67.1 % were only detected to present significantly reduced expression at T24. This lead us to wonder how the significantly changed gene expression lists overlap, addressing the difference in all time points. To see if we can further categorise differential gene expression, we compared the gene lists at the four time points, describing this overlap in an UpSet plot of up- and down-regulated expression in heat stress (Fig. 22E-F). The largest group of significant gene changes in both groups was compiled of changes that only occurred at T24. Among up-regulated genes, we found the next biggest groups to be gene changes that were detected at T8 to T24, only at T4, and then changes that were present at all time points. In the down-regulated genes, we found consistent changes at all time points to present the second largest group, with T8-T24 the third, and T12-T24 the next biggest groups.

Overall, there was a very clear time-dependency in the development of transcript level changes throughout the experiment. Key genes of the canonical HSR described a transcript "burst" in early heat stress, before gradually returning to more moderate, albeit still elevated transcript levels. This development described a type of adaptive effect as a result of an adaptation to the new conditions, and developing towards the establishment of a new equilibrium of the system.
Comparison of genes significantly changed in expression at all time points revealed a surprisingly small fraction of overlapping changes, especially between T4 and T24. We only found 141 genes to be up-regulated at all time points, while the group of down-regulated genes at all time points was slightly bigger with 502 genes. We detected a significantly higher number of genes that showed variation at T24, indicating that the long-term exposure to stress has wide reaching effects that only become measurable at later stages. We further attempted to discern these and identify if it presents an overall increase in gene expression variation, or if we can identify precise mechanisms impacted at this time point. As UpSet graphs only show the overall presence of a gene in multiple lists, it did not let us assess the specific trajectory, or over-representation of a certain group of genes. To identify more refined changes, we assessed if we could group gene changes into clusters or describe specific trends, as the heat stress response appeared to be a highly dynamic process.

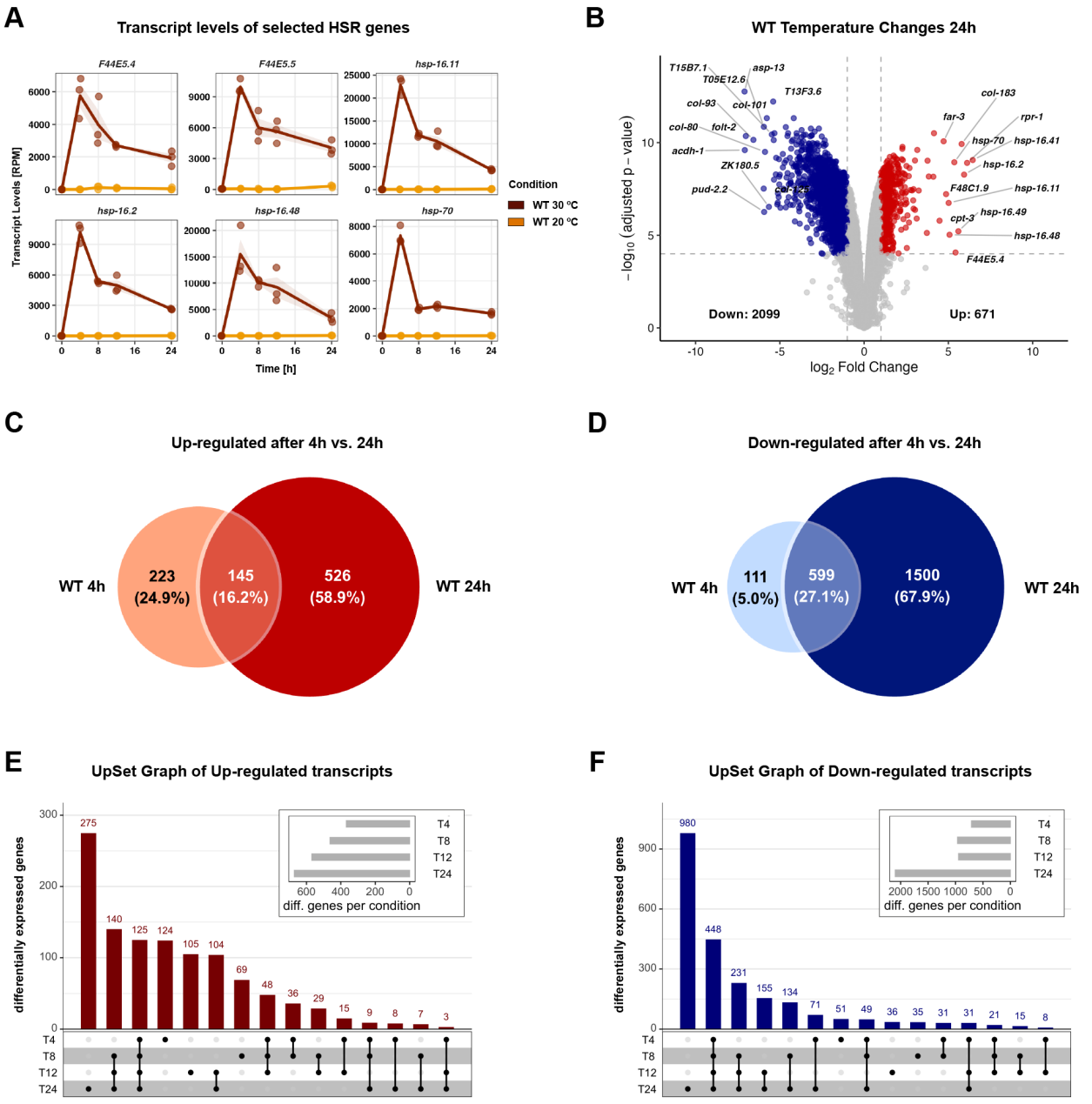

Figure 22: ***Overlap of heat shock dependent expression changes at different time points.*** *(A) Volcano plot comparing merged transcript isoforms >10RPM of wild type day 1 animals raised at 20 °C or 30 °C after 24 hours of treatment. (B) UpSetGraph representing the overlap of gene transcripts significantly changed at any of the time points during exposure to 30 °C. (C) Venn diagram showing overlap of transcripts significantly increased at 4 and 24 hours of treatment at 30 °C. (D) Venn diagram showing overlap of transcripts significantly reduced at 4 and 24 hours of treatment at 30 °C. (E) Biological Processes GO terms of genes significantly higher expressed at 30 °C after 24 hours of heat stress. (F) Biological Processes GO terms of genes significantly lower expressed at 30 °C after 24 hours of heat stress.*

Novel trends in the heat shock response

To identify trends of expression changes in the time resolved response to heat stress, we performed k-means clustering of z-score normalised gene expression as an unbiased approach of grouping genes by their expression pattern. To reduce noise and focus on heat induced changes, we selected genes that showed significantly increased or decreased expression at any of the time points. We identified a good separation of clusters by grouping them in 12 individual clusters, ensuring a clean separation of trends without any significant outliers, representing grouped expression behaviour. Following clustering we assessed clusters for representation of novel trends by looking for gene groups that are not described in the canonical HSR. By investigation of genes in these gene groups and trends we intended to facilitate the identification of changes in global trends of gene expression patterns to ultimately compare them to DMD transcripts to identify causes for stress hypersensitivity.

We categorised the produced probe trend plots into three sub-groups, with genes either showing an upwards trend, an overall downward trajectory, or showing a transient up- or down-regulation which returned to similar expression levels at the negative control. Here, we confirmed that most genes were in fact down-regulated, with a clear separation of gradual reduction or rapid drop in transcript levels at T4 (Supplementary Fig. 1). We analysed genes and gene groups annotated to respective clusters, and further investigated gene groups that showed dynamics that have not previously been outlined in the HSR. The two biggest clusters were cluster 4 and 8, comprised of genes with a strong down-regulation in heat stress. Cluster 4 (Fig. 21A) included 808 genes following this trend, which showed a strong decline in transcript levels from T0 to T4, before continuing on a softer decline for the remaining experiment. Assessing this cluster further, we identified a group of aspartyl proteases to be well represented in this cluster. Next, we analysed the biggest cluster with 1053 genes showing a reduction of transcript levels to almost 0 at T4, and staying at low transcript levels for the remainder of the stress treatment (Fig. 21C). This cluster included genes from the mitochondrial genome, which showed a rapid drop of transcript levels throughout and remained low until the end. Finally, we were interested in a cluster of 68 genes which showed a significant increase in transcript levels in the middle time points, before returning to near baseline levels at T24 (Fig. 21E). Here, we found a group of histones to contribute to this cluster, with the strongest increase in expression levels coming from *his-38* and *his-40* (Fig. 21F).

Overall, it appeared that there was a clear separation of gene expression, which we categorised in defined clusters. The canonical HSR genes reached their highest expression levels after 4 hours before slowly dropping again throughout the time course. Next to the expected transcription changes described extensively in the HSF-1-dependent HSR, we detected trends in the data that pointed us towards unexpected mechanisms and changes that we considered potentially causal in hypersensitivity. The most persistent and significant trend we found throughout the experiment was the down-regulation of genes related to proteolysis (Fig. 21D). Strikingly, we identified a group of aspartyl proteases to contribute to this effect, with a gradual reduction in transcript levels throughout the experiment (Fig. 23B). In addition to this significant trend, we found another strong change assessing the trends with a consistent down-regulation in heat stress. Here, we detected a strong representation of mitochondrion related genes (Fig. 23D).

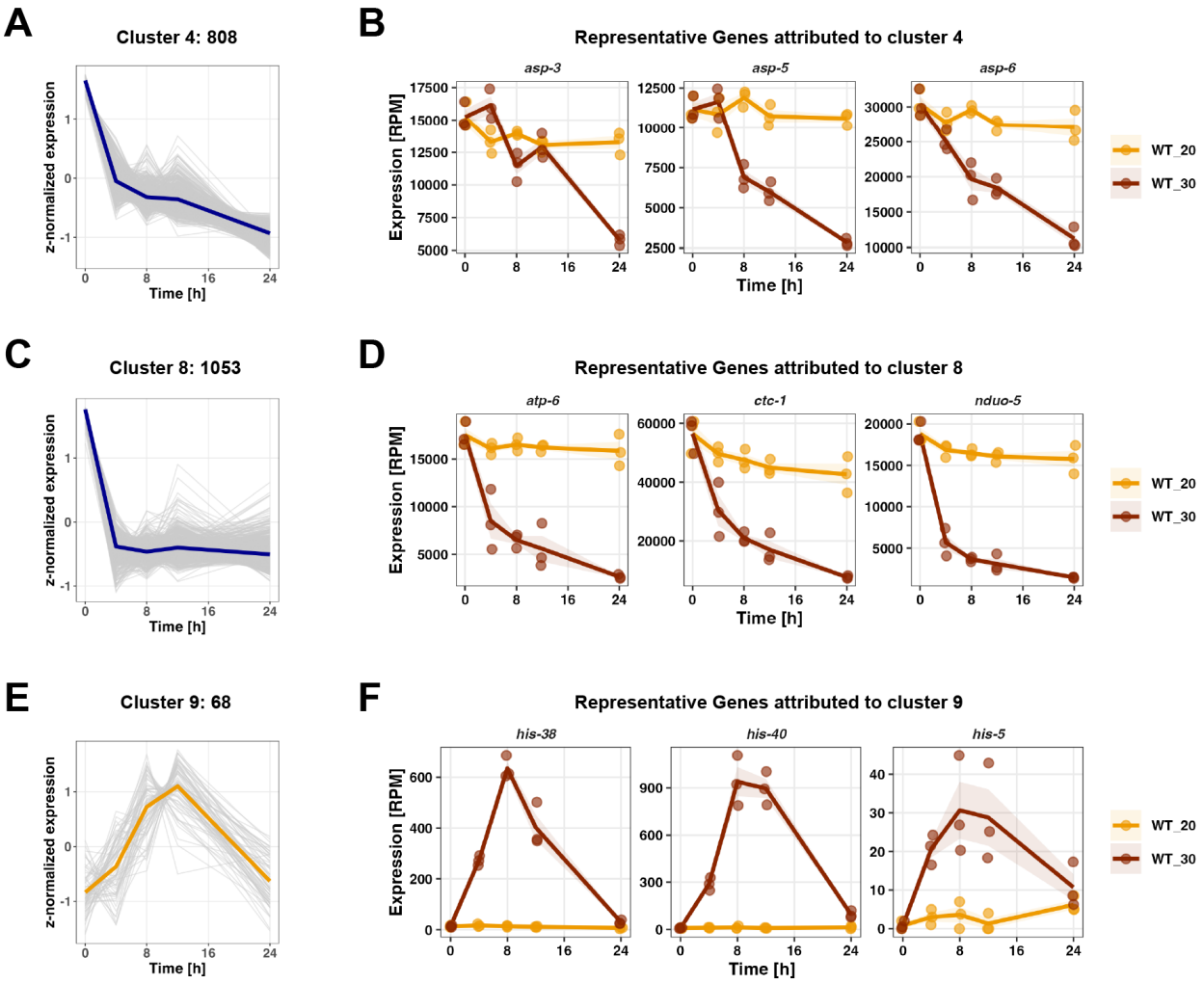

Figure 23: ***Novel trends identified in heat shock time course.*** *Probe trend plot of z-score normalised transcript levels of transcript isoforms >10RPM. Genes were clustered into 12 groups using k-means clustering, and annotated to a subgroup based on their trajectory. Clusters with an overall upwards trend are marked in red, downwards in blue, and clusters that show a transient change in yellow. (A) Line graph of z-score normalised transcript levels of 808 genes representing cluster 4. (B) Line graphs of selected genes from cluster 4. (C) Line graph of z-score normalised transcript levels of 1053 genes representing cluster 8. (D) Line graphs of selected genes from cluster 8. (E) Line graph of z-score normalised transcript levels of 68 genes representing cluster 4. (F) Line graphs of selected genes from cluster 9.*

2.3.2 Combining chronic and acute stress to identify determinants of resilience

This RNA-seq experiment was designed to identify causal changes determining heat stress hypersensitivity in the *dys-1(eg33)* mutant. We reasoned that any difference in gene expression, either in baseline transcript level changes, or in the expression changes during heat stress, could hint at mechanisms involved in this phenotype. We therefore systematically compared the profiles of baseline and stress induced transcriptomes of the wild type and *dys-1(eg33)* mutant animals, investigating the data for gene expression differences. Initially, we compared unstressed samples to see if we could find an explanation in consistent expression variation, before confirming if the DMD model showed any variation in amplitude or dynamics of key components of the HSR. Lastly, we would assess the novel trends identified in the wild type, to ultimately compile a list of genes which describe any type of alterations in comparison to the wild type.

Consistent baseline changes in DMD expression patterns

Initially, we compared wild type and DMD baseline transcript levels of day 1 animals at individual time points to normalise for expression changes that are only detected in a specific window. As this only represented a snapshot of the experiment at individual time points, we then mapped baseline transcriptome overlap of the untreated controls at every time point in an UpSet plot, to identify genes which showed a consistent change, reducing noise and false positives.

A volcano plot portraying differential gene expression of day 1 animals at T4 showed a strong genotype effect in genes being expressed at lower levels in the *dys-1(eg33)* mutant (Fig. 24A). Here, we could detect 316 genes to be significantly down-, and 35 genes to be significantly up-regulated at T4. Visualisation of the overlap of significantly changed genes at different untreated time points in an UpSet graph showed that a group of 56 genes were significantly changed at T4, T8, T12, and T24 (Fig. 24B). We further assessed if this group of genes was related to a specific process or mechanism. Assessment of GO terms did not show a strong over-representation of any process in the respective gene group, but indicated collagen and cuticle development genes to be part of the group (Fig. 24C). We then plotted all 56 gens in a heatmap to assess their variability (Fig. 24D). Generally, genes fell into two groups, with 33 genes showing overall lower expression in the *dys-1(eg33)* mutant, and 23 genes showing elevated expression. In the genes that were lower expressed there was a further separation of genes that showed dynamic expression in the wild type, while remaining mostly unchanged in the mutant.

Taken together, we detected significantly changed expression in a number of genes, with the majority showing a significantly lower expression in the DMD model when compared to the wild type. Assessment of experimental controls and published signatures by comparison to a public transcriptome data set confirmed the altered expression of muscle related genes such as *myo-6*, and the causal mutant gene *dys-1*. Assessing gens that were consistently changed at every time point, we found representation of epigenetic modulators like *jmjd-3.1* and *sdc-3*. Additionally, we discovered genes related to mitochondria to be expressed at higher levels in the transcription factor *sptf-3*, and the OXPHOS component *cox-4*.

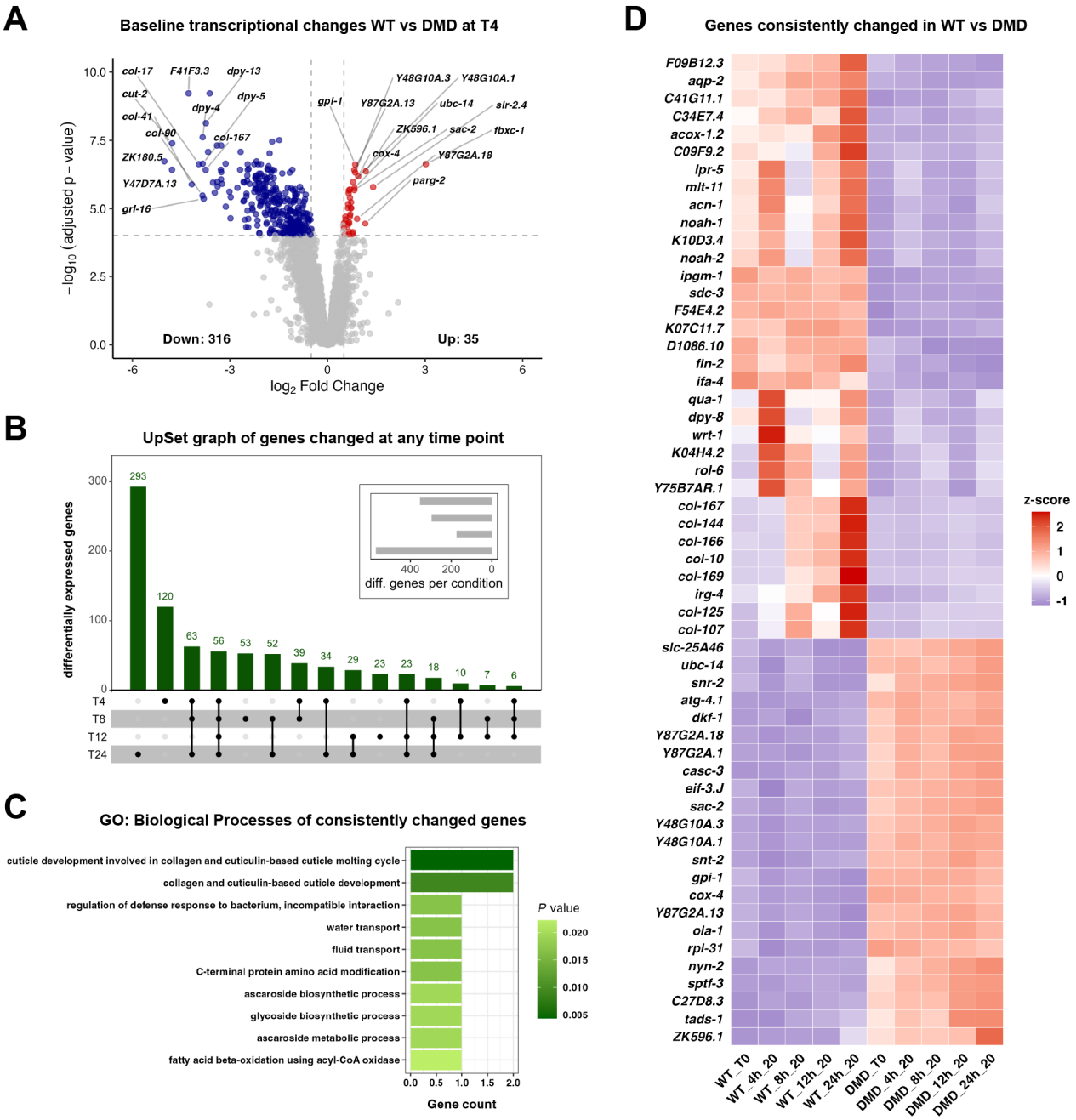

Figure 24: ***Baseline transcriptomic changes in C. elegans mutant for DMD.*** *(A) Volcano plot comparing merged transcript isoforms >10RPM of wild type day 1 animals of wild type and dys-1(eg33) mutant raised at 20 °C for 4 hours after experiment start. (B) UpSet graph of genes significantly changed in the dys-1(eg33) mutant at any time between T4 and T24. (C) GO term enrichment analysis of genes significantly changed between wild type and dys-1(eg33) animals at every time point. (D) Heatmap of genes significantly changed between wild type and dys-1(eg33) animals at every time point.*

Differences in the DMD heat shock response

Next to significant changes in baseline expression, we were particularly interested in changes of HSR dynamics. For this, we applied two methods to analyse the data for changes based on variation in gene expression changes during heat stress. First, we compared significant expression differences in the DMD model in heat stress at different time points, before mapping these changes to the response of the wild type. This more manual approach would represent an assessment of the canonical HSR, as it controls for gene changes at individual time points, and by that would be more suited to identify qualitative comparison to identify genes that are changed or not changed at a given time point. We would then assess genes solely differentially expressed in either of the strains, to look for heat-dependent gene changes absent in the *dys-1(eg33)* mutant, or only identified in the frailty model. In a more systematic approach, we would computationally determine differentially expressed genes between wildtype and mutant as a factor of the interaction term, determining variance as a factor of genotype and temperature in one parameter, using linear modelling with limma. This computational approach also accounts for directionality of expression changes, and identifies genes that behave differently in the two genotypes throughout in response to the temperature change. From both approaches, we aimed to compile a list of genes that could be potential drivers of hypersensitivity. To enable testing of this causality in RNAi mediated knockdown of genes, we were more intrigued by genes that showed an increased expression in the DMD model, to assess if knockdown could restore thermorecovery in acute stress assays.

First, we analysed significant transcript changes of the *dys-1(eg33)* mutant at T4 as performed for the wild type, to determine heat induced changes in treatment at 30 °C. We then mapped the DMD mutant changes to the changes of the wild type at T4 to assess the overlap of the genes changed in heat stress in the initial phase (Fig. 25A). The strongest up-regulated genes were shared and included *hsp-16.2*, *hsp-16.48*, and *hsp-16.41*, while the strongest down-regulation was detected in *asp-13*, *col-93*, and *pept-1* in both genotypes. We then systematically compared the differential expression of wild type and DMD mutant at T4. This comparison revealed 58.5 % in the up-regulated, and 61.1 % of the down-regulated genes to be shared between wild type and mutant (Fig. 25C/E). As observed before, we found the genes down-regulated in both strains upon heat stress to heavily feature proteolysis (Fig. 25B). To see if the genes deferentially expressed in either genotype are related to any specific processes, we assessed if they would fall into particular biological processes in GO term analysis. Here, we identified a strong representation of genes related to cuticle development and ECM organisation (Fig. 25D). In contrast, genes exclusively changed in the wild type showed representation of genes related to fatty-acid metabolism and other metabolic processes (Fig. 25F).

Overall, the DMD model showed a strong induction of the canonical HSR, with all main drivers detected in the wild type showing significantly higher expression in the DMD mutant during heat stress. Assessing differences in heat-dependent expression changes between wild type and DMD mutant, we could identify ECM composition and cuticle development genes to be exclusively changed in the DMD mutant, while the wild type showed alterations in metabolism which were absent in the *dys-1(eg33)* mutant at T4. As this comparison exclusively captured changes at an individual time point, we performed a more comprehensive analysis under the consideration of all data, to make results more robust and reveal individual genes whose expression was changed as a factor of both genotype and temperature.

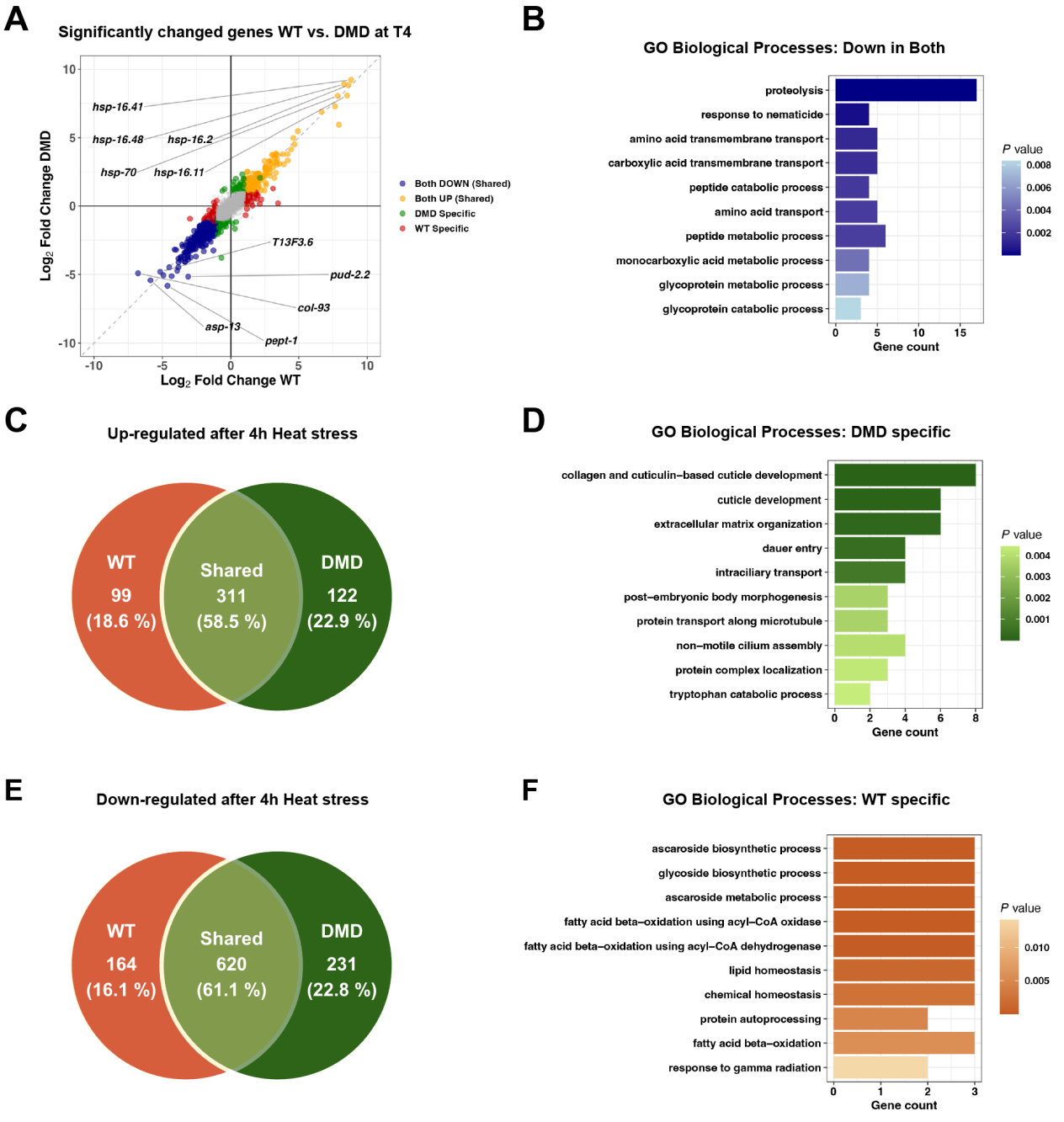

Figure 25: ***Identified trends in the heat shock time course.*** *(A) Volcano plot comparing significantly changed gene transcripts of wild type and dys-1(eg33) mutant day 1 animals after 4 hours of treatment at 30 °C. (B) GO term enrichment analysis of genes significantly changed in wild type and dys-1(eg33) animals after 4 hours of treatment at 30 °C. (C) Venn diagram showing overlap of transcripts significantly increased at 4 hours of treatment at 30 °C between wild type and dys-1(eg33) mutant. (D) GO term enrichment analysis of genes significantly changed only in dys-1(eg33) animals after 4 hours of treatment at 30 °C. (E) Venn diagram showing overlap of transcripts significantly reduced at 4 hours of treatment at 30 °C between wild type and dys-1(eg33) mutant. (F) GO term enrichment analysis of genes significantly changed only in wild type animals after 4 hours of treatment at 30 °C.*

Differences identified by the interaction term

The limma framework offers a robust statistical approach for transcriptomic analysis by including multi-factor information across samples, thereby stabilizing variance estimates and increasing statistical power. In a multi-factor experimental design involving both genotype and temperature, limma's linear modeling capability is particularly advantageous for dissecting the complex regulatory landscape. By incorporating an interaction term (genotype+temperature), the model moves beyond the identification of independent main effects to discern genes whose expression profile in response to thermal shift is conditioned by the underlying genetic background. This statistical synergy allows for the precise identification of the "genotype-specific environmental response" effectively isolating cases where a mutation disrupts the homeostatic plasticity. Here, we used this model to portray expression changes that are determined by this interaction term, to identify genes which show opposing expression patterns in the *dys-1(eg33)* mutant.

Following determination of significant expression changes based on the interaction term, we visualised significant changes in volcano plots. Comparison at T24 revealed 213 genes to show elevated expression, and reduce transcript levels of 6 genes according to the interaction term (Fig. 26A). From all respective volcano plots at all time points we collected the genes to plot expression patterns in a heatmap. Overall, we detected 239 genes which were detected to be changed at any time point. We analysed individual gene profiles and identified a set of genes we considered to be relevant in this context (Fig. 26B). Next to five sets of gene groups, we identified differences in expression patterns of the histone *his-40*, and *hsp-4*, which were detected by analysis of the interaction term. Changes detected in expression of aspartyl proteases were plotted in line graphs (Fig. 26C). Here, the wild type follows a general trend of reduced transcript levels in heat stress which progresses over time. In contrast, the *dys-1(eg33)* mutant described a softer reduction in *asp-2*, *asp-3*, and *asp-4*. *asp-1* transcript levels increased in the DMD mutant throughout the experiment, while the wild type showed a strong reduction at T24. In *asp-6*, *dys-1(eg33)* transcript levels did not appear to change, while the wild type showed a gradual reduction. A similar trend was observed in transient histone up-regulation, where the *dys-1(eg33)* mutant only showed elevated expression levels at lower amplitude to the wild type (Fig. 26D). Assessing a group of *spp* genes, we detected a reduction in expression in heat stress, which was stronger in the wild type compared to the DMD mutant in most cases. *spp-2* was an outlier, as it mildly increased in transcript levels until T12, before doubling its expression levels in the wild type, while the *dys-1(eg33)* expression remained stable from T12 to T24. We also found differential expression of a group of enzymes active in the innate immune response (Fig. 26F). Here, *lys-1* and *lys-2* were transiently up-regulated in the wild type, while *lys-8* was down-regulated in comparison to the negative control in the wild type. In all cases, the *dys-1(eg33)* mutant did not reduce transcript levels in later stages as observed in the wild type. Lastly, we identified *myo* genes to be represented in the interaction term (Fig. 26G). This was not caused by changes in stress expression patterns, but showed variation of baseline expression, where expression in the wild type gradually increased in the untreated controls, while DMD mutant levels declined.

Overall, we detected 239 genes to be significantly changed as a function of genotype+temperature, and found the majority of these genes to be expressed at higher transcript levels in the DMD mutant. Considering the individual gene expression line graphs, it appears that in many of these cases the mutant follows the trend of the wild type expression pattern, but falls short in the extent of these changes. Representation of *myo* genes in differential expression served as a control, as the *dys-1(eg33)* mutant is well described as a model for muscle frailty. Assessment of transcript levels of aspartyl proteases in heat stress revealed that the strong down-regulation in the wild type was much softer in the DMD mutant. A clear outlier was *asp-1*, as the wild

type showed expression below baseline, while the mutant showed elevated expression levels at T24. The DMD mutant described an opposing trend, and was considered a top candidate for RNAi screening, as it represented the type of expression change we aimed to uncover, as it has the same baseline level but shows a contrasting expression pattern in heat stress. Additionally, we found *spp-10* and *lys-8* to show similar effects, as they show lower levels than baseline in the wild type at T24, while *dys-1(eg33)* levels were higher than baseline at this time point.

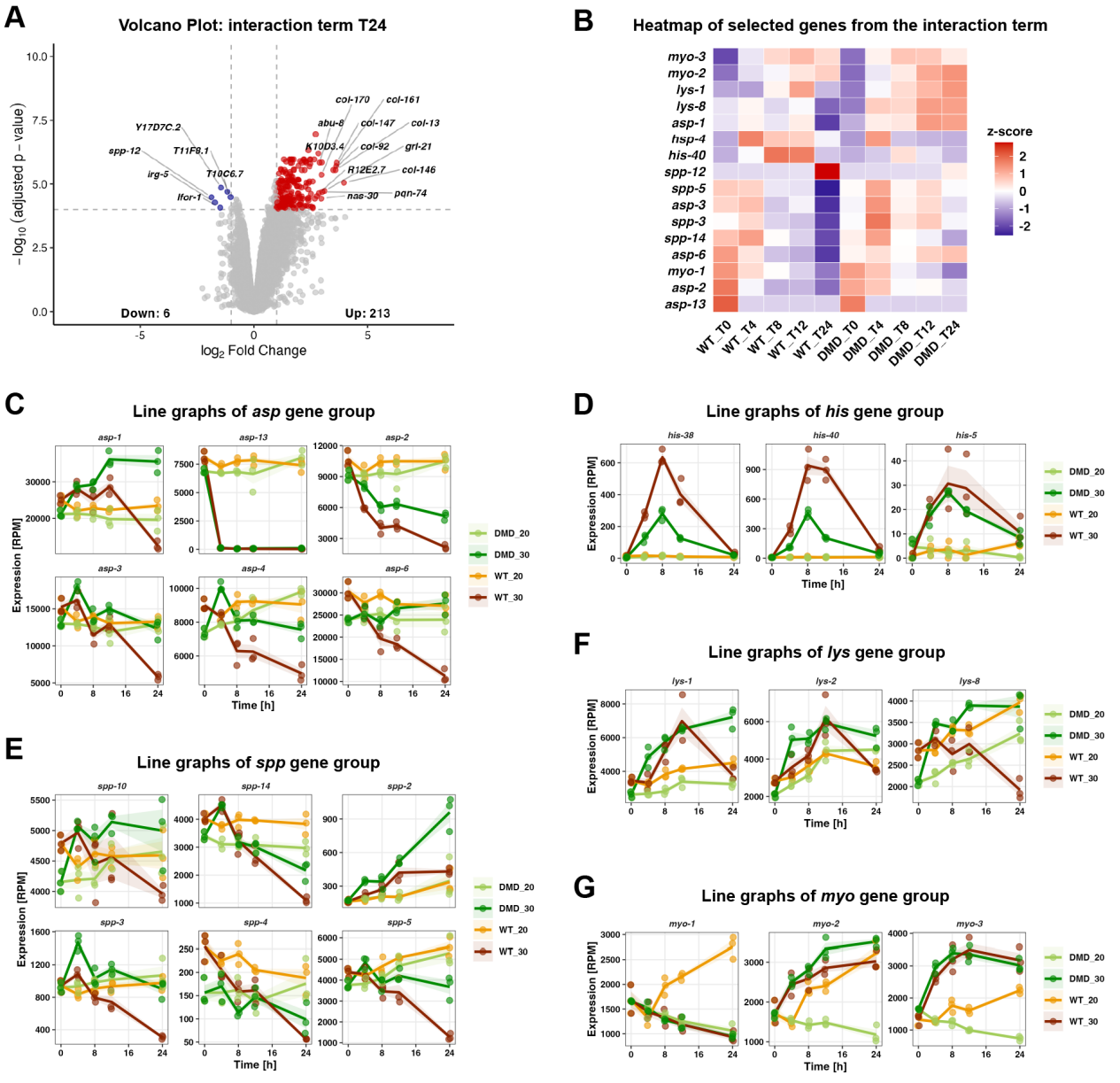

Figure 26: ***Changes captured by the interaction term.*** *(A) Volcano plot comparing significantly changed gene transcripts as a factor of the interaction term (genotype+temperature) of wild type and dys-1(eg33) mutant day 1 animals after 24 hours of treatment at 30 °C. (B) Heatmap of selected genes identified by analysis of the interaction term at any time point of treatment at 30 °C (C) Line graphs of genes from the asp gene group comparing wild type and dys-1(eg33) mutant transcript levels of day 1 adults in heat stress time course. (D) Line graphs of genes from the his gene group (E) Line graphs of genes from the spp gene group (F) Line graphs of genes from the lys gene group. (G) Line graphs of genes from the myo gene group.*

2.3.3 Stress response cross-talk and homeostatic capacity in DMD

Having observed a degree of stress response cross-talk using transgenic reporters, we assessed the transcript levels of components and markers of the stress response mechanisms reacting to mitochondrial and ER stress. We detected an increase in *hsp-4*p::GFP signal(*zcIs4*) in heat stress, which would require a preceding transcriptional response. As we detected *hsp-4* as a hit by analysis of the interaction term, we wondered if there is a significant difference in expression of this and potentially other stress markers of the UPR^{ER}. Additionally, we identified the mitochondrial transcription factor *sptf-3* to show significantly higher transcript levels in the DMD model, while we identified another key component of the UPR^{mito}, the transcription factor *atfs-1*, to be among the genes showing variation in expression during heat stress at T24. We therefore mapped expression levels of representative genes of the responses throughout the experiment in line graphs, comparing wild type and DMD levels.

Representing the induction of the canonical HSR, we plotted the expression of a set of heat responsive chaperones in the response to stress (Fig. 27A). The transcript levels showed an explosive increase at T4, before decreasing again in the next time points. *hsp-90* was an outlier in this pattern, as it maintained high transcript levels, and almost returned to the T4 levels at later stages, while the other genes maintained a lower expression. We could not detect significant variation between the wild type and the DMD model in this response. To outline the effect of heat stress on the UPR^{mito}, we assessed transcript levels of the transcription factors *atfs-1* and *sptf-3*, and the *atfs-1* targets *hsp-6* and *hsp-60* (Fig. 27B). Transcript levels of *atfs-1* were strongly reduced at T4, before describing a slow recovery towards baseline levels in the wild type. The DMD model maintained the reduced levels after T4 throughout. The chaperones described different trends, as *hsp-6* increased strongly at T4, and maintained high levels, while *hsp-60* only appeared to show a mild increase at T24. The DMD model described a stronger reduction in *hsp-6* levels after elevation at T4, with a clear separation from the wild type at T24. Regarding *hsp-60*, it did not show any increase as observed in the wild type. Assessment of the transcription factor *sptf-3* showed a consistent difference in transcript levels between wild type and DMD, with DMD expression being significantly higher. *sptf-3* expression was not affected by stress. To assess induction of the UPR^{ER}, we compared expression of the ER stress response markers *hsp-3* and *hsp-4*, next to the genes involved for their induction, *ire-1* and *xbp-1* (Fig. 27C). The two chaperones described a similar trend as the HSR chaperones, sharply increasing in transcript levels at T4, before declining throughout the remaining time points. The wild type hereby described a gradual reduction, while the reduction of transcripts in the DMD model was more rapid, with the *hsp-4* levels even returning to baseline at T24. Both strains showed signs of ire-1 and xbp-1 activation, also presenting a rapid increase in expression during stress, but maintaining these elevated levels throughout. The DMD model showed a mild variation in expression of *xbp-1*, as it appeared to increase further at T24, while the wild type remained stable transcript levels.

As outlined in the comparison of the canonical HSR, we only found mild variations in the main effectors of the HSR. Comparing the most relevant genes in the UPR^{mito}, *atfs-1*, and the downstream markers *hsp-6* and *hsp-60*, we found the wild type to show higher transcript levels especially at the 24 hour time point. The UPR^{mito} did appear to be impacted by the stress, with the DMD model presenting a weaker response, as *atfs-1* remained at lower levels without returning to baseline expression, and describing a lower expression of *hsp-6* and *hsp-60* especially at T24. Based on this observation, we wondered if this alteration in mitochondrial stress dynamics during heat stress could indicate a vulnerability of the DMD model, which has been reported to carry a mitochondrial burden (Higashitani et al. 2023), while heat stress is reported to strongly affect mitochondria

(Momma et al. 2017). We therefore included treatments targeting this mechanism in the candidate screen, to assess if there is a causal link between this observation and stress hypersensitivity. Additionally, comparison of the ER stress response markers *hsp-3* and *hsp-4* revealed a reduced induction of these chaperones in the DMD model. Considering that we observed a reduced induction of the transgenic *hsp-4*p::GFP signal(*zcIs4*) in TM stress, this observation matches the hypothesis that the DMD model shows a reduced capacity of the UPR^{ER}.

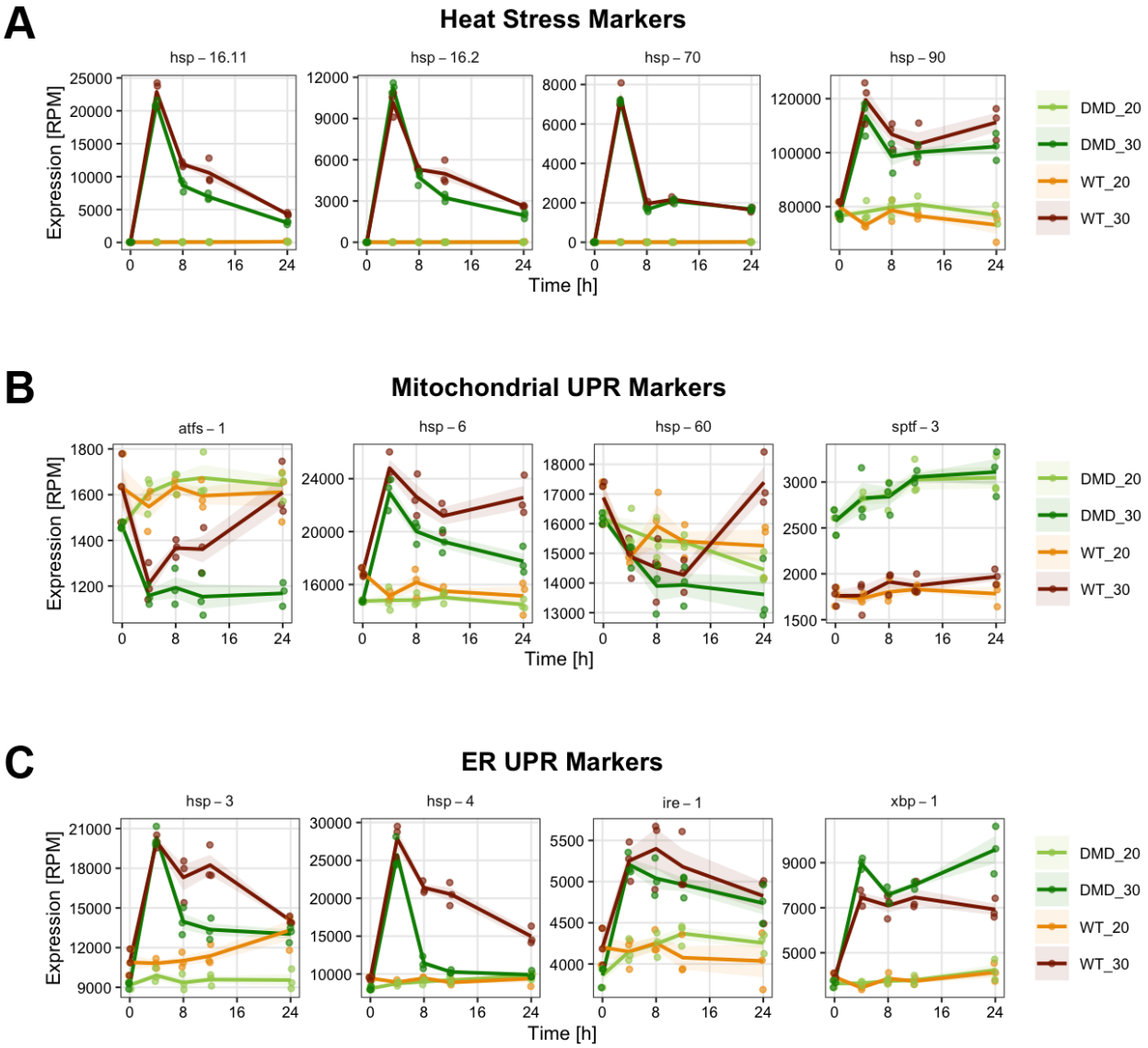

Figure 27: ***Stress response cross-talk in heat stress time course.*** *(A) Line graphs comparing expression of selected heat stress markers in day 1 adults of wild type and dys-1(eg33) mutant in time course stress at 30 °C. (B) Line graphs comparing expression of selected mitochondrial stress genes in day 1 adults of wild type and dys-1(eg33) mutant in time course stress at 30 °C. (C) Line graphs comparing expression of selected ER stress genes in day 1 adults of wild type and dys-1(eg33) mutant in time course stress at 30 °C.*

2.3.4 RNAi candidate screen reveals novel ways to improve heat resilience

Building on the genes we identified to be changed in the RNA-seq experiment, uncovering both baseline and dynamic changes, we compiled a list of genes we considered to be potentially causal candidates in *dys-1(eg33)* heat hypersensitivity. First, we looked at genes that showed an increased expression in the DMD model, arguing that if this increase in transcript levels is causal in stress hypersensitivity, RNAi mediated knockdown of expression would to some extent restore more wild-type-like expression. We would then expose them to heat stress in a thermorecovery assay, to assess if the respective knockdown affects heat stress frailty of the *dys-1(eg33)* mutant. The candidate genes selected for thermorecovery by RNAi mediated knockdown were chosen based on a set of criteria. They were either consistently higher expressed in DMD or showed a significantly higher expression than the wild type during heat stress, and were connected to specific functions related to a stress response or motility phenotype.

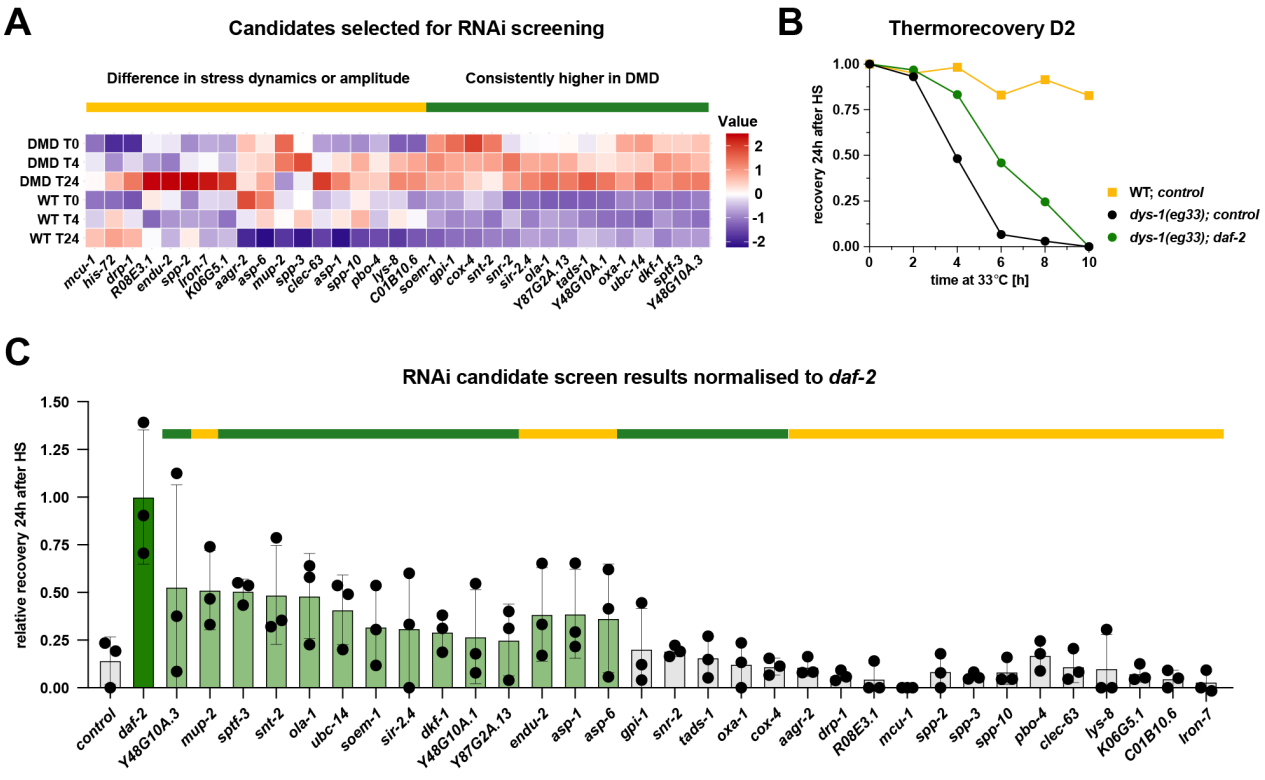

Figure 28: ***Thermorecovery screen of selected candidates.*** *(A) Heatmap of selected genes comparing transcript levels of day 1 animals of wild type and dys-1(eg33) mutant at 0, 4 and 24 hours of treatment at 30 °C. (B) Thermorecovery time course assay of day 1 animals comparing the recovery from heat shock for 2 to 10 hours at 33 °C of wild type, dys-1(eg33) aninmals on control or daf-2 RNAi. (B) Thermorecovery assay of day 1 adult animals of the dys-1(eg33) mutant raised on RNAi after 6 hours of heat stress at 33 °C.*

To test this, we selected 33 candidates which fell into these two categories, showing differences in baseline expression or describing variation in stress dynamics, which we visualised in a heatmap comparing expression at T0, T4 and T24 (Fig. 28A). To assess if it was in principle possible to improve thermorecovery by RNAi, we performed thermorecovery time course of DMD animals on control versus *daf-2 RNAi* in comparison to

the wild type (Fig. 28B). Control DMD animals showed a strong reduction in recovery rates from 2 hours of exposure to stress, and recovered at less than 10 % after exposure to 6 hours of treatment at 33 °C. *daf-2* RNAi treated animals recovered at higher rates throughout the experiment, with the strongest separation after 6 hours, showing a recovery rate of just under 50 % in comparison to the 10 % in the control. Next, we performed a thermorecovery candidate screen to compare stress recovery of day 1 *dys-1(eg33)* mutant animals raised on RNAi for the selected candidates (Fig. 28B). *daf-2* RNAi was used as a positive control for improving *dys-1(eg33)* hypersensitivity, and served as a benchmark in recovery screening. We assessed thermorecovery of the candidates normalised to recovery rates of the positive control, and categorised them into groups based on their average recovery across replicates. 14 candidates showed an increased average recovery of over 10 %, and were selected for further testing. We confirmed that RNAi is in principle sufficient to improve thermorecovery phenotypes using *daf-2* RNAi. We further identified 14 candidates which improved thermorecovery over the set threshold of 10 %, with the strongest effect observed in *Y48G10A.3*, *mup-2*, *sptf-3*, *snt-2*, and *ola-1*, which reached recovery rates of about 50 % of the *daf-2* RNAi control.

Themorecovery time course confirms broad beneficial effect of 4 candidates

We excluded 6 candidates which did not reproduce the results, before testing the remaining 8 candidates in a time course, as we reasoned adding time as a factor would show if the effects are robust or an artifact of the specific conditions. We performed time course thermorecovery on day 1 adult animals of the DMD mutant, comparing recovery of populations raised on control, *daf-2*, or candidate RNAi exposed to 33 °C for 2 to 10 hours (Fig. 29). The control showed a gradual decline, recovering at about 30 % after 4 hours of stress, and not showing any recovery at 6 hours. The *daf-2* control population recovered at higher rates at all time points, with about 70 % recovery at 4 hours, and 20 % after 6 hours of stress. The candidates *asp-6*, *soem-1*, and *ubc-14* showed no effect or just a mild effect of improved recovery. *snt-2* RNAi showed a strong increase of recovery after 4 hours, reaching recovery of about 60 %, while remaining time points showed control recovery rates. Treatment with *asp-1*, *sptf-3*, *ola-1*, and *Y48G10A.3* RNAi improved thermorecovery at more than one time point, with *sptf-3* RNAi showing elevated recovery rates compared to the control at every time point.

In this experiment we identified four candidates which showed an increase in thermorecovery in the *dys-1(eg33)* mutant upon RNAi mediated knockdown, namely *asp-1*, *sptf-3*, *ola-1*, and *Y48G10A.3*. These candidates appeared to be interesting in their own respects. We had targeted *asp-1* as a representative of a group of aspartyl proteases showing a decrease of transcript levels in heat stress, and describing an opposing trend in the DMD model, where it was up-regulated at T24. Knockdown in thermorecovery appeared to have a benefit on recovery outcome, indicating a causal role of changes in proteolysis in DMD. Further assessment of this process could investigate if knockdown of additional proteases that follow this discrepancy between wild type and DMD model show a similar effect, even though we did not see it in the knockdown of *asp-6*. The most convincing candidate was the transcription factor *sptf-3*, which showed improvement at most time points and almost reached recovery levels of the *daf-2* RNAi positive control in this experiment. It is described as a transcription regulator relevant in development, but has recently been shown to act in the UPR^{mito} on a level with *atfs-1* (Hemerling et al. 2023). The ATP hydrolase *ola-1* is involved in thermotaxis, and has been described as a regulator of the ISR (Chen et al. 2015). This indicates a connection of the modulation of this response to impact heat survival, which would describe another case of the interaction of distinct mechanisms in the response to stress determining resilience.

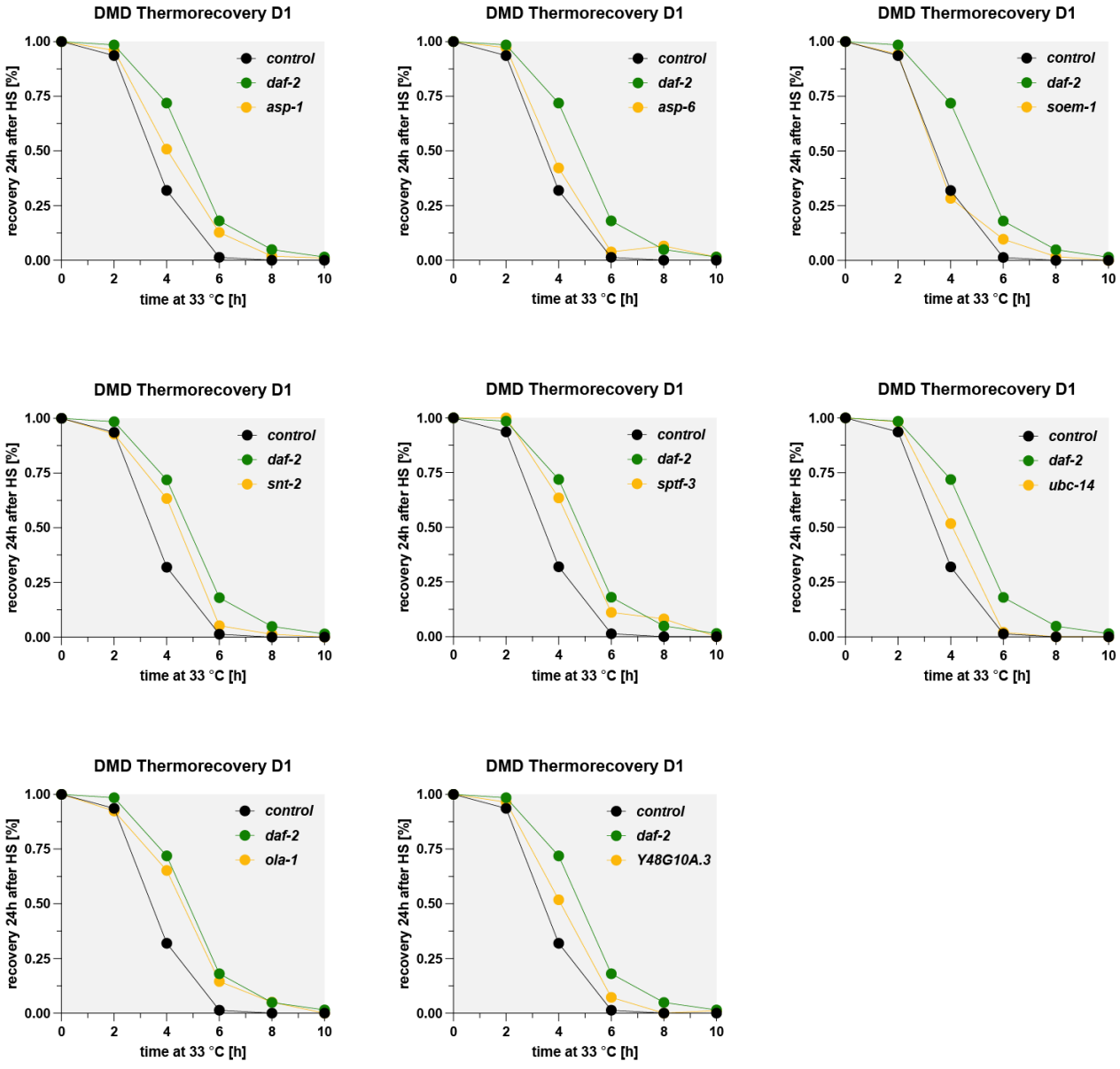

Figure 29: ***Thermorecovery time course of selected candidates.*** *Thermorecovery time course assay using day 1 adults of dys-1(eg33) raised on daf-2 or candidate RNAi following exposure to heat stress at 33 °C for 2 to 10 hours. Every time point represents an individual population on 6 cm RNAi plates from a randomised experimental setup in a heat-adjustable incubator. Every plate contained at least 50 adult animals.*

Conclusion of DMD changes in heat stress RNAseq and candidate testing

Taken together, we identified a range of genes that showed significant changes in the *C. elegans* DMD model from baseline expression and in changes of HSR dynamics. RNA-seq analysis revealed that the *dys-1(eg33)* mutant can mount an effective canonical HSR, and followed observed trends such as the reduced expression of genes encoded on the mitochondrial genome. Comparison of further processes we found differentially regulated in heat, we found a reduced transient expression of a set of histones, and a reduced down-regulation of aspartyl proteases as a part of the strongest down-regulated trend in proteolysis. Assessment of stress response mechanisms additionally uncovered a reduced expression of stress markers of the UPR^{mito} in the DMD model upon stress, while it showed increased levels of the related transcription factor *sptf-3*. Similar to *hsp-6*, we also identified a stronger reduction of transcript levels in the UPR^{ER} chaperones *hsp-3* and *hsp-4*. From these trends and individual changes, we compiled a list of genes we tested in thermorecovery upon RNAi mediated knockdown. Even though we did detect changes on protein and transcript level in genes related to the UPR^{ER}, we did not include these genes, as this approach we were limited to genes that showed an increased expression in the DMD model.

Overall, we identified four candidates indicating mechanisms involved in heat resilience, which could be further investigated in individual studies. Based on the alterations of the UPR^{mito} and the implication of mitochondria in heat stress and DMD phenotypes, we decided to focus on the effects of *sptf-3* knockdown. Additionally, we reasoned that its role as a transcription factor could make modulation more effective as it would induce a broader effect, also modulating downstream *sptf-3* signaling.

2.4 Improving UPR^{mito} capacity alleviates stress hypersensitivity in *C. elegans* DMD

2.4.1 Modulation of SPTF-3 improves mitochondrial frailty in DMD

The transcription factor *sptf-3* has been described as a positive regulator of the UPR^{mito} (Hemerling et al. 2023). Having shown that RNAi mediated knockdown of *sptf-3* was sufficient to improve thermorecovery in the hypersensitive DMD mutant, we wondered how these benefits are achieved and what the effect of this treatment on other frailty phenotypes would be. We therefore aimed to assess the effects of *sptf-3* RNAi on AA stress in motility, and investigate the state of the UPR^{mito}. For this, we assessed mRNA levels of relevant markers in RNAi treatment during heat stress, and addressed reporter induction of the transgenic *hsp-6*p::GFP(*zcIS13*) reporter.

First, we assessed thermorecovery of the DMD model and the wild type on day 1 adult animals raised on control, *daf-2*, and *sptf-3* RNAi (Fig. 30A-B). In the DMD mutant, populations raised on *daf-2* recovered at 50 % on average, while treatment on *sptf-3* RNAi resulted in recovery of about 35 % from heat stress at 33 °C. The wild type was exposed to heat stress at 34 °C for 6 hours to achieve a better separation of treatments. The control population recovered at just under 50 %, with the *daf-2* positive control showing almost full recovery, and *sptf-3* RNAi populations recovering at about 10 %. Next, we assessed *dys-1(eg33)* day 1 animals raised on *sptf-3* RNAi for locomotion after treatment with AA for 24 hours (Fig. 30C). Individuals raised on control RNAi and placed on DMSO showed body bend rates with an average of just over 30 bends in 30 seconds, with a significant reduction to almost no movement in most individuals. This effect was observed in both conditions. To investigate the involvement of the UPR^{mito}, we assessed mRNA levels of the stress responsive chaperones *hsp-6* and *hsp-60*, and *nduo-1* as a mitochondrial gene involved in OXPHOS, comparing transcript levels on baseline and in heat stress (Fig. 30D). In the wild type, we detected an increase in *hsp-6* and *hsp-60* transcript levels in heat stress, which was not affected in RNAi treatment. Expression of *nduo-1* was generally reduced in heat stress, and was mildly elevated in the *sptf-3* RNAi condition. The DMD model generally followed the same trends, with *hsp-6* and *hsp-60* being up, and *nduo-1* reduced in heat stress. The increase in *hsp-6* and *hsp-60* appeared to be reduced in *atfs-1* RNAi, while *sptf-3* RNAi appeared to increase baseline expression levels. The reduction of expression of *nduo-1* in heat stress appeared stronger in the DMD model, with *sptf-3* RNAi showing higher levels in stress than the respective control. Further, we assessed GFP expression in the *hsp-6*p::GFP(*zcIs13*) transgenic reporter raised on RNAi (Fig. 30E-F). Here, we observed a significant increase in signal in worms raised on *sptf-3* RNAi. This effect was detected in both the wild type and *dys-1(eg33)* mutant, although the increase in signal in the DMD model appeared to be more significant. Additionally, *atfs-1* RNAi depleted the background signal completely and prohibited expression of the reporter.

Taken together we confirm a robust improvement of thermorecovery in *dys-1(eg33)* mutants during *sptf-3* knockdown. This is in contrast to the effects in the wild type, where we found RNAi mediated knockdown of *sptf-3* to significantly reduce thermorecovery. This contrasting effect might be explained by *sptf-3* transcript levels, as decreasing them in DMD could lead to a more wild-type-like expression, while additional reduction as portrayed by the wild type could be detrimental. Considering its role in the UPR^{mito}, it was surprising that we did not find any improvement in mitochondrial stress, however, we could not show that any treatment did benefit the mitochondrial stress phenotype, and the assay might not be suited for as a readout for improvement by RNAi. Of note, *sptf-3* RNAi did not affect baseline locomotion, and therefore did not show any impact of

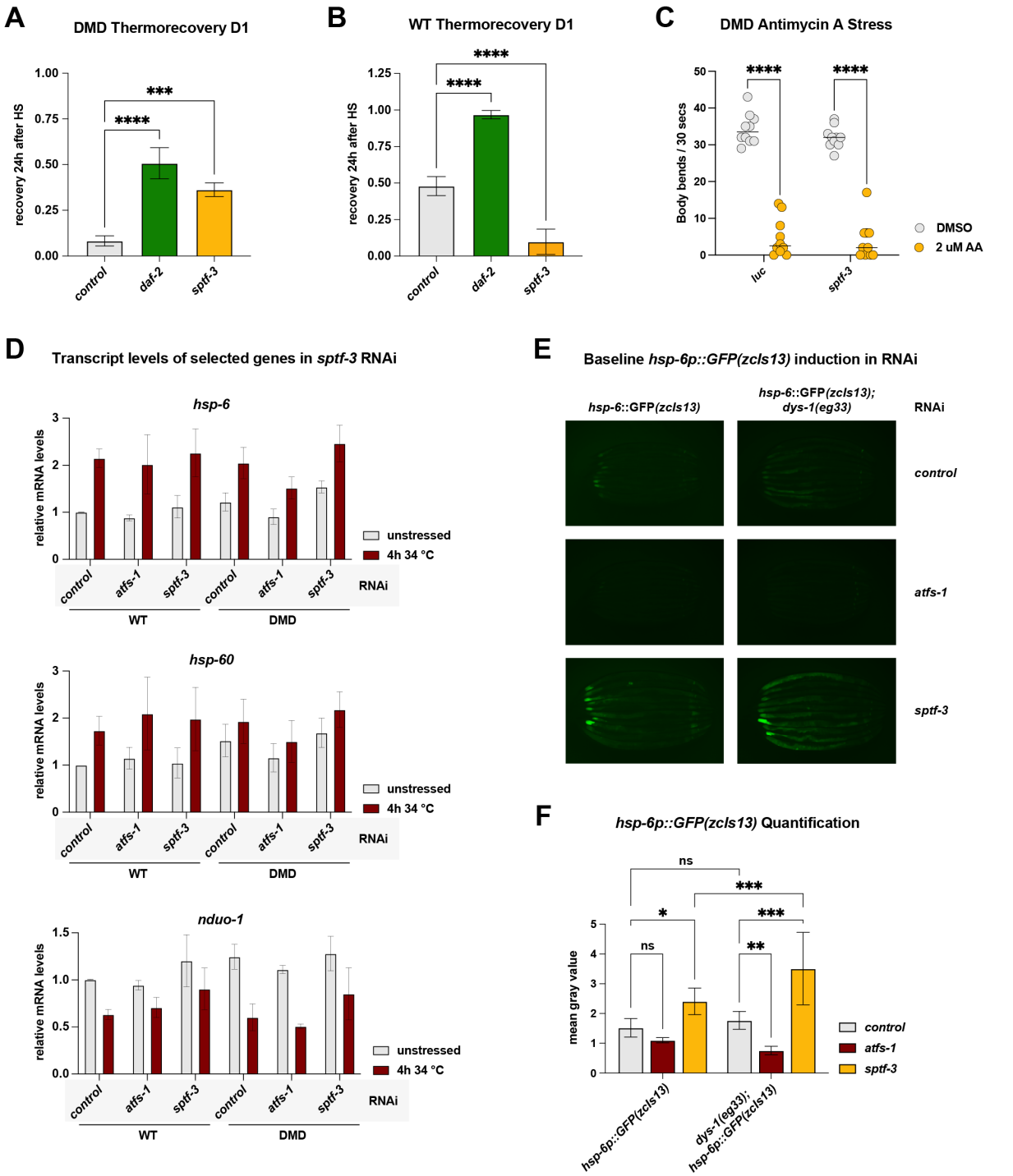

Figure 30: ***Effects of sptf-3 RNAi on dys-1(eg33) stress response and resilience.*** *(A) Thermorecovery assay using day 1 adults of dys-1(eg33) mutant raised on control, daf-2, or sptf-3 RNAi comparing recovery after exposure to 33 °C for 6 hours. (B) Thermorecovery assay using day 1 adults of the wild type raised on RNAi comparing recovery after exposure to 34 °C for 6 hours. (C) Locomotion assay comparing body bend rates of day 1 animals of the dys-1(eg33) mutant raised on control or sptf-3 RNAi after treatment with 2 μM Antimycin A. (D) Stress induction assay on day 1 animals raised on RNAi comparing transcript levels of selected genes after heat stress of 34 °C for 4 hours using qPCR. (E) Imaging of baseline GFP signal of the hsp-6p::GFP(zcIs13) reporter in wild type or dys-1(eg33) mutant background raised on control, atfs-1, or sptf-3 RNAi. (F) Quantification of hsp-6p::GFP(zcIs13) reporter signal measured as mean gray value of individual animals. Compared are the induction levels between worms raised on control, atfs-1, or sptf-3 RNAi.*

the classical DMD phenotype related to muscle frailty. Additionally, we remain to explain how the knockdown of a suspected positive regulator of *atfs-1* and the UPR^{mito} would lead to an increase in *hsp-6*p::GFP(*zcIS13*) GFP levels. Assessment of *hsp-6* mRNA levels by qPCR only revealed a mild increase in mRNA levels in *sptf-3* RNAi, with *hsp-60* levels slightly higher in the *dys-1(eg33)* mutant, but not further increased by *sptf-3* RNAi.

2.4.2 Over-activation mutant for ATFS-1 improves resilience in *C. elegans* DMD

Having identified an activation of *hsp-6*p::GFP(*zcIs13*) in the *sptf-3* RNAi treatment, we wondered if other means of activating this response could recapitulate this effect. A well established way of increasing the capacity of the UPR^{mito} is the activation of the key transcription factor *atfs-1*. Two gain-of-function mutants, QC115(*et15*) and QC117(*et17*), consistently activate the expression of the responsive chaperones as a consequence of mutations in the promoter of *atfs-1* (Rauthan et al. 2013). In these strains, gain-of-function of *atfs-1* results in a consistent activation of the *hsp-6*p::GFP(*zcIS13*) reporter, and increases transcript levels of a range of stress response markers (Rauthan et al. 2013). Additionally, the mutants have been shown to affect resilience, improving stress tolerance in various contexts (Soo et al. 2021b). We therefore decided to cross this mutant in the *dys-1(eg33)* mutant background, to investigate if increasing UPR^{mito} capacity by a consecutive *atfs-1* signaling is sufficient to improve thermorecvovery. To facilitate assessment of UPR^{mito} activity, we combined the two mutations in the background of the *hsp-6*p::GFP(*zcIs13*) transgenic reporter.

atfs-1(et17) mutation improves thermorecovery in *dys-1(eg33)* mutant

We aimed to compare multiple *atfs-1* activator mutants, before choosing a suited mutation for crossing into the DMD mutant. Following this, we wondered how this would affect the recovery of the DMD mutant, and what the impact on UPR^{mito} signaling in atfs-1 over-activity looked like. For this we assessed heat stress response in thermorecovery and investigated the status of the UPR^{mito} using the *hsp-6*p::GFP*(zcIs13)* transgenic reporter and RT-qPCR.

First, we compared thermorecovery of two *atfs-1* activator mutants with the wild type following heat stress at 34 °C for 6 hours (Fig. 31A). The wild type recovered at less than 10 % average recovery, while populations of *atfs-1(et15)* recovered at over 80 %, and *atfs-1(et17)* mutants at over 50 % of individuals. Next, we addressed if *atfs-1* activation would also have this effect in DMD thermorecovery. For this, we exposed day 1 adult animals of wild type, the *hsp-6*p::GFP*(zcIs13)* reporter, the *dys-1(eg33)* mutant with and without the reporter, and the triple mutant also carrying the *atfs-1(et17)* mutation to heat stress at 33 °C for 6 hours (Fig. 31B). Wild type and transgenic reporter animals showed recovery rates of over 80 %, while the DMD mutant and the respective reporter strain recovered at between 10 and 20 % of the population. The triple mutant showed a significantly higher recovery rate at an average of just under 50 %. We could further show that this effect was dependent on *atfs-1*, as RNAi mediated knockdown of *atfs-1* resulted in a significant reduction of thermorecovery (Fig. 31C). To confirm the downstream effects of *atfs-1* activation, and elucidate the relation to *sptf-3*, we assessed transgenic reporter induction of *hsp-6*p::GFP*(zcIs13)* (Fig. 31D-E). We detected a strong baseline induction of reporter singal in the *atfs-1(et17)* mutant, which appeared to be increased in *sptf-3* RNAi. This signal was fully lost upon *atfs-1* RNAi.

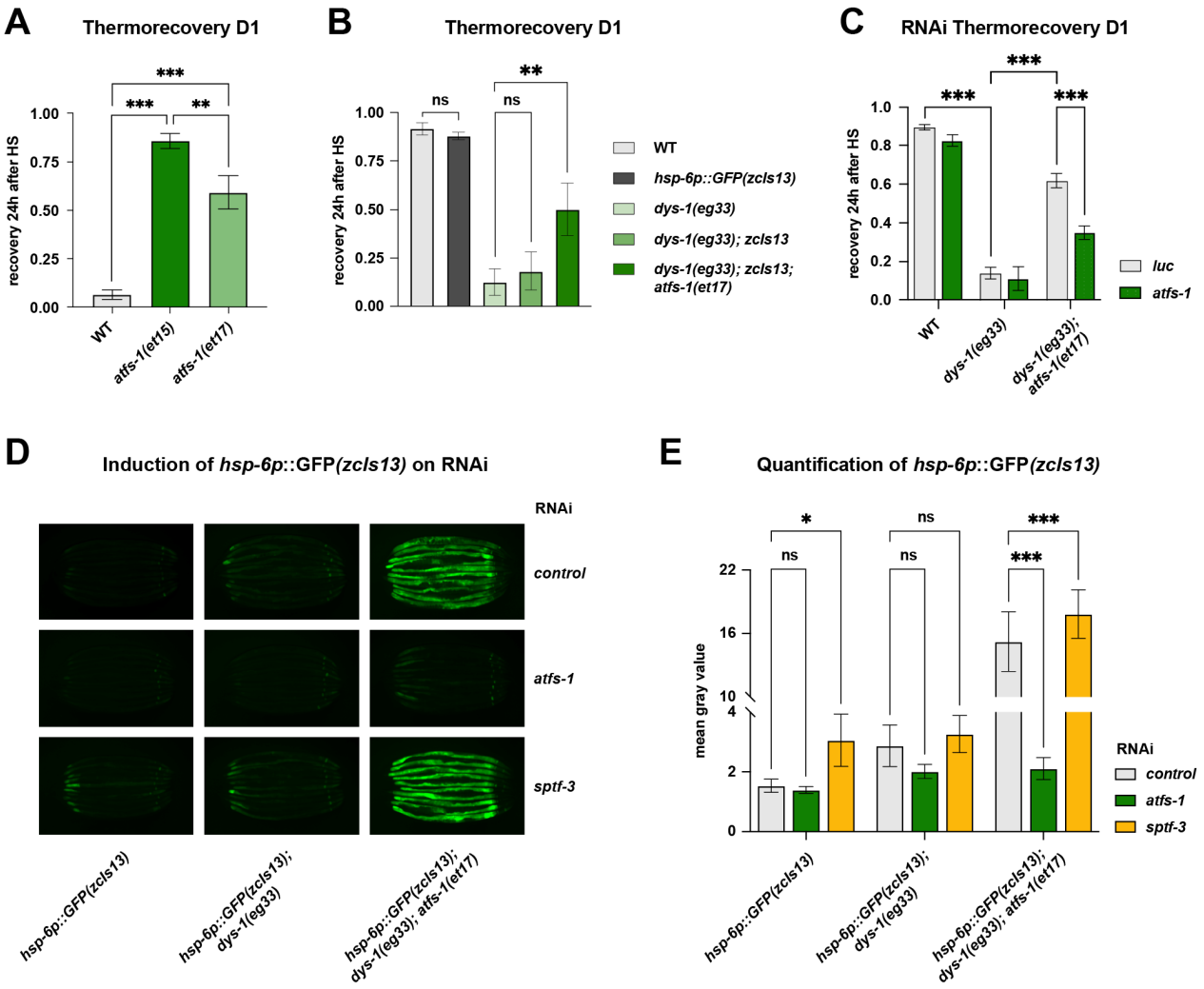

Figure 31: ***atfs-1 over-activation improves heat resilience in C. elegans DMD.*** *(A) Thermorecovery assay using day 1 adults of wild type, atfs-1(et15) or atfs-1(at17) mutant comparing recovery from heat stress at 34 °C for 6 hours. (B) Thermorecovery assay using day 1 adults of wild type, hsp-6p::GFP(zcIS13), dys-1(eg33) mutant, cross of dys-1(eg33) and zcIs13 reporter, or triple cross of dys-1(eg33), zcIs13, and atfs-1(et17) mutant comparing recovery from heat stress at 33 °C for 6 hours. (C) Thermorecovery assay using day 1 adults of wild type, dys-1(eg33) mutant, or cross of dys-1(eg33) and atfs-1(et17) mutant raised on control, or atfs-1 RNAi comparing recovery after exposure to 33 °C for 6 hours. (D) Imaging of baseline GFP signal of the hsp-6p::GFP(zcIs13) reporter in wild type, dys-1(eg33), and cross of dys-1(eg33) and atfs-1(et17) mutant background raised on control, atfs-1, or sptf-3 RNAi. (E) Quantification of hsp-6p::GFP(zcIs13) reporter signal measured as mean gray value of individual animals. Compared are the induction levels between worms raised on control, atfs-1, or sptf-3 RNAi.*

We confirmed an increased thermorecovery in the *atfs-1* activator mutants, as implied in the literature (Rauthan et al. 2013). We observed a stronger improvement of thermorecovery in the QC115 strain corresponding to the *et15* mutation, which is described to be a stronger activator of *atfs-1*. Based on this, there seemed to be a positive correlation between strength of activation and level of improvement. As the stronger activator also showed a delay in development, we decided to proceed with the more moderate activator mutation in *atfs-1(et17)*, as this still showed a significant improvement in thermorecovery.
The triple mutant did show a significant improvement in thermorecovery compared to the *dys-1(eg33)* strains. Importantly, the *hsp-6*p::GFP*(zcIs13)* reporter in either wild type or *dys-1(eg33)* background did not impact heat stress recovery by itself, and improvement of thermorecovery was dependent on *atfs-1*. Seeing this strong effect on the recovery phenotype, we wanted to know what the effects on molecular level on the expression of related genes looked like, and if these could explain the alleviation ion stress hypersensitivity of the *dys-1(eg33)* mutant.

atfs-1(et17) over-activation affects mitochondrial genome expression in heat stress

To assess the effects of the *atfs-1(et17)* mutation on mitochondria related genes and stress dynamics, we employed RT-qPCR comparing transcript levels of wild type, *dys-1(eg33)* mutant, and the double mutant with *atfs-1(et17)* in heat stress induction after 4 hours at 34 °C (Fig. 32). We assessed expression levels of *hsp-70(C12C8.1)*, serving as control for the HSR, and a set of genes relevant in the mitochondrial response to stress, as well as components of OXPHOS encoded on the mitochondrial genome, which we had identified in RNA-seq as being down-regulated in heat stress.
We found *hsp-70(C12C8.1)* to be significantly up-regulated in all strains. Assessing the expression of *gst-4*, a gene involved in SKN-1 signaling, we observed a reduction in transcript levels in acute heat stress, with a less severe reduction in the strains carrying the *dys-1(eg33)* mutation. We assessed transcript levels of *sptf-3*, *hsp-6* and *hsp-60* as representative markers of UPR^{mito} activity. Surprisingly, we did not detect significantly higher transcript levels of *hsp-6* or *hsp-60* in *atfs-1(et17)* on baseline, while it did show a stronger increase in *hsp-6* expression in heat stress. Assessing markers for mitochondrial energy metabolism revealed significantly higher transcript levels of genes encoded on the mitochondrial genome in *atfs-1(et17)*. Most prominently, the expression of *nudo-1*, *nduo-4*, and *atp-6* was strongly elevated on baseline, and transcript levels of *nduo-1* and *atp-6* did not follow a downward trend contrary to wild type and *dys-1(eg33)* mutant.

Taken together, we did not see a clear transcriptional signature of *atfs-1* activation in the UPR^{mito} of the *atfs-1(et17)* mutant, although we clearly found this on protein level in the transgenic reporter. Surprisingly, we found a strong effect on gene expression from the mitochondrial genome. This connection has been made before, describing a direct regulation of OXPHOS components by *atfs-1* (Nargund et al. 2015). However, this has not been described in the context of increased stress resilience. While the increased thermorecovery could be conveyed by an increase in UPR^{mito} capacity, we wondered if it could also be affected by an increase in OXPHOS activity. Alleviation of stress hypersensitivity in DMD could then be mediated by increased availability of energy produced in mitochondria, which are chronically affected in DMD. As we expected this process to also be heavily affected by mitochondrial stress, we next assessed if the *atfs-1(et17)* mutation could also alleviate AA stress hypersensitivity in DMD.

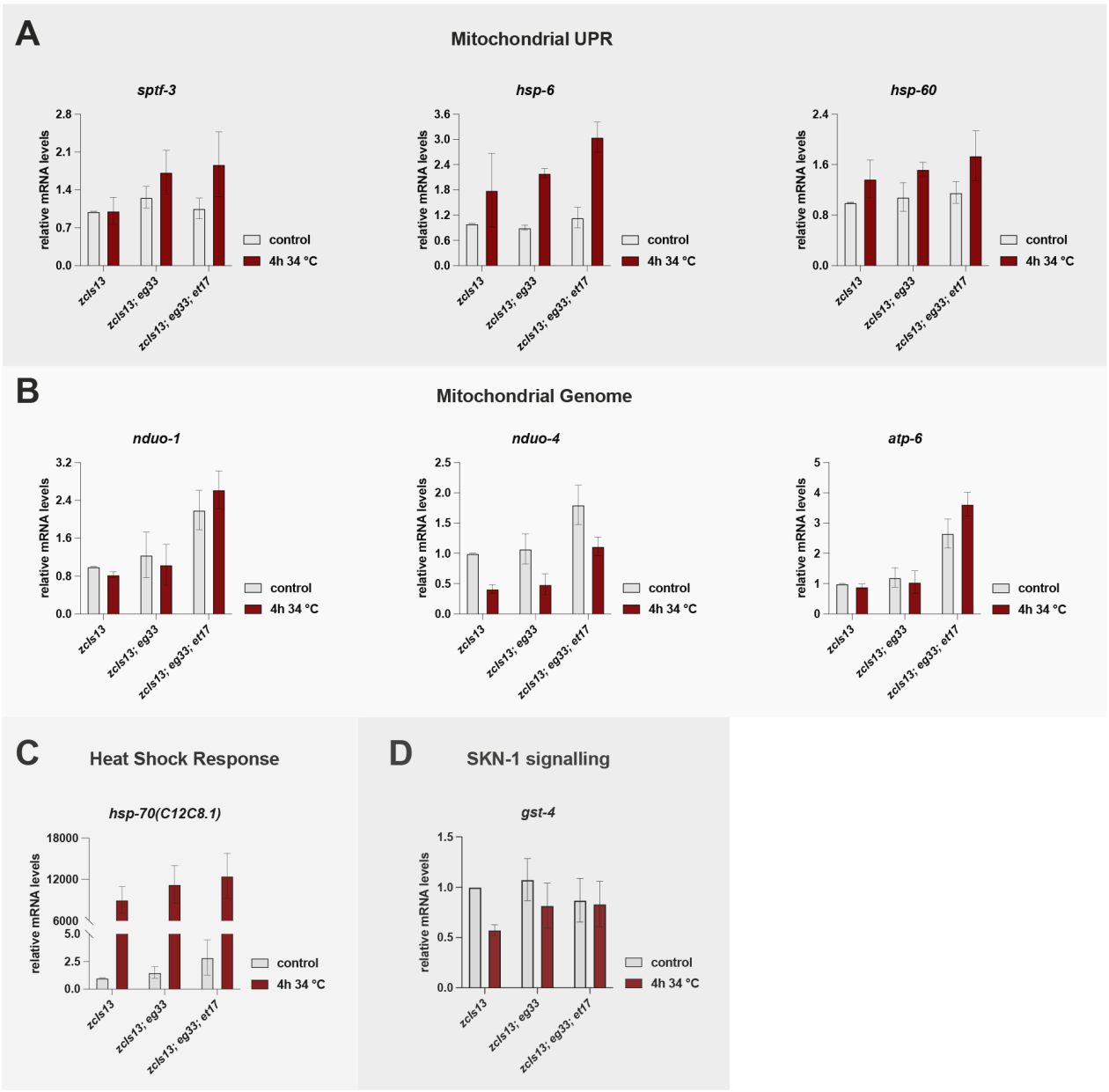

Figure 32: ***atfs-1 gain-of-function increases mitochondrial genome expression.*** *Stress induction assay on day 1 animals comparing transcript levels of selected genes after heat stress of 34 °C for 4 hours using qPCR. Plotted are mRNA levels for (A) mitochondrial UPR markers sptf-3, hsp-6, and hsp-60. (B) Transcript levels of nduo-1, nduo-4, and atp-6, genes encoded on the mitochondrial genome active in OXPHOS. (C) Expression of the HSR chaperone hsp-70. (D) Expression of gst-4, active in SKN-1 signaling.*

atfs-1(et17) mutation improves mitochondrial stress response in DMD model

To assess the effects of the *atfs-1(et17)* mutation in mitochondrial stress, we exposed day 1 animals of the wild type, *dys-1(eg33)* mutant, and the *dys-1(eg33)/atfs-1(et17)* double mutant to AA and investigated *hsp-6*p::GFP*(zcIs13)* reporter induction, stress behaviour in locomotion, and mRNA levels using qPCR. Next to an increased baseline signal, we identified a significantly stronger activation of *hsp-6*p::GFP*(zcIs13)* reporter expression in the *atfs-1(et17)* mutant (Fig. 33A-B). Comparing locomotion following treatment of day 1 adults with 5 μM AA for 24 hours, we showed the triple mutant to describe a less severe drop in body bend rates than the individual *dys-1(eg33)* mutant. The wild type showed a significant reduction of about 10 body bends / 30 seconds in AA treatment, while the DMD model fell from 30 to under 10 average body bends / 30 seconds. The *dys-1(eg33)/atfs-1(et17)* mutants showed a mild but not significant reduction of locomotion in the untreated condition, but performed significantly better than *the dys-1(eg33)* mutant after stress treatment. Assessing mRNA levels after short treatment with 10 μM Antimycin A for 4 hours was not sufficient to induce an increase in transcript levels of *hsp-6* or *hsp-60* via RT-qPCR (Fig. 33D). Expression of *nduo-1* and *ctc-1* was generally elevated in *dys-1(eg33)/atfs-1(et17)* mutants.

Taken together, we identified a robust increase in *hsp-6*p::GFP*(zcIs13)* reporter induction, and showed that the *atfs-1(et17)* mutation alleviated mitochondrial stress hypersensitivity in the DMD mutant. The *atfs-1(et17)* mutation also increased the maximum induction of the stress response in acute stress measured as GFP in the *hsp-6*p::GFP*(zcIs13)* reporter, indicating an overall improvement of the UPR^{mito}.

The role of *atfs-1(et17)* in DMD resilience by improving mitochondrial health

In conclusion, we show that the activator mutation *atfs-1(et17)* is sufficient to improve thermal and mitochondrial stress hypersensitivity in the *C. elegans* DMD model *dys-1(eg33)*. Using the transgenic *hsp-6*p::GFP*(zcIs13)* reporter, we show that the mutation not just increases baseline expression, but also extends the maximum signal in acute stress. Additionally, we uncover a strong increase in the expression of OXPHOS genes encoded on the mitochondrial genome. It remains to be shown if this is contributing to improved resilience in the DMD model, but we hypothesise that this could benefit energy availability in DMD, supporting responsiveness to acute stress in this model for mitochondrial frailty. To assess if improved resilience in the DMD mutant was conveyed by a broader effect of increased mitochondrial health, we next looked for other means to benefit this process.

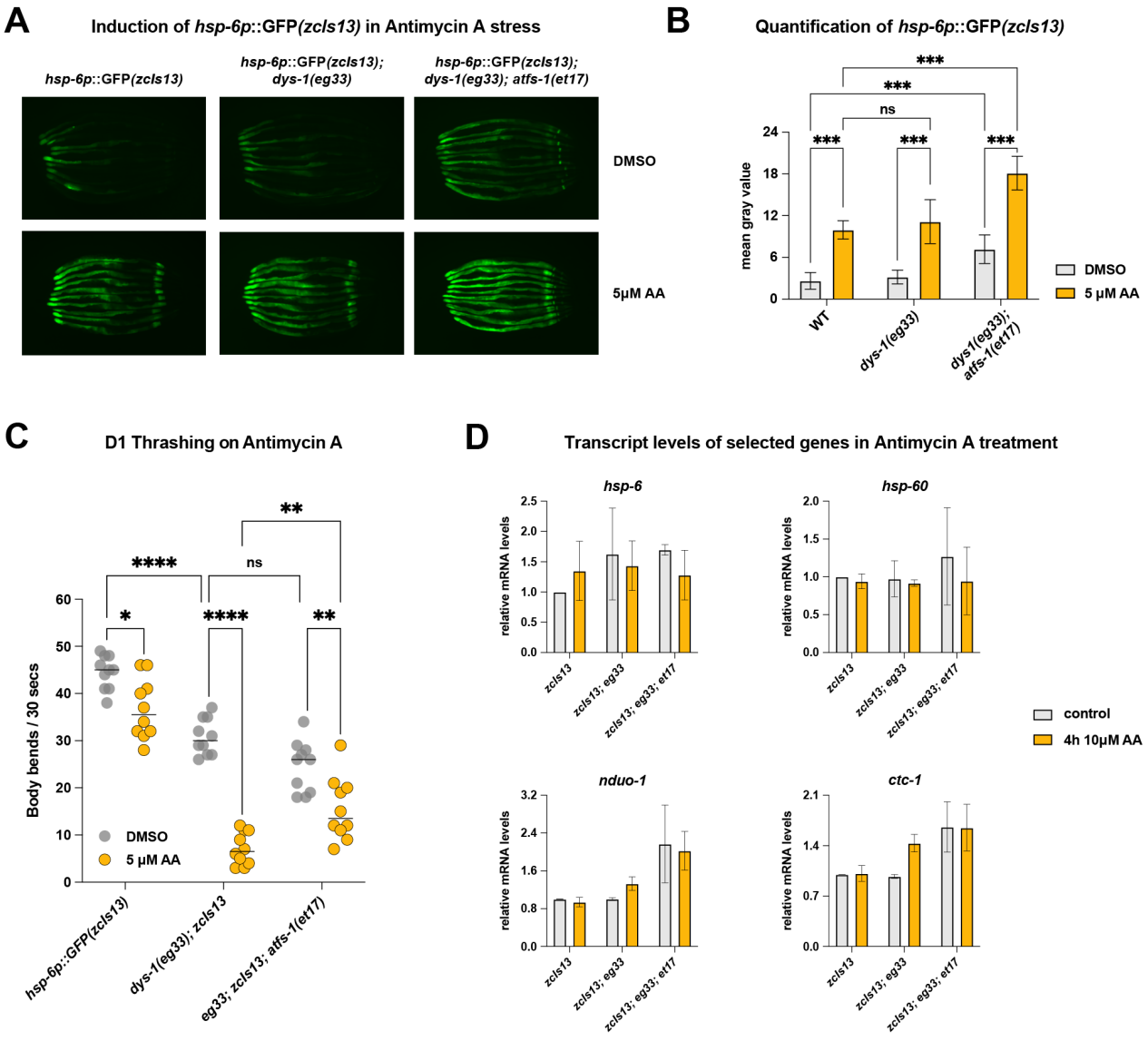

Figure 33: ***atfs-1 over-activation improves mitochondrial stress resilience in C. elegans DMD.*** *(A) Mitochondrial stress assay using day 1 animals of wild type, dys-1(eg33), and cross of dys-1(eg33) and atfs-1(et17) in the hsp-6p::GFP(zcIs13) reporter background comparing GFP induction after treatment with 5 µM Antimycin A for 24 hours. (B) Quantification of hsp-6p::GFP(zcIs13) reporter signal measured as mean gray value of individual animals comparing Antimycin A induction of GFP between wild type, dys-1(eg33), and dys-1(eg33) and atfs-1(et17) double mutant. (C) Locomotion assay comparing body bend rates of day 1 animals of wild type, dys-1(eg33), and dys-1(eg33) and atfs-1(et17) double mutant after treatment with 5 µM Antimycin A for 24 hours. (D) Stress induction assay on day 1 animals comparing transcript levels of selected genes after treatment with 10 µM Antimycin A for 4 hours using qPCR.*

2.4.3 Inducing the mitochondrial UPR with *nuo-6* RNAi improves thermorecovery

Other means to induce the mitochondrial UPR include the knockdown of the NADH Ubiquinone Oxidoreductase *nuo-6* (Yang and Hekimi 2010b). This has been reported to improve mitochondrial health by mitohormesis, and is understood as a robust way of chronically inducing the *atfs-1* dependent UPR^{mt} at low amplitude to generate overall health benefits.

Assessing *hsp-6*p::GFP*(zcIs13)* reporter induction in RNAi, we detected a strong induction of GFP upon RNAi mediated knockdown of *nuo-6*, which was significantly stronger in the *atfs-1(et17)* activator mutant (Fig. 34A-B). We detected GFP induction to be significantly higher in the *dys-1(eg33)* mutant, with the strongest signal showing a 100 % increase in signal from wild type to *atfs-1(et17)* in *nuo-6* RNAi. We then assessed thermorecovery on day 1 of adulthood in worms raised on control or *nuo-6* RNAi, comparing recovery after 33 °C for 6 hours (Fig. 34C). We identified a significant increase in thermorecovery in *nuo-6* RNAi treated worms in both strains carrying the *dys-1(eg33)* mutation. The *atfs-1(et17)* activator mutant showed significantly higher recovery rates than the DMD model on baseline, which was further improved by *nuo-6* RNAi, correlating with the intensity of reporter induction. Overall, we identified a strong activation of the *hsp-6*p::GFP*(zcIs13)* reporter, which coincided with an improvement in thermorecovery.

Improving mitochondrial biogenesis and energy metabolism in DMD

Improvement of mitochondrial health emerges as a promising path to alleviate DMD stress hypersensitivity. We identified *nuo-6* RNAi as another means to improve thermorecovery in the *dys-1(eg33)* mutant. As with the *atfs-1(et17)* activator, this effect was not exclusive for the DMD model, and also affected the wild type. It would be intriguing to assess further paths of boosting mitochondrial health to assess if this is a general method to improve stress resilience.

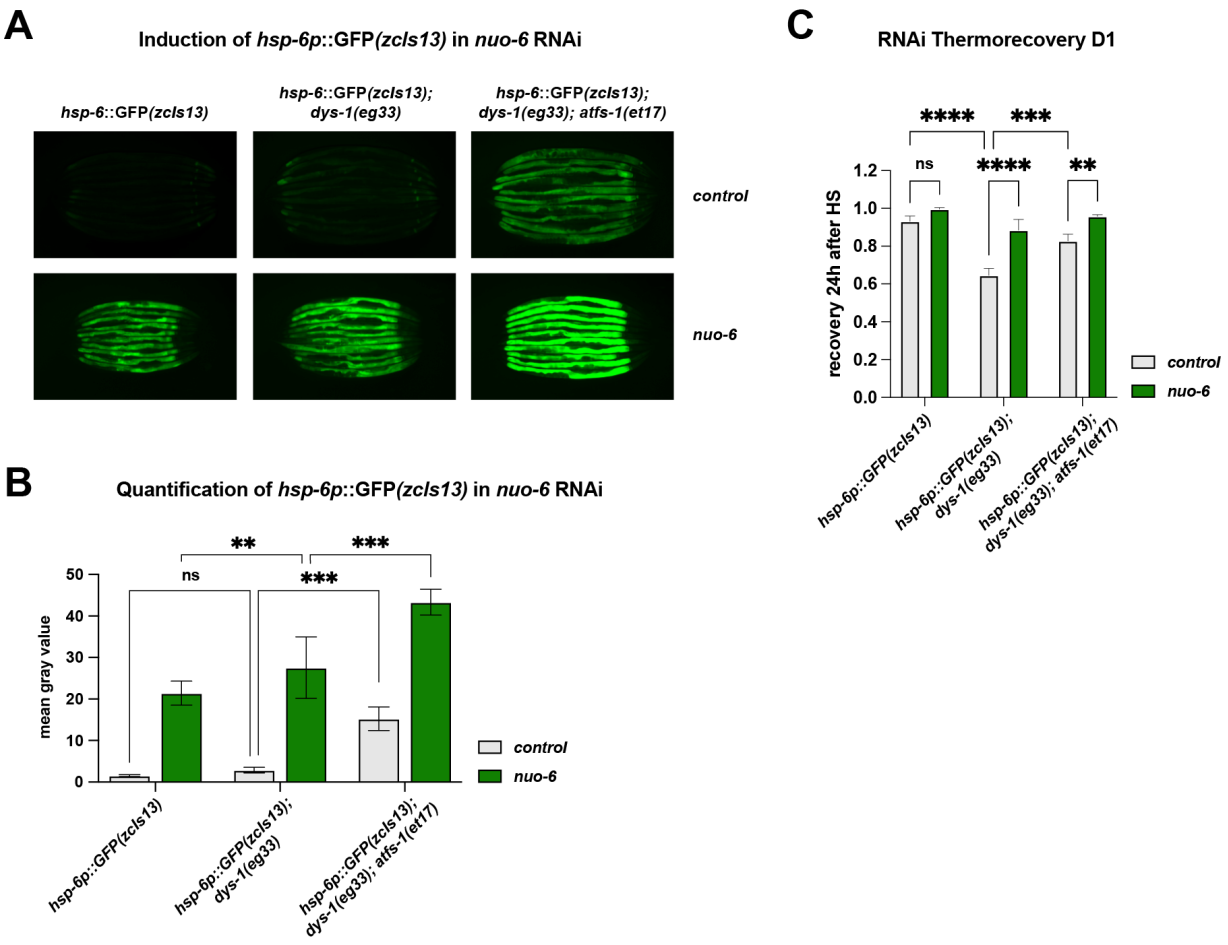

Figure 34: ***Improvement of heat resilience in nuo-6 knockdown.*** *(A) Imaging of baseline GFP signal of the hsp-6p::GFP(zcIs13) reporter in wild type, dys-1(eg33) mutant, and dys-1(eg33) and atfs-1(et17) double mutant raised on control or nuo-6 RNAi. (B) Quantification of hsp-6p::GFP(zcIs13) reporter signal measured as mean gray value of individual animals. Compared are the induction levels between worms raised on control or nuo-6 RNAi. (C) Thermorecovery assay using day 1 adults of wild type, dys-1(eg33) mutant, and dys-1(eg33) and atfs-1(et17) double mutant raised on control or nuo-6 RNAi comparing recovery after exposure to 33 °C for 6 hours.*

3 DISCUSSION

3.1 Modulating resilience to improve stress survival in *C. elegans*

In this study, we aimed to identify modulators of disease through the comparison of dynamic gene expression changes during the response to stress. To this end, we needed to identify suited models and readouts that quantify frailty and resilience, before assessing the molecular changes causing these effects. We set out to test our underlying hypothesis and assess whether a chronic burden on cellular homeostasis would reduce response capacity to acute stress. For this, we needed to establish key metrics to assess disease models for reduced resilience, determining suited parameters to describe a reduction of stress response capacity. Having identified these conditions in combination with a disease model which shows frailty in these physiological assays, we would then elucidate the molecular processes determining resilience to ultimately identify the causal drivers of changes in stress resilience.

3.1.1 Measuring resilience and stress response capacity in *C. elegans*

The nematode *C. elegans* has proven its strength in the assessment of physical readouts upon genetic perturbation and the characterisation of mutants. Fast generation turnover and the scalability of the model to obtain large amounts of RNA and protein add to the utility in experiments analysing molecular changes in transcription, translation, or metabolism, expanding the use to not just assess physiology, but dive into the underlying molecular mechanisms determining resilience. Utilising this, we confirmed that the *C. elegans* mutant *dys-1(eg33)* constitutes phenotypes synonymous with mammalian DMD. This model has been extensively studied as a model for muscle frailty (Hewitt et al. 2018; Ellwood et al. 2022), showing reduced strength and locomotion. Adding to this frailty, it was shown that the physiological phenotype can be improved by treatments in principle (Ellwood et al. 2022; Wu et al. 2022), which was crucial to not just understand the causes of frailty, but on the endeavour to modulate and improve frailty phenotypes. Quantifying locomotion throughout life, we showed that the muscle frailty phenotype is also progressing faster than in wild type controls (Fig. 8C), making the *dys-1(eg33)* mutant a model for progressive muscle loss. This adds an intriguing aspect to the use of this model, as it shows that there is more to this mutation than simply muscle failure. The animals are capable of moving and by that present muscle functionality. Considering the description of the consequences of the mutation, it appears the scaffolding function is not essential for muscle function, but rather involved in stability of the sarcolemma (Ellwood, Piasecki, and Szewczyk 2021), which is ultimately relevant in the maintenance of muscle function. Additionally, the mutant has been shown to increase Ca^{2+} influx into the cytosol and subsequently mitochondria (Higashitani et al. 2023), which is believed to have significant effects on the cell and metabolism. Overall, it carries a clear chronic burden on the homeostatic system showing reduced muscle function, which we show to be progressively reduced in aging, and a range of secondary effects burdening cellular health.

According to the project paradigm, we expect a reduced responsiveness to acute perturbation in the presence of a chronic burden. To test this, we applied different physiological assays describing the response to stress. We chose assays that recapitulate not just the ability to endure perturbation by assessing stress tolerance, but

aimed to capture the recovery from perturbation, as we understand resilience as the ability to endure, adapt to, and recover from stress to return to a healthy state. We therefore decided to assess fitness after stress treatment as a means to capture all aspects of resilience, testing if the animals were able to not simply survive a stress, but regain functional health. The recovery from heat was introduced as a metric of stress response capacity (Labbadia and Morimoto 2015), and showed reliable dose dependent reduction in recovery (Fig. 9A-B). Complementing this, we found treatment with Antimycin A (AA) to reduce locomotion after extended periods of treatment at low concentrations.

We leveraged this to describe an increased susceptibility to both of these stresses in the *dys-1(eg33)* mutant, showing reduced recovery rates from heat stress, and a significantly stronger impact on locomotion of stress treatment with AA (Fig. 9C). We suggest that the increased sensitivity to stress, either induced with heat or the ETC complex III blocker AA, was caused by a reduction in stress response capacity, indicated by the failure of responsive mechanisms to resolve the stress to the same extent as in the wild type. Especially in the heat treatment, the variation in recovery rates was visible, as although we measured the ability to move normally following recovery, the majority of *dys-1(eg33)* animals were not only unable to move, but were in fact dead. We further showed that this hypersensitivity was not caused by the inability to mount a functional stress response in principle (Fig. 18). The canonical stress response mechanisms in response to the stress in which we detected hypersensitivity did not appear to be altered looking at key markers and transgenic reporters. However, as this method is not representative for the entirety of the response, we required a more detailed analysis of this response on a broad molecular level, which we further assessed using RNA-seq. While we detected a significantly lower UPR^{ER} induction when investigating the induction of the responsive chaperone *hsp-4* using Tunicamycin (TM), we did not detect any effects on the physiology of adult nematodes in TM stress.

Overall, we show that the DMD mutant *dys-1(eg33)* is hypersensitive to heat and mitochondrial stress. Using the established methods and tools to assess resilience, we further showed that the mutants are capable of mounting a stress response, with a weaker induction in TM Stress. This hints at a reduction in ER stress signalling capacities, however, we could not determine if this was at the stage of stress sensing, since we could not find a physiological phenotype related to this reduced signal induction.

3.1.2 Experimental challenges for quantification of resilience

To define the best metrics for assessment of resilience in *C. elegans*, we assessed a range of disease models and physiological assays to identify the best model and readout. During this process, it became clear that we required tightly defined parameters to make sure the chosen models and assays fulfil a certain set of criteria. While models for protein aggregation are great for portraying progressive loss of proteostasis and reduced health at older ages, we realised that we had to look for a more prominent phenotype in early life to make molecular analysis feasible. It has proven to be more difficult than expected, as the efficiency of physiological assays to measure and quantify resilience depends on stress dosage and duration, prominence and penetrance of a phenotype, and the correct metrics to measure. This was crucial to describe a phenotype with good separation from the control to later enable identification of successful rescue in an attempted treatment of a condition.
Initially, we assessed models for protein aggregation and the comparison of two temperature sensitive mutants, *glp-1(bn18)* and *gon-2(q388)*. However, we could not identify the correct metrics for any of these comparisons, based on the absence of a frailty phenotype at the chosen age, and an insufficient penetrance of sterility of *gon-2(q388)* at the non-permissive temperature. This highlights the importance of setting criteria and

requirements in regards to the experimental setup, as even a great model might not be suited for a specific readout, and vice versa.

Comparison of conventional rescue treatments for DMD and resilience phenotypes

Following the identification of stress hypersensitivity in the *dys-1(eg33)* mutant, we employed a variety of treatments published to improve DMD phenotypes in *C. elegans* (Higashitani et al. 2023; Hewitt et al. 2018). This included various compounds (Fig. 10), and specific mutations linked to processes shown to be involved in certain disease relevant phenotypes (11). We could not detect an improvement in any of the treatments, which we could not annotate to a lack of efficiency of the compound, as we lacked the relevant controls to confirm target engagement. However, it was surprising that we did not detect any benefits in resilience or locomotion in a *dys-1(eg33);mcu-1(ju1154)* double mutant. This loss-of-function mutation for the mitochondrial calcium uniporter prohibits the uptake of calcium into mitochondria, which is a key phenotype in *C. elegans* DMD (Higashitani et al. 2023) and has been observed as an aspect of neurodegeneration (Alvarez et al. 2020). Neither genetic knockout or pharmacological inhibition with Ru360 improved locomotion in our experiments (Fig. 11). Strikingly, we did not detect any benefit in locomotion over 4 days of adulthood, and even found the double mutant to be more sensitive to heat stress than the *dys-1(eg33)* mutation alone.While there could be different reasons for the lack of this phenotype, this observation goes against published effects of this mutation (Higashitani et al. 2023).
Interestingly, we found most double mutants with *dys-1(eg33)* to show increased sensitivity to stress, as next to the *mcu-1(ju1154)* mutation the *hsp-6p*::GFP*(gpIs1);dys-1(eg33)* reporter double mutant was also more sensitive to heat stress (Fig. 9). In the context of resilience and considering the paradigm of limited overall resources in an organism, this might be explained by the additional burden the system experiences by needing to express additional protein in the reporter system, or attempting to release the calcium now accumulating in the cytosol. Turning this around, we could show that a strong increase in thermorecovery in a *daf-2(e1370)* mutant came at the cost of locomotion (Fig. 12).

In establishing relevant assays and exploration of suited models, we also drew inspiration from fundamental work on resilience in *C. elegans* pioneered by the group of Richard Moriomoto (Labbadia and Morimoto 2014). They describe a range of readouts for resilience and touch on key mechanisms, also covering a connection of physiology and molecular responses. They utilise the modulation of *jmjd-3.1* expression and show its effects as a strong determinant of resilience (Labbadia and Morimoto 2015). However, we were looking for a process that actively orchestrates stress response mechanisms, independent from epigenetic changes and developmental programs.
Overall, the establishment of assays and treatments was complex, and especially negative results in compound treatments are difficult to interpret, as confirmation of target engagement is challenging. Especially in *C. elegans*, where we find a multitude of possibilities why a compound is not effective, from problems in compound uptake into the organism through the cuticle, delivery from the intestine to other organs, or sheer incompatibility with the expected target. Strikingly, we could not circumvent limiting effects by maximising the respective drug dose. The challenges encountered during experimental design in the assessment of resilience and frailty show that the analysis of these characteristics needs to be precisely designed, and always depend on the specific scientific question it aims to answer. Clearly defining criteria and requirements for both the right model and the physiological assay were instrumental to identify the ideal parameters to portray a physiological frailty and stress hypersensitivity.

3.1.3 On the overlap of stress responses

In this study we aimed to analyse gene expression differences between the wild type and a stress sensitive disease model to uncover changes in the stress response expression patterns. We reason that by this we can elucidate how stress response pathways interact to drive physiological resilience mechanisms toward restoration of homeostasis. A recent study has discussed the connection of stress responses and shows the induction of ER stress markers in heat stress (Alcala et al. 2026). This overlap of stress responses has been addressed in previous research using the transgenic *hsp-4*p::GFP(*zcIs4*) reporter (Yoneda et al. 2004). Consistently, we find *hsp-4* mildly up-regulated in heat shock, where it is regulated in dependence of HSF-1 (Brunquell et al. 2016). While there is evidence for overlap, none of the available data address the dynamics of this interaction, or the nature of this interaction. By assessing the expression of key genes active in the UPR^{ER} and UPR^{mito} in heat stress, we aimed to differentiate if they act in parallel or depend on an initial response by the HSF-1 dependent stress response.

Confirming that heat stress affects more than the canonical HSR, we saw a mild induction of the UPR^{ER} stress marker *hsp-4* during treatment with moderate heat stress (Fig. 19). We find induction of the reporter after 8 hours, however, after 24 hours at 30 °Cthe signal had decreased again. We therefore find this to be a transient effect, contrary to the canonical HSR which continuously increased throughout this experimental setting (Fig. 13). Molecular analysis of these effects in a RNAseq heat stress time course confirmed these effects on transcript level (Fig. 27). Here, we identified a "burst" in transcript levels of the UPR^{ER} chaperones *hsp-3* and *hsp-4* in response to moderate heat stress after 4 hours at 30 °C(Fig. 27). Transcript levels declined throughout the later time points, which matches the observations on protein level in the reporter. Additionally, we saw a clear increase in components of the IRE-1/XBP-1 branch of the UPR upstream of chaperone expression. All these effects were found at moderate heat stress, and we reason that increased temperatures could cause much stronger effects on the UPR^{ER}. The induction dynamics followed the same trend as canonical HSR chaperones, and assessing public data for HSF-1 dependency, it appears that induction of at least *hsp-4* could be dependent on HSF-1 (Brunquell et al. 2016). It would be important to address this further in epistasis experiments to outline this interaction in more detail.
Assessing induction of the UPR^{mito} via expression of the stress responsive chaperone *hsp-6*, we confirmed this to also be affected by heat stress, as it visibly lost its baseline expression after 24 hours (Fig. 19). Assessing transcript levels in RNA-seq showed an initial increase in *hsp-6* transcript levels, following the trend of other chaperones being strongly induced after 4 hours (Fig. 27). However, transcript levels of the main driver of the UPR^{mito}, *atfs-1*, were reduced in heat stress. Without further analysis it remains to be shown how this dynamic process is affected by heat stress, but there appears to be a significant impact in response to heat stress, which we further confirm by modulating this stress response mechanism to affect heat stress recovery outcomes.

Additionally, *hsp-4* appeared to be affected by mitochondrial stress with strong local expression in the distal area of the intestine in long-term exposure to AA (Fig. 19). As this stress causes very local effects in mitochondria, this is intriguing in comparison to heat which affects the entirety of the cell. Therefore this fragmented induction in AA stress could be the result of direct stress response cross-talk, as mitochondria are physically connected to the ER (Liu et al. 2019). This connects the induction of oxidative stress in the mitochondria to the response mechanism at the ER. In contrast to the markers of UPR^{ER} and UPR^{mito}, the expression of *hsp-16.2* was exclusively induced in heat stress.

Monitoring the ISR in *C. elegans*

Investigating the activity of the Integrated Stress Response (ISR) in *C. elegans* proved to be a huge challenge, as the available tools were shown to be compromised (Fig. 16). In collaboration with the laboratory of Nicolas Lehrbach, we designed and tested a variety of alternative reporters for ISR activity and *atf-4* expression to address these technical limitations (Fig. 35). However, experiments utilizing an endogenously GFP-tagged *atf-4* transgene revealed that its expression was independent of typical stress inducers like heat or TM stress. These findings challenge the assumed conservation of the ISR in nematodes and underscore the vital importance of rigorous controls and the constant questioning of scientific hypotheses.
What remains to be explained are the effects observed in reduced mRNA translation in heat stress in the absence of ISR activity in the ISR inhibition mutant *eif-2α(syb1385)*. This observation challenges the understanding of the ISR as the driving mechanism in reduced mRNA translation during heat stress. As an alternative mechanism, it is shown that the HSF-1-facilitated reduction of translation can also regulate proteostasis (Howard et al. 2016). This raises critical questions regarding the extent of ISR dependency in these processes and adds another angle to the potential cross-talk between these regulatory pathways in heat stress.

Taken together, we find strong evidence for the induction of UPR^{ER} and involvement of the UPR^{mito} in heat stress. Furthermore, we show local expression of *hsp-4* in AA stress. It remains to be shown how these response mechanisms interact in detail, and how they converge to determine resilience.

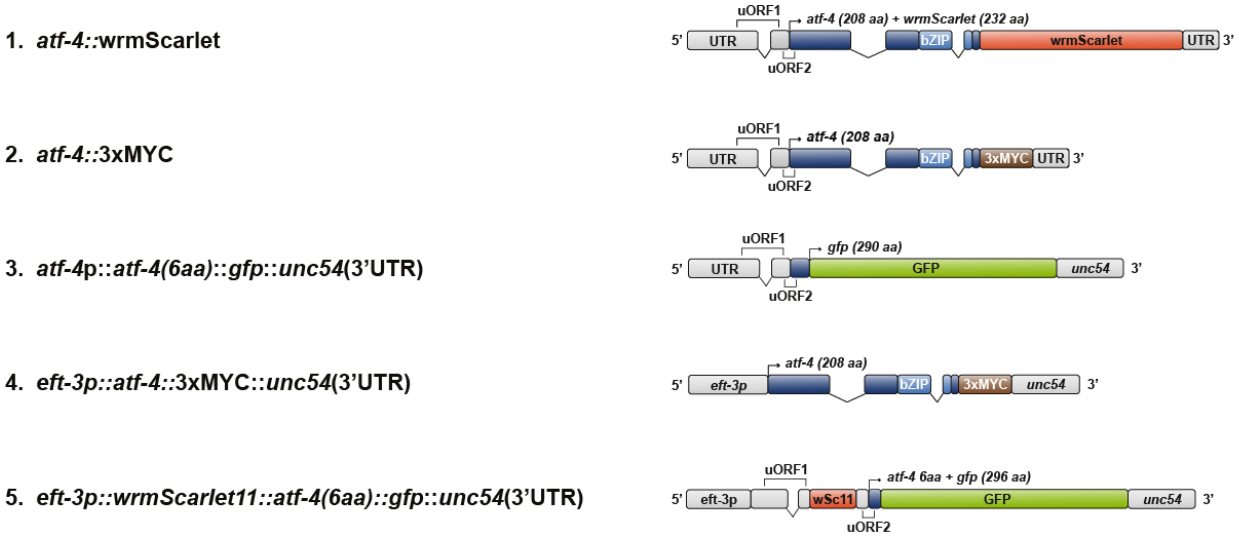

Figure 35: ***Transgenes designed to report on ISR activity.*** *Schematic overview of 5 transgenes designed as part of this project. Transgenes 1 and 2 were designed as endogenous edits to be introduced into the genome by CRISPR-Cas9. Transgenes 3-5 were designed as artificial transgenes to be introduced as extra-chromosomal arrays.*

3.2 Elucidating stress dynamics to explain heat hypersensitivity

We argue that comparison of steady-state transcriptomes is not sufficient to reveal relevant changes causing stress hypersensitivity in the *dys-1(eg33)* mutant, as expression during stress is highly dynamic and precisely wired. To advance our understanding of the relevant processes and how they vary in the DMD model, we employed RNA-seq in a time course stress experiment to outline the differences in gene expression changes in the frail *dys-1(eg33)* mutant.

3.2.1 Effects of the canonical heat shock response

In initial dose finding experiments using a transgenic reporter expressing GFP under the promoter of the HSR chaperone *hsp-16.2*, we could outline the dose-dependent induction of the response over 24 hours (Fig. 13). We chose to continue assessment of the underlying molecular changes in heat stress exposure at a temperature of 30 °C, describing the stress dose that caused a strong induction of the signal, without overwhelming the system and avoiding saturation of the response. This decision was made to ensure we would not exhaust the response, and ensure we could outline a dynamic process during the induction of the HSR. The aim was to expand on a snapshot of stress induction by comparison of unstressed and stressed conditions, toward outlining the muli-phasic changes experienced during heat stress over time. We reasoned that transient and adaptive gene changes are commonly masked by assessing a single time point, and this would add significant value to the understanding of the HSR. Previous studies have assessed time course heat induction using RNA-seq (Jovic et al. 2017). However, the chosen stress was severe and they showed that treated animals died as a consequence of their treatment. We therefore think that their data is contaminated by pro-death signaling. While this data set certainly covers key changes in the canonical HSR and gives an insight on affected mechanisms, the overwhelming stress stimulus is unlikely to enable a detailed and sensitive coverage of heat shock response dynamics, and does not recapitulate physiological perturbation. We aimed to address the shortcomings of the experimental design by using a moderate stress to enable a separation of changes by time and induction intensity. Additionally, we expand the use of this experiment to uncover changes in the response of the hypersensitive *dys-1(eg33)* mutant.

Confirming that stress induction was efficient and serving as key control in this experiment, we find a strong signature of the HSF-1 dependent HSR after 4 hours of heat stress (Fig. 21). The most affected genes are well-described effectors of the HSR, with 7 of the 10 most significantly changed up-regulated genes being well-characterised targets of HSF-1 (Brunquell et al. 2016). We identified a burst in expression in the initial phase of the time course after 4 hours, before slowly decreasing again after, describing the on-demand transcriptional induction facilitated by HSF-1 (Fig. 22A). Considering the observations in experiments with the fluorescent reporter, where we saw a consistent increase of the signal over 24 hours on protein level (Fig. 13), this shows the dynamic nature of the process from initial transcription changes to functional response on protein level. This touches on a clear limitation of this experiment, as HSR dynamics include more than transcriptional changes and protein turnover, protein interaction, and protein half life are key metrics that functionally affect adaptation and stress response mechanisms. This observation of an initial peak and slow return to lower transcript levels was observed throughout the experiment for genes associated with the canonical HSR. They were, however, consistently stronger expressed than in the untreated controls, indicating the crucial role of the HSF-1 dependent response throughout.

This slow decline in the transcript levels of main effectors when exposed to stress could be a simple

normalisation following an overshoot of the response in the initial response phase, or an adaptation to the new conditions. As we were aiming to capture expression changes relevant in resilience, this could be informative, as resilience is more than the simple ability to mount a programmed response, and also includes an adaptation and re-establishment of homeostasis in response to a perturbation. Expanding our approach, it would add significant value to also assess recovery after a stress, as there could be programmed mechanisms to return to normal function in stress recovery. This would reflect the conditions in the natural habitat of *C. elegans*, as they are exposed to temperature changes throughout the day and life, which could also be recapitulated experimentally.

3.2.2 Novel implications in heat stress

Investigating stress dynamics in a time course uncovered a variety of changes that would have been missed by steady-state transcriptome comparison. Adding to changes describing the canonical HSR, we found several processes that have not been described as mechanisms affected by heat. Serving as an insightful control to cross-check our results, we used two reference data sets assessing the effects of specific HSF-1 signalling and broad heat stress induction to confirm results and support our observations (Sural et al. 2019; Brunquell et al. 2016). In one approach, signatures are generated from the comparison of an HSF-1 over-activation mutant that carries a mutation in the HSF-1 negative regulator HSB-1 (Sural et al. 2019). Furthermore, we utilised work describing the HSF-1 dependent and independent signatures in the HSR in an attempt to identify stress response mechanisms not relying on HSF-1 (Brunquell et al. 2016). These resources outline a clear signature for HSF-1, and build a strong foundation supporting the interpretation of our data, serving as control in observations and understanding novel trends. Analysis of stress dynamics revealed three main processes we identify to be involved or affected by the HSR, and confirm our observations by comparison to the reference data sets.

Understanding the role of mitochondrial gene expression in heat stress

First, we noted a strong reduction in the expression of genes encoded on the mitochondrial genome with a significant drop of transcript levels from the earliest time point (Fig. 23D). Assessing transcript levels of mitochondria related genes encoded by the nuclear genome, as described in the mitocarta (Rath et al. 2020), we confirmed that these changes were not caused by an under-representation of mitochondrial DNA as an RNA-seq artifact. It appeared to be a coordinated reduction in transcript levels from the mitochondrial genome in heat stress, and could indicate a programmed mechanism during heat stress. Considering potential explanations for this observation, we wondered if this was driven by an active regulatory process, or indirect effects of changes in overarching cellular dynamics. Heat stress exerts wide-reaching systemic effects on cellular proteostasis, where the canonical Heat Shock Response (HSR) classically coordinates the clearance of misfolded proteins by inducing chaperone expression and tuning translation to prevent further proteotoxic load (Singh et al. 2024). Beyond the cytosol, thermal stress profoundly impacts mitochondrial homeostasis, leading to the loss of membrane potential, generation of reactive oxygen species (ROS), and the change of mitochondrial morphology (Shutt and McBride 2013; Iba et al. 2025). During stress, mitochondria undergo a complex change of dynamics with moderate stress causing Stress-Induced Mitochondrial Hyperfusion (SIMH) as a survival strategy (Tondera et al. 2009; Shutt and McBride 2013). However, prolonged or extreme stress can shift these dynamics to induce mitochondrial fragmentation and signal for cell death (Bliek 2009; Das

and Chakrabarti 2020). Surprisingly, we identify markers for either process to be heavily affected in heat stress, suggesting that the mitochondrial stress response is not a binary switch but a complex process. Overall, the balance of fission and fusion is highly sensitive to changes in cellular homeostasis and reacts to stress by the induction of various active response mechanisms. While we observe a significant reduction in transcript levels of genes from the mitochondrial genome, it remains speculative whether this stems from a programmed transcriptional suppression or is simply a consequence of altered mitochondrial mass and dynamics.

Understanding the role of histones in heat stress

We further uncover the transient increase in transcript levels of a subset of histones (Fig. 23F), which were exclusively induced in heat stress at time points where the transcript levels of the canonical HSR were already declining (Fig. 22A). The most relevant genes describing the strongest trend in this effect were *his-38* and *his-40*, which showed their highest transcript levels after 8 hours of treatment, before returning to their baseline expression after 24 hours. This transient response could indicate an active role in the response to heat stress, and is also represented in data sets describing HSF-1 signatures (Sural et al. 2020). The expression of histones has previously been linked to heat stress, as the knockout of certain H3.3 expressing genes did reduce viability in heat stress (Delaney et al. 2018). While it does not imply our main candidates *his-38* or *his-40*, they show a functional link between the expression of histones and heat stress survival. Interestingly, combining this with observations made in the reduced transcripts of genes on the mitochondrial genome, this advances a recent hypothesis suggesting a HSF-1 dependent suppression of gene expression from the mitochondrial genome, hypothesising that histones are shuttled to mitochondria to support compacting of the mitochondrial genome (Sural et al. 2020). The authors show the presence of histones in mitochondria, however, further experimental evidence would be required to fully outline this relationship. Taken together, we show transient expression of histones as a suspected secondary response in heat stress. Future research should investigate if this is an actively regulated process indicating a demand for histones during heat stress, and if it is required for stress survival.

Understanding the role of aspartic proteases in heat stress

We find the by far largest group of genes down-regulated throughout the stress time course to be genes linked to proteolysis. We identified aspartic proteases to significantly contribute to this effect and describe a consistent trend, with expression levels consistently dropping throughout the experiment (Fig. 23B). Interestingly, the aspartic protease *asp-13* was among the strongest down-regulated genes at every individual time point. Referring to the literature, various aspartic proteases can be found down-regulated in both RNAseq reference data sets. Aspartic proteases are a highly conserved class of proteolytic enzymes characterized by two aspartic acid residues in their active site. *asp-3* and *asp-4* have been shown to play an important role in necrotic cell death (Syntichaki et al. 2002). Along with the cysteine protease *vha-12*, which we also find down-regulated in our data, they are required for the execution of necrosis triggered by hyperactive ion channels or heat stroke. Surprisingly, *asp-1* has been shown to be only expressed in development in the intestine (Tcherepanova et al. 2000). Our data strongly contradicts this, as we detect a stable expression of *asp-1* in adult animals of both genotypes, which was not affected by larval development as these levels were stable throughout the experiment and worms were raised on FUdR.

Research on aspartic proteases appears to be limited, with almost no literature on expression changes

in stress, albeit being present in reference data sets (Sural et al. 2019; Brunquell et al. 2016). In proteostasis and protein quality control, proteases usually ensure that misfolded nascent polypeptides are degraded before they can form toxic aggregates. As misfolding of proteins is increased in heat stress, the he overall reduction in proteolysis would seem counter intuitive. However, we hypothesize this could serve as a mechanism to prohibit cleavage of nascent proteins like chaperones expressed in response to stress, to protect the response machinery during re-establishment of homeostasis. Supporting this would be the improved thermorecovery we observe upon RNAi mediated knockdown of *asp-1* (Fig. 29). As another possibility, we considered the reduction of protease transcript levels to come from a reduction in food ingestion. We base this theory on the expression patterns of aspartic proteases, which is strongest in the intestine for all *asp* genes we found deferentially expressed in the wild type (Gao et al. 2023). Environmental stress, including heat, has been shown to significantly reduce food uptake (Furones et al. 2026). An alternative explanation could therefore be that there is simply no requirement for proteins active in digestion mechanisms during extended periods of stress. The gradual reduction in expression levels compared to the rapid changes we observe in the chaperones of the HSR could support this, as a decline in protease demand in the intestine would likely be slow, being the consequence of a reduced signalling for the expression of proteases. Contradicting this idea are the observations in the *dys-1(eg33)* mutant, where we see a much weaker reduction in transcript levels. It would be surprising if the mutant would show a difference in ingestion during stress, as they are overall much stronger affected by heat in the shown hypersensitivity phenotypes. Future research should focus on the impacts of impairing protease function, and assess the effect of impairment of food uptake on aspartic protease expression. This could prove informative by showing if other means of impairing food uptake can mimic the heat stress induced effects.

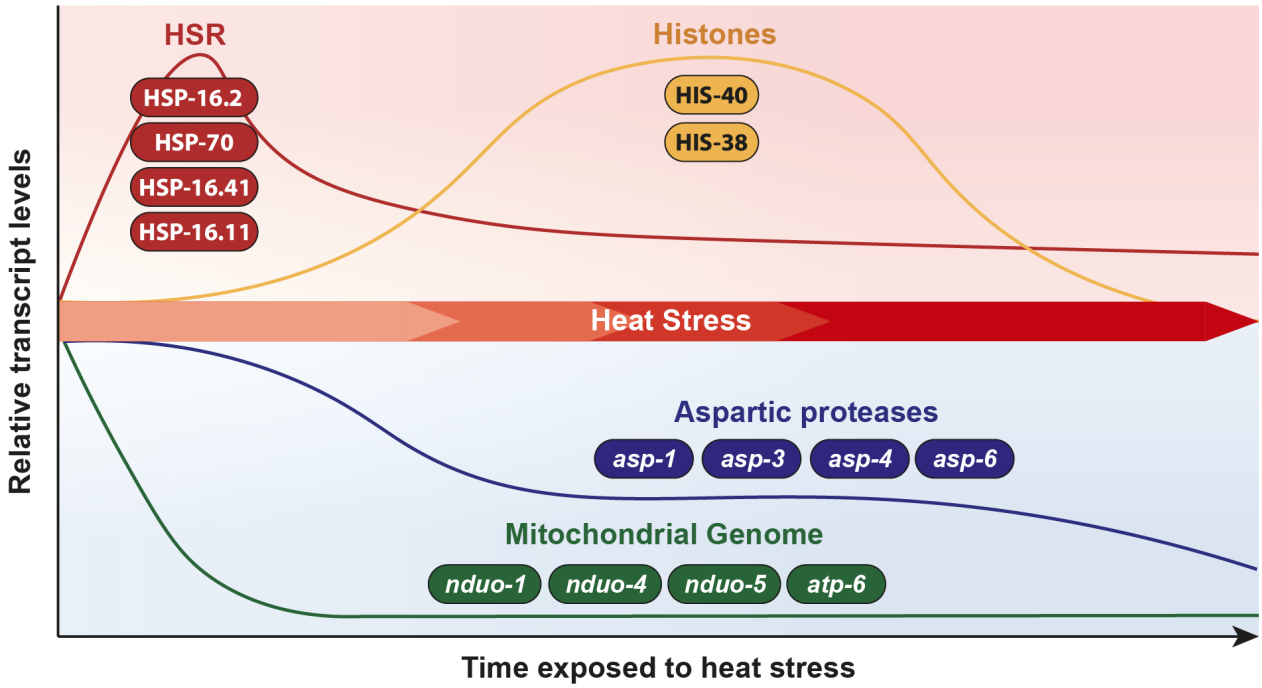

Figure 36: ***Trends of the heat shock response.*** *Schematic overview of processes altered in heat stress based on trends in transcript levels in RNA-seq time course. Positive trends in the red box describe up-regulated processes, negative trends in the blue box describe down-regulated processes. Next to effects of the canonical HSR, we find a transient increase of transcript levels in histones, with the strongest representatives being his-38 and his-40, and a down-regulation of aspartic proteases and genes encoded on the mitochondrial genome active in OXPHOS.*

Summarising novel trends in the response to heat shock

Taken together, we observe several novel trends in our RNAseq experiment which open new angles on the HSR. As our experiment covers more than initial effects of heat stress induction, we uncover transient changes in histone expression, and a gradual decline in transcript levels of diverse processes. This expands our understanding of the effects of heat stress, adding to the canonical HSR dependent on HSF-1. We also identify changes only occurring at later stages of the HSR, indicating an adaptation to new conditions, which could be crucial in understanding recovery as an additional factor determining resilience past initial stress response mechanisms. This experiment gives an interesting insight on how these processes interact to support adaptation and recovery from a global acute stress affecting the organism. Regarding differences of transcript levels of histones, aspartic proteases and genes encoded on the mitochondrial genome, we suggest that future experiments should focus on elucidating if these are actively regulated process in response to heat stress, or simply the result of the wide-reaching consequences of a global stress on the organism.

3.3 Alleviating stress hypersensitivity in *C. elegans dys-1(eg33)* mutant

The aim of this study was to identify modulators of disease by comparison of wild type and disease gene expression during stress. We employed physiological assays to characterise frailty in the context of resilience, and assessed stress response dynamics using transgenic reporters to capture relevant transcriptome changes during heat stress. Comparing wild type and disease dynamics, we describe transcript level changes in a hypersensitive mutant to uncover mechanisms driving homeostatic frailty in disease.

3.3.1 Characterising stress hypersensitivity in *dys-1(eg33)* mutant

The phenotypes that are described in the *dys-1(eg33)* mutant are diverse and cover a variety of mechanisms that appear to be affected by the gene truncation. Observation of reduced lifespan, and behaviour in different compound treatments have been utilised to study the aspects of muscle-related phenotypes, mostly focused on locomotion and mitochondrial morphology (Ellwood, Piasecki, and Szewczyk 2021; Hewitt et al. 2018; Sudevan et al. 2019). Here, we leverage the *dys-1(eg33)* mutant as a model for stress response hypersensitivity. First, we showed stress hypersensitivity of the *dys-1(eg33)* mutant in heat and mitochondrial stress (Fig. 9). This makes the DMD mutant a suited model for homeostatic frailty, adding to its use constituting progressive muscle loss assessed as reduced locomotion in age (Fig. 8). The observed sensitivity to thermal stress we detect aligns with the understanding of the model showing calcium imbalance, as heat stress acts as a catalyst for cytosolic calcium leakage, which in turn triggers mitochondrial fragmentation (Momma et al. 2017). Analysis of key effectors of canonical stress response pathways using transgenic fluorescent reporters did not show any significant changes of the expression of stress markers in response to heat or mitochondrial stress (Fig. 18). The only difference we identified was in the intensity of induction of *hsp-4* in ER stress, which we could not tie to a frailty phenotype in adult *dys-1(eg33)* mutants. Overall, we showed that the *dys-1(eg33)* mutant is capable of mounting a heat shock response, with all key markers following the expected trends and dynamics of the wild type, albeit at lower amplitude in ER stress. Studies in mdx mice have shown that the ER environment in dystrophic muscle is severely compromised by calcium Ca^{2+} leakage through ryanodine receptors (RyR), triggering the PERK branch of the UPR^{ER} and consequently the ISR (Krishna et al. 2023). Additionally, the disturbance of calcium homeostasis at the ER in muscle cells has been linked to reduced muscle function, and restoring calcium signaling between the ER and mitochondria alleviated detrimental

phenotypes (Pauly et al. 2017). However, we did not detect a physiological readout in the *dys-1(eg33)* mutant upon disturbance of the ER, and therefore proceeded to assess the response to heat stress.

3.3.2 Uncovering potential drivers of stress hypersensitivity in *dys-1(eg33)* mutant

Adding acute heat stress to the chronic burden experienced in the *dys-1(eg33)* mutant revealed a variety of differences in the comparison of stress dynamics to the wild type. However, transcript changes as defined in the canonical HSR were not significantly changed in the *dys-1(eg33)* mutant (Fig. 27A), supporting initial observations in fluorescent reporter induction. When assessing transcript levels of established stress response markers of additional stress response pathways, we observed changes in the UPR^{mito} in the *dys-1(eg33)* mutant. Here, the initial changes of the main drivers *atfs-1*, *hsp-6*, and *hsp-60*, described the same trajectory as the wild type. In contrast, from the 8 hour time point onward it appeared that the mutant transcript levels remained consistently lower, while the wild type maintained elevated expression of *hsp-6*, and *atfs-1* transcript levels returned to pre-stress conditions.

Assessing the novel heat stress trends we identified, the transient up-regulation of histones in the wild type appeared to be much weaker in the *dys-1(eg33)* mutants, only showing up-regulation to about 50 % of the mRNA levels observed in the wild type (Fig. 26D). However, the DMD model did not show any significant changes in the expression from the mitochondrial genome, as transcript levels were reduced as described in wild type dynamics. The reduction of expression of the aspartic proteases, however, appeared to overall be weaker than in the wild type (Fig. 26C). Strikingly, the protease *asp-1* appeared to even increase in expression levels after 24 hours in the *dys-1(eg33)* mutant. Compared to the wild type, which showed significantly lower transcript levels than baseline in the extended stress period, the DMD model developed in the opposite direction. The regulation of aspartic proteases has been linked to dysregulation of calcium homeostasis, with high levels of expression of ASP-3 and ASP-4 being involved in facilitating necrosis and neurodegeneration (Syntichaki et al. 2002; Glaser et al. 2019; Ludtmann and Abramov 2018). Considering this link intensifies the potential involvement of Ca^{2+} imbalance in homeostatic frailty in DMD, and urges more direct assessment of calcium metabolism in the *dys-1(eg33)* mutant to investigate causality. Ultimately, we have identified a variety of changes in stress dynamics comparing stress induction of the wild type with a model that is sensitive to stress in the *dys-1(eg33)* mutant. From all detected differences in steady-state and dynamic changes in expression we compiled a list of candidates showing elevated levels when compared to the wild type, which we further assessed in RNAi mediated knockdown experiments for their potential to alleviate stress hypersensitivity of the *dys-1(eg33)* mutant in thermorecovery.

3.3.3 Modulating stress hypersensitivity in *dys-1(eg33)* mutant

In *C. elegans*, the reduction of Insulin/IGF-1 signaling (IIS) is one of the most potent ways to enhance resistance to multiple forms of environmental stress, particularly heat stress (Hsu, Murphy, and Kenyon 2003). Accordingly, we find that the *dys-1(eg33); daf-2(e1370)* double mutant recovers significantly better after heat stress (Fig. 12). This aligns with previous research showing the reduced decline of muscle function, and alleviation of reduced lifespan in the *dys-1(eg33)* mutant upon IIS modulation (Oh and Kim 2013). Surprisingly, we did not detect any benefits in locomotion. In contrast, we even detected motility to be significantly lower in the double mutant. This could indicate a trade-off in improved stress response capacity at the cost of locomotion, however, it might just not be the ideal metric to assess these effects.

From the compiled list of candidates with expression differences in steady-state or dynamic changes in expression, we tested the potential to improve thermorecovery upon knockdown. With this approach we found 5 candidates to significantly improve thermorecovery after heat stress treatment at varying stress exposure durations (Fig. 29). Surprisingly, *asp-1* was the only successful candidate identified from dynamic changes to show a mild improvement upon knockdown, while the remaining candidates were found from expression differences on baseline. This does not strengthen the benefit of adding acute stress to identify causal changes, however, it could also be a result of the clear limitations of the RNAi candidate screen. While we know that RNAi can be sufficient to improve thermorecovery in *daf-2* RNAi, it is impossible to assess the efficiency of individual RNAi treatments, and similar to the limitations in compound treatments, we can't control for the reduction of the respective target expression without specific fluorescent reporters. Therefore we cannot prove that modulation of the remaining candidate genes does not improve thermorecovery.
The most consistent candidate, with an increased recovery at all chosen conditions and at times outperforming the positive control of *daf-2* RNAi, the transcription factor SPTF-3 emerged as the top candidate from the thermorecovery improvement screen, and was further assessed for its potential in improving frailty phenotypes in the *dys-1(eg33)* mutant. We believe that the overall approach can be leveraged further by comparison of other disease models that show a variation in resilience in specific stress contexts. Additionally, the remaining candidates that showed improvement of thermorecovery upon knockdown present intriguing observations to follow up in separate studies.

3.3.4 The role of SPTF-3 and the UPR^{mt} in *C. elegans* DMD

The transcription factor SPTF-3 is a positive regulator of the *atfs-1*-dependent UPR^{mt} and orchestrates mitochondrial biogenesis in response to a variety of stimuli related to reduced availability of resources (Hemerling et al. 2023). We hypothesise that the increased baseline expression of this TF in the *dys-1(eg33)* mutant could stem from chronic mitochondrial stress and elevated Ca^{2+} influx (Higashitani et al. 2023). A persistent activation of the UPR^{mt} could deplete the homeostatic stress capacity in acute perturbation, making the system more vulnerable to additional stress like heat, which increases metabolic demand and exacerbates calcium-induced mitochondrial damage (Momma et al. 2017). Boosting mitochondrial biogenesis, indicated by elevated *sptf-3* levels, could be interpreted as a countermeasure to buffer for mitochondrial burden.
To further investigate this, we assessed previous studies that outline the steady-state transcriptome of *dys-1(eg33)* and *dys-1(cx18)* mutants, the authors analyse transcript levels in larval and adult samples (Hrach et al. 2020). They find genes linked to increased mitochondrial homeostasis to be up-regulated early in the DMD mutants, while later changes are linked to muscle-structure maintenance. In the *dys-1(cx18)* mutant, resulting in a shorter truncated protein than in *dys-1(eg33)*, they found the two UPR^{mt} chaperones HSP-60 and HSP-6 to be up-regulated (Hrach et al. 2020). However, we could not confirm this hypothesis by assessment of *hsp-6*p::GFP(*zcIs13*) reporter induction, as we did not find any baseline induction which would support a chronic UPR^{mt} activation, and in turn identify an increase in signal upon knockdown of *sptf-3* (Fig. 30).

Additional trends that align with our results include the increase in *asp-1* and *asp-6* levels, and lower levels of the histones *his-38* and *his-40*. Surprisingly, they only find *sptf-3* to be subtly higher expressed in early stages. This could be explained by the exclusive selection for expression levels in the muscle in their study, while we assess whole worm RNA-seq data. It therefore also remains an intriguing question "where" all this occurs. *dys-1(eg33)* is mostly interpreted as a model for muscle frailty, which would be supported by the specific effects of calcium-leakage in muscle cells upon heat stress (Momma et al. 2017). Further

research should focus on the effects of the *dys-1(eg33)* mutation in different tissues, and investigate if the stress hypersensitivity originates exclusively in the muscle, or if there is an organism-wide vulnerability.
In regards to the identified changes in transcript levels of aspartic proteases during stress, the expression of proteases in calcium imbalance has previously been linked to the muscle frailty and necrosis of the *dys-1(cx18)* mutant (Joyce et al. 2012). Here, the authors describe how calcium-dependent protease *clp-1*, but also the aspartyl proteases *asp-3*, *asp-4* and in a lesser capacity *asp-1*, are involved in facilitating necrosis. This indicates a connection between frailty phenotypes in *C. elegans* DMD, calcium imbalance, and proteolysis, which we now identify to be affected further by heat. It remains to be tested if this process is actively involved in heat stress lethality, or is merely a side effect made prominent by acute perturbation.

Overall, we identified a previously undescribed involvement of SPTF-3 in DMD-related stress hypersensitivity, where reduction of increased baseline expression is sufficient to partially rescue heat stress hypersensitivity in *dys-1(eg33)* mutants. We show that RNAi mediated knockdown of *sptf-3* induces the UPR^{mito}, which led us to the investigation of other means to induce the UPR^{mito} as methods to alleviate stress hypersensitivity in the DMD model. Thus, we show that increasing ATFS-1 activity in gain-of-function mutants, or via RNAi-mediated knockdown of *nuo-6*, which is linked to mitohormesis and the bolstering of acute stress response capacity (Yang and Hekimi 2010a), can also improve thermorecovery in wild type and *dys-1(eg33)* mutants. Future experiments should address if these effects are mediated by an increase in UPR^{mito} response capacity, or secondary effects relayed to mitochondrial biogenesis and health. Furthermore, we remain to show how knockdown of *sptf-3* can induce the UPR^{mito}, as it is contradictory being understood as a positive regulator of the UPR^{mito}.

3.3.5 Implications in mammalian DMD

The conservation of functional domains within the *C. elegans* dystrophin protein makes the nematode an effective model to describe the structural and mechanical detriments observed in mammalian DMD. Because the core components of the dystrophin-glycoprotein complex (DGC) are evolutionarily conserved, the loss of sarcolemma integrity and altered signaling cascades in the worm closely describe those in mammals (Ellwood, Piasecki, and Szewczyk 2021). This enables *C. elegans* to serve as a high-throughput proxy for identifying aspects of DMD frailty, and identify methods of genetic and pharmacological modulation that prevent muscle function decline or improve cellular resilience during stress.
In mammalian DMD, mutations in the dystrophin gene lead to progressive muscle wasting, fibrosis, and respiratory failure (Duan et al. 2021). Here, we show that *C. elegans* not just mirrors muscle frailty, but also recapitulates the aspect of a progressive muscle loss, by far exceeding the reduction in muscle function observed in wild type aging (Fig. 8). Studies in mdx mice and human biopsies reveal that these muscles are characterized by chronic calcium overload, excessive reactive oxygen species (ROS) production, and mitochondria that are already severely dysfunctional and fragmented (Kelly-Worden and Thomas 2014; Duan et al. 2021). It remains to be convincingly shown if this mitochondrial burden is merely a secondary consequence or a central driver of the disease, as the metabolic exhaustion of the muscle fibers accelerates necrotic cell death and prevents effective regeneration. While the structural effects of the *dys-1* mutations are similar, we remain to show if the signaling and resilience phenotypes we detect in *C. elegans* also translate to mammalian DMD.

Our discoveries in the *C. elegans dys-1(eg33)* model regarding SPTF-3 have significant parallels in mammalian DMD. Strikingly, activation of the mammalian ortholog of SPTF-3, Sp1, has been shown to be involved in

the muscle's response to chronic injury and metabolic stress (Lv et al. 2023). The authors describe it as a target for the treatment with Naringenin (NAR), which they use to alleviate muscle frailty phenotypes in mdx mice. Furthermore, Sp1 and Sp3 have been shown to regulate expression of Dp71 in myoblasts, a dytrophin protein abundant in the brain and non-muscle tissues in mammals (León et al. 2005). These studies indicate a context-dependent direct interaction of Sp1 and dystrophin, which could add significant insight to our observations.
Additionally, analysis of mdx mouse model and human DMD biopsies have revealed heightened ER stress markers BiP (Moorwood and Barton 2014). Considering our observations regarding alterations in UPR^{ER} induction (Fig. 18), this could indicate a direct link of a DMD model to alterations in stress response capacity. Assessing further functions, Sp1 can also act as a mediator of the fibrotic response, working alongside SMAD proteins to drive the expression of Connective Tissue Growth Factor (CTGF) and collagen genes (Córdova et al. 2015).

Overall, research in mammalian DMD models suggests that our findings could be highly relevant in higher organisms, especially regarding the involvement of the transcription factor Sp1. The discovery that improving mitochondrial stress response capacity and biogenesis in dependence of *sptf-3* enhances resilience in *C. elegans* DMD models suggests that bolstering UPR^{mito} capacity could impact human disease outcomes. While current frontline treatments such as corticosteroids focus on reducing inflammation, and modern gene therapies aim to restore structural function, targeting mitochondrial resilience offers a complementary therapeutic approach. This shift toward improving "organismal resilience" rather than structural repair represents a promising frontier in multi-modal DMD therapy.

Summarising the aspects of stress hypersensitivity in *C. elegans* DMD mutant *dys-1(eg33)*

Here, we characterise the *C. elegans dys-1(eg33)* mutant as a model for stress hypersensitivity in thermal and mitochondrial stress, outline the stress-dependent transcriptome changes in heat stress, and propose ways to alleviate this stress hypersensitivity. Taken together, we identify processes related to calcium imbalance, proteolysis and UPR^{mt} to show variation in stress behaviour in the *dys-1(eg33)* mutant. As these processes converge at mitochondria, we further assessed how modulation of mitochondrial dynamics could affect stress survival, and find that improving UPR^{mt} capacity is sufficient to alleviate the stress hypersensitivity phenotype in the *dys-1(eg33)* mutant. These effects were achieved by depletion of *sptf-3* or *nuo-6*, or by gain-of-function mutations of the key UPR^{mito} driver ATFS-1.

3.4 Improving stress response capacity in *C. elegans*

In this study we uncover changes in the stress response expression patterns of the *dys-1(eg33)* mutant, which we use to understand how stress response mechanisms interact to return the organism to a state of homeostasis. Beyond this, our objective was to utilise these insights to develop interventions to restore organismal resilience. After comparison of various treatments, modulation of the UPR^{mito} emerged as the most robust conveyor of improved thermorecovery.

3.4.1 Boosting the UPR^{mt} to increase stress resilience

To improve thermorecovery in the *dys-1(eg33)* mutants, we chose a set of *atfs-1* gain-of-function mutants, generated in a forward genetic screen selecting for activator mutations of reporter signal of the transgenic *hsp-6p*::GFP(*zcIs13*) reporter ((Rauthan et al. 2013)). Interestingly, these mutants have been described to improve stress resistance in specific contexts, while not improving lifespan (Pede et al. 2025). This describes a trade-off where this mechanism promotes survival in acute stress scenarios, without carrying a long-term benefit. We also find this to be connected to a prominent pro-health concept within dietary restriction, which has not just been shown to improve stress resistance, but also shown to impact *atfs-1* through food deprivation (Naresh et al. 2022).

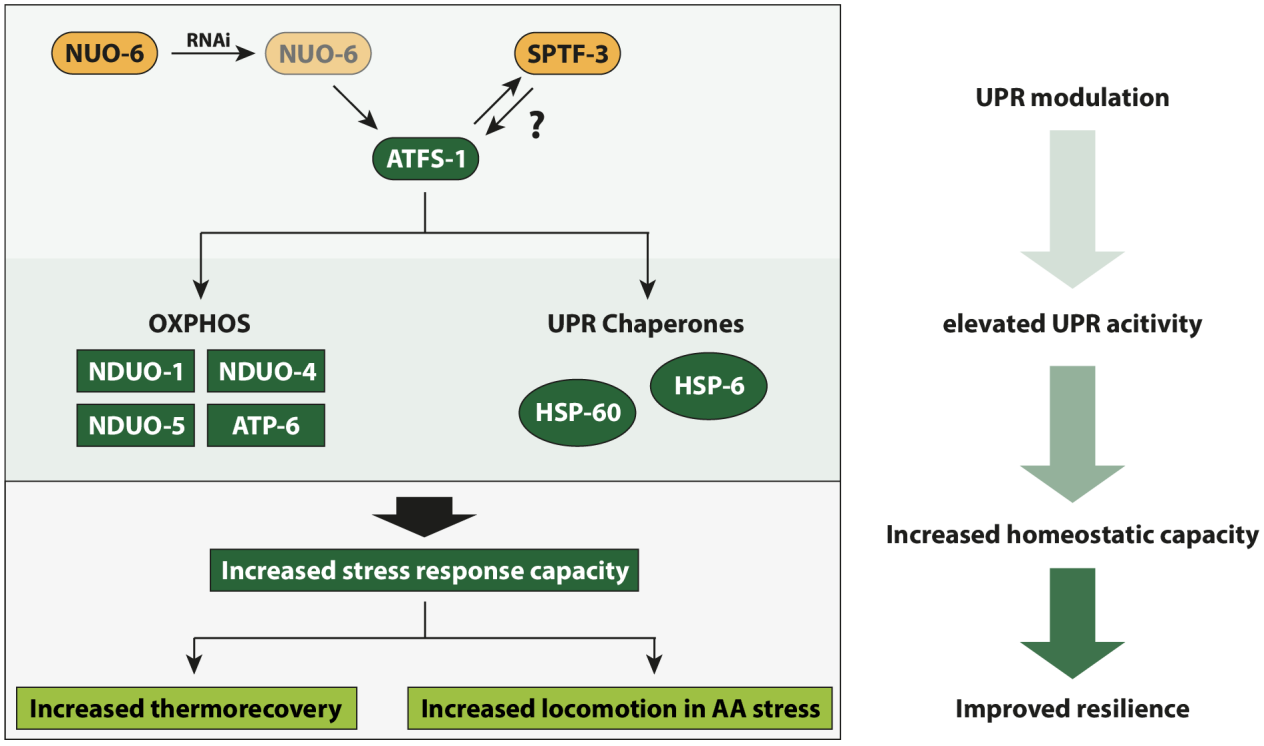

Figure 37: ***Boosting UPR^{mito} activity improves resilience by increasing homeostatic capacity.*** *Increasing UPR^{mito} signaling by modulation of gene expression of sptf-3 or nuo-6, as well as gain-of-function of the TF atfs-1, leads to elevated transcript levels of mitochondrial OXPHOS genes and chaperones. This subsequently increases stress response capacity, measured as increased thermorecovery and motility following mitochondrial stress.*

Assessment of these strains in our assays confirmed a robust improvement of thermorecovery in the *atfs-1* activator mutants (Fig. 31). This coincides with a strong activation of the *hsp-6*p::GFP(*zcIs13*) reporter, confirming increased UPR^{mt} activity in this strain. Surprisingly, we did not find this strong activation on transcript level when assessing mRNA levels using qPCR (Fig. 32B). We could, however, show that *atfs-1* gain-of-function leads to a clear increase in transcription of OXPHOS genes encoded on the mitochondrial genome, measured in expression of *nduo-1*, *nduo-4*, and *atp-6*. Furthermore, SKN-1 signalling did not appear to be involved in this effect, as the levels of *gst-4* were not changed in the *atfs-1(et17)* mutant as the transcript levels of mitochondrial genome genes.

In the future, this should be expanded to also compare transcript levels of genes involved in OXPHOS encoded on the genome, to confirm the overall increase in mitochondrial activity. Without these results, we can only speculate if elevated transcript levels of these genes indicate increased energy metabolism, increased mitochondrial biogenesis, or other non-specific effects. However, it appears an intriguing observation, as this increase might give a first hint at processes involved in the alleviation of DMD stress hypersensitivity. We hypothesise that the ability of the *dys-1(eg33)* mutant to respond to stress might be impaired by a chronic mitochondrial burden, which reduces the responsiveness to acute stress response mechanisms and other energy demanding processes. Improvement in mitochondrial efficiency and energy metabolism, which is indicated by elevation of OXPHOS components, could bolster mitochondrial resilience in the DMD model, and partially restore stress response capacity.

Accordingly, *atfs-1* has been connected to an increased OXPHOS activity in UPR^{mito} (Nargund et al. 2015). ATFS-1 is shown to directly bind the promoters of OXPHOS genes, and suggest a balanced regulation of OXPHOS genes and stress responsive chaperones depending on the stress load. This recapitulates our results, and explains the increased levels of mitochondrial gene expression in the gain-of-function mutant. Furthermore, this expands the regulatory role of *atfs-1* in orchestrating mitochondrial energy metabolism. Combining this with our observation of a strong down-regulation of these genes in heat stress, increasing the baseline levels and softening down-regulation of OXPHOS components in the *atfs-1* gain-of-function could significantly improve the capacity to buffer the stress effects. This indicates that boosting energy levels facilitated by the UPR^{mito} could prime the organism to be more resilient in acute stress scenarios. Following up on these observations, we considered other methods of boosting UPR^{mito} capacity. One way of achieving this is by modulating the expression of the NADH Ubiquinone Oxidoreductase *nuo-6* (Wu et al. 2018). We could show that RNAi mediated knockdown of *nuo-6* improved thermorecovery (Fig. 34), indicating that mild stress, in addition to *atfs-1* gain-of-function, can bolster stress response capacity. Therefore, we reason that moderate activation of the UPR^{mito} increases stress response capacity, and consequently improves resilience in heat and mitochondrial stress (Fig. 37).

3.4.2 Boosting stress response capacity to elevate the resilience threshold

In our research hypothesis we state that any chronic burden would act as a constant drain that diminishes response capacity to acute stress by adaptive mechanisms. We reason that *dys-1(eg33)* mutants carry a chronic burden, making them more sensitive to acute stress. We have shown this experimentally, supporting the idea that animals with a chronic burden reach a respective "breaking point", where the stress load exceeds the resilience threshold earlier than wild type animals (Fig. 1). Based on the alleviation of the hypersensitivity in *atfs-1* gain-of-function and UPR^{mito} over-activation, we now expand this model. We argue that by increasing UPR^{mito} capacity we don't necessarily reduce the chronic burden, but increase the resilience threshold, to extend the time acute stress can be endured before reaching the breaking point (Fig. 38). This is supported by results connected to *daf-2* modulation, where general health benefits mediated by *daf-2* mutation increase thermorecovery (Fig. 12). As the double mutant of *dys-1(eg33); daf-2(e1370)* remains more sensitive than the individual *dys-1(eg33)* mutant, we reason that the underlying chronic burden is not resolved, but rather that the *daf-2* related benefits increase overall capacity to cope with the stress. However, this paradigm will require extensive further testing, and remains to be a conceptual opinion on how stress response mechanisms determine resilience.

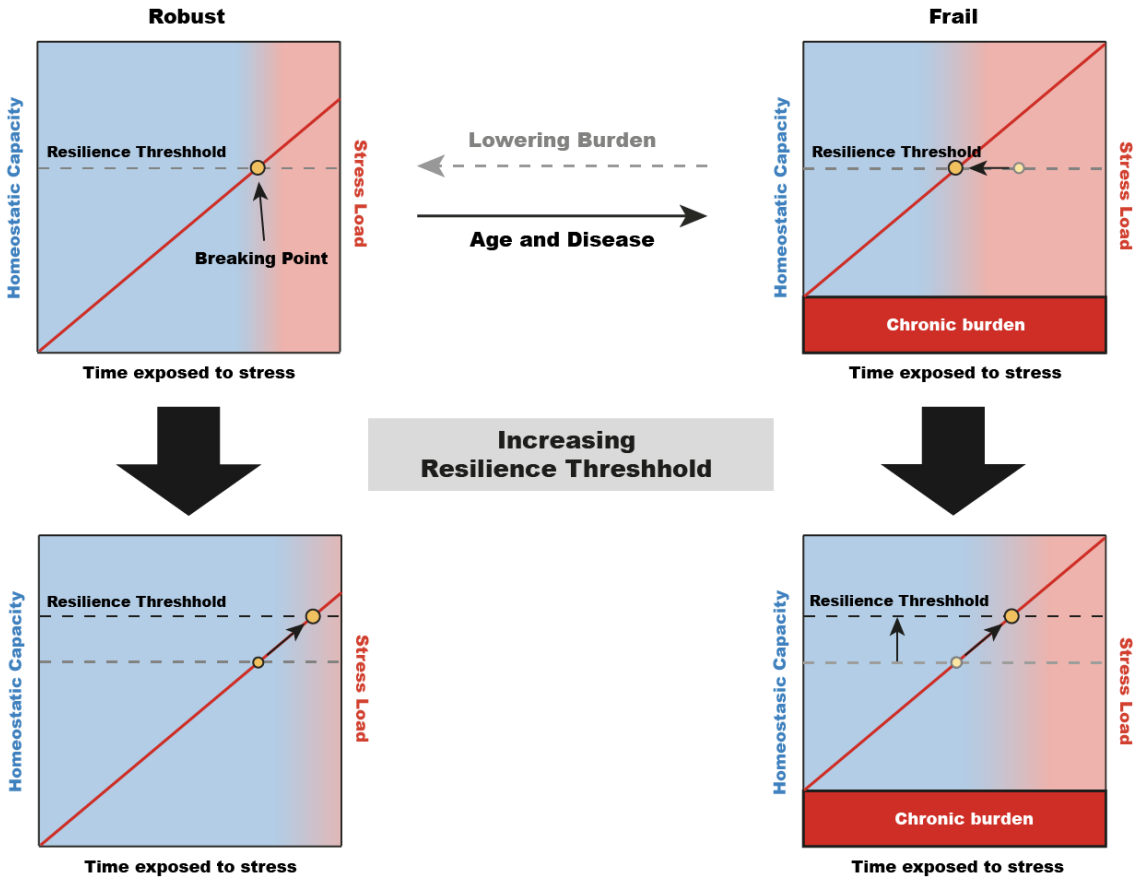

Figure 38: ***Boosting UPR^{mito} capacity improves resilience by increasing resilience threshold.*** *During constant exposure to stress, the stress accumulates over time building an increasing burden on the system. If the stress load reaches a level exceeding the resilience threshold, the system takes damage from which it will not be able to recover, representing the breaking point. This resilience threshold is determined by the combined stress response capacity, which can be tuned by boosting individual response mechanisms to elevate acute responsiveness, and prolong the time a stress can be endured before reaching the breaking point.*

4 FUTURE DIRECTIONS

4.1 Boosting resilience and energy metabolism to improve health

4.1.1 Increasing stress response capacity to improve resilience

As an important landmark in aging, the loss of proteostasis capacity weighs on the ability to effectively respond to external perturbation (Hoppe and Cohen 2020; Labbadia and Morimoto 2014). In a demographic shift, understanding the underlying processes remains as important as ever. We show that by increasing UPR^{mito} activity in the *dys-1(eg33)* mutant we can improve resilience and alleviate stress hypersensitivity. By tuning this stress response mechanism, we identify improvement of stress recovery in mitochondrial and heat stress (Fig. 31+33). Furthermore, we identified the ATFS-1-dependent induction of mitochondrial chaperones to correlate with survival improvement in *atfs-1* gain-of-function mutants and knockdown of *nuo-6* (Fig. 34). We intend to further assess if this induction of the UPR^{mito} indeed represents an increase in stress response capacity, or if these effects work through secondary mechanisms such as increased turnover of mitochondria or mitohormesis. However, this appears a good starting point for studying the potential of modulating resilience in disease, to buffer the age-related decline observed in proteostasis capacity.

Regarding the use of the *C. elegans dys-1(eg33)* mutant in resilience studies, it emerges as a powerful tool to identify and experimentally test general improvements of resilience. Furthermore, the hypersensitivity can be alleviated by different ways targeting the improvement of resilience mechanisms. A logical next step will be the detailed molecular comparison of the partially rescued double mutant *dys-1(eg33);atfs-1(et17)*. Using a synonymous framework we applied to outline the dynamic changes leading to *dys-1(eg33)* hypersensitivity, we will assess heat stress dynamics in the double mutant to identify altered gene expression restoring gene expression in *dys-1(eg33)* to more wild-type like patterns. Expanding this idea, we intend to include a comparison of the effects observed in *dys-1(eg33);daf-2(e1370)* (Fig. 12) to discern how improved thermorecovery is achieved in these two strains. We suggest it would be valuable to investigate if the beneficial effects in stress recovery are facilitated by distinct mechanisms, or if they converge in a programmed mechanism determining stress resilience.

Surprisingly, UPR^{mito} activation in the *atfs-1* gain-of-function mutant fails to improve lifespan (Bennett et al. 2014). This supports the idea of lifespan being to some extent uncoupled from healthspan (Bansal et al. 2015), however, improvement of proteostasis is thought to improve overall health as it directly counteracts an aging hallmark. We aim to address this dilemma, and understand how tuning these processes can support the delicate regulation of proteostasis mechanisms to not only improve acute stress response capacity, but sustainably improve healthspan.

4.1.2 Mapping stress response interaction to describe resilience

Comparison of steady state levels is commonly used to describe disease model gene expression changes (Hrach et al. 2020). However, we reason that in protesotatic diseases this is not sufficient to portray the complexity of the effects of a disease on the proteostasis network. Assessing gene expression changes in heat stress using transgenic reporters and RNA sequencing has revealed the dynamic nature of stress response mechanisms, and how tightly distinct stress response pathways are connected. We wanted to identify pivotal points in this interaction and uncover causal drivers of frailty in disease. As a result, we could show differences in expression dynamics of the UPR^{mito} in the *dys-1(eg33)* mutant, and discover ATFS-1 as a pivotal factor, as modulation of its activity directly affects heat stress recovery.

As heat is a broad stress which affects the entire organism, it is not surprising that this stress also touches on other response mechanisms. However, effects like the reduced baseline expression of the *hsp-6*p::GFP(*zcIs13*) reporter in endured heat stress (Fig. 19) indicate that there could be more to this than a passive induction of various stress responses. In a more systematic approach, we want to address this from different angles to investigate if these potential interactions are multi-lateral, addressing if boosting the HSF-1 driven response affects mitochondrial and ER stress capacity, or if these effects are exclusive for heat stress. By this, we intend to outline the proteostasis network and pinpoint more nodes like ATFS-1 which serve as modulators of the interaction in this network. *C. elegans* is a reliable model for assessment of stress responses, and many stress response pathways are conserved (Rodriguez et al. 2013). Therefore discoveries in *C. elegans* should translate to higher organisms and help improve the understanding of how resilience is programmed in mammalian models and humans, to ultimately guiding interventions aimed at improving cellular and organismal resilience.

As another comparison that will inform this research, we show that the induction of the transgenic reporter *hsp-4*p::GFP(*zcIs4*) has revealed a significantly reduced induction of the UPR^{ER} in the *dys-1(eg33)* mutant (Fig. 9). This indicates changes in the wiring of the UPR^{ER} in the *dys-1(eg33)* mutant, and would encourage further analysis of the induction by TM in RNA sequencing time course. Overall, the comparison of dynamic gene expression in stress has revealed changes in disease which would be masked in steady-state transcriptomics. We therefore propose to standardise the use of time course RNA-seq to facilitate identification of malfunction in stress response mechanisms in disease.

4.1.3 Mitochondria and Histones in heat stress

We uncovered a systematic and gradual decline in transcript levels of genes encoded by the mitochondrial genome during moderate heat stress (Fig. 23B). This striking effect was detected for mitochondrial genes. However, this also suggests that this could be driven by effects in mitochondrial dynamics, as the reduced expression could be the result of a reduction in mitochondrial content rather than a programmed down-regulation. We aim to experimentally distinguish this. By assessment of mitophagy rates, respiration, and metabolism we intend to assess mitochondrial dynamics and energy metabolism to understand the changes determining these effects. If we could discover a regulatory mechanism that drives a reduction of mitochondrial metabolism in cellular stress, the modulation of this could have significant impact on treatments of a range of diseases, and aging itself, as it is also defined by mitochondrial dysfunction and disturbance of energy metabolism (Sun, Youle, and Finkel 2016; López-Otín et al. 2023).

Furthermore, we detected a transient up-regulation of histones (Fig. 23F), which we also identified in reference data sets (Sural et al. 2019; Brunquell et al. 2016). This is especially intriguing in the context of a recent study, which proposes the role of HSF-1 signaling in modulation of mitochondrial function via histones (Sural et al. 2020). They identify involvement of one of our most significantly changed histones, *his-38*, and describe an active mechanism connecting reduced transcription from the mitochondrial genome to nuclear encoded histones (Sural et al. 2020). We therefore aim to assess the active role of histones in the response to stress, addressing if they are required in thermorecovery and reduction of transcription from the mitochondrial genome. By outlining the regulation by HSF-1, we will add significant insights into the role of histones in the response to heat stress. The transient nature of the expression pattern is unique among HSF-1 regulated genes, and we suggest that elucidating this multi-phasic response will contribute to the understanding of resilience.

4.1.4 Understanding the role of proteolysis in heat stress

Aspartic proteases are highly conserved across species (Davies 1990). If we can show that they are actively down-regulated in stress, and if this mechanism proves to be malfunctional in diseases like DMD, this could be a path for future interventions. Equivalent to trends in mitochondrial gene expression, we observed a reduction in gene expression of genes related to proteolysis. We aim to distinguish if this is actively contributing to heat resilience or a consequence of secondary effects. The systematic reduction in the transcript levels of a group of aspartic proteases in heat stress was much less severe in most of the assessed *asp* genes in the *dys-1(eg33)* mutant. Especially considering *asp-1*, which shows opposing development in heat stress (Fig. 26), this could hint at a relevant role in processes determining resilience.
Furthermore, we showed that knockdown of *asp-1* could alleviate stress hypersensitivity in *dys-1(eg33)* mutants, highlighting the relevance of this observation (Fig. 29). Next, we aim to elucidate how the modulation of aspartyl proteases, especially *asp-1*, affects thermorecovery. Considering potential redundancy in function of *asp* genes, we will explore methods to affect broad proteolysis mechanisms, to identify if they hold an active role in stress responses, or are altered as a downstream consequence.

4.2 Implications for frailty in DMD

4.2.1 Outlining the mechanism causing stress hypersensitivity in DMD

As the *C. elegans* mutation is equivalent to mammalian truncation mutants causal in DMD (Ellwood, Piasecki, and Szewczyk 2021), we aimed to understand the impact on nematode resilience as a way to inform mammalian disease phenotypes. We discovered a strong hypersensitivity of the *C. elegans dys-1(eg33)* mutant in heat and mitochondrial stress (Fig. 9). Comparing the steady state and dynamic expression of stress responses, we showed differences in UPR^{mito} and UPR^{ER} transcript levels in heat stress, which we leveraged to discover the modulation of UPR^{mito} capacity as a method to alleviate stress hypersensitivity. We now need to test if these effects are indeed conserved in higher organisms, and if modulation of the UPR^{mito} of mammals, such as the mdx mouse, can achieve similar beneficial effects.
Additionally, we aim to uncover the causes for reduced UPR^{mito} capacity underlying this, and pinpoint which downstream effects are involved in salvaging DMD pathology in the nematode. Analysing mitochondrial dynamics and health parameters by quantifying oxygen consumption rates and metabolomics will help us understand the determinants of hypersensitivity conveyed by mitochondria, and support understanding of the mechanism of rescue treatments. If we can find driving aspects of this muscle disease in the worm, leveraging

this in the mammalian system might open new angles that are not addressed by current treatments.

Building on the strength of using dynamic expression differences in comparison of *dys-1(eg33)* mutant transcriptomes, a comparison of the mutant to a treated condition appears of significant value. This would enable us to discern the precise expression differences caused by the *atfs-1(et17)* mutation on the expression profile of the *dys-1(eg33)* mutant, and highlight genes actively contributing to improved resilience. By this, we could triangulate respective changes and map the involved processes. Systematic overlap of changes of different successful treatments will then enable us to precisely outline disease relevant pathways.

Further, we aim to assess the effects of UPR^{mito} modulation are universal and transfer to other disease models, as modulation of the UPR^{mito} by *atfs-1* gain-of-function in heat stress appears to be generally beneficial (Fig. 31). Strikingly, the modulation of SPTF-3 seems to only benefit the DMD model, and it only improved resilience and not motility (Fig. 30). In this context it would be interesting to see what the specific effects of SPTF-3 modulation in DMD are, if the specific interaction with ATFS-1 is involved, and if it can affect resilience in other disease models. Considering that it did not affect locomotion, it appears that this effect is downstream of muscle deficiency, or even an independent effect. Overall, the value of this observation in the broader context of the disease remains to be elucidated, and adding data of UPR^{mito} in mammals appears to be the next milestone in harnessing these findings for application in DMD treatment.

4.2.2 Implications in sarcopenia

Our discoveries could also benefit sarcopenia research, as mitochondrial proteostasis and stress response capacity are among the processes affected in age-related muscle frailty (Merlini, Bonaldo, and Marzetti 2015; Higashitani et al. 2023). If the causal detriments are indeed related to stress response capacity, and if we succeed in determining the driving factors in hypersensitivity and progressive frailty, treatments discovered in DMD might be transferable to sarcopenia. First, we need to show that our observations are indeed represented in mammalian data. To this end, we will compare public data for DMD and sarcopenia to assess if we find trends matching our observation in the nematode.

4.3 Tuning the UPR^{mt} in heat stress

4.3.1 The role of ATFS-1 in heat stress

Building upon the observation that ATFS-1 activation, via gain-of-function mutations or mitochondrial stress induction by *nuo-6* knockdown, significantly bolsters heat stress recovery (Fig. 31+34), future research should prioritize deconstructing these effects to understand how modulating the UPR^{mito} can improve heat stress response. We aim to discern if the effects are caused directly by enhancing UPR^{mito} capacity, or if they achieve their benefits through energy metabolism and mitochondrial content. This could add insights on the requirement of efficienet energy metabolism in resilience, and sugegst mitochiondria as a main target in resilinec eresearch. The striking down-regulation of the mitochondrial genome observed in heat stress, which we found lifted in *atfs-1* mutants with improved stress recovery, hints at a key role of this in overall resilience. Ultimately, determining how ATFS-1 sustains mitochondrial genome integrity under proteotoxic load may provide a novel blueprint for rescuing the metabolic failure observed in DMD and age-related sarcopenia.

4.3.2 Tuning mitochondrial dynamics to increase resilience

Modulating the UPR^{mito} directly can prove challenging, as it also causes detrimental effects in excessive signaling (Shpilka and Haynes 2018). By deciphering the stress response mechanism in detail, we obtain results that can inform treatments independent from direct UPR^{mito} modulation. If we can show that distinct downstream factors of the UPR^{mito} are sufficient to rescue reduced resilience in age an ddisease, this would open new avenues to alleviate homeostatic burdens of cellular burdens. In line with this, targeting mitochondrial processes at different levels emerges as a potent path to improve heat stress response capacity. As a strategy for further research, we propose a comparative analysis of the effects of targeting distinct mechanisms in mitochondria using compounds. Literature suggests that increased NAD+ levels (Mouchiroud et al. 2013), boosting mitophagy using Urolithin A Ryu et al. 2016; D'Amico et al. 2021; Luan et al. 2021; Andreux et al. 2019), or treatment with Metformin (Onken and Driscoll 2010), all show potential in improvement of resilience. It would be valuable to compare these compounds in our assays and discern how they affect mitochondrial mechanisms, to ultimately uncover the crucial drivers of mitochondria-related determinants of resilience independent of the sensitive key driver of the UPR^{mito}.

4.4 Concluding remarks

In summary, we showed that disease models can be leveraged to identify changes in gene expression during stress to reveal modulators of stress resilience. We identified an exhaustion of the UPR^{mito} as a contributing factor to stress hypersensitivity in a *C. elegans* model for DMD, leading us to the identification of increased mitochondrial stress response capacity as a reliable means to improve resilience. While this was a data driven approach, we learned from published effects of UPR^{mito} modulation, which has been shown to affect stress resilience in various contexts. However, we add to this understanding specifically outlining dynamic transcriptional responses, and highlighting the beneficial effects of UPR^{mito} activity in heat stress recovery. Future research should focus on how this is achieved, to discern if this is driven by increased energy metabolism and mitochondrial biogenesis supporting recovery, or direct activation of protein folding by chaperones.

Regarding our overarching questions, we showed that the *dys-1(eg33)* mutant as a model for DMD is indeed hypersensitive to stress. Comparing gene expression changes, we outlined the dynamic expression changes in heat stress time course to describe changes in stress response mechanism. We ultimately leveraged these discoveries to alleviate stress hypersensitivity in the *dys-1(eg33)* mutant by modulating the UPR^{mito}, and propose this as a method to improve *C. elegans* resilience in disease.

While some important questions remain to be answered by future research, we reason that the overall approach is a promising way of assessing resilience to reveal changes in stress response dynamics. Comparison of dynamic expression changes revealed numerous processes which appear to be altered in the chosen disease model, adding significant value to comparison of steady-state transcriptomics. We suggest that understanding the determinants of resilience and how the wiring of responsive mechanisms is altered by chronic burdens in disease, is the key to finding novel ways to boost resilience and cellular health. We argue that this will enable the treatment of a range of diseases characterised by homeostatic frailty, as it supports the cell to buffer diverse stress more efficiently, in contrast to targeting individual processes.

5 MATERIALS AND METHODS

5.1 *C. elegans* handling and methodology

5.1.1 *C. elegans* strains and maintenance

All *C. elegans* strains were maintained at 20 °C on nematode growth medium (NGM) agar plates seeded with *Escherichia coli* (*E. coli*) strain OP50, unless specified. Strains obtained from the Caenorhabditis Genetics Center (CGC) or National BioResource Project (NBRP) were crossed into the lab N2 background at least twice. Strains used in this study are listed in Table 1 with their respective genotype and source. Crossing and genotyping of strains is described in 5.1.2. Synchronization of strains for experiments was achieved by bleaching, unless specified.

Table 1: C. elegans strains used in this study

Strain	Genotype	Backcrossed	Source
MSD331	N2 Bristol wild type	NA	CGC
MSD624	rps-9p::rps-9D94N::rps-9 3'UTR integrated in MSD615	NA	this study
MSD505	*pkIs2386[unc-54p::alpha-syn::YFP; unc-119(+)]*	2x	Denzel lab
MSD535	*gcn-2(ok871)* II	2x	Denzel lab
MSD498	daf-2(e1370) III	4x	Denzel lab
CZ199982	mcu-1(ju1154)	0x	CGC
MSD648	*dys-1(eg33)* I; mcu-1(ju1154)	2x	this study
MSD635	*dys-1(eg33)* I	2x	this study
MSD636	*dys-1(eg33)* I; daf-2(e1370) III	2x	this study
MSD633	*dys-1(eg33)* I; hsp-4p::GFP(zcIs4) V	2x	this study
MSD628	*dys-1(eg33)* I; hsp-6p::GFP(zcIs13) V	2x	this study
MSD627	*dys-1(eg33)* I; hsp-16.2p::GFP(gpIs1)	2x	this study
MSD615	oxTi556 I; unc-119(ed3) III.	4x	this study
BZ33	*dys-1(eg33)* I	NA	CGC
MSD589	hsp-4p::GFP(zcIs4) V	4x	Denzel lab
MSD460	eIF2alpha (syb1385), S51A "phospho-dead"	2x	Denzel lab
MSD314	"Patf-4(uORF)::GFP" faulty reporter	2x	Denzel lab
MSD582	"Patf-4(uORF)::GFP"; gcn-2(ok871); eIF2alpha (syb1385)	2x	Denzel lab
SJ4058	hsp-60p::GFP(zcIs9) V	2x	Denzel lab
SJ4100	hsp-6p::GFP(zcIs13) V	2x	Denzel lab
SJ4005	hsp-4p::GFP(zcIs4) V	2x	Denzel lab
MSD348	*pycr-1(wrm22)* X	2x	Denzel lab
TJ375	gpIs1 [hsp-16.2p::GFP]	0x	CGC
DG2389	glp-1(bn18) III.	0x	CGC
EJ1158	gon-2(q388) I.	0x	CGC
MSD441	mls133[unc-54p::Q35:YFP]	2x	Denzel lab

5.1.2 *C. elegans* crossing

Male worms for crossing were generated by incubation of L4 larvae of the respective genotype at 30 °C for 8 hours. Crossing of strains was performed by placing 3 hermaphrodite L4 with 12 adult male worms on 3 cm NGM plates. From successful crosses, indicated by 50% male progeny, 5 individual worms of the uniform F1 were singled on 6 cm NGM plates for further genotyping of the F2 generation for homozygous worms. For confirmation of respective genotype, individual adults were lysed in single worm lysis buffer (10 mM Tris pH 8, 50 mM KCl, 3 mM $MgCl_2$, 0,45% v/v Triton X 100, 0,45% v/v Tween 20, Proteinase K 100 μg/ml). Genotyping was performed using primers listed in 2. Genotyping for the *dys-1(eg33)* mutation was performed by adding a restriction step targeting a AhdI restriction site generated by the mutation. Crosses involving any of the fluorescent reporters was supported by fluorescent microscopy, screening for baseline fluorescence.

Table 2: Genotyping primers used in this study

Gene	Forward primer	Reverse primer
dys-1	CCAACAACTGAAACTGGGCATAAC	TTGACTCTCAGATTCCTCGTTTGG
daf-2	CATCAATGCGTACTCCTCATCCAG	AGTCGCTCAAGTTTTGCCATCGAG
mcu-1	GCTCGACGGTAGAATTGTTTAGTG	CACCGTAAAATTAGTTTCCAGGCG
rps-9 in MSD624	GGCGAGGAGGTCATCAAAGAGTTC	GGGCCTGGAAATTAGTGTTGCATG

5.1.3 *C. elegans* microinjection using FLInt

The strain MSD624 was generated by CRISPR/Cas9 facilitated integration of a transgene into the FLInt locus in *oxTi556* of the MSD615 strain. CRISPR guides were used as described in Malaiwong, Porta-de-la-Riva, and Krieg 2023, and sourced from IDT, together with the tracrRNA, and SpCas9 protein. The template was designed in Benchling and included homolgy arms designed to be suited for integration of large constructs and chosen to be 50 bp, based on efficiency aspects described in Paix et al. 2014. The template was ordered integrated in a vector from VectorBuilder, to be linearised and combined with the CRISPR components in the injection mix.

Table 3: Injection mix composition

Component	Concentration	Source
template DNA	100 ng/μl	VectorBuilder
SpCas9	6.25 μM	IDT
crRNA	15 μM	IDT

Injection into the distal gonads was performed using a Carl Zeiss Axio Imager Z1 microscope with a manual micromanipulator scaffolding a Femtojet4 microinjector. Early day 1 adult animals of MSD615 were placed in oil on 2% agarose pads, and transferred to NGM plates at 25 °C following injection to improve CRISPR/Cas9 efficiency. Adults of the F1 generation were screened for loss of tdTomato signal, and singled for genotyping for integration of the transgene.

5.1.4 Compound treatments

Treatmentment with compounds was performed either in liquid, poured into NGM plates, or added on top of the NGM plates. For treatment with Idebenone, Ru360 Treatment in liquid was only applied as stated in initial stress induction experiments, all other experiments used plates with the compound added to the media before pouring, as sytated in 4. To induce ER stress, we transferred worms on NGM plates containing various concentrations of tunicamycin, ranging from 1 μg/ml to 100 μg/ml in 1% DMSO. Mitochondrial stress was induced using the complex III blocker Antimycin A (AA) at low doses. Worms were transferred on plates containing 1 to 10 μg/ml AA.

Table 4: Compounds used in this study

Compound	Usage	Conc. / Solvent	Source
Antimycin A	Mitochondrial Stress; Complex III blocker	2-100 μM / DMSO	Sigma-Aldrich
Idebenone	Coenzyme Q10 (CoQ10) supplementation	1-100 μM / DMSO	Sigma-Aldrich
Melatonin	Antioxidant	1 mM / DMSO	Sigma-Aldrich
Chloroquine	lysosomotropic agent that inhibits autophagy	1 mM / ddH_2O	Sigma-Aldrich
Arimoclomol	Heat Shock Protein (HSP) co-inducer	100 nM / DMSO	MedChemExp
Teprenone	non-toxic inducer of HSP70	100 μM / DMSO	Fisher Scientific
G418	Blocking of translation elongation	125-250 μM / ddH_2O	Merck
Tunicamycin	ER stress by inhibition of N-glycosylation	1-100 μg/ml / DMSO	Merck
Paraquat	Induction of the formation of Superoxide	10-20 mM / ddH_2O	Sigma-Aldrich
Puromycin	Integration in proteins to monitor translation	500 μg/ml / ddH_2O	Sigma-Aldrich
Ru360	Inhibition of *mcu-1*	5 μM / ddH_2O	Calbiochem

5.1.5 Locomotion assay

Animals were raised on NGM or RNAi plates as indicated. Locomotion was assessed in liquid by transferring individual worms to a 5 μl drop of M9 buffer on unseeded NGM plates. Following an adaptation period of 30s, full body bends were counted over 30s. At least 12 animals were scored per experiment and condition. For locomotion in aging, animals were assessed on day 1 to 5, 8, 11, and 15. Every second day animals were transferred to fresh plates to avoid contamination with larvae.

5.1.6 Thermorecovery assay

For stress recovery assay, worms were synchronized by bleaching and grown on either standard 6 cm NGM or RNAi plates as indicated, until reaching young adult stage. At 68 hours post hatch, plates were transferred to an incubator at 33 °C, 34 °C or 35 °C. The standard for experiments involving the *dys-1(eg33)* mutant, labelled DMD thermorecovery, was 33 °C, while the wild type was commonly assessed at 34 °C. Following treatment, plates were returned to 20 °C and recovered for at least 16 hours before analysing recovery from heat stress, scored as natural movement in response to prodding. Each condition contained 3 replicates of at least 40 individuals, unless specified. For time course thermorecovery, individual time points were scored on one replicate plate of over 60 individuals per plate.

5.1.7 Lifespan assay

For lifespan analysis, strains were synchronized by egg laying for 2 hours. From the progeny, L4 stage larvae were placed on 6 cm NGM plates seeded with OP50 *E. coli* at 20 °C, defined as day 0. Per condition, 15 worms were placed on 10 plates, and survival was monitored every 2-3 days. During the first 10 days, worms were manually transferred every 2 days to avoid contamination with progeny. Survival was scored by gentle prodding, worms that did not respond to repeated touch were scored as dead and removed from the plates. Individuals that crawled off the plate, showed egg lay deficiency, or a ruptured vulva phenotype, were removed and censored. Lifespan experiments were blinded and performed at least 2x independently. Survival curves were plotted using GraphPad Prism (Version 11.0.2 (100)).

5.1.8 Generation time assay

For investigation of generation time, synchronised eggs were grown on NGM plates until reaching reproductive stage. The time from placing the egg to the first egg laid by the worm was defined as the generation time. For each strain 15 animals were placed on individual plates after 55 hours, and transferred every hour until producing the first progeny.

5.1.9 Development assay

For investigation of development during treatment with G418 (Merck) or TM (Merck), synchronised eggs were placed on NGM plates containing 125-250 μM G418 or 1-4 μg/ml TM. Eggs were counted at placement, and development past the L4 stage was assessed after 3 days of growth at 20 °C. The ratio of developed worms to placed eggs was calculated and plotted in GraphPad Prism (Version 11.0.2 (100)). Every experiment was performed in triplicates.

5.1.10 *C. elegans* imaging

For worm imaging, animals were aligned in stacks of 10 on ice-cold unseeded 3cm NGM plates, and imaged using a M205 FCA Stereo Fluorescent microscope (LEICA). Images were acquired using the Leica Application Suite X. Fluorescent reporter signal was measured as mean grey value in ImageJ2 (Version: 2.16.0/1.54p), and portrayed using GraphPad Prism (Version 11.0.2 (100)).

5.1.11 RNA interference

RNAi-mediated knockdown of target genes was achieved by feeding with HT115 bacteria carrying a vector for inducible expression of respective dsRNA, and ampicillin resistance. Expression was induced by addition of isopropyl-β-D-1-thiogalactopyranoside (IPTG). Bacteria were seeded on NGM plates containing 0.4 mM IPTG (Roth), and 100 μg/ml ampicillin (Merck Millipore). Individual clones were validated by sanger sequencing (Plasmidsaurus) following plasmid extraction and purification using a Zyppy Plasmid Miniprep Kit (Zymo). Bacterial clones used in this study are listed in table 5.

5.2 Molecular biology

5.2.1 RNA extraction

Following respective treatment, worms were collected in 10 ml of 4 °C M9 buffer and washed in cold M9 once. Worms were frozen in 300 μl TRI-reagent (QIAGEN), and RNA was extracted using Direct-zol RNA Miniprep Kit (Zymo). Purity and concentration of the RNA were assessed and confirmed using a NanoPhotometer NP80 (IMPLEN), Qubit fluorometer (Invitrogen), and TapeStation (Agilent Technologies) for selected samples. Standard protocols as described by the manufacturers were followed.

5.2.2 RT-qPCR

Analysis of transcript levels was performed using RT-qPCR on samples collected from day 1 adult animals. Following extraction of RNA as described, RNA was transcribed to complementary DNA (cDNA) using iScript Reverse Transcription Supermix (Bio-Rad). From the cDNA, 384-well plates were set up for qPCR with Power SYBR Green PCR Master Mix (Applied Biosystems) as the measurable fluorophore, and respective primers listed in table 6. Measurement was performed using a QuantStudio™ 7 Pro thermocycler (Applied Biosystems) and respective software. mRNA levels were determined by calculation of the $\Delta\Delta CT$ normalised to the expression of *pmp-3*. Three independent experiments were conducted, unless specified.

5.2.3 Western blotting

Following respective treatment, day 1 adult worms were collected in 10 ml of 4°C M9 buffer and washed in cold M9 twice. Worm pellets were frozen in liquid nitrogen until protein extraction. For protein extraction, worms were thawed and re-suspended in RIPA buffer (Thermo Scientific), supplemented with cOmplete Protease Inhibitor (Roche), and PhosphoSTOP (Roche). Samples were lysed using a Q800R3 Sonicator (QSONICA), at 30% amplitude for 10 pulses of 30 seconds. Lysed samples were centrifuged for 10 minutes at 15.000 rpm, before protein concentration in the supernatant was determined by bicinchoninic acid assay (BCA) (Thermo Fisher). Normalised protein samples in Laemmli buffer (Thermo Fisher) were separated by sodium dodecyl sulfate polyacrylamide gel electrophoresis (SDS-PAGE) and transferred to nitrocellulose membranes using a Trans-Blot Turbo system (Bio-Rad). Membranes were blocked in either 5 % milk in TBST or 2 % bovine serum albumin (BSA) in TBST, depending on the respective antibody. Puromycin (Merck Millipore; 1:10.000), and Living Colors GFP (Clontech; 1:10.000) antibodies were used in milk, phospho-eIF2α (Cell Signaling; 1:2.000) was used in BSA. For normalisation, we stained total protein levels using the Revert 520 Total Protein Stain for Western Blot Normalization (Licor). Secondary antibodies coupled to Horseradish peroxidase (HRP) were detected using Immobilon ECL UltraPlus Western HRP Substrate (Millipore), and visualised using the chemiluminescence channel of the Odyssey imaging system (Licor). Quantification of protein levels was performed using the EmpiriaStudio software (Licor), and analysed using Prism (Version 11.0.0 (93)).

5.2.4 RNA sequencing

Sample collection and RNA extraction

Wild type and *dys-1(eg33)* mutant worms for this experiment were raised on 10 cm NGM plates for 62

hours, before transferring them to 10 cm plates containing 10 μM FUdR. Transfer was performed by washing worms off in M9 buffer, and distributing them in even volume on 27 FUdR plates per genotype. Following incubation on FUdR plates for 24 more hours at 20 °C, respective plates were placed in an incubator at 30 °C. Respective control plates were kept at 20 °C. Plates were randomised across genotype and condition in their respective groups.

At their respective time point, worms were washed off from their plates and collected in ice-cold M9 buffer. Animals were washed once with M9 to redcue contamination risk with remaining bacteria. Supernatant was taken off following centrifugation at 2000 xg for 2 min, and worms were snap-frozen in liquid nitrogen. RNA extraction was performed at a later stage in three replicate groups to reduce batch effects. RNA was quantified using a NanoPhotometer NP80 (IMPLEN), Qubit fluorometer (Invitrogen), and TapeStation (Agilent Technologies). 500 ng of RNA per sample were handed over to the Genomics hub in a randomised 96-well plate.

Library preparation and sequencing

RNA library prep and sequencing was performed by the Altos Genomics Hub in Cambridge (UK) and San Diego (California, USA). RNA was isolated from collected samples as described in 5.2.2. Library preparation was performed using the Watchmaker RNA Library Prep Kit (Watchmaker) according to protocol provided by the manufacturer. The pooled libraries were sequenced with the Illumina NextSeq 2000 system using paired-end sequencing.

Data processing and mapping

Raw sequencing reads were subjected to quality trimming and adapter removal using Trim Galore (version 0.6.7) with Cutadapt (version 3.4). Comprehensive quality control reports summarising all initial and post-alignment metrics like read distribution, coverage, and duplication rates were generated using MultiQC. Reads were mapped to the WBcel235 reference transcriptome using STAR. Transcript-level quantification was performed using Salmon (version 1.10.1) via a quasi-mapping approach. Merged transcript gene counts were imported to R (Version 2025.09.2+418 (2025.09.2+418)) for data analysis.

5.3 Statistics and data analysis

5.3.1 R studio

All data analysis was performed in R studio (Version 2025.09.2+418 (2025.09.2+418)). Differential expression analysis was performed on 54 *C. elegans* transcriptomic samples using the limma-voom empirical Bayes framework. High-throughput sequencing counts were first filtered by included unsupervised variance based filtering to remove lowly expressed features, retaining only genes with a minimum of c counts per million (CPM) in at least n samples, where n corresponds to the smallest experimental group size. Following filtering, library sizes were normalized using the Trimmed Mean of M-values (TMM) method to account for composition bias across the 54 libraries.

To assess differential expression, specific comparisons were extracted using a contrast matrix. To stabilize the variance and increase statistical power for the relatively small per-group sample sizes within the 54-sample cohort, the empirical Bayes (eBayes) method was applied. This approach moderates the genewise residual variances toward a global trend, resulting in moderated t-statistics and associated p-values. Significant differentially expressed genes (DEGs) were defined using a Benjamini-Hochberg (BH) false discovery rate (FDR) adjustment to control for multiple testing. To assess data similarity and visualize transcriptional profiles across the 54 samples, expression values were normalized using Unit Vector Scaling. This transformation ensures that the boundaries for each individual gene are constrained within a fixed range between -1 and 1 to remain independent of the absolute transcript levels of other genes in the data set.

Principle component analysis was performed on all transcripts with an expression of >10 RPM. GO term analysis was performed using enrichR, referencing to the 2018 GO dbs. Line graphs were plotted with ggplot2. UpSet graphs were generated from significantly changed genes as defined by limma and plotted using UpSetR. Clustering was performed on z-score normalised expression patterns using k-means clustering on 12 centers at set.seed(42). Genes were pre-selected for genes that showed significant changes at any of the time point in wild type heat stress induction. Heatmaps were generated from merged-gene counts using ggplot2.

5.3.2 Statistical significance tests

Results are presented as means +/±SD or means +/±SEM, unless stated otherwise. Statistical tests were performed using one-way or two-way ANOVA with Dunnet's multiple comparison test. Significance levels were *p<0.05, **p<0.01, ***p<0.001, and ****p<0.0001 versus wild type control. Experiments were performed with three biological replicates, unless stated otherwise.

Table 5: RNAi clones used in this study

Target	Sequence	Source
luciferase	negative control	Denzel lab
sptf-3	Y40B1A.4	Ahringer library
atfs-1	ZC376.7	Horizon library
daf-2	Y55D5A.5	Denzel lab
Y48G10A.3	Y48G10A.3	Horizon library
mup-2	T22E5.5	Horizon library
snt-2	F42G9.7	Ahringer library
ola-1	W08E3.3	Ahringer library
ubc-14	G_YK4617	Horizon library
soem-1	Y87G2A.a	Ahringer library
sir-2.4	sjj2_C06A5.11	Ahringer library suppl.
dkf-1	W09C5.5	Horizon library
Y48G10A.1	Y48G10A.1	Horizon library
Y87G2A.13	Y87G2A.13	Horizon library
endu-2	M60.2	Ahringer library
asp-1	Y39B6A.20	Horizon library
asp-6	F21F8.7	Horizon library
gpi-1	Y87G2A.8	Horizon library
snr-2	W08E3.1	Ahringer library
tads-1	C01A2.5	Ahringer library
oxa-1	C01A2.3	Ahringer library
cox-4	W09C5.8	Horizon library
aagr-2	R05F9.12	Horizon library
drp-1	T12E12.4	Horizon library
R08E3.1	R08E3.1	Ahringer library
mcu-1	K02B2.3	Ahringer library
spp-2	T08A9.12.1	Ahringer library
spp-3	T08A9.7.1	Ahringer library
spp-10	C28C12.7	Horizon library
pbo-4	K09C8.1	Horizon library
clec-63	F35C5.6	Horizon library
lys-8	C17G10.5	Horizon library
K06G5.1	K06G5.1	Horizon library
C01B10.6	C01B10.6	Horizon library
lron-7	K03A1.2	Horizon library
xbp-1	R74.3	Horizon library
nuo-6	W01A8.4	Ahringer library

Table 6: qPCR primers used in this study

Target	Forward primer	Reverse primer
hsp-6	GTTATCGAGAACGCAGAAGGAG	CATCCTTAGTAGCTTGACGCTG
hsp-60	AGGGATTCGAGAGCATTCGTCAAG	TGTGGCGACTTGAGCGATCTCTTC
clpp-1	TCAAAGCGAAAGTGGCAAA	TGCACTTATCATTTGTATTGTGTCA
atfs-1	CAATCACCATCAAAATCGGCG	CTTGCTCAATGTCCATTTCGAAC
sptf-3	CAACAACACCTGATGGATCAC	GGAATGAATTGCACCTGTCTC
mtss-1	GATCTCCAAGTCTACCGTCC	GTCATCAACCTCTTGCTTGC
hmg-5	AAAGAAGTACACAGACGAAGC	TTTCTGGAGGACGACATGG
ctc-1	GGTGAACAGTCTACCCACC	GCTAAATCTACTCTACTTCCAGG
nduo-1	AGCGTCATTTATTGGGAAGAAGAC	AAGCTTGTGCTAATCCCATAAATGT
nduo-4	GCACACGGTTATACATCTACACTTATG	GATGTATGATAAAATTCACCAATAAGG
nduo-5	AGATGAGATTTATTGGGTATTTCTAG	CACCTAGACGATTAGTTAATGCTG
polg-1	CTGCCTAATACCGTTGCCTTCTT	TTGGAGCCGTCCGGATT
cox-4	GCCGACTGGAAGAACTTGTC	GCGGAGATCACCTTCCAGTA
F44E5.4 (*hsp-70*)	TGATACCCATCTCGGAGGAG	GTGGATTGGGTGAAATGTCC
C12C8.1 (*hsp-70*)	CTACATGCAAAGCGATTGGA	GGCGTAGTCTTGTTCCCTTC
jmjd-3.1	GTGACAATGAAACGACGTTG	TTCGCTTGAAGTAGAAGCAG
pmp-3	CGGTGTTAAAACTCACTGGAGA	TCGTGAAGTTCCATAACACGA
sod-3	ACTGCTCGCACTGCTTCAA	CATAGTCTGGGCGGACATTT
trx-2	TTGATTTCCACGCAGAATG	TGGCGAGAAGAACACTTCCT
cts-1	CTCGACAACTTCCCAGATAACC	GGTACAGGTTGCGATAGATGATAGC
gst-4	CTGAAGCCAACGACTCCATT	GCGTAAGCTTCTTCCTCTGC
atp-6	TGCTGCTGTAGCGTGATTAAG	ACTGTTAAAGCAAGTGGACGAG
ctb-1	TGGTGTTACAGGGGCAACAT	TGGCCTCATTATAGGGTCAGC
ctc-2	GTAGTTTATTGTTGGGAGTTTTAGTG	CACAATAATTCACCAAACTGATACTC
hsp-4	GTGGCAAACGCGTACTGTGATGA	CGCAACGTATGATGGAGTGATTC

6 REFERENCES

Alcala, Athena et al. (2026). “A non-canonical role for UPRER during heat stress in C. elegans”. In: *bioRxiv*, p. 2026.01.08.698479.

Alvarez, Javier et al. (2020). “The Role of Ca2+ Signaling in Aging and Neurodegeneration: Insights from Caenorhabditis elegans Models”. In: *Cells* 9.1, p. 204.

Amorim, João A. et al. (2022). “Mitochondrial and metabolic dysfunction in ageing and age-related diseases”. In: *Nature Reviews Endocrinology* 18.4, pp. 243–258.

Andreux, Pénélope A. et al. (2019). “The mitophagy activator urolithin A is safe and induces a molecular signature of improved mitochondrial and cellular health in humans”. In: *Nature Metabolism* 1.6, pp. 595–603.

Arantes-Oliveira, Nuno et al. (2002). “Regulation of Life-Span by Germ-Line Stem Cells in Caenorhabditis elegans”. In: *Science* 295.5554, pp. 502–505.

Arunagiri, Anoop et al. (2019). “Proinsulin misfolding is an early event in the progression to type 2 diabetes”. In: *eLife* 8, e44532.

Atella, Vincenzo et al. (2019). “Trends in age-related disease burden and healthcare utilization”. In: *Aging Cell* 18.1, e12861.

Back, Sung Hoon and Randal J. Kaufman (2012). “Endoplasmic Reticulum Stress and Type 2 Diabetes”. In: *Annual Review of Biochemistry* 81.1, pp. 767–793.

Baines, Katie Nicoll et al. (2017). “Aging Effects of Caenorhabditis elegans Ryanodine Receptor Variants Corresponding to Human Myopathic Mutations”. In: *G3: Genes, Genomes, Genetics* 7.5, pp. 1451–1461.

Baker, George T. and Richard L. Sprott (1988). “Biomarkers of aging”. In: *Experimental Gerontology* 23.4-5, pp. 223–239.

Balch, William E. et al. (2008). “Adapting Proteostasis for Disease Intervention”. In: *Science* 319.5865, pp. 916–919.

Bansal, Ankita et al. (2015). “Uncoupling lifespan and healthspan in Caenorhabditis elegans longevity mutants”. In: *Proceedings of the National Academy of Sciences* 112.3, E277–E286.

Bar-Ziv, Raz et al. (2020). “Measurements of physiological stress responses in C. elegans.” In: *Journal of visualized experiments : JoVE* 159, pp. 10.3791/61001.

Bargmann, Cornelia I., Erika Hartwieg, and H. Robert Horvitz (1993). “Odorant-selective genes and neurons mediate olfaction in C. elegans”. In: *Cell* 74.3, pp. 515–527.

Barzilai, Nir et al. (2016). “Metformin as a Tool to Target Aging”. In: *Cell Metabolism* 23.6, pp. 1060–1065.

Ben-Zvi, Anat, Elizabeth A. Miller, and Richard I. Morimoto (2009). “Collapse of proteostasis represents an early molecular event in Caenorhabditis elegans aging”. In: *Proceedings of the National Academy of Sciences* 106.35, pp. 14914–14919.

Bennett, Christopher F. et al. (2014). “Activation of the mitochondrial unfolded protein response does not predict longevity in Caenorhabditis elegans”. In: *Nature Communications* 5.1, p. 3483.

Bliek, Alexander M van der (2009). “Fussy mitochondria fuse in response to stress”. In: *The EMBO Journal* 28.11, pp. 1533–1534.

Brand, M.D (2000). “Uncoupling to survive? The role of mitochondrial inefficiency in ageing”. In: *Experimental Gerontology* 35.6-7, pp. 811–820.

Brenner, S (1974). “THE GENETICS OF CAENORHABDITIS ELEGANS”. In: *Genetics* 77.1, pp. 71–94.

Brown, Marishka K. and Nirinjini Naidoo (2012). “The endoplasmic reticulum stress response in aging and age-related diseases”. In: *Frontiers in Physiology* 3, p. 263.

Brunquell, Jessica et al. (2016). “The genome-wide role of HSF-1 in the regulation of gene expression in Caenorhabditis elegans”. In: *BMC Genomics.* 17.1, p. 559.

Bulfield, G et al. (1984). “X chromosome-linked muscular dystrophy (mdx) in the mouse.” In: *Proceedings of the National Academy of Sciences* 81.4, pp. 1189–1192.

Buyse, Gunnar M. et al. (2013). “Effects of glucocorticoids and idebenone on respiratory function in patients with duchenne muscular dystrophy”. In: *Pediatric Pulmonology* 48.9, pp. 912–920.

Calfon, Marcella et al. (2002). “IRE1 couples endoplasmic reticulum load to secretory capacity by processing the XBP-1 mRNA”. In: *Nature* 415.6867, pp. 92–96.

Campbell, Daniel and Steven Zuryn (2024). “The mechanisms and roles of mitochondrial dynamics in C. elegans”. In: *Seminars in Cell & Developmental Biology* 156, pp. 266–275.

Cárdenas, César et al. (2010). “Essential Regulation of Cell Bioenergetics by Constitutive InsP3 Receptor Ca2+ Transfer to Mitochondria”. In: *Cell* 142.2, pp. 270–283.

Chapin, Hannah C. et al. (2015). “Tissue-specific autophagy responses to aging and stress in C. elegans”. In: *Aging (Albany NY)* 7.6, pp. 419–432.

Charmpilas, Nikolaos, Qiaochu Li, and Thorsten Hoppe (2025). “The mitochondrial unfolded protein response: acting near and far”. In: *Biological Chemistry* 0.0.

Chaudhuri, Jyotiska, Manish Parihar, and Andre Pires-daSilva (2011). “An Introduction to Worm Lab: from Culturing Worms to Mutagenesis”. In: *Journal of Visualized Experiments* 47.

Chen, Huarong et al. (2015). “OLA1 regulates protein synthesis and integrated stress response by inhibiting eIF2 ternary complex formation”. In: *Scientific Reports* 5.1, p. 13241.

Cheng, Yu-Wei, Jie Liu, and Toren Finkel (2023). “Mitohormesis”. In: *Cell Metabolism* 35.11, pp. 1872–1886.

Cho, Junhyo et al. (2025). “Determination of health status during aging using bending and pumping rates at various survival rates in Caenorhabditis elegans”. In: *Scientific Reports* 15.1, p. 9057.

Chondronasiou, Dafni et al. (2022). “Multi-omic rejuvenation of naturally aged tissues by a single cycle of transient reprogramming”. In: *Aging Cell* 21.3, e13578.

Cohen, Sheldon et al. (2012). “Chronic stress, glucocorticoid receptor resistance, inflammation, and disease risk”. In: *Proceedings of the National Academy of Sciences* 109.16, pp. 5995–5999.

Collaborators, GBD 2019 Demographics et al. (2020). “Global age-sex-specific fertility, mortality, healthy life expectancy (HALE), and population estimates in 204 countries and territories, 1950–2019: a comprehensive demographic analysis for the Global Burden of Disease Study 2019”. In: *The Lancet* 396.10258, pp. 1160–1203.

Córdova, Gonzalo et al. (2015). “SMAD3 and SP1/SP3 Transcription Factors Collaborate to Regulate Connective Tissue Growth Factor Gene Expression in Myoblasts in Response to Transforming Growth Factor β”. In: *Journal of Cellular Biochemistry* 116.9, pp. 1880–1887.

Costa-Mattioli, Mauro and Peter Walter (2020). “The integrated stress response: From mechanism to disease”. In: *Science* 368.6489, eaat5314.

Crudele, Julie M. (2025). “Safety and efficacy of commercially administered elevidys (delandistrogene moxeparvovec-rokl)”. In: *Molecular Therapy* 34.1, pp. 10–11.

Cruz-Jentoft, Alfonso J and Avan A Sayer (2019). “Sarcopenia”. In: *The Lancet* 393.10191, pp. 2636–2646.

D’Amico, Davide et al. (2021). “Impact of the Natural Compound Urolithin A on Health, Disease, and Aging”. In: *Trends in Molecular Medicine* 27.7, pp. 687–699.

Das, Rajdeep and Oishee Chakrabarti (2020). “Mitochondrial hyperfusion: a friend or a foe”. In: *Biochemical Society Transactions* 48.2, pp. 631–644.

Davies, D R (1990). “The Structure and Function of the Aspartic Proteinases”. In: *Annual Review of Biophysics and Biophysical Chemistry* 19.1, pp. 189–215.

Deconinck, Nicolas and Bernard Dan (2007). “Pathophysiology of Duchenne Muscular Dystrophy: Current Hypotheses”. In: *Pediatric Neurology* 36.1, pp. 1–7.

Delaney, Kamila et al. (2018). “Differential Expression of Histone H3.3 Genes and Their Role in Modulating Temperature Stress Response in Caenorhabditis elegans”. In: *Genetics* 209.2, pp. 551–565.

DementiaForecasting (2022). “Estimation of the global prevalence of dementia in 2019 and forecasted prevalence in 2050: an analysis for the Global Burden of Disease Study 2019”. In: *The Lancet Public Health* 7.2, e105–e125.

Derisbourg, Maxime J., Matías D. Hartman, and Martin S. Denzel (2021). “Modulating the integrated stress response to slow aging and ameliorate age-related pathology”. In: *Nature Aging* 1.9, pp. 760–768.

Derisbourg, Maxime J. et al. (2021). “Mutagenesis screen uncovers lifespan extension through integrated stress response inhibition without reduced mRNA translation”. In: *Nature Communications* 12.1, p. 1678.

Dickinson, Daniel J et al. (2013). “Engineering the Caenorhabditis elegans genome using Cas9-triggered homologous recombination”. In: *Nature Methods* 10.10, pp. 1028–1034.

Dilberger, Benjamin et al. (2019). “Mitochondrial Oxidative Stress Impairs Energy Metabolism and Reduces Stress Resistance and Longevity of C. elegans”. In: *Oxidative Medicine and Cellular Longevity* 2019.1, p. 6840540.

Duan, Dongsheng et al. (2021). “Duchenne muscular dystrophy”. In: *Nature Reviews Disease Primers* 7.1, p. 13.

Dubinin, Mikhail V. et al. (2020). “Duchenne muscular dystrophy is associated with the inhibition of calcium uniport in mitochondria and an increased sensitivity of the organelles to the calcium-induced permeability transition”. In: *Biochimica et Biophysica Acta (BBA) - Molecular Basis of Disease* 1866.5, p. 165674.

Dues, Dylan J et al. (2019). “Resistance to Stress Can Be Experimentally Dissociated From Longevity”. In: *The Journals of Gerontology: Series A* 74.8, pp. 1206–1214.

Ellwood, Rebecca A., Mathew Piasecki, and Nathaniel J. Szewczyk (2021). “Caenorhabditis elegans as a Model System for Duchenne Muscular Dystrophy”. In: *International Journal of Molecular Sciences* 22.9, p. 4891.

Ellwood, Rebecca A. et al. (2021). “Mitochondrial hydrogen sulfide supplementation improves health in the C. elegans Duchenne muscular dystrophy model”. In: *Proceedings of the National Academy of Sciences* 118.9, e2018342118.

Ellwood, Rebecca A. et al. (2022). “Sulfur amino acid supplementation displays therapeutic potential in a C. elegans model of Duchenne muscular dystrophy”. In: *Communications Biology* 5.1, p. 1255.

Ewald, Collin Y. et al. (2015). “Dauer-independent insulin/IGF-1-signalling implicates collagen remodelling in longevity”. In: *Nature* 519.7541, pp. 97–101.

Falzarano, Maria Sofia et al. (2015). “Duchenne Muscular Dystrophy: From Diagnosis to Therapy”. In: *Molecules* 20.10, pp. 18168–18184.

Fire, Andrew et al. (1998). “Potent and specific genetic interference by double-stranded RNA in Caenorhabditis elegans”. In: *Nature* 391.6669, pp. 806–811.

Fischer, Fabian et al. (2022). “Ingestion of single guide RNAs induces gene overexpression and extends lifespan in Caenorhabditis elegans via CRISPR activation”. In: *Journal of Biological Chemistry* 298.7, p. 102085.

Flanigan, K. et al. (2025). “22OUpdate on INSPIRE DUCHENNE: a phase 1/2 study of SGT-003, a next-generation microdystrophin gene therapy for Duchenne muscular dystrophy”. In: *Neuromuscular Disorders* 53, p. 106188.

Fontana, Luigi and Linda Partridge (2015). “Promoting Health and Longevity through Diet: From Model Organisms to Humans”. In: *Cell* 161.1, pp. 106–118.

Francesco, Andrea Di et al. (2018). “A time to fast”. In: *Science* 362.6416, pp. 770–775.

Friedland, Ari E et al. (2013). “Heritable genome editing in C. elegans via a CRISPR-Cas9 system”. In: *Nature Methods* 10.8, pp. 741–743.

Frøkjær-Jensen, Christian et al. (2008). “Single-copy insertion of transgenes in Caenorhabditis elegans”. In: *Nature Genetics* 40.11, pp. 1375–1383.

Fulop, T. et al. (2010). “Aging, frailty and age-related diseases”. In: *Biogerontology* 11.5, pp. 547–563.

Furones, Samuel et al. (2026). “Quantification of C. elegans food intake under food stressors exposure: A fluorescence-based approach for food safety assessment”. In: *Food Bioscience* 80, p. 108956.

Gao, Shihong Max et al. (2023). “Aging Atlas Reveals Cell-Type-Specific Regulation of Pro-longevity Strategies”. In: *bioRxiv*, p. 2023.02.28.530490.

Garmany, Armin, Satsuki Yamada, and Andre Terzic (2021). “Longevity leap: mind the healthspan gap”. In: *npj Regenerative Medicine* 6.1, p. 57.

Gaud, Aurélie et al. (2004). “Prednisone reduces muscle degeneration in dystrophin-deficient Caenorhabditis elegans”. In: *Neuromuscular Disorders* 14.6, pp. 365–370.

Ghemrawi, Rose and Mostafa Khair (2020). “Endoplasmic Reticulum Stress and Unfolded Protein Response in Neurodegenerative Diseases”. In: *International Journal of Molecular Sciences* 21.17, p. 6127.

Gianfredi, Vincenza et al. (2025). “Aging, longevity, and healthy aging: the public health approach”. In: *Aging Clinical and Experimental Research* 37.1, p. 125.

Glaser, Talita et al. (2019). “Calcium signalling: A common target in neurological disorders and neurogenesis”. In: *Seminars in Cell & Developmental Biology* 95, pp. 25–33.

Group, UK Prospective Diabetes Study (UKPDS) (1998). “Effect of intensive blood-glucose control with metformin on complications in overweight patients with type 2 diabetes (UKPDS 34)”. In: *The Lancet* 352.9131, pp. 854–865.

Guo, Jun et al. (2022). “Aging and aging-related diseases: from molecular mechanisms to interventions and treatments”. In: *Signal Transduction and Targeted Therapy* 7.1, p. 391.

Gürler, Metin and Özlem Özsoy (2018). “Exploring the relationship between life expectancy at birth and economic growth in 56 developing countries”. In: *Journal of Global Health Reports* 3.

Haeussler, Simon and Barbara Conradt (2022). “The Unfolded Protein Response, Methods and Protocols”. In: *Methods in Molecular Biology* 2378, pp. 249–259.

Haigis, Marcia C. and Bruce A. Yankner (2010). “The Aging Stress Response”. In: *Molecular Cell* 40.2, pp. 333–344.

Halling, Jens Frey and Henriette Pilegaard (2020). “PGC-1-mediated regulation of mitochondrial function and physiological implications”. In: *Applied Physiology, Nutrition, and Metabolism* 45.9, pp. 927–936.

Hansen, Malene et al. (2008). “A Role for Autophagy in the Extension of Lifespan by Dietary Restriction in C. elegans”. In: *PLoS Genetics* 4.2, e24.

Harrison, David E. et al. (2009). “Rapamycin fed late in life extends lifespan in genetically heterogeneous mice”. In: *Nature* 460.7253, pp. 392–395.

Hawley, John A. and Jill J. Leckey (2015). “Carbohydrate Dependence During Prolonged, Intense Endurance Exercise”. In: *Sports Medicine* 45.Suppl 1, pp. 5–12.

Haynes, Cole M. and David Ron (2010). “The mitochondrial UPR – protecting organelle protein homeostasis”. In: *Journal of Cell Science* 123.22, pp. 3849–3855.

Haynes, Cole M. et al. (2007). “ClpP Mediates Activation of a Mitochondrial Unfolded Protein Response in C. elegans”. In: *Developmental Cell* 13.4, pp. 467–480.

Haynes, Cole M. et al. (2010). “The Matrix Peptide Exporter HAF-1 Signals a Mitochondrial UPR by Activating the Transcription Factor ZC376.7 in C. elegans”. In: *Molecular Cell* 37.4, pp. 529–540.

Hemerling, Johannes CW et al. (2023). “SPTF-3/SP1 orchestrates mitochondrial biogenesis upon ribosomal stress and acute starvation”. In: *bioRxiv*, p. 2023.08.18.553493.

Hewitt, Jennifer E. et al. (2018). “Muscle strength deficiency and mitochondrial dysfunction in a muscular dystrophy model of Caenorhabditis elegans and its functional response to drugs”. In: *Disease Models & Mechanisms* 11.12, p. dmm036137.

Higashitani, Atsushi et al. (2023). “Increased mitochondrial Ca2+ contributes to health decline with age and Duchene muscular dystrophy in C. elegans”. In: *The FASEB Journal* 37.4, e22851.

Hipp, Mark S., Prasad Kasturi, and F. Ulrich Hartl (2019). “The proteostasis network and its decline in ageing”. In: *Nature Reviews Molecular Cell Biology* 20.7, pp. 421–435.

Hipp, Mark S., Sae-Hun Park, and F. Ulrich Hartl (2014). “Proteostasis impairment in protein-misfolding and -aggregation diseases”. In: *Trends in Cell Biology* 24.9, pp. 506–514.

Hirata, Takuya et al. (2024). “Chloroquine decreases cardiac fibrosis and improves cardiac function in a mouse model of Duchenne muscular dystrophy”. In: *PLOS ONE* 19.1, e0297083.

Hobert, Oliver and Paula Loria (2016). “Green Fluorescent Protein”. In: *Methods of Biochemical Analysis* 47, pp. 203–226.

Höhfeld, Jörg et al. (2021). “Maintaining proteostasis under mechanical stress”. In: *EMBO reports* 22.8, EMBR202152507.

Hoppe, Thorsten and Ehud Cohen (2020). “Organismal Protein Homeostasis Mechanisms”. In: *Genetics* 215.4, pp. 889–901.

Horvath, Steve (2013). “DNA methylation age of human tissues and cell types”. In: *Genome Biology* 14.10, p. 3156.

Houthoofd, Koen et al. (2003). “Life extension via dietary restriction is independent of the Ins/IGF-1 signalling pathway in Caenorhabditis elegans”. In: *Experimental Gerontology* 38.9, pp. 947–954.

Howard, Amber C. et al. (2016). “Reducing translation through eIF4G/IFG-1 improves survival under ER stress that depends on heat shock factor HSF-1 in Caenorhabditis elegans”. In: *Aging Cell* 15.6, pp. 1027–1038.

Hrach, Heather C et al. (2020). “Transcriptome changes during the initiation and progression of Duchenne muscular dystrophy in Caenorhabditis elegans”. In: *Human Molecular Genetics* 29.10, pp. 1607–1623.

Hsin, Honor and Cynthia Kenyon (1999). “Signals from the reproductive system regulate the lifespan of C. elegans”. In: *Nature* 399.6734, pp. 362–366.

Hsu, Ao-Lin, Coleen T. Murphy, and Cynthia Kenyon (2003). “Regulation of Aging and Age-Related Disease by DAF-16 and Heat-Shock Factor”. In: *Science* 300.5622, pp. 1142–1145.

Hughes, KJ et al. (2018). “Exercise exacerbates decline in the musculature of an animal model of Duchenne muscular dystrophy”. In: *bioRxiv*, p. 360388.

Hughes, Stacie E et al. (2007). “Genetic and Pharmacological Factors That Influence Reproductive Aging in Nematodes”. In: *PLoS Genetics* 3.2, e25.

Hutter, Harald (2006). “C. elegans, Methods and Applications”. In: *Methods in molecular biology (Clifton, N.J.)* 351, pp. 155–173.

Hyatt, Hayden et al. (2019). “Mitochondrial dysfunction induces muscle atrophy during prolonged inactivity: A review of the causes and effects”. In: *Archives of Biochemistry and Biophysics* 662, pp. 49–60.

Iba, Toshiaki et al. (2025). “Heat stress-induced mitochondrial damage and its impact on leukocyte function”. In: *Journal of Intensive Care* 13.1, p. 61.

Impey, Samuel G. et al. (2018). “Fuel for the Work Required: A Theoretical Framework for Carbohydrate Periodization and the Glycogen Threshold Hypothesis”. In: *Sports Medicine* 48.5, pp. 1031–1048.

Ishii, Naoaki et al. (2004). “Coenzyme Q10 can prolong C. elegans lifespan by lowering oxidative stress”. In: *Mechanisms of Ageing and Development* 125.1, pp. 41–46.

Jaba, Elisabeta, Christiana Brigitte Balan, and Ioan-Bogdan Robu (2014). “The Relationship between Life Expectancy at Birth and Health Expenditures Estimated by a Cross-country and Time-series Analysis”. In: *Procedia Economics and Finance* 15, pp. 108–114.

Jayaraj, Gopal G., Mark S. Hipp, and F. Ulrich Hartl (2020). “Functional Modules of the Proteostasis Network”. In: *Cold Spring Harbor Perspectives in Biology* 12.1, a033951.

Jorgensen, Erik M. and Susan E. Mango (2002). “The art and design of genetic screens: Caenorhabditis elegans”. In: *Nature Reviews Genetics* 3.5, pp. 356–369.

Jovic, Katharina et al. (2017). “Temporal dynamics of gene expression in heat-stressed Caenorhabditis elegans”. In: *PLoS ONE* 12.12, e0189445.

Joyce, Peter I. et al. (2012). “The Atypical Calpains: Evolutionary Analyses and Roles in Caenorhabditis elegans Cellular Degeneration”. In: *PLoS Genetics* 8.3, e1002602.

Kamath, Ravi S et al. (2000). “Effectiveness of specific RNA-mediated interference through ingested double-stranded RNA in Caenorhabditis elegans”. In: *Genome Biology* 2.1, research0002.1.

Kamath, Ravi S. et al. (2003). “Systematic functional analysis of the Caenorhabditis elegans genome using RNAi”. In: *Nature* 421.6920, pp. 231–237.

Kelly-Worden, Marie and Emily Thomas (2014). “Mitochondrial Dysfunction in Duchenne Muscular Dystrophy”. In: *Open Journal of Endocrine and Metabolic Diseases* 2014.08, pp. 211–218.

Kennedy, Brian K. et al. (2014). “Geroscience: Linking Aging to Chronic Disease”. In: *Cell* 159.4, pp. 709–713.

Kenyon, Cynthia et al. (1993). “A C. elegans mutant that lives twice as long as wild type”. In: *Nature* 366.6454, pp. 461–464.

Kirkwood, Thomas B.L. (2005). “Understanding the Odd Science of Aging”. In: *Cell* 120.4, pp. 437–447.

Klaips, Courtney L., Gopal Gunanathan Jayaraj, and F. Ulrich Hartl (2018). “Pathways of cellular proteostasis in aging and disease”. In: *Journal of Cell Biology* 217.1, pp. 51–63.

Klass, Michael R. (1983). “A method for the isolation of longevity mutants in the nematode Caenorhabditis elegans and initial results”. In: *Mechanisms of Ageing and Development* 22.3-4, pp. 279–286.

Krishna, Swathy et al. (2023). “Indicators of increased ER stress and UPR in aged D2-mdx and human dystrophic skeletal muscles”. In: *Frontiers in Physiology* 14, p. 1152576.

Kumsta, Caroline et al. (2017). “Hormetic heat stress and HSF-1 induce autophagy to improve survival and proteostasis in C. elegans”. In: *Nature Communications* 8.1, p. 14337.

Kyriakou, Eleni, Eirini Taouktsi, and Popi Syntichaki (2022). “The Thermal Stress Coping Network of the Nematode Caenorhabditis elegans”. In: *International Journal of Molecular Sciences* 23.23, p. 14907.

Labbadia, Johnathan and Richard I. Morimoto (2014). “The Biology of Proteostasis in Aging and Disease”. In: *Annual Review of Biochemistry* 84.1, pp. 1–30.

– (2015). “Repression of the Heat Shock Response Is a Programmed Event at the Onset of Reproduction”. In: *Molecular Cell* 59.4, pp. 639–650.

Labbadia, Johnathan et al. (2017). “Mitochondrial Stress Restores the Heat Shock Response and Prevents Proteostasis Collapse during Aging”. In: *Cell Reports* 21.6, pp. 1481–1494.

Lakso, Merja et al. (2003). “Dopaminergic neuronal loss and motor deficits in Caenorhabditis elegans overexpressing human -synuclein”. In: *Journal of Neurochemistry* 86.1, pp. 165–172.

Law, Charity W et al. (2014). “voom: precision weights unlock linear model analysis tools for RNA-seq read counts”. In: *Genome Biology* 15.2, R29.

Laybutt, D. R. et al. (2007). “Endoplasmic reticulum stress contributes to beta cell apoptosis in type 2 diabetes”. In: *Diabetologia* 50.4, pp. 752–763.

Lee, Ann-Hwee, Neal N. Iwakoshi, and Laurie H. Glimcher (2003). “XBP-1 Regulates a Subset of Endoplasmic Reticulum Resident Chaperone Genes in the Unfolded Protein Response”. In: *Molecular and Cellular Biology* 23.21, pp. 7448–7459.

Lei, Yingying et al. (2024). “Molecular mechanism of ATF6 in unfolded protein response and its role in disease”. In: *Heliyon* 10.5, e25937.

León, Mario Bermúdez de et al. (2005). “Dystrophin Dp71 Expression Is Down-regulated during Myogenesis ROLE OF Sp1 AND Sp3 ON THE Dp71 PROMOTER ACTIVITY*”. In: *Journal of Biological Chemistry* 280.7, pp. 5290–5299.

Leong, Darryl P et al. (2015). “Prognostic value of grip strength: findings from the Prospective Urban Rural Epidemiology (PURE) study”. In: *The Lancet* 386.9990, pp. 266–273.

Levine, Morgan E. et al. (2018). “An epigenetic biomarker of aging for lifespan and healthspan”. In: *Aging (Albany NY)* 10.4, pp. 573–591.

Li, Chenchen et al. (2026). “AI-driven aging digital twins: A roadmap for clinical translation in precision geriatrics”. In: *Ageing Research Reviews* 113, p. 102931.

Li, Jian et al. (2016). “E2F coregulates an essential HSF developmental program that is distinct from the heat-shock response”. In: *Genes & Development* 30.18, pp. 2062–2075.

Li, Jing, Sang Gyun Kim, and John Blenis (2014). “Rapamycin: One Drug, Many Effects”. In: *Cell Metabolism* 19.3, pp. 373–379.

Link, Christopher D et al. (1999). “Direct observation of stress response in Caenorhabditis elegans using a reporter transgene”. In: *Cell Stress & Chaperones* 4.4, p. 235.

Lithgow, G J et al. (1995). “Thermotolerance and extended life-span conferred by single-gene mutations and induced by thermal stress.” In: *Proceedings of the National Academy of Sciences* 92.16, pp. 7540–7544.

Liu, Jie et al. (2013). “Functional Aging in the Nervous System Contributes to Age-Dependent Motor Activity Decline in C. elegans”. In: *Cell Metabolism* 18.3, pp. 392–402.

Liu, Yasmine J. et al. (2019). “Mitochondrial translation and dynamics synergistically extend lifespan in C. elegans through HLH-30”. In: *bioRxiv*, p. 871079.

López-Otín, Carlos et al. (2013). “The Hallmarks of Aging”. In: *Cell* 153.6, pp. 1194–1217.

– (2023). “Hallmarks of aging: An expanding universe”. In: *Cell* 186.2, pp. 243–278.

Lu, Ake T. et al. (2019). “DNA methylation GrimAge strongly predicts lifespan and healthspan”. In: *Aging (Albany NY)* 11.2, pp. 303–327.

Lu, Yuancheng et al. (2020). “Reprogramming to recover youthful epigenetic information and restore vision”. In: *Nature* 588.7836, pp. 124–129.

Luan, Peiling et al. (2021). “Urolithin A improves muscle function by inducing mitophagy in muscular dystrophy”. In: *Science Translational Medicine* 13.588.

Ludtmann, Marthe H.R. and Andrey Y. Abramov (2018). “Mitochondrial calcium imbalance in Parkinson’s disease”. In: *Neuroscience Letters* 663, pp. 86–90.

Luo, Zhenhuan et al. (2022). “Gene activation in Caenorhabditis elegans using the Campylobacter jejuni CRISPR-Cas9 feeding system”. In: *G3* 12.6, jkac068.

Lv, Zhenyu et al. (2023). “Naringenin improves muscle endurance via activation of the Sp1-ERRγ transcriptional axis”. In: *Cell Reports* 42.11, p. 113288.

Lv, Ziquan and Yajie Guo (2020). “Metformin and Its Benefits for Various Diseases”. In: *Frontiers in Endocrinology* 11, p. 191.

Mair, William et al. (2009). “Optimizing Dietary Restriction for Genetic Epistasis Analysis and Gene Discovery in C. elegans”. In: *PLoS ONE* 4.2, e4535.

Malaiwong, Nawaphat, Montserrat Porta-de-la-Riva, and Michael Krieg (2023). “FLInt: Single Shot Safe Harbor Transgene Integration via Fluorescent Landmark Interference”. In: *bioRxiv*, p. 2023.01.19.524728.

Malaiwong, Nawaphat et al. (2026). “FLInt 2.0: Robust and customizable single shot integration in C. elegans”. In: *bioRxiv*, p. 2026.01.12.699147.

Mandsager, Kyle et al. (2018). “Association of Cardiorespiratory Fitness With Long-term Mortality Among Adults Undergoing Exercise Treadmill Testing”. In: *JAMA Network Open* 1.6, e183605.

Matthews, Emma et al. (2016). “Corticosteroids for the treatment of Duchenne muscular dystrophy”. In: *Cochrane Database of Systematic Reviews* 2016.5, CD003725.

Maurel, M. et al. (2014). “Getting RIDD of RNA: IRE1 in cell fate regulation”. In: *Trends in Biochemical Sciences* 39.5, pp. 245–254.

McColl, Gawain et al. (2010). “Insulin-like Signaling Determines Survival during Stress via Posttranscriptional Mechanisms in C. elegans”. In: *Cell Metabolism* 12.3, pp. 260–272.

McDonald, Craig M. et al. (2016). “Idebenone reduces respiratory complications in patients with Duchenne muscular dystrophy”. In: *Neuromuscular Disorders* 26.8, pp. 473–480.

Mello, C.C. et al. (1991). “Efficient gene transfer in C.elegans: extrachromosomal maintenance and integration of transforming sequences.” In: *The EMBO Journal* 10.12, pp. 3959–3970.

Merlini, Luciano, Paolo Bonaldo, and Emanuele Marzetti (2015). “Editorial: Pathophysiological Mechanisms of Sarcopenia in Aging and in Muscular Dystrophy: A Translational Approach”. In: *Frontiers in Aging Neuroscience* 7, p. 153.

Miller, D.M. et al. (1999). “Two-Color GFP Expression System for C. elegans”. In: *BioTechniques* 26.5, pp. 914–921.

Momma, Kenta et al. (2017). “Heat-Induced Calcium Leakage Causes Mitochondrial Damage in Caenorhabditis elegans Body-Wall Muscles”. In: *Genetics* 206.4, pp. 1985–1994.

Moorwood, Catherine and Elisabeth R. Barton (2014). “Caspase-12 ablation preserves muscle function in the mdx mouse”. In: *Human Molecular Genetics* 23.20, pp. 5325–5341.

Morimoto, Richard I. (2008). “Proteotoxic stress and inducible chaperone networks in neurodegenerative disease and aging”. In: *Genes & Development* 22.11, pp. 1427–1438.

Morley, James F. and Richard I. Morimoto (2004). “Regulation of Longevity in Caenorhabditis elegans by Heat Shock Factor and Molecular Chaperones”. In: *Molecular Biology of the Cell* 15.2, pp. 657–664.

Morley, James F. et al. (2002). “The threshold for polyglutamine-expansion protein aggregation and cellular toxicity is dynamic and influenced by aging in Caenorhabditis elegans”. In: *Proceedings of the National Academy of Sciences* 99.16, pp. 10417–10422.

Mouchiroud, Laurent et al. (2013). “The NAD+/Sirtuin Pathway Modulates Longevity through Activation of Mitochondrial UPR and FOXO Signaling”. In: *Cell* 154.2, pp. 430–441.

Murphy, Coleen T. et al. (2003). “Genes that act downstream of DAF-16 to influence the lifespan of Caenorhabditis elegans”. In: *Nature* 424.6946, pp. 277–283.

Mutz, Julian, Raquel Iniesta, and Cathryn M. Lewis (2024). “Metabolomic age (MileAge) predicts health and life span: A comparison of multiple machine learning algorithms”. In: *Science Advances* 10.51, eadp3743.

Narendra, Derek P. and Richard J. Youle (2011). “Targeting Mitochondrial Dysfunction: Role for PINK1 and Parkin in Mitochondrial Quality Control”. In: *Antioxidants & Redox Signaling* 14.10, pp. 1929–1938.

Naresh, Nandhitha Uma et al. (2022). “Mitochondrial genome recovery by ATFS-1 is essential for development after starvation”. In: *Cell Reports* 41.13, p. 111875.

Nargund, Amrita M. et al. (2012). “Mitochondrial Import Efficiency of ATFS-1 Regulates Mitochondrial UPR Activation”. In: *Science* 337.6094, pp. 587–590.

Nargund, Amrita M. et al. (2015). “Mitochondrial and Nuclear Accumulation of the Transcription Factor ATFS-1 Promotes OXPHOS Recovery during the UPRmt”. In: *Molecular Cell* 58.1, pp. 123–133.

Ocampo, Alejandro et al. (2016). “In Vivo Amelioration of Age-Associated Hallmarks by Partial Reprogramming”. In: *Cell* 167.7, 1719–1733.e12.

Oh, Kelly Hyunju and Hongkyun Kim (2013). “Reduced IGF signaling prevents muscle cell death in a Caenorhabditis elegans model of muscular dystrophy”. In: *Proceedings of the National Academy of Sciences* 110.47, pp. 19024–19029.

Onken, Brian and Monica Driscoll (2010). “Metformin Induces a Dietary Restriction–Like State and the Oxidative Stress Response to Extend C. elegans Healthspan via AMPK, LKB1, and SKN-1”. In: *PLoS ONE* 5.1, e8758.

Paix, Alexandre et al. (2014). “Scalable and Versatile Genome Editing Using Linear DNAs with Microhomology to Cas9 Sites in Caenorhabditis elegans”. In: *Genetics* 198.4, pp. 1347–1356.

Pakos-Zebrucka, Karolina et al. (2016). “The integrated stress response”. In: *EMBO reports* 17.10, pp. 1374–1395.

Palikaras, Konstantinos, Eirini Lionaki, and Nektarios Tavernarakis (2015). “Coordination of mitophagy and mitochondrial biogenesis during ageing in C. elegans”. In: *Nature* 521.7553, pp. 525–528.

Pan, Xin et al. (2013). “The physiological role of mitochondrial calcium revealed by mice lacking the mitochondrial calcium uniporter”. In: *Nature Cell Biology* 15.12, pp. 1464–1472.

Pauly, Marion et al. (2017). “ER stress disturbs SR/ER-mitochondria Ca2+ transfer: Implications in Duchenne muscular dystrophy”. In: *Biochimica et Biophysica Acta (BBA) - Molecular Basis of Disease* 1863.9, pp. 2229–2239.

Pede, Alexa Di et al. (2025). “Mild activation of the mitochondrial unfolded protein response increases lifespan without increasing resistance to stress”. In: *Open Biology* 15.4, p. 240358.

Penke, Botond et al. (2018). “Heat Shock Proteins and Autophagy Pathways in Neuroprotection: from Molecular Bases to Pharmacological Interventions”. In: *International Journal of Molecular Sciences* 19.1, p. 325.

Petrungaro, Carmelina et al. (2015). “The Ca2+-Dependent Release of the Mia40-Induced MICU1-MICU2 Dimer from MCU Regulates Mitochondrial Ca2+ Uptake”. In: *Cell Metabolism* 22.4, pp. 721–733.

Phillips, Stuart M. (2006). “Dietary protein for athletes: from requirements to metabolic advantage”. In: *Applied Physiology, Nutrition, and Metabolism* 31.6, pp. 647–654.

Pincus, David et al. (2010). “BiP Binding to the ER-Stress Sensor Ire1 Tunes the Homeostatic Behavior of the Unfolded Protein Response”. In: *PLoS Biology* 8.7, e1000415.

Rahman, Mizanur et al. (2020). “NemaLife chip: a micropillar-based microfluidic culture device optimized for aging studies in crawling C. elegans”. In: *Scientific Reports* 10.1, p. 16190.

Ranabhat, Chhabi L. et al. (2018). “The Influence of Universal Health Coverage on Life Expectancy at Birth (LEAB) and Healthy Life Expectancy (HALE): A Multi-Country Cross-Sectional Study”. In: *Frontiers in Pharmacology* 9, p. 960.

Rath, Sneha et al. (2020). “MitoCarta3.0: an updated mitochondrial proteome now with sub-organelle localization and pathway annotations”. In: *Nucleic Acids Research* 49.D1, pp. D1541–D1547.

Rauthan, Manish et al. (2013). “The mitochondrial unfolded protein response activator ATFS-1 protects cells from inhibition of the mevalonate pathway”. In: *Proceedings of the National Academy of Sciences* 110.15, pp. 5981–5986.

Reinke, Valerie et al. (2000). “A Global Profile of Germline Gene Expression in C. elegans”. In: *Molecular Cell* 6.3, pp. 605–616.

Ristow, Michael and Kathrin Schmeisser (2014). “Mitohormesis: Promoting Health and Lifespan by Increased Levels of Reactive Oxygen Species (ROS)”. In: *Dose-Response* 12.2, dose–response.13-035.Ristow.

Rodriguez, Miriam et al. (2013). “Worms under stress: C. elegans stress response and its relevance to complex human disease and aging”. In: *Trends in Genetics* 29.6, pp. 367–374.

Romussi, Stefano et al. (2024). “C. elegans: a prominent platform for modeling and drug screening in neurological disorders”. In: *Expert Opinion on Drug Discovery* 19.5, pp. 565–585.

Ron, David and Peter Walter (2007). “Signal integration in the endoplasmic reticulum unfolded protein response”. In: *Nature Reviews Molecular Cell Biology* 8.7, pp. 519–529.

Roussos, Antonis et al. (2023). “Caenorhabditis elegans as a Model System to Study Human Neurodegenerative Disorders”. In: *Biomolecules* 13.3, p. 478.

Roux, Antoine E. et al. (2022). “The complete cell atlas of an aging multicellular organism”. In: *bioRxiv*, p. 2022.06.15.496201.

Ryu, Dongryeol et al. (2016). “Urolithin A induces mitophagy and prolongs lifespan in C. elegans and increases muscle function in rodents”. In: *Nature Medicine* 22.8, pp. 879–888.

Salzer, Liesa and Michael Witting (2021). “Quo Vadis Caenorhabditis elegans Metabolomics—A Review of Current Methods and Applications to Explore Metabolism in the Nematode”. In: *Metabolites* 11.5, p. 284.

San-Millán, Iñigo and George A. Brooks (2018). “Assessment of Metabolic Flexibility by Means of Measuring Blood Lactate, Fat, and Carbohydrate Oxidation Responses to Exercise in Professional Endurance Athletes and Less-Fit Individuals”. In: *Sports Medicine* 48.2, pp. 467–479.

Santra, Mantu, Ken A. Dill, and Adam M. R. de Graff (2019). “Proteostasis collapse is a driver of cell aging and death”. In: *Proceedings of the National Academy of Sciences* 116.44, pp. 22173–22178.

Scheltens, Philip et al. (2021). “Alzheimer’s disease”. In: *The Lancet* 397.EMBO J 36 2017, pp. 1577–1590.

Schreiner, William P et al. (2019). “Remodeling of the Caenorhabditis elegans non-coding RNA transcriptome by heat shock”. In: *Nucleic Acids Research* 47.18, pp. 9829–9841.

Shalgi, Reut et al. (2013). “Widespread Regulation of Translation by Elongation Pausing in Heat Shock”. In: *Molecular Cell* 49.3, pp. 439–452.

Shcherbakov, Dimitri et al. (2022). “Premature aging in mice with error-prone protein synthesis”. In: *Science Advances* 8.9, eabl9051.

Shpilka, Tomer and Cole M. Haynes (2018). “The mitochondrial UPR: mechanisms, physiological functions and implications in ageing”. In: *Nature Reviews Molecular Cell Biology* 19.2, pp. 109–120.

Shutt, Timothy E. and Heidi M. McBride (2013). “Staying cool in difficult times: Mitochondrial dynamics, quality control and the stress response”. In: *Biochimica et Biophysica Acta (BBA) - Molecular Cell Research* 1833.2, pp. 417–424.

Sidrauski, Carmela et al. (2015). “The small molecule ISRIB reverses the effects of eIF2α phosphorylation on translation and stress granule assembly”. In: *eLife* 4, e05033.

Singh, Manish Kumar et al. (2024). “Heat Shock Response and Heat Shock Proteins: Current Understanding and Future Opportunities in Human Diseases”. In: *International Journal of Molecular Sciences* 25.8, p. 4209.

Soo, Sonja K et al. (2021a). “Activation of mitochondrial unfolded protein response protects against multiple exogenous stressors”. In: *Life Science Alliance* 4.12, e202101182.

Soo, Sonja K. et al. (2021b). “Mitochondrial unfolded protein response transcription factor ATFS-1 increases resistance to exogenous stressors through upregulation of multiple stress response pathways”. In: *bioRxiv*, p. 2021.04.26.441408.

Stanley, Taylor R. et al. (2024). “Activation of the heat shock response as a therapeutic strategy for tau toxicity”. In: *Disease Models & Mechanisms* 17.9, p. dmm050635.

Statzer, Cyril et al. (2022). “ATF-4 and hydrogen sulfide signalling mediate longevity in response to inhibition of translation or mTORC1”. In: *Nature Communications* 13.1, p. 967.

Steinkraus, Katherine A. et al. (2008). “Dietary restriction suppresses proteotoxicity and enhances longevity by an hsf-1-dependent mechanism in Caenorhabditis elegans”. In: *Aging Cell* 7.3, pp. 394–404.

Sudevan, Surabhi et al. (2019). “Mitochondrial dysfunction causes Ca2+ overload and ECM degradation–mediated muscle damage in C. elegans”. In: *The FASEB Journal* 33.8, pp. 9540–9550.

Sun, Andrew Y and Eric J Lambie (1997). “gon-2, a Gene Required for Gonadogenesis in Caenorhabditis elegans”. In: *Genetics* 147.3, pp. 1077–1089.

Sun, Nuo, Richard J. Youle, and Toren Finkel (2016). “The Mitochondrial Basis of Aging”. In: *Molecular Cell* 61.5, pp. 654–666.

Sural, Surojit et al. (2019). “HSB-1 Inhibition and HSF-1 Overexpression Trigger Overlapping Transcriptional Changes To Promote Longevity in Caenorhabditis elegans”. In: *G3: Genes, Genomes, Genetics* 9.5, pp. 1679–1692.

Sural, Surojit et al. (2020). “HSB-1/HSF-1 pathway modulates histone H4 in mitochondria to control mtDNA transcription and longevity”. In: *Science Advances* 6.43, eaaz4452.

Syntichaki, Popi et al. (2002). “Specific aspartyl and calpain proteases are required for neurodegeneration in C. elegans”. In: *Nature* 419.6910, pp. 939–944.

Takahashi, Kazutoshi and Shinya Yamanaka (2006). “Induction of Pluripotent Stem Cells from Mouse Embryonic and Adult Fibroblast Cultures by Defined Factors”. In: *Cell* 126.4, pp. 663–676.

Takahashi, Kazutoshi et al. (2007). “Induction of Pluripotent Stem Cells from Adult Human Fibroblasts by Defined Factors”. In: *Cell* 131.5, pp. 861–872.

Taylor, Rebecca C. and Andrew Dillin (2013). “XBP-1 Is a Cell-Nonautonomous Regulator of Stress Resistance and Longevity”. In: *Cell* 153.7, pp. 1435–1447.

Tcherepanova, Irina et al. (2000). “Aspartic Proteases from the Nematode Caenorhabditis elegans STRUCTURAL ORGANIZATION AND DEVELOPMENTAL AND CELL-SPECIFIC EXPRESSION OF asp-1 *”. In: *Journal of Biological Chemistry* 275.34, pp. 26359–26369.

Tondera, Daniel et al. (2009). “SLP-2 is required for stress-induced mitochondrial hyperfusion”. In: *The EMBO Journal* 28.11, pp. 1589–1600.

Tsang, William Y. and Bernard D. Lemire (2003). “The role of mitochondria in the life of the nematode, Caenorhabditis elegans”. In: *Biochimica et Biophysica Acta (BBA) - Molecular Basis of Disease* 1638.2, pp. 91–105.

Ukraintseva, Svetlana, Anatoliy I. Yashin, and Konstantin G. Arbeev (2016). “Resilience Versus Robustness in Aging”. In: *Journals of Gerontology Series A: Biomedical Sciences and Medical Sciences* 71.11, pp. 1533–1534.

Ukraintseva, Svetlana et al. (2021). “Decline in biological resilience as key manifestation of aging: Potential mechanisms and role in health and longevity”. In: *Mechanisms of Ageing and Development* 194, p. 111418.

Verhaart, Ingrid E. C. and Annemieke Aartsma-Rus (2019). “Therapeutic developments for Duchenne muscular dystrophy”. In: *Nature Reviews Neurology* 15.7, pp. 373–386.

Vivek-Ananth, R P et al. (2025). “Effects of Curcumin and Sulforaphane on C. elegans Healthspan: Independent and Combined Impacts”. In: *Innovation in Aging* 9.Supplement$_2$, igaf122.2541.

Walter, Peter and David Ron (2011). “The Unfolded Protein Response: From Stress Pathway to Homeostatic Regulation”. In: *Science* 334.6059, pp. 1081–1086.

Wek, R C, H -Y Jiang, and T G Anthony (2006). “Coping with stress: eIF2 kinases and translational control”. In: *Biochemical Society Transactions* 34.1, pp. 7–11.

Whitson, Heather E. et al. (2016). “Physical Resilience in Older Adults: Systematic Review and Development of an Emerging Construct”. In: *Journals of Gerontology Series A: Biomedical Sciences and Medical Sciences* 71.4, pp. 489–495.

Wilczok, Dominika (2025). “Deep learning and generative artificial intelligence in aging research and healthy longevity medicine”. In: *Aging (Albany NY)* 17.1, pp. 251–275.

Wilmanski, Tomasz et al. (2021). “Gut microbiome pattern reflects healthy ageing and predicts survival in humans”. In: *Nature Metabolism* 3.2, pp. 274–286.

Wu, Xintong et al. (2022). “Mitochonic Acid 5 Improves Duchenne Muscular Dystrophy and Parkinson’s Disease Model of Caenorhabditis elegans”. In: *International Journal of Molecular Sciences* 23.17, p. 9572.

Wu, Ziyun et al. (2018). “Mitochondrial unfolded protein response transcription factor ATFS-1 promotes longevity in a long-lived mitochondrial mutant through activation of stress response pathways”. In: *BMC Biology* 16.1, p. 147.

Xu, Fan et al. (2023). “Reprogramming of the transcriptome after heat stress mediates heat hormesis in Caenorhabditis elegans”. In: *Nature Communications* 14.1, p. 4176.

Xu, L Amanda et al. (2026). “Automated analysis of C. elegans behavior by LabGym: an open-source, AI-powered platform”. In: *G3: Genes, Genomes, Genetics*, jkag120.

Yamasaki, Satoshi and Paul Anderson (2008). “Reprogramming mRNA translation during stress”. In: *Current Opinion in Cell Biology* 20.2, pp. 222–226.

Yang, Liu et al. (2021). “Pyrroloquinoline quinone extends Caenorhabditis elegans ’ longevity through the insulin/IGF1 signaling pathway-mediated activation of autophagy”. In: *Food & Function* 12.22, pp. 11319–11330.

Yang, Wen and Siegfried Hekimi (2010a). “A Mitochondrial Superoxide Signal Triggers Increased Longevity in Caenorhabditis elegans”. In: *PLoS Biology* 8.12, e1000556.

– (2010b). “Two modes of mitochondrial dysfunction lead independently to lifespan extension in Caenorhabditis elegans”. In: *Aging Cell* 9.3, pp. 433–447.

Yasuda, Kensuke et al. (2021). “Cortisol promotes stress tolerance via DAF-16 in Caenorhabditis elegans”. In: *Biochemistry and Biophysics Reports* 26, p. 100961.

Yoneda, Takunari et al. (2004). “Compartment-specific perturbation of protein handling activates genes encoding mitochondrial chaperones”. In: *Journal of Cell Science* 117.18, pp. 4055–4066.

Yuan, Shuai and Susanna C. Larsson (2023). “Epidemiology of sarcopenia: Prevalence, risk factors, and consequences”. In: *Metabolism* 144, p. 155533.

Zabłocka, Barbara, Dariusz C. Górecki, and Krzysztof Zabłocki (2021). “Disrupted Calcium Homeostasis in Duchenne Muscular Dystrophy: A Common Mechanism behind Diverse Consequences”. In: *International Journal of Molecular Sciences* 22.20, p. 11040.

Zavagno, Giulia et al. (2024). “Rapid measurement of ageing by automated monitoring of movement of C. elegans populations”. In: *GeroScience* 46.2, pp. 2281–2293.

Zhan, Hong et al. (2014). “In vivo single-molecule imaging identifies altered dynamics of calcium channels in dystrophin-mutant C. elegans”. In: *Nature Communications* 5.1, p. 4974.

Zhu, Peng-fei et al. (2026). “ISRIB as a prototype eIF2B activator: Pharmacology, mechanisms, and translational potential in aging-related cognitive disorders”. In: *Pharmacological Research* 228, p. 108228.

7 APPENDICES

7.1 Supplementary Material

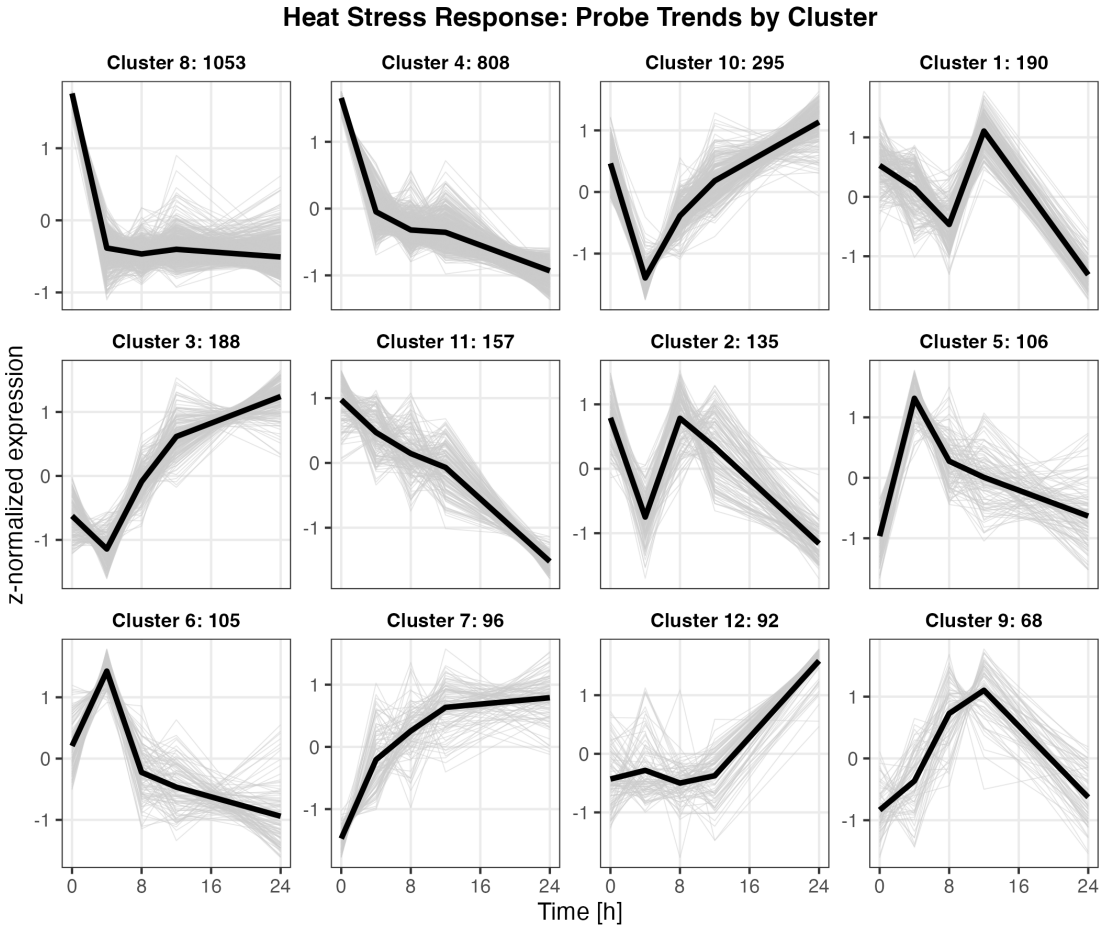

7.2 Contributions

RNA library prep and sequencing was performed by the Altos Genomics hub at Altos in Cambridge (UK) and San Diego (California, USA).

Bioinformatic analyses were performed in collaboration with the Bioinformatics hub at Altos, Cambridge Institute of Science. Limma modelling was performed by Ricard Argelaguet and adapted for further analysis by Jan Eike Dinort.